Department of Applied Geology

Gold transport in aqueous *versus* organic fluids: Experimental data and natural observations for describing ore-forming systems

Lars-S. Crede

This thesis is presented for the Degree of

Doctor of Philosophy

of

Curtin University

July 2018

Declaration

To the best of my knowledge and belief this thesis contains no material previously published by any other person except where due acknowledgment has been made. This thesis contains no material which has been accepted for the award of any other degree or diploma in any university.

Perth, 11th of July 2018

Signature

Abstract

The association of carbonaceous matter (CM) with ore deposits of metals such as gold has long been recognized but is still poorly understood. CM is commonly accepted as a reducing or scavenging agent for metals out of hydrothermal aqueous ore fluids. A few studies on e.g., Carlin-type Gold (Au) deposits and some experimental studies though, suggest that liquid hydrocarbons can transport Au. Still the understanding of how Au may be transported by liquid hydrocarbons is very limited. Thus, this Ph.D. – project aimed to answer in what amounts Au may be transported by oil and how oil competes with hydrothermal aqueous fluids by performing partition experiments; how Au is transported in oil by performing synchrotron X-ray absorption spectroscopy (XAS) experiments; and whether proof for a hydrocarbon phase transport of Au is present in samples from the McLaughlin Au-Hg deposit to support the hypothesis of a hydrocarbon phase Au transport, or to prove it wrong.

To perform Au partition experiments a new method was developed to allow *in-situ* sampling of both fluids, the oil and the aqueous solution. To achieve this a HFS-340Z hydrothermal flow system (Coretest Systems, Inc.) was modified and used as a batch reactor, so that the density stratified aqueous solution (brine, 10 wt% NaCl) and the oil, *n*-dodecane ($CH_3(CH_2)_{10}CH_3$; DD) or 1-dodecanethiol ($CH_3(CH_2)_{10}CH_2SH$; DDT), can be sampled simultaneously at temperature (up to 150 °C). The samples were then processed for Au analyzes by inductively coupled plasma mass spectrometry (ICP-MS). First partition experiments with brine and DD revealed that Au partitioning is independent of temperature in the range of 105 °C to 150 °C and that the ("trusted") partition coefficient ($D_{Au}^{org/aq}$; org = oil; aq = brine) is 0.1 0.1 ± 0.04. Partition experiments between brine and DDT also appear to be temperature independent in the same temperature range with an $D_{Au}^{org/aq}$ after data processing of 19 ± 21 and Au concentrations of ppm levels. These results suggest that, while the alkane DD is unlikely to transport Au, thiolate ligands such as DDT can contribute significantly to Au transport and that oils have the capacity to transport more Au than hydrothermal aqueous fluids at these conditions.

The speciation and the structural properties of gold complexes in DD or DDT in contact with aqueous solutions (brine and pure water) from 25 °C to 250 °C were investigated by XAS experiments performed at the European Synchrotron Facility in Grenoble, France. Below

125 °C Au(III)Cl is dominant in the DD and the adjacent aqueous solution with a refined coordination number (CN) of chloride 4.0(3) and a Au-Cl bond length of 2.28 Å, consistent with the tetrachloroaurate complex ($AuCl_4^-$). An Au(I) complex dominates in both water and adjacent DDT with a CN of sulfur ~2.0, suggesting a $[RS\text{-}Au\text{-}SR]^-$ (RS = DDT with deprotonated thiol group) complex with Au-S bond lengths ranging from 2.29(1) Å to 2.31(3) Å. Sulfur is always present in natural oils and thus these results suggests, that Au(I) - organothiol complexes are the dominant form of Au below 125 °C. At temperatures ≥ 125 °C gold was reduced to Au(0) in all solutions investigated, suggesting that organo-stabilized nanoparticles may be the major form of gold to be scavenged, concentrated or transported in natural oils at these conditions.

The above noted experimental results established that oils can act as excellent Au distributors. To complete the argument for a hydrocarbon phase Au transport samples from the McLaughlin Au-HG deposit, which is associated with CM ranging from liquid oil to solid bitumen, were investigated. Investigation of the textural relationships between CM and Au mineralization of samples from the McLaughlin Au-Hg deposit and analyzes of Au concentrations in liquid oil in these samples revealed proof of a hydrocarbon phase Au mobilization at least within the deposit. Textural evidence indicates an alternating and sometimes parallel introduction of silica - rich hydrothermal fluids and hydrocarbon fluids. Au concentrations in ppm levels in liquid oil demonstrate that Au is and was mobile within the deposit in organic liquids, and was possibly introduced with liquid oil in addition to other hydrothermal fluids. Since oil can migrate over long distances (km scale) it is able to act as an ore fluids.

Acknowledgements

There are many people who were a great support during this PhD project. Thank you all so much. First of all, I cannot thank Katy Evans enough or express how much her support was worth for me. Katy always knew what was important and did an awesome job helping me to structure my often unstructured thoughts. She was simply the best. I wish her all the best for her exciting future. I want to thank Kirsten Rempel. She was the person who gave me the chance to work on this exciting project and have this great experience in Western Australia. Thank you so much for that, Kirsten. Many thanks to Joël Brugger and Weihua Liu who played a substantial part in the success of the XAS part of this project and who made the trip to the ESRF in France a great time. Then I want to thank Julien Bourdet for his great introduction to hydrocarbon fluid inclusions. Although the fluid inclusion study was not that fruitful, I learned a lot from Julien and am very thankful for that and the time he took to point me in the right direction. Andy Wieczorek helped me maintain the experimental equipment in the lab and was a huge time and money saver. I would have become much older without him in the early stages of the PhD, thanks Andy. Here, I also want to thank Prok Vasilyev who turned the lab into an enjoyable environment shortly after I started my PhD. I am deeply grateful of the help received from Barbara Etschmann, Denis Testemale, Shirley (Siyu Hu), Frank Reith, Kliti Grice, Peter Hopper and Ichiko Sugiyama. Many thanks to Andrew Putnis, his awesome dinner parties, and his support for the lab. Tobias Wengorsch helped me to take some great quality photos and was always there to discuss the weirdness of science, thanks Tobi! I am also very thankful of Shaun Height and his patience with me. He sometimes came to Curtin just for me to pick up ONE sample. Andreas Beinlich, Thomas Becker, William Rickard, and Kari Pitts spend a lot of time with me working on parts of the project that did not pay out in the end. Thank you so much for your help! I also want to thank G. Pokrovski and A. Giże for their excellent reviews and comments.

Last but not least, I am very grateful to Franzi who agreed to come with me to Western Australia for a little adventure. I hope I did not forget anyone, if so please be angry with me. I hope to be back one day, see you then!

I was supported by the Curtin International Postgraduate Research Scholarship (CIPRS)/ Department of Applied Geology – ARC Discovery Project Scholarship #52507.

Table of Contents

List of Figures

List of Tables

List of Equations

Nomenclature

$D^{org/aq}$	Partition coefficient of Au between the oil and the brine
c_{Au}^{org}	Au concentration in the oil
c_{Au}^{aq}	Au concentration in the brine
Au_{recov}	Fraction of Au recovered after the experiment in % of the initially added amount of Au
DD	*n*-dodecane ($CH_3(CH_2)_{10}CH_3$)
DDT	1-dodecanethiol ($CH_3(CH_2)_{10}CH_2SH$)
CM	Carbonaceous matter

Chapter 1

Introduction

1.1 Introduction

Carbonaceous matter (CM) can be associated with a variety of different types of ore deposits including e.g., epithermal Au-Ag(-Hg) deposits (Sherlock, 1992; Pearcy and Burruss, 1993; Mastalerz et al., 2000; Sherlock, 2000); Carlin-type Au deposits (Radtke and Scheiner, 1970; Hausen and Park, 1986; Emsbo and Koenig, 2007; Gu et al., 2012; Groves et al., 2016); orogenic Au deposits (Mirasol-Robert et al., 2017); Mississippi Valley-type Pb-Zn deposits (e.g., Parnell, 1988; Giże and Barnes, 1989; Kesler et al., 1994), 'Kupferschiefer' copper deposits (e.g., Kucha, 1981; Kucha and Przylowicz, 1999; Sawlowicz et al., 2000), sediment-hosted U deposits (Landais, 1996; Spirakis, 1996), and Witwatersrand-type Au-U deposits (Fuchs et al., 2016). In addition, high concentrations of ore metals measured in natural crude oil and bitumen (Hennet et al., 1988; Manning and Giże, 1993; Filby, 1994; Samedova et al., 2009; Vorapalawut et al., 2011) suggest petroleum phase metal transport. Still, the common association of hydrocarbons and ores, and the role of hydrocarbons in the mobilization, transport, concentration, deposition, and preservation stages of ore formation processes are controversial and not fully understood, although there is extensive literature describing and interpreting the occurrence of organic matter in ore deposits (e. g., Parnell, 1988; Parnell et al., 1993; Giordano et al., 2000; Glikson and Mastalerz, 2000). Two of the main reasons for the unclear relationship are the lack and difficulty of experiments on the interaction of hydrocarbons, metals, and rocks, and the difficulty with identification of the paragenetic relationship and history of the organic matter and the ore. Consequently, this data is missing in current ore-formation models, but is needed to alleviate the increasing difficulty of finding new ore deposits.

1.1.1 Roles of CM

The main roles of organic matter in the literature in ore formation processes are (e. g., Parnell et al., 1993; Giordano et al., 2000; Glikson and Mastalerz, 2000, and references within):

- Mechanical filtering of metals out of aqueous fluids
- Providing reducing conditions or acting as an active reductant leading to ore mineral precipitation
- Active biological involvement e. g., uptake in plants

- Organic ligands dissolved in aqueous (hydrothermal) fluids transporting metals

These widely accepted roles for organic matter in ore formation processes mainly focus on the last stage of any ore formation, the concentration and deposition stage. There are exceptions of course, such as in the Witwatersrand basin South Africa, where petroleum-phase transport was proposed in the form of mobile liquid hydrocarbons that originated from shales and contributed to the mobilization and re-deposition of uranium and gold (Fuchs et al., 2015; Fuchs et al., 2016). Simplified, there are three pre-requisites for the formation of any ore deposit: source, transport, and precipitation (deposition) including concentration (Giże, 2000). The possibility of liquid hydrocarbons such as petroleum, to actively transport metals is often dismissed in favor of aqueous fluids. Further, evidence for organic matter acting as a source for gold the first stage of the ore formation process -- is lacking. This lack of evidence is in contrast to that for zinc or lead in black shales for example, which are possible sources for some ore deposit types (Large et al., 2011). As zinc is a borderline soft metal and lead is a soft metal it is possible that other soft elements such as gold, platinum, or mercury also can be concentrated in organic-rich shales.

The most widespread evidence of a role for organic matter in the ore formation process is in the precipitation phase. There are several functions that organic matter can perform in the precipitation stage. Most common is the mechanical filtering of metals/sulfur out of later hydrothermal aqueous fluids (e. g. Molnár et al., 2016), and by acting as a reducing agent leading to gold precipitation due to the reduction of sulfate to solid state sulfite; a process that is suggested for the Carlin Au-deposit (Giże, 2000). Furthermore, graphite is known to be an active reductant in shear-zone hosted gold deposits (Gize, 1999; Giże, 2000; Giże et al., 2000). Early studies showed that living organic matter is involved by taking up metals as gold, when the plants are in the vicinity of gold bearing geological structures (e.g., gold veinlets; Warren and Delavault, 1950). This process can be assigned to the source and precipitation/concentration stage, with the implication that the organic matter enriched in gold is preserved and again introduced into the geological cycle. In sedimentary environments, organic matter is involved in the formation of metal sulfides in carbonaceous sediments during diagenesis (Saxby, 1973).

As noted above, a variety of different ore deposits are associated with organic matter e. g., the Kupferschiefer (Cu-Zn-Pb) in Poland and Germany, the sedimentary Witwatersrand

U-Au deposits in South Africa, the McArthur River SEDEX Pb-Zn deposit in Australia, the Pine Point Mississippi Valley-type deposit in Canada, or the McLaughlin Au deposit in the United States, California, to just name a few famous deposits. In most uranium deposits for example, organic matter is believed to be a key component of the genetic model (Leventhal, 1980; Leventhal et al., 1986; Landais, 1996; Spirakis, 1996). The Grants Uranium district in New Mexico has a linear correlation between organic matter and the ore within host units (Granger, 1966; Leventhal and Threlkeld, 1978; Leventhal et al., 1986) to a degree that it is almost impossible to find organic matter that is not mineralized or to find primary ore without organic matter. Carbonaceous matter for example is an intimate part of the chemical structure of the uranium bearing thucholite (Ellsworth, 1928). The ore minerals uraninite and coffinite are intimately mixed with organic matter (Granger, 1966) suggesting that organic matter is necessary for the deposition of uranium, possibly due to the transport of organic matter and uranium within the same ground water flow paths and subsequent co-precipitation (Leventhal and Giordano, 2000).

Organic matter is often found in Carlin-type Au deposits (Hulen and Collister, 1999; Emsbo and Koenig, 2007) and Au-Hg epithermal vein deposits (Sherlock, 2005) that frequently have abundant carbonaceous matter in the original mineralized horizon (Berger and Bagby, 1993). A good example for the still ongoing discussion on the role of hydrocarbons is the Carlin deposit. At the Carlin deposit, the organic-rich zones are often, but not necessarily, gold bearing. This led some researchers (Radtke and Scheiner, 1970) to conclude that the organic matter was introduced with the gold, and suggested that the concentration of organic matter occurred during hydrothermal mineralization and alteration (e. g. Radtke, 1981; Hausen and Park, 1986). Later studies proposed that petroleum migration predated gold mineralization (Kuehn, 1989), and that the organic matter was only involved during the deposition process (Giże et al., 2000) by provision of a reducing environment. This interpretation is supported by the general acceptance that aqueous brines act as the transport fluid for metals into the ore deposit. The lack of a consistent relationship between CM and Au in Carlin-type deposits is considered as a consequence of the superposition of the record of two independent fluids (petroleum and aqueous brine) using the same migration pathways (Giże, 2000). However, Emsbo and Koenig (2007) claim that clear evidence of organic matter acting as the transport medium was found at the northern Carlin-trend (Emsbo and Koenig, 2007), where gold and other trace elements are homogenously distributed within the bitumen grains. The authors propose that, if the gold was introduced after the bitumen, then it would be distributed on the outer bitumen grain margins.

Additionally, Emsbo and Koenig (2007) claim that the mineralization caused by hydrothermal fluids in the Carlin-type deposits is older than the bitumen generation and migration, due to the absence of alteration of the bitumen and surrounding rocks by hydrothermal Carlin-type fluids. If this is the case then the presence of Au in bitumen indicates gold transportation in organic fluids. The mineralization order and point in time of bitumen generation and migration after Emsbo and Koenig (2007) is the opposite of what Kuehn (1989) proposed. These views are yet to be reconciled; Groves et al. (2016) reported that hydrocarbons play a major role in the formation of giant gold provinces such as in the Carlin gold province, but also state that its precise role is still unclear and that the interrelated factors leading to the formation of the Carlin Au province are unique.

The organic phase transport of ore metals forms only a small fraction of the current literature, due to lack of available data. This is a crucial issue, as understanding of the chemical transport mechanism is the key to understanding mobilization and deposition mechanisms, due to the involvement of ore fluids in all three stages: mobilization, transport, and deposition.

1.1.2 Au transport by CM

Metal transport with organic involvement is limited to low-temperature deposits (< 250 °C), due to the degradation of organic compounds at higher temperatures. Thus, investigation of the role of CM in gold deposits focuses on hydrothermal conditions at relatively low pressure and temperature. For effective transport, the possible ligands that may transport Au must be present in a high enough concentration, be persistent enough to not degrade during metal extraction from the source and transport, and be stable enough to result in sufficient metal solubilities to concentrate the metals into ore bodies.

The dominant dissolved organic ligands in hydrothermal aqueous fluids are mono- and dicarboxylate species, and to a lesser degree organosulfur and phenolic compounds (see review in Giordano et al., 2000). The available, but not so recent literature suggests that CM may contribute to gold transport in the form of metal-organic complexes that are dissolved in aqueous fluids, mainly sulfur-based ligands and to a lesser degree nitrogen-based ligands dissolved in aqueous ore fluids (e.g., Wood, 1996; Giordano, 2000; Giże, 2000; Wood, 2000), where the gold cation is bonded directly to electron-donor atoms other than carbon (Langmuir, 1979).

Because the Au^{+} ion classifies as a soft Lewis acid it forms complexes with soft, easily polarizable ligands (Pearson, 1968). Thus, Au bonds very strongly with CN^{-}, which is produced by some plants and microorganisms (Fairbrother et al., 2009), with S-bearing functional groups (Figure 1-1), and then, less strong, with nitrogen (e.g., amine) and oxygen (Vlassopoulos et al., 1990; Wood, 1996; Liu et al., 2014; Ta et al., 2014). Au(I) cyanide complexes can be stable in the environment for extended time periods (Ta et al., 2014), and thus may be a potential ligand for gold transport. Au – thiol bonds, for example Au bonds to thiomalate (Figure 1-1) and thioglucose, are the main gold-active species in biological systems (Cotton and Wilkinson, 1988; Giże, 2000; Etschmann et al., 2016; Zammit et al., 2016).

A liquid crude oil (also referred to as liquid bitumen, liquid hydrocarbon, or liquid oil) transporting metals is usually considered to have a secondary role, as it is coexisting with aqueous ore fluids in the same sedimentary basin, contributing to the ore metal transport only to a small degree (Giordano, 2000). However, wherever the two fluids are physically in contact, there will be partitioning of the metals between the two phases. Tetrapyrrole ligands were thought to be the main chemical to transport metals in a petroleum phase (Giordano, 2000). Solvent-extractable tetrapyrrole structures are porphyrins (Figure 1-1), which are able to form metal-porphyrin complexes that strongly fractionate into the organic phase in a water-organic phase system. It is known that porphyrins form stable to very stable complexes with V, Ni, Fe, Cu and Co, and thus are able to contribute significantly to the organic phase transport. However, gold is not reported to form porphyrin complexes to any great extent, due to its large ionic radii, as ions with radii near 0.65 Å are preferred in metal-porphyrin complexes. It is assumed that the soft metal gold interacts in the organic phase most strongly with soft, sulfur- and nitrogen-based ligands, just as it does in the hydrothermal aqueous phase.

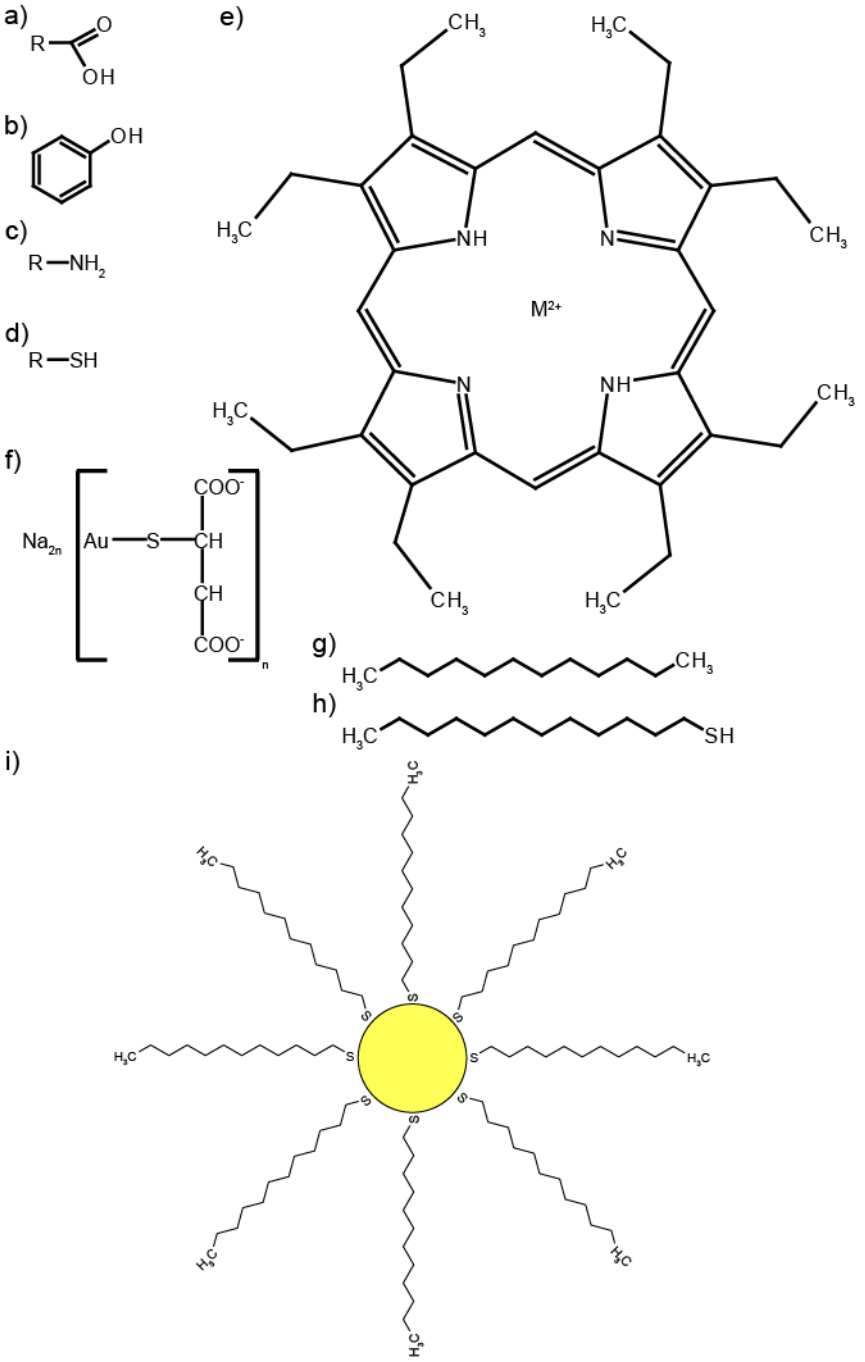

Figure 1-1: Some of the ligands that can form metal organic complexes. (a) carboxyls; (b) phenolic hydroxyls; (c) amino groups; (d) thiol; (e) metal porphyrin complex (after Giordano, 2000), (f) sodium aurothiomalate (after Elder and Eidsness, 1987), n-dodecane (g), 1-dodecanethiol (h), and (i) a AuNP capped with 1-dodecanethiol (after Daniel and Astruc, 2004 and references therein).

1.1.3 Au transport in the form of Au nanoparticles (AuNPs)

The means by which gold could be transported in organic liquids is mostly unknown, but observations in nature may give hints to the actual state of gold during the transport process. Gold nanoparticles are coming more and more into focus in recent years, due to better technologies to characterize gold nanoparticles, and to their myriad uses (e.g., Daniel

and Astruc, 2004; Jain et al., 2007; Sardar et al., 2009; Ansar et al., 2013; Alex and Tiwari, 2015). Gold nanoparticles may also contribute to Au transport in liquid CM (Osterloh et al., 2004; Reith et al., 2010; Stankus et al., 2010; Lohman et al., 2012; Pearce et al., 2016; Reith and Cornelis, 2017). A comprehensive review on possible formation mechanisms of natural gold nanoparticles, and their role in the precipitation of primary and secondary gold is given in Hough et al. (2011), and references therein. Gold nanoparticles can, for example, be transported and deposited from magmatic vapors onto vent walls (Meeker et al., 1991; Taran et al., 2000; Simmons and Brown, 2007; Larocque et al., 2008); occur as a combined colloid of silica and gold (Frondel, 1938); be incorporated in the host sulfide by solid solution (Simon et al., 1999; Reich et al., 2005); be incorporated as nanoparticles when Au concentrations exceed the gold solubility in the sulfide (Palenik et al., 2004; Reich et al., 2005); or form Au by coagulation from a nanoparticle suspension (Saunders, 1990) in hypogene environments. In supergene deposits gold is thought to be a secondary precipitate that was transported and deposited from solution (Hough et al., 2009) or nanoparticulate colloidal suspensions (Hough et al., 2008). Pearce et al. (2016) argues that the several magnitudes higher gold concentration in orogenic gold deposits compared to aqueous ore-forming fluids and crustal rocks cannot be explained by high fluid volumes, based on microstructural analysis of alteration around gold grains. Instead, these workers propose that silica stabilized colloids stable at temperatures excessing 350 °C, and able to transport large amounts of gold, were responsible for the gold deposit formation.

AuNPs are of great interest in nanoscience research, materials science, inorganic chemistry, surface science, and medicine, for example to diagnose and treat cancer. Lohman et al. (2012) conducted solubility experiments with different ligated gold nanoparticles in several organic solvents. The authors found a strong dependence of the solubility on the type of ligand and the choice of solvent. A negative chemisorption enthalpy of -126 kJ/mole of thiol on gold surfaces was reported (Lavrich et al., 1998) indicating a strong attraction between gold and thiols. Edinger et al. (1997) found that metallic gold in ethanolic thiol solutions is corroded, with the thiol acting as the active oxidant. This effect is strongly reduced when using hexane as a solvent, also confirming a solvent dependence and a preference of gold building complexes with polarizable ligands. In the same process the corrosion and dissolution of gold ceases due to self-assembled monolayers (SAM) forming at the gold surface (Figure 1-1) leading to a passivation of the formerly reactive interface (Zamborini and Crooks, 1998). The organothiols build up the SAM by bonding with the AuNP *via* a Au-S bond (Figure 1-1) with the unreactive end pointing away from the AuNP (Daniel

and Astruc, 2004). The formation of self-assembled monolayers on AuNPs allows influence on the properties and size of the AuNPs (Häkkinen, 2012; Alex and Tiwari, 2015). Organothiols (R-SH; Figure 1-1) are commonly used to form these SAM *via* the addition of a reductant to a gold(III) solution (see Daniel and Astruc, 2004, and references therein for syntheses). With increasing temperatures (20°C to 60°C) the SAM will be rearranged (Heath et al., 1997) until oxidation of the thiols in the SAM occurs at 100°C, when in contact with air (Delamarche et al., 1994).

On the basis of the above, it may be that AuNPs are stabilized in natural hydrocarbon liquids by thiols. Thiol-Au NP complexes could provide a highly effective hydrocarbon phase gold transport, due to the potentially higher gold concentrations transported in the form of AuNPs compared to covalently bonded single gold atoms and ligands.

1.1.4 Experimental data on metals in oil and aqueous fluids

To date, only a few experimental studies on the solubility of metals in organic compounds have been performed. These studies suggest that gold may be dissolved and transported in organic liquids, even when aqueous fluid is present. Miedaner et al. (2005) conducted solubility experiments of mercury in organic liquids and found that 821 ppm, 647 ppm and 280 ppm of Hg is soluble in octane, dodecane and toluene at 200°C, respectively. As the gold-mercury deposits of the Californian coast ranges are often associated with organic matter (e. g. Liu et al., 1993a; Sherlock, 2005), these experimental results not only suggest that organic matter may be very important for Hg mobilization, but also for Au mobilization.

Au solubility studies show that 2 to 3 ppb Au are soluble in crude oil at 100°C, and up to 18 ppb of Au at 200°C (Williams-Jones and Migdisov, 2007). Further experiments conducted by (Fuchs et al., 2011) showed that a maximum of 39 ppb to 48 ppb of Au is soluble in crude oil at 250°C, and that the solubility is significantly lower at higher and lower temperatures. Furthermore, their experiments indicated a gold solubility dependence on the molecular structure of the oil, as the solubility decreases in refined oil fractions. The potential of crude oils to mobilize and concentrate Au was shown by the experiments conducted Migdisov et al. (2017) with maximum Au solubility's of up to 50 ppb Au at 250 °C, which is enough for crude oils to be considered as ore fluids.

Emsbo et al. (2009) conducted mixing experiments between brine solutions spiked with 8 to 10 ppm of gold and other metals and crude oil. The metals, except for vanadium, were almost entirely partitioned into the oil phase. Liu et al. (1993b) and (Zhuang et al., 1999) performed portioning experiments between gold doped aqueous solutions and crude oils, resulting in a Au transfer from the aqueous solution to the oil of 98% and 99%, respectively.

In contrast, there is plenty of data available on the solubility, transport mechanisms, and speciation of Au in hydrothermal aqueous ore fluids (e.g., Henley, 1973; Seward, 1973; Renders and Seward, 1989; Shenberger and Barnes, 1989; Hayashi and Ohmoto, 1991; Seward, 1993; Gammons and Williams-Jones, 1995; Benning and Seward, 1996; Gammons et al., 1997; Murphy and LaGrange, 1998; Murphy et al., 2000; Stefánsson and Seward, 2004; Tagirov et al., 2005; Pokrovski et al., 2009a; Pokrovski et al., 2009b; Pokrovski et al., 2014; Seward et al., 2014; Mei et al., 2017). Under hydrothermal conditions Au is transported by building complexes with hydrogen sulfide ligands in acidic to neutral aqueous fluids ≤350 °C, and to a lesser degree gold chloride complexes (Pokrovski et al., 2009a; Pokrovski et al., 2009b; Liu et al., 2014). There is a big range of Au solubility in hydrothermal aqueous fluids/liquids depending mainly on composition and temperature.

Considering the extensive research on hydrothermal aqueous liquids compared to the amount of research on organic liquids, it is interesting to consider if research has been somewhat one-sided, leading to biased conclusions on the role of organic matter during hydrothermal ore-deposit formation.

1.2 Objectives

(1) To provide new data on the ability or non-ability of organic liquids to transport gold. To do this, a primary aim of this PhD project was to develop a method for Au partition experiments between aqueous fluids and oil that allows *in-situ* sampling of the oil and the aqueous fluid at the specific temperature. This method was then used to perform gold partition experiments to generate Au partition coefficients between a brine solution (10wt% NaCl) and 1-dodecanethiol ($CH_3(CH_2)_{10}CH_2SH$; DDT) and *n*-dodecane ($CH_3(CH_2)_{10}CH_3$; DD). Results from this work are presented in Chapters 2 and 3.

(2) To identify the speciation of Au in organic and co-existing aqueous fluids, and to interpret the results in the context of possible Au transport by organic liquids, and, if applicable, the precipitation and deposition of Au. To accomplish this objective, X-ray absorption spectroscopy (XAS) was performed at the European Synchrotron Facility (ESRF) to constrain the oxidation state and host complexes for Au bonded in oils (DD and DDT) and co-existing aqueous fluids. The results from this work are presented in Chapter 4.

(3) To study the role of organic material in the formation of a natural ore deposit. Samples from the Au-Hg McLaughlin mine, Geysers/Clear Lake area, California, USA, were studied to investigate the close spatial relationship of Au mineralization and the abundant hydrocarbon material with the objective of better understanding the role of hydrocarbons in the Au-Hg McLaughlin deposit. The results from this work are presented in Chapter 5.

1.3 Significance

Due to the lack of experimental data on ore-metals such as gold and their solubility and partitioning behavior between organic and aqueous fluids, it is difficult to satisfactorily determine the role of organic matter in the formation process of ore deposits, in spite of the common association between organic matter, gold and other ore metals. Considering that field studies on ore deposits are focused on the end product of the formation process, it becomes even more important to conduct experiments to study the dynamic processes before ore deposition. Data on the partitioning of gold between organic and aqueous liquids is required to further understand ore deposit formation processes, since the two liquids or fluids can be present in the same ore systems.

A better understanding of the links between organic matter and ore deposits is not only crucial for research, but also for the exploration, mining and mineral industry, where the lack of discovering new mining targets has a costly impact on the industry. This study can lead to a better understanding of deposit characteristics and therefore to new exploration indicators, that are of high value for the minerals and mining industry.

An understanding of the partitioning processes of gold between aqueous and organic liquids may also be significant for the oil and gas industry as well, by enhancing oil refining processes, and additionally by increasing the understanding of oils as a possible metal source.

References

Alex, S. and Tiwari, A. (2015) Functionalized gold nanoparticles: synthesis, properties and applications—a review. *J. Nanosci. Nanotechnol.* **15**, 1869-1894.

Ansar, S.M., Perera, G.S., Jiang, D., Holler, R.A. and Zhang, D. (2013) Organothiols self-assembled onto gold: evidence for deprotonation of the sulfur-bound hydrogen and charge transfer from thiolate. *J. Phys. Chem. C* **117**, 8793-8798.

Benning, L.G. and Seward, T.M. (1996) Hydrosulphide complexing of Au (I) in hydrothermal solutions from 150–400 C and 500–1500 bar. *Geochim. Cosmochim. Acta* **60**, 1849-1871.

Berger, B.R. and Bagby, W.C. (1993) The geology and origin of Carlin-type gold deposits, in: Foster, R.P. (Ed.), Gold Metallogeny and Exploration. Springer Netherlands, pp. 210-248.Cotton, F.A. and Wilkinson, G. (1988) Advanced inorganic chemistry. Wiley New York.

Daniel, M.-C. and Astruc, D. (2004) Gold nanoparticles: assembly, supramolecular chemistry, quantum-size-related properties, and applications toward biology, catalysis, and nanotechnology. *Chem. Rev.* **104**, 293-346.

Delamarche, E.a.a., Michel, B., Kang, H. and Gerber, C. (1994) Thermal stability of self-assembled monolayers. *Langmuir* **10**, 4103-4108.

Edinger, K., Grunze, M. and Wöll, C. (1997) Corrosion of gold by alkane thiols. *Phys. Chem. Chem. Phys.* **101**, 1811-1815.

Elder, R.C. and Eidsness, M.K. (1987) Synchrotron X-ray studies of metal-based drugs and metabolites. *Chem. Rev.* **87**, 1027-1046.

Ellsworth, H. V. (1928). (I) Thuchohte, a remarkable primary carbon mineral from the vicinity of Parry Sound, Ontario.(II) Cyrtolite intergrowth associated with the Parry Sound thucholite. *American Mineralogist: Journal of Earth and Planetary Materials*, *13*(8), 419-441.

Emsbo, P. and Koenig, A.E. (2007) Transport of Au in petroleum: Evidence from the northern Carlin trend, Nevada, in: al., C.J.A.e. (Ed.), *Mineral Eploration and Research: Digging Deeper*. Proc. 9th Biennial SGA Meeting, Millpress, Dublin, pp. 695-698.

Emsbo, P., Williams-Jones, A.E., Koenig, A.E. and Wilson, S.A. (2009) Petroleum as an Agent of Metal Transport: Metallogenic and Exploration Implications, in: Williams, P.J. (Ed.), In, P.J. Williams (ed.) *Smart Science for Exploration and Mining*. Proc. 10th Biennial SGA Meeting, James Cook Univ. Earth & Enviro. Studies, pp. 99-101.

Etschmann, B., Brugger, J., Fairbrother, L., Grosse, C., Nies, D., Martinez-Criado, G. and Reith, F. (2016) Applying the Midas touch: Differing toxicity of mobile gold and platinum complexes drives biomineralization in the bacterium Cupriavidus metallidurans. *Chem. Geol.* **438**, 103-111.

Fairbrother, L., Shapter, J., Brugger, J., Southam, G., Pring, A. and Reith, F. (2009) Effect of the cyanide-producing bacterium Chromobacterium violaceum on ultraflat Au surfaces. *Chem. Geol.* **265**, 313-320.

Filby, R.H. (1994) Origin and nature of trace element species in crude oils, bitumens and kerogens: implications for correlation and other geochemical studies. *Geol. Soc. Spec. Publ.* **78**, 203-219.

Frondel, C. (1938) Stability of colloidal gold under hydrothermal conditions. *Econ. Geol.* **33**, 1-20.

Fuchs, S., Migdisov, A. and Williams-Jones, A.E. (2011) The transport of gold in petroleum: An experimental study, Goldschmidt. *Mineral Mag.*, Prague, Czech Republic, p. 871.

Fuchs, S., Schumann, D., Williams-Jones, A.E. and Vali, H. (2015) The growth and concentration of uranium and titanium minerals in hydrocarbons of the Carbon Leader Reef, Witwatersrand Supergroup, South Africa. *Chem. Geol.* **393-394**, 55-66.

Fuchs, S., Williams-Jones, A.E., Jackson, S.E. and Przybylowicz, W.J. (2016) Metal distribution in pyrobitumen of the Carbon Leader Reef, Witwatersrand Supergroup, South Africa: Evidence for liquid hydrocarbon ore fluids. *Chem. Geol.* **426**, 45-59.

Gammons, C.H. and Williams-Jones, A. (1995) The solubility of Au Ag alloy+ AgCl in HCl/NaCl solutions at 300° C: New data on the stability of Au (1) chloride complexes in hydrothermal fluids. *Geochim. Cosmochim. Acta* **59**, 3453-3468.

Gammons, C.H., Yu, Y. and Williams-Jones, A. (1997) The disproportionation of gold (I) chloride complexes at 25 to 200 C. *Geochim. Cosmochim. Acta* **61**, 1971-1983.

Giordano, T. (2000) Organic matter as a transport agent in ore-forming systems. *Rev. Econ. Geol.* **9**, 133-155.

Giordano, T.H., Kettler, R.M. and Wood, S.A. (2000) Ore genesis and exploration: the roles of organic matter. Society of Economic Geologists.

Giże, A. (2000) The organic geochemistry of gold, platinum, uranium and mercury deposits. *Rev. Econ. Geol.: Ore Genesisis and Exploration: The Roles of Organic Matter*, 217-250.

Giże, A. and Barnes, H. (1989) Organic processes in Mississippi Valley-type ore genesis, 28th International Geological Congress Abstracts, pp. 557-558.

Giże, A.P. (1999) A special issue on organic matter and ore deposits: Interactions, applications, and case studies - Introduction. *Econ. Geol. and the Bull. Soc. of Economic Geologists* **94**, 963-965.

Giże, A.P., Kuehn, C., Furlong, K. and Gaunt, J. (2000) Organic maturation modeling applied to ore genesis and exploration. *Rev. Econ. Geol.* **9**, 87-104.

Glikson, M. and Mastalerz, M. (2000) Organic matter and mineralisation: thermal alteration, hydrocarbon generation and role in metallogenesis. Springer Science & Business Media.

Granger, H.C. (1966) Analytical data on samples collected at Ambrosia Lake, New Mexico, 1958 through 1962. US Geological Survey], 1966.

Groves, D.I., Goldfarb, R.J. and Santosh, M. (2016) The conjunction of factors that lead to formation of giant gold provinces and deposits in non-arc settings. *Geosc. Frontiers* **7**, 303-314.

Gu, X.X., Zhang, Y.M., Li, B.H., Dong, S.Y., Xue, C.J. and Fu, S.H. (2012) Hydrocarbon- and ore-bearing basinal fluids: a possible link between gold mineralization and hydrocarbon accumulation in the Youjiang basin, South China. *Miner. Deposita* **47**, 663-682.

Häkkinen, H. (2012) The gold-sulfur interface at the nanoscale. *Nature chemistry* **4**, 443-455.

Hausen, D.M. and Park, W.C. (1986) Observations on the association of gold mineralization with organic matter in Carlin-type ores. *Organics and ore deposits, Proceedings: Denver Region Exploration Geologists Society*, 119-136.

Hayashi, K.-i. and Ohmoto, H. (1991) Solubility of gold in NaCl-and H2S-bearing aqueous solutions at 250–350°C. *Geochim. Cosmochim. Acta* **55**, 2111-2126.

Heath, J.R., Knobler, C.M. and Leff, D.V. (1997) Pressure/temperature phase diagrams and superlattices of organically functionalized metal nanocrystal monolayers: the influence of particle size, size distribution, and surface passivant. *J. Phys. Chem. B* **101**, 189-197.

Henley, R.W. (1973) Solubility of gold in hydrothermal chloride solutions. *Chem. Geol.* **11**, 73-87.

Hennet, R.J.C., Crerar, D.A. and Schwartz, J. (1988) Organic complexes in hydrothermal systems. *Econ. Geol.* **83**, 742-764.

Hough, R., Butt, C. and Buhner, J. (2009) The mineralogy, crystallography and metallography of gold. *Elements* **5**, 297-302.

Hough, R., Noble, R., Hitchen, G., Hart, R., Reddy, S., Saunders, M., Clode, P., Vaughan, D., Lowe, J. and Gray, D. (2008) Naturally occurring gold nanoparticles and nanoplates. *Geology* **36**, 571-574.

Hough, R., Noble, R. and Reich, M. (2011) Natural gold nanoparticles. *Ore Geol. Rev.* **42**, 55-61.

Hulen, J.B. and Collister, J.W. (1999) The oil-bearing, carlin-type gold deposits of Yankee Basin, Alligator Ridge District, Nevada. *Econ. Geol.* **94**, 1029-1049.

Jain, P.K., Huang, X., El-Sayed, I.H. and El-Sayed, M.A. (2007) Review of some interesting surface plasmon resonance-enhanced properties of noble metal nanoparticles and their applications to biosystems. *Plasmonics* **2**, 107-118.

Kesler, S., Jones, H., Furman, F., Sassen, R., Anderson, W. and Kyle, J. (1994) Role of crude oil in the genesis of Mississippi Valley-type deposits: Evidence from the Cincinnati arch. *Geology* **22**, 609-612.

Kucha, H. (1981) Precious metal alloys and organic matter in the Zechstein copper deposits, Poland. *Mineral. Petrol.* **28**, 1-16.

Kucha, H. and Przylowicz, W. (1999) Noble metals in organic matter and clay-organic matrices, Kupferschiefer, Poland. *Econ. Geol.* **94**, 1137-1162.

Kuehn, C.A. (1989) Studies of disseminated gold deposits near Carlin, Nevada: Evidence for a deep geologic setting of ore formation.

Landais, P. (1996) Organic geochemistry of sedimentary uranium ore deposits. *Ore Geol. Rev.* **11**, 33-51.

Langmuir, D. (1979) Techniques of estimating thermodynamic properties for some aqueous complexes of geochemical interest.

Large, R.R., Bull, S.W. and Maslennikov, V.V. (2011) A Carbonaceous Sedimentary Source-Rock Model for Carlin-Type and Orogenic Gold Deposits. *Econ. Geol.* **106**, 331-358.

Larocque, A.C., Stimac, J.A., Siebe, C., Greengrass, K., Chapman, R. and Mejia, S.R. (2008) Deposition of a high-sulfidation Au assemblage from a magmatic volatile phase, Volcán Popocatépetl, Mexico. *Journal of Volcanology and Geothermal Research* **170**, 51-60.

Lavrich, D.J., Wetterer, S.M., Bernasek, S.L. and Scoles, G. (1998) Physisorption and chemisorption of alkanethiols and alkyl sulfides on Au (111). *J. Phys. Chem. B* **102**, 3456-3465.

Leventhal, J. (1980) Organic geochemistry and uranium in Grants mineral belt. *Mem.-NM Bur. Mines Miner. Resour.;(United States)* **38**.

Leventhal, J. and Giordano, T. (2000) The nature and roles of organic matter associated with ores and ore-forming systems: An introduction. *Rev. Econ. Geol* **9**, 1-26.

Leventhal, J.S., Daws, T.A. and Frye, J.S. (1986) Organic geochemical analysis of sedimentary organic matter associated with uranium. *Appl. Geochem.* **1**, 241-247.

Leventhal, J.S. and Threlkeld, C.N. (1978) Carbon-13/carbon-12 isotope fractionation of organic matter associated with uranium ores induced by alpha irradiation. *Science* **202**, 430-432.

Liu, D., Fu, J. and Jia, R. (1993a) Bitumen and dispersed organic matter related to mineralization in stratabound deposits, South China, Bitumens in Ore Deposits. Springer, pp. 171-177.

Liu, J., Fu, J. and Lu, J. (1993b) Experimental study on interaction between organic matter and gold. *'Sci. Geol. Sin.' In Chinese.* **28**, 246-253.

Liu, W., Etschmann, B., Testemale, D., Hazemann, J.-L., Rempel, K., Müller, H. and Brugger, J. (2014) Gold transport in hydrothermal fluids: Competition among the Cl^-, Br^-, HS^- and NH_3(aq) ligands. *Chem. Geol.* **376**, 11-19.

Lohman, B.C., Powell, J.A., Cingarapu, S., Aakeroy, C.B., Chakrabarti, A., Klabunde, K.J., Law, B.M. and Sorensen, C.M. (2012) Solubility of gold nanoparticles as a function of ligand shell and alkane solvent. *Phys. Chem. Chem. Phys.* **14**, 6509-6513.

Manning, D.A. and Giże, A.P. (1993) The role of organic matter in ore transport processes, Org. Geochem. Springer, pp. 547-563.

Mastalerz, M., Bustin, R., Sinclair, A., Stankiewicz, B. and Thomson, M. (2000) Implications of hydrocarbons in gold-bearing epithermal systems: Selected examples from the Canadian Cordillera, Organic Matter and Mineralisation: Thermal Alteration, Hydrocarbon Generation and Role in Metallogenesis. Springer, pp. 359-377.

Meeker, K.A., Chuan, R.L., Kyle, P.R. and Palais, J.M. (1991) Emission of elemental gold particles from Mount Erebus, Ross Island, Antarctica. *Geophysical Research Letters* **18**, 1405-1408.

Mei, Y., Liu, W., Brugger, J., Migdisov, A.A. and Williams-Jones, A.E. (2017) Hydration Is the Key for Gold Transport in CO2–HCl–H2O Vapor. *ACS Earth and Space Chemistry*.

Miedaner, M.M., Migdisov, A.A. and Williams-Jones, A.E. (2005) Solubility of metallic mercury in octane, dodecane and toluene at temperatures between 100 degrees C and 200 degrees C. *Geochim. Cosmochim. Acta* **69**, 5511-5516.

Migdisov, A., Guo, X., Williams-Jones, A., Sun, C., Vasyukova, O., Sugiyama, I., Fuchs, S., Pearce, K. and Roback, R. (2017) Hydrocarbons as ore fluids. *Geochem. Persp. Lett.* **5**, 47-52.

Mirasol-Robert, A., Grotheer, H., Bourdet, J., Suvorova, A., Grice, K., McCuaig, T.C. and Greenwood, P.F. (2017) Evidence and origin of different types of sedimentary organic matter from a Paleoproterozoic orogenic Au deposit. *Precambrian Research* **299**, 319-338.

Molnár, F., Oduro, H., Cook, N.D., Pohjolainen, E., Takács, Á., O'Brien, H., Pakkanen, L., Johanson, B. and Wirth, R. (2016) Association of gold with uraninite and pyrobitumen in the metavolcanic rock hosted hydrothermal Au-U mineralisation at Rompas, Peräpohja Schist Belt, northern Finland. *Miner. Deposita*, 1-22.

Murphy, P. and LaGrange, M. (1998) Raman spectroscopy of gold chloro-hydroxy speciation in fluids at ambient temperature and pressure: a re-evaluation of the effects of pH and chloride concentration. *Geochim. Cosmochim. Acta* **62**, 3515-3526.

Murphy, P.J., Stevens, G. and LaGrange, M.S. (2000) The effects of temperature and pressure on gold-chloride speciation in hydrothermal fluids: A Raman spectroscopic study. *Geochim. Cosmochim. Acta* **64**, 479-494.

Osterloh, F., Hiramatsu, H., Porter, R. and Guo, T. (2004) Alkanethiol-induced structural rearrangements in silica-gold core-shell-type nanoparticle clusters: An opportunity for chemical sensor engineering. *Langmuir* **20**, 5553-5558.

Palenik, C.S., Utsunomiya, S., Reich, M., Kesler, S.E., Wang, L. and Ewing, R.C. (2004) "Invisible „gold revealed: Direct imaging of gold nanoparticles in a Carlin-type deposit. *Am. Mineral.* **89**, 1359-1366.

Parnell, J. (1988) Metal Enrichments in Solid Bitumens - a Review. *Miner. Deposita* **23**, 191-199.

Parnell, J., Kucha, H. and Landais, P. (1993) Bitumens in ore deposits. Springer Science & Business Media.

Pearce, M.A., Gazley, M.F., Fisher, L.A., Hough, R., Saunders, M. and Kong, C. (2016) Nanoparticles and Gold Deposit Formation, Goldschmidt, Yokohama, Japan, p. 2455.

Pearcy, E. and Burruss, R. (1993) Hydrocarbons and gold mineralization in the hot-spring deposit at Cherry Hill, California, Bitumens in Ore Deposits. Springer, pp. 117-137.

Pearson, R.G. (1968) Hard and soft acids and bases, HSAB, part 1: Fundamental principles. *J. chem. Educ* **45**, 581.

Pokrovski, G.S., Akinfiev, N.N., Borisova, A.Y., Zotov, A.V. and Kouzmanov, K. (2014) Gold speciation and transport in geological fluids: insights from experiments and physical-chemical modelling. *Geol. Soc. Spec. Publ.* **402(1)**, 9-70.

Pokrovski, G.S., Tagirov, B.R., Schott, J., Bazarkina, E.F., Hazermann, J.L. and Proux, O. (2009a) An in situ X-ray absorption spectroscopy study of gold-chloride complexing in hydrothermal fluids. *Chem. Geol.* **259**, 17-29.

Pokrovski, G.S., Tagirov, B.R., Schott, J., Hazemann, J.L. and Proux, O. (2009b) A new view on gold speciation in sulfur-bearing hydrothermal fluids from in situ X-ray absorption spectroscopy and quantum-chemical modeling. *Geochim. Cosmochim. Acta* **73**, 5406-5427.

Radtke, A.S. (1981) Geology of the Carlin gold deposit, Nevada, Open-File Report, - ed.

Radtke, A.S. and Scheiner, B.J. (1970) Studies of hydrothermal gold deposition - (pt.) 1, carlin gold deposit, nevada, the role of carbonaceous materials in gold deposition. *Econ. Geol.* **65**, 87-102.

Reich, M., Kesler, S.E., Utsunomiya, S., Palenik, C.S., Chryssoulis, S.L. and Ewing, R.C. (2005) Solubility of gold in arsenian pyrite. *Geochim. Cosmochim. Acta* **69**, 2781-2796.

Reith, F. and Cornelis, G. (2017) Effect of soil properties on gold-and platinum nanoparticle mobility. *Chem. Geol.* **466**, 446-453.

Reith, F., Fairbrother, L., Nolze, G., Wilhelmi, O., Clode, P.L., Gregg, A., Parsons, J.E., Wakelin, S.A., Pring, A. and Hough, R. (2010) Nanoparticle factories: Biofilms hold the key to gold dispersion and nugget formation. *Geology* **38**, 843-846.

Renders, P. and Seward, T. (1989) The stability of hydrosulphido-and sulphido-complexes of Au (I) and Ag (I) at 25 C. *Geochim. Cosmochim. Acta* **53**, 245-253.

Samedova, F., Guseinova, B., Kuliev, A. and Alieva, F. (2009) Trace elements in crude oil from some new South Caspian oil fields. *Petroleum Chemistry* **49**, 288-291.

Sardar, R., Funston, A.M., Mulvaney, P. and Murray, R.W. (2009) Gold nanoparticles: past, present, and future. *Langmuir* **25**, 13840-13851.

Saunders, J.A. (1990) Colloidal transport of gold and silica in epithermal precious-metal systems: Evidence from the Sleeper deposit, Nevada. *Geology* **18**, 757-760.

Sawlowicz, Z., Gize, A. and Rospondek, M. (2000) Organic matter from Zechstein copper deposits (Kupferschiefer) in Poland, Organic Matter and Mineralisation: Thermal Alteration, Hydrocarbon Generation and Role in Metallogenesis. Springer, pp. 220-242.

Saxby, J. D. (1973). Diagenesis of metal-organic complexes in sediments: formation of metal sulphides from cystine complexes. Chemical Geology, 12(4), 241-248.

Seward, T. (1993) The hydrothermal geochemistry of gold, Gold metallogeny and exploration. Springer, pp. 37-62.

Seward, T., Williams-Jones, A. and Migdisov, A. (2014) 13.2 The Chemistry of Metal Transport and Deposition by Ore-Forming Hydrothermal Fluids. *Treatise on Geochemistry (Second Edition), Elsevier, Oxford*, 29-57.

Seward, T.M. (1973) Thio complexes of gold and the transport of gold in hydrothermal ore solutions. *Geochim. Cosmochim. Acta* **37**, 379-399.

Shenberger, D.M. and Barnes, H.L. (1989) Solubility of gold in aqueous sulfide solutions from 150 to 350°C. *Geochim. Cosmochim. Acta* **53**, 269-278.

Sherlock, R. (1992) The empirical relationship between gold-mercury mineralization and hydrocarbons, in the northern Coast Ranges, California, GAC-MAC Joint Annual Meeting, Program with Abstracts.

Sherlock, R. (2000) The association of gold—mercury mineralization and hydrocarbons in the coast ranges of northern California, Organic Matter and Mineralisation: Thermal Alteration, Hydrocarbon Generation and Role in Metallogenesis. Springer, pp. 378-399.

Sherlock, R.L. (2005) The relationship between the McLaughlin gold-mercury deposit and active hydrothermal systems in the Geysers-Clear Lake area, northern Coast Ranges, California. *Ore Geol. Rev.* **26**, 349-382.

Simmons, S.F. and Brown, K.L. (2007) The flux of gold and related metals through a volcanic arc, Taupo Volcanic Zone, New Zealand. *Geology* **35**, 1099-1102.

Simon, G., Huang, H., Penner-Hahn, J.E., Kesler, S.E. and Kao, L.-S. (1999) Oxidation state of gold and arsenic in gold-bearing arsenian pyrite. *Am. Mineral.* **84**, 1071-1079.

Spirakis, C.S. (1996) The roles of organic matter in the formation of uranium deposits in sedimentary rocks. *Ore Geol. Rev.* **11**, 53-69.

Stankus, D.P., Lohse, S.E., Hutchison, J.E. and Nason, J.A. (2010) Interactions between natural organic matter and gold nanoparticles stabilized with different organic capping agents. *Environ. Sci. Technol.* **45**, 3238-3244.

Stefánsson, A. and Seward, T. (2004) Gold (I) complexing in aqueous sulphide solutions to 500 C at 500 bar. *Geochim. Cosmochim. Acta* **68**, 4121-4143.

Ta, C., Reith, F., Brugger, J.l., Pring, A. and Lenehan, C.E. (2014) Analysis of gold (I/III)-complexes by HPLC-ICP-MS demonstrates gold (III) stability in surface waters. *Environ. Sci. Technol.* **48**, 5737-5744.

Tagirov, B.R., Salvi, S., Schott, J. and Baranova, N.N. (2005) Experimental study of gold-hydrosulphide complexing in aqueous solutions at 350–500°C, 500 and 1000 bars using mineral buffers. *Geochim. Cosmochim. Acta* **69**, 2119-2132.

Taran, Y.A., Bernard, A., Gavilanes, J.-C. and Africano, F. (2000) Native gold in mineral precipitates from high-temperature volcanic gases of Colima volcano, Mexico. *Appl. Geochem.* **15**, 337-346.

Vlassopoulos, D., Wood, S.A. and Mucci, A. (1990) Gold speciation in natural waters: II. The importance of organic complexing—Experiments with some simple model ligands. *Geochim. Cosmochim. Acta* **54**, 1575-1586.

Vorapalawut, N., Pohl, P., Bouyssiere, B., Shiowatana, J. and Lobinski, R. (2011) Multielement analysis of petroleum samples by laser ablation double focusing sector field inductively coupled plasma mass spectrometry (LA-ICP MS). *J. Anal. At. Spectrom.* **26**, 618-622.

Warren, H.V. and Delavault, R.E. (1950) Gold and silver content of some trees and horsetails in British Columbia. *Geological Society of America Bulletin* **61**, 123-128.

Williams-Jones, A. and Migdisov, A. (2007) The solubility of gold in crude oil: implications for ore genesis, Proceedings of the 9th Biennal SGA Meeting, Millpress, Dublin, pp. 765-768.

Wood, S. (1996) The role of humic substances in the transport and fixation of metals of economic interest (Au, Pt, Pd, U, V). *Ore Geol. Rev.* **11**, 1-31.

Wood, S. (2000) Organic matter: supergene enrichment and dispersion. *Ore Genesis and Exploration: The Roles of organic matter. Reviews in Economic Geology* **9**, 157-192.

Zamborini, F.P. and Crooks, R.M. (1998) Corrosion passivation of gold by n-alkanethiol self-assembled monolayers: effect of chain length and end group. *Langmuir* **14**, 3279-3286.

Zammit, C.M., Weiland, F., Brugger, J., Wade, B., Winderbaum, L.J., Nies, D.H., Southam, G., Hoffmann, P. and Reith, F. (2016) Proteomic responses to gold (III)-toxicity in the bacterium Cupriavidus metallidurans CH34. *Metallomics* **8**, 1204-1216.

Zhuang, H.P., Lu, J.L., Fu, J.M., Ren, C.G. and Zou, D.G. (1999) Crude oil as carrier of gold: petrological and geochemical evidence from Lannigou gold deposit in southwestern Guizhou, China. *Sci. China Ser. D* **42**, 216-224.

Copyright statement

Chapter 2

An experimental method for gold partitioning between two immiscible fluids: brine and *n*-dodecane

Lars-S. Crede, Kirsten U. Rempel, Si-Yu Hu, Katy A. Evans

A modified version of this chapter was published with Chemical Geology (https://doi.org/10.1016/j.chemgeo.2018.09.034)

Abstract

Organic matter can be found in many different types of ore deposits, but its role in ore-forming processes is not yet fully understood. Here, we present an experimental method that can be used to determine the partition coefficient ($D_{Au}^{org/aq}$: partition coefficient of Au between an hydrocarbon and an aqueous fluid*)* of gold between two immiscible liquids, and thus whether liquid hydrocarbon fluids such as petroleum can act as ore fluids and transport gold or other metals of interest. To investigate liquid hydrocarbons in the presence of an aqueous liquid doped with gold, we modified the HFS-340Z hydrothermal flow system (Coretest Systems, Inc.) to enable sampling at hydrothermal *P-T* conditions (≤ 150 °C and ~5 bar) of each of two density-stratified immiscible liquids. A saline aqueous solution (10 wt% NaCl) was doped with gold and heated with *n*-dodecane ($CH_3(CH_2)_{10}CH_3$) to 105 °C and 150 °C. Each brine sample was directly followed by an organic sample until three samples of each liquid were taken. Aqua regia was added to the brine samples to stabilize the gold before ICP-MS analyses. Each organic sample was digested chemically with a mixture of ultra-pure nitric acid and hydrogen peroxide to generate carbon free solutions prior to ICP-MS analysis. This procedure generates reproducible partition coefficients for gold, or presumably any other metal, between hydrocarbon and aqueous liquids, if passivation procedures of the HFS-340Z hydrothermal flow system are strictly followed and error sources are monitored rigorously. The preferred $D_{Au}^{org/aq}$ between *n*-dodecane and the brine is 0.05 ± 0.04.

2.1 Introduction

Organic matter is a common constituent of various types of ore deposits, such as Carlin-type Au and epithermal Ag-Au-(Hg) deposits (e.g., Hofstra et al., 1991; Bowell et al., 1999; Zhuang et al., 1999; Sherlock, 2000; Emsbo and Koenig, 2007), Mississippi Valley-type Pb-Zn deposits (e.g., Parnell, 1988), or sediment hosted uranium deposits (e.g., Landais, 1996; Spirakis, 1996; Fuchs et al., 2015; Fuchs et al., 2016), and is often interpreted as a reducing agent involved in deposition of metals from hydrothermal ore fluids (Giże, 1999; Giże, 2000). However, experiments (Liu et al., 1993; Lu and Zhuang, 1996; Miedaner et al., 2005) and analyses of crude oils and petroleum in gold deposits (e.g., Zhuang et al., 1999; Emsbo and Koenig, 2007) suggest that organic fluids such as petroleum may also act to dissolve and transport metals, a critical factor not considered in most current ore deposit models. Further confirmation or repudiation of this 'missing link' in our understanding of ore-forming processes is not possible due to an almost complete absence of experimental data on metal-organic fluid interactions.

Gold partitioning experiments by Liu et al. (1993) at 25 °C using crude oil and an aqueous solution containing 500 ppm gold resulted in a transfer of 98% of the gold to the oil. Similarly, 99% of the gold was transferred into the oil phase in thermal simulation experiments at 150 °C in a coexisting system of crude oil, brine and rock (Zhuang et al., 1999). Few studies of this type are available in the peer-reviewed literature, but the following experimental results have been recorded in conference proceedings. In contrast to partition experiments and the thermal simulation experiment, solubility experiments indicate much lower gold concentrations with 2 to 3 ppb gold in crude oil at 100 °C, and up to 18 ppb of gold at 200 °C (Williams-Jones and Migdisov, 2007). Other work documented that 39–48 ppb gold can be present in crude oil at 250 °C, and that the solubility is significantly lower at temperatures higher and lower than 250 °C (Fuchs et al., 2011). In mixing experiments between crude oil and brine solutions spiked with 8 to 10 ppm of gold, palladium, platinum, or vanadium, the metals, except for V, were almost entirely partitioned into the oil phase at concentrations ranging between 50 ppm and 100 ppm (Emsbo et al., 2009).

In this study, we present a method for gold partitioning experiments between two density-stratified immiscible liquids -- an aqueous brine and a one-component oil consisting of *n*-dodecane (Figure 2-1). The alkane *n*-dodecane is not representative of natural oils. In

fact, it has no functional groups to form metal organic complexes (e.g., Giordano, 2000), and is therefore not expected to complex significantly with Au. However, the physical characteristics such as melting point, boiling point, and stability under a broad range of redox and temperature conditions are suitable for the purposes of the study, and there are a number of structurally related compounds that do bear functional groups with the potential to complex Au, such as 1-dodecanethiol. The alkane *n*-dodecane therefore is optimal for method development purposes and to demonstrate the feasibility of gold partition experiments between aqueous and oil based fluids.

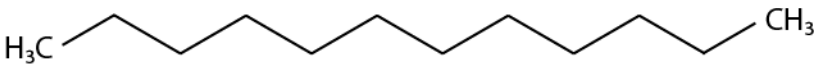

Figure 2-1: 2D structure of n-dodecane

The experimental set-up is similar to those used for aqueous vapor-liquid fractionation experiments (Pokrovski et al., 2008; Rempel et al., 2012), with the addition of *in-situ* sampling of each liquid at hydrothermal *P-T* conditions, ≤ 150 °C and ~5 bar for this study. Temperatures were chosen to be in the liquid oil window (<160 °C), but to allow high enough pressures for sampling from the top (section 2) 105 °C were chosen over 100 °C. In addition to presenting the method, we will comment on problems encountered during the method development. Furthermore, the methodology can also be used to conduct partition experiments with other elements and metals than gold, and with immiscible liquids of more complex compositions to generate fundamental data for geological processes in the upper earth crust.

2.2 Methodology

Here, the final method is described. Preliminary experiments performed during method development are described in section 3. The advantage of the HFS-340Z hydrothermal flow system chosen for the experiments is that samples can be taken simultaneously from the top and from the bottom. In-situ sampling gives the advantage that several samples can be taken from one experiment over time. The titanium vessel enables reusability and is inert in contact with most chemicals. A disadvantage is the time consuming experiment preparation and the time consuming cleaning process.

2.2.1 Equipment

The partitioning experiments were conducted in an adapted HFS-340Z hydrothermal flow system purchased from Coretest Systems, Inc. (Figure 2-2) that was used as a closed system. The system comprises a flexible titanium sampling cell loaded with the immiscible liquids, which are contained within a stainless steel pressure vessel partially filled with a low viscosity liquid (H_2O) that applies a confining pressure to the titanium sampling cell. For simplification, the cell will be referred to as the Ti-cell. Note that the Ti-cell is not flexible at the chosen pressure and temperature conditions (more details in section 2.2). The Ti-cell has a volume of 410 ml, which was reduced to 225 ml by inserting Teflon rods to reduce the volume of chemicals needed per experiment. The pressure vessel and Ti-cell are installed within a vertical tube furnace. All components in contact with the experimental liquids are made of commercially pure Grade 2 Ti alloy passivated with nitric acid (at ~100 °C for 24h) to create a surface coating of inert TiO_2. The aqueous liquid used for our experiments was a brine (125 ml, 10wt% NaCl) with a density of ~1.06 g/ml at 25 °C that was doped with 1 to 25 ppm gold ($[Au^{III}Cl_4]^-$), while the *n*-dodecane (40-50 ml, $CH_3(CH_2)_{10}CH_3$) is less dense, with a density of 0.749 g/ml at 25 °C. Au was added in the form of a 1000 ppm Au plasma standard solution (10wt% $HCl_{(aq)}$). Sampling lines at the top and bottom of the Ti-cell allow for simultaneous sampling of the two density-stratified immiscible liquids. The upper sampling line extends down to the center of the Ti-cell, past the air in the headspace, and into the organic liquid layer, if filled with the appropriate proportions (ca. 125 ml aqueous liquid *versus* 40 ml to 50 ml of organic liquid). The length of this sampling line (extended tube) can be varied during the set-up to the desired length. In our case, the extended tube reaches ~16 cm, to the center of the Ti-cell. The sampling lines on the Ti-cell lead to two valves with fittings to sample directly into a sample container, a PP (polypropylene) vial for the aqueous samples and a titanium autoclave (Ti grade 2) for the organic samples. Attached to the valves are 1 cm long clear PVC (polyvinyl chloride) tubes to allow for visual examination of the sampled liquid. Using a two-way valve, the top line is also connected to a pressure transducer to record the pressure inside the Ti-cell. Titanium frit filters (10 µm pore size) can be integrated into both sampling lines to filter out undissolved particles (Figure 2-2). We tested the set-up with and without the titanium frits and omitted the titanium frits in our final setup for reasons discussed below.

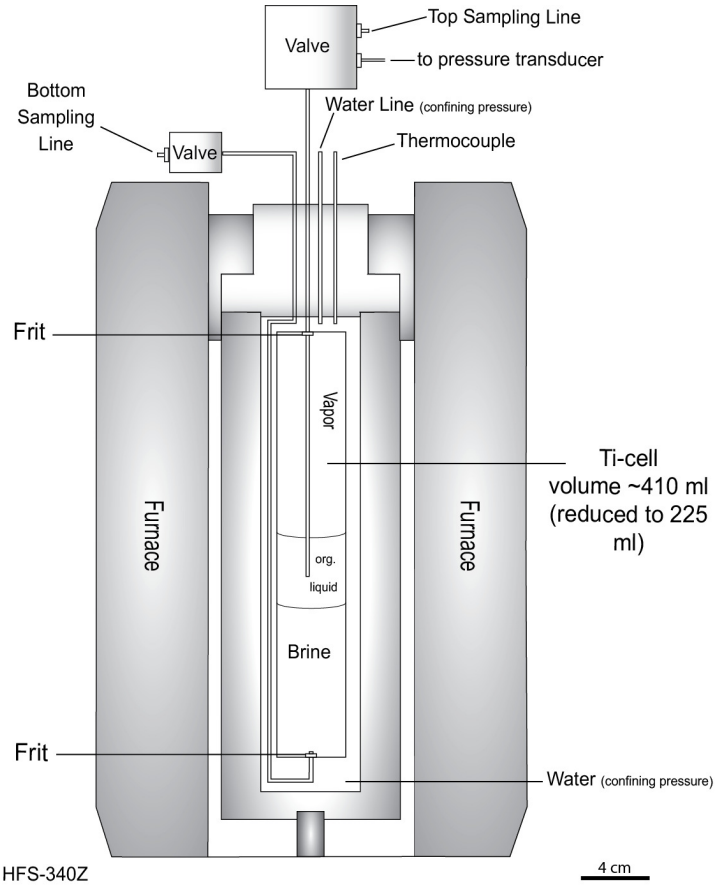

Figure 2-2: Schematic diagram of the HFS-340Z hydrothermal flow system, Coretest Systems, Inc. The volume of the titanium cell was reduced to 225 ml by inserting Teflon rods.

2.2.2 Materials and experimental strategy

A schematic chart of the experimental procedure is given in Figure 2-3. Diluted ultra-pure NaOH and HCl were used to modify the pH of the aqueous brine to the desired value (pH_{Start}) prior to loading. The remaining atmosphere (air) in the headspace above the liquids was 40 to 50 ml. The atmosphere was not flushed due to the reducing conditions of the experiment (see section 2.5.5). The confining pressure was set to 5 bar for all experiments. However, the flexible Ti-cell is rigid enough to withstand this relatively low confining pressure, so the pressure in the Ti-cell, as measured by the pressure transducer, is controlled by the temperature and salinity of the brine and is constrained to saturated water vapour pressure for the 10 wt% brine. Following loading, the Ti-cell was heated slowly to the desired temperature, taking ~12 h to reach 105 °C and ~15 h to reach 150 °C (halite + water + vapor liquid; Driesner and Heinrich, 2007). A temperature of 105 °C was needed to generate enough pressure to sample from the top-line. A further consideration in specification of a temperature range was the need to generate conditions within the liquid oil window i.e. less than 160°C. The apparatus was left at the final temperature for 6 h before sampling. Before

each aqueous and organic sample pair was taken, both sampling valves were opened to release unreacted liquids contained in the tubes between the Ti-cell and the valves (~2 ml unreacted liquid per sampling line), and up to 5 ml to rinse the lines. For each experiment, three sample pairs of brine and organic liquid were taken at roughly equal pressure and the same temperature, with each brine sample directly followed by one of organic liquid. The subsequent fluid volume loss resulted in a pressure decrease of up to 0.5 bar between sampling events. Samples were directly released into the vial (brine) and the titanium autoclave (*n*-dodecane), and visually examined in the vial (brine) and while the liquid was released (*n*-dodecane) to recognise mixed phase samples. After each sampling event, the system was allowed some time to adapt to the new conditions. Once the pressure was stable, the next sample was taken. The temperature was not affected by the volume loss. To assess whether equilibrium conditions were reached, a time series experiment was made (PE10), with samples after 18 h and again after 42 h (section 4.3). In PE 10, the ratio of *n*-dodecane to brine was changed to 80 ml *n*-dodecane to 90 ml brine to move the brine further away from the top sampling line. The Au in HCl standard solution was added in this experiment directly into the Ti-cell after loading the brine, followed by *n*-dodecane. Directly after sampling (all experiments), the pH of the aqueous sample was determined (pH_{End}). By releasing aliquots of either liquid through the valves, the pressure during individual experiments can be decreased. Alternatively, the confining pressure and temperature can be adjusted during the experiments to modify *P-T* conditions as required, but this was not done in these experiments.

Partitioning experiments between aqueous brine (10 wt% NaCl) and *n*-dodecane were conducted at 105 °C (18 h) and 150 °C (21 h). Each experiment was repeated three to four times at the same *P-T-X* conditions to assess the repeatability of the gold partitioning results. During the sampling series, the volume of the aqueous liquid decreases more rapidly than that of organic liquid, and the volume of the air in the headspace increases with decreasing pressure. The aqueous samples were between 5 to 8 ml and the volume of the organic sample was 0.1 to 1.0 ml. The volume loss upon sampling and rinsing the sampling lines (dead liquid volume) varied a little. After each experiment, the Ti-cell, the sampling lines and valves were first rinsed several times with Milli-Q water, then with a aqua regia solution (35% HCl and 67% HNO_3, 3:1 ratio), followed by Milli-Q water again (lines and valves were rinsed by attaching a vacuum pump). This procedure was applied after each experiment. In addition we tested passivating the Ti-cell after a set of 3 to 5 experiments and after each experiment with nitric acid (20%) over 8 h at 150 °C to create a surface coating of inert TiO_2 (24 h

including heating and cooling time), and to break down remains of the *n*-dodecane in our final method. To remove any remaining nitric acid, the Ti-cell, sampling lines, and valves were rinsed several times with Milli-Q water, prior to heating the Ti-cell with 200 ml of Milli-Q to 150 °C for 8 h (24 h including heating and cooling time).

2.2.3 Sample processing

After transferring the brine samples into vials, we added 6 ml of aqua regia to stabilize the gold solution, and diluted the samples with Milli-Q water to 45 ml for ICP-MS analysis of gold. During earlier experiments, aqua regia was not added to the aqueous sample solution, resulting in a systematic reduction in gold concentrations by 30--40%.

The *n*-dodecane samples were digested in in-house made 45 ml screw top titanium autoclaves to produce carbon-free, homogeneous aqueous solutions suitable for ICP-MS analyses, using a method based on the microwave assisted digestion technique described by Wondimu et al. (2000). Their method was modified *via* addition of a Vulcan laboratory furnace and the titanium autoclaves with 45 ml volumes, and a rinsing step was added, resulting in two aqueous solutions per organic sample as described below.

For the digestion, 7.5 ml of ultra-pure HNO_3 (nitric acid, 67%) and 2.5 ml of H_2O_2 (hydrogen peroxide, 30%) were added to each of the three titanium autoclaves containing the samples. The autoclaves were sealed, heated to 100 °C for 1 h, and opened briefly to release the initial gases produced in order to reduce the pressure inside the autoclaves. The autoclaves were then heated at a rate of 5 °C/min, completing the digestion at 125 °C (24 h). Preliminary experiments revealed that the most effective ratio for digestion is a maximum of 0.5 ml oil to 7.5 ml HNO_3 and 2.5 ml H_2O_2. Note that this reaction is strongly exothermic and volumes must be limited to prevent over-pressure in the autoclaves with potentially undesirable consequences, such as deformation and breach of the autoclaves. The digestion process plays a dual role in that it also passivates the titanium autoclaves resulting in a surface coating of inert TiO_2. The volume of acids can be reduced proportionally for smaller volumes of organic liquid.

After digestion, the digested solution was set aside for analysis. The titanium autoclaves were then filled with an aqua regia solution based on ultra-pure HCl (35%) and HNO_3 (67%), and heated to 125 °C (24 h) to dissolve any residual gold and rinse the autoclave,

creating a second solution for analysis. The two solutions originating from each organic sample were diluted to 45 ml with Milli-Q water separately. After each digestion the titanium autoclaves were rinsed in Milli-Q water, cleaned in an aqua regia bath for ≥24 h, rinsed in Milli-Q water, soaked in a Milli-Q water bath (24 h), and dried in an oven at 100 °C.

All three solutions for each sample pair (two from the organic liquid, and one brine) were analyzed by ICP-MS at *LabWest Minerals Analysis Pty Ltd* in Perth using a Perkin Elmer Nexion 300 inductively coupled plasma mass spectrometer. The time period between the end of sample processing and analyses by ICP-MS in the final method stage was one to two weeks (samples 1 to 10; section 4); in the early method development stage the time period was up to three weeks. The detection limit for gold was 0.05 ppb, which is equivalent to 10 ppb to 150 ppb in the *n*-dodecane samples, depending on the mass of the sample, and 0.3 to 0.5 ppb in the brine samples. Blank digestion runs in the titanium autoclaves (no sample and gold, chemicals only) were performed after 30 and 42 digestions to monitor gold loss to the titanium autoclaves (Table 2-1). In addition to Au analyses, Cl concentrations in the organic samples were analyzed by inductively coupled plasma optical emission spectrometry (ICP-OES) in six partition experiments (PE) during the early stages of method development. The Na and Cl concentration was also analyzed in a second analysis of the samples of one partition experiment 9 months after the experiment (PE42; Table 2-2) and in the time series experiment (Table 2-3; PE 10). Au concentrations in PE 42 were also measured after this extended time period to assess any changes in gold stability in the processed samples over time. The Na and Cl concentrations were only analyzed in the first solutions of a few selected experiments, after digesting the samples with HNO_3 and H_2O_2 to allow for evaluation of Na and Cl concentrations in the *n*-dodecane samples.

The organic sample digestion creates two solutions that were analyzed separately by ICP-MS, so the absolute mass of gold in the two solutions was summed to calculate the gold concentration in the original sample. The partition coefficients for gold between the organic liquid (org) and the aqueous liquid (aq) were calculated using a mass concentration ratio:

$$D_{Au}^{org/aq} = c_{Au}^{org} / c_{Au}^{aq} \qquad \text{Eq. 2-1}$$

$D_{Au}^{org/aq}$ is the partition coefficient, c_{Au}^{org} is the gold concentration of the organic liquid, by mass, and c_{Au}^{aq} is the gold concentration of the aqueous liquid, by mass. Uncertainties in

the partition coefficients were calculated by standard error propagation, assuming the individual components of the error are uncorrelated (Table 2-3). The largest contribution to the uncertainty originates from the variation of the gold concentrations of the three samples taken per experiment. Mass balance calculations were applied to determine the gold recovery (Au_{recov}) by dividing the total gold determined from the samples by total gold loaded.

$$Au_{recov} = m^{sampled}_{Au\ total} / m^{loaded}_{Au\ total} \qquad \text{Eq. 2-2}$$

The gold recovery is a useful monitor of gold loss during the partition experiment. A scheme summarizing the experimental and sample processing steps is given in Figure 2-3.

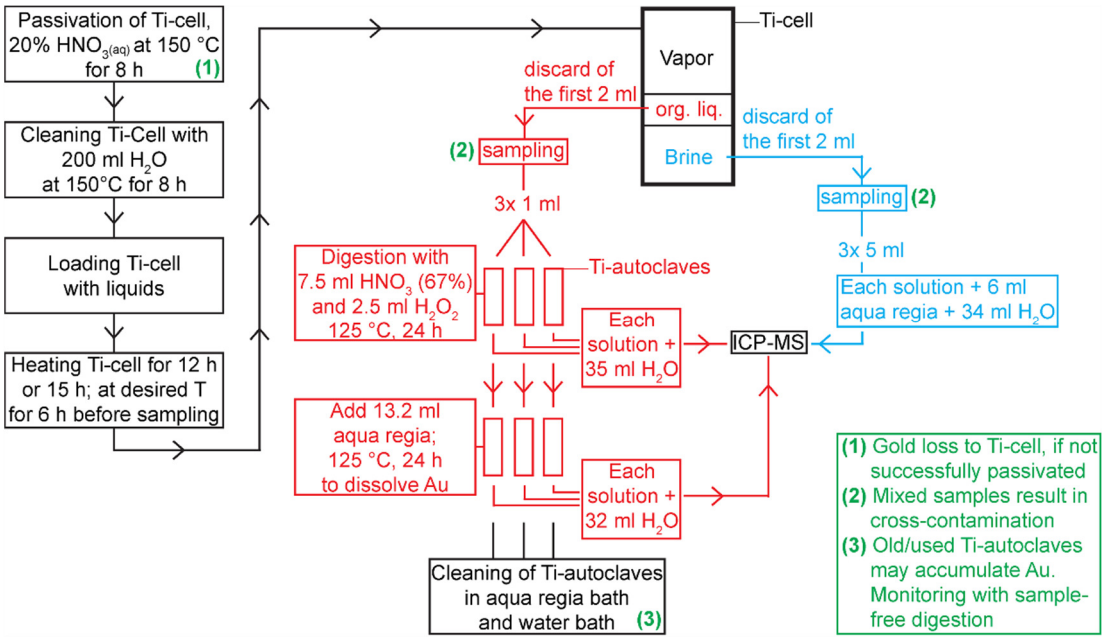

Figure 2-3: Experimental and sample processing scheme. Numbers and text in green emphasize the major difficulties that were encountered in the preliminary method development stage, which need to be carefully avoided (see section 3 and 5).

2.2.4 GC-MS

Gas Chromatography Mass Spectroscopy (GC-MS) was used to determine if *n*-dodecane breaks down during the partitioning experiments at 105 °C and 150 °C. Post run *n*-dodecane samples were rinsed through magnesium sulfate (pre-washed with *n*-hexane) to desorb water from the samples and then diluted (~100000 times) with *n*-hexane to prepare the samples for GC-MS. The sample results were compared to the GC-MS spectra of the initial, pure chemical compound (> 99%). GC-MS analyses were performed using a Hewlett

Packard 6890A gas chromatograph (GC) interfaced to a Hewlett Packard 5973 mass spectrometer (MS). The GC was fitted with a 60 m × 0.25 mm in diameter WCOT (wall coated open tubular) fused silica column coated with a 0.25 µm phenyl arylene polymer phase (DB-5MS, J&W Scientific). The GC oven was programmed from 40 °C (hold 1 minute), then heated to 320 °C at 20 °C/min with a final hold time of 15 min. Ultra-high purity helium was used as carrier gas with a constant flow of 1.1 ml/min. Sample injection was 1 µl, pulsed splitless at 310 °C. The MS was operated at 70 eV with a source temperature of 230 °C. Mass spectra were acquired in full scan mode (m/z 50-550 at 2.9 scans/sec).

2.3 Observations and results during preliminary method development

2.3.1 Method development, tests, blanks, and gold loss

Gold introduction into the brine was tested with Au(I)Cl, Au(III)Cl_3 (powder) and the gold plasma standard (final method: $HAuCl_4$ in 10wt% HCl $_{(aq)}$). The Au(I)Cl does not dissolve completely in the brine (at 25-90 °C), thus undissolved particles were added to the experiment, making it difficult to ascertain how much dissolved gold was present during the experiment. The strongly hydroscopic nature of Au(III)Cl_3 made it difficult to load an exact amount of gold. Thus, using the gold powders unnecessarily increases the uncertainty in the mass balance calculation for determining gold recovery, and the presence of Au particles presents a contamination risk for determination of dissolved Au in the samples. The gold plasma standard (1000 ppm Au in 10wt% HCl) proved to be the most efficient way to introduce gold to the brine, although the pH has to be adjusted if acidic conditions are not desired.

During testing of the experimental method we initially used gas-tight, inert syringes attached to the valves to sample the liquids. Aqua regia was rinsed through the syringes and added to the sample solution that was analyzed by ICP-MS at *LabWest Minerals Analysis Pty Ltd*. After sampling, the syringes were cleaned with aqua regia and Milli-Q water again. Even after cleaning, analysis of aqua regia rinsed through the syringes yielded gold concentrations of ~100 ppb (organic sample) and ~300 ppb (aqueous sample, Table 2-1). Thus, it is recommended to always sample directly into the final vial for the brine, and into the autoclave for the digestion of the organic liquid, rather than using contamination-prone syringes or other containers before transferring the samples into the final container.

Several types of blanks were run to investigate the possibility of gold loss or contamination throughout the sampling and digestion procedure. Aqua regia rinsed through the sampling lines (including the valves) contained up to 15 ppb gold (Table 2-1), and acidic solutions used for a blank digestion run in titanium autoclaves that had been used for 30 digestions of organic samples ranged from below the detection limit of 0.05 ppb to ~6 ppb gold (Table 2-1), calculated to represent the equivalent gold concentration in a *n*-dodecane sample of 1 ml. One blank run after 42 digestions yielded a significant gold concentration of 360 ppb indicating gold accumulation on the walls of the autoclave.

Table 2-1: C_{Au} of blank digestions, sampling lines, and syringes

Sample	C_{Au} [ppb]	Nr. of Dig.[c]
Blank 1	4	30
Blank 2	6	30
Blank 3	b. d.[d]	30
Blank 4	5	30
Blank 5	360	42
Syringe Org[a]	90	-
Syringe Aq[b]	320	-
Sampl. Lines	15	-

[a)] used for sampling dodecane
[b)] used for sampling the brine
[c)] Number of digestions in Ti-autoclaves prior to blank
[d)] below detection limit

Scanning electron microscopy (SEM) and energy dispersive X-ray spectroscopy (EDX) (Hitachi TM 3030) investigation of the two Ti sealing disks from the base of the Ti-cell (sealing the Ti-cell at the bottom, and in contact with the brine during the experiment) revealed that passivation with nitric acid every couple of experiments was only partially successful (Figure 2-4). While one disk shows no observable gold particles, the other disk shows areas that are mostly passivated and areas that are not passivated. The non-passivated areas are the host for numerous precipitated gold particles, indicating that gold precipitated from solution onto non-passivated areas of the Ti-cell walls during the experiments. The gold particles ranged in size from nm to µm scale. The larger particles appear to have formed by accumulation of many smaller particles (Figure 2-4). The accumulation of gold particles is the most likely explanation for low gold recoveries (Table 2-3). During the early method development, the Ti-cell was passivated only after sets of several experiments (3 to 5), but the frequency of passivation was increased to before each experiment in the final method to reduce the gold

loss. The proportion of gold recovered was found to correlate negatively with the number of runs since passivation of the Ti-cell (see section 4).

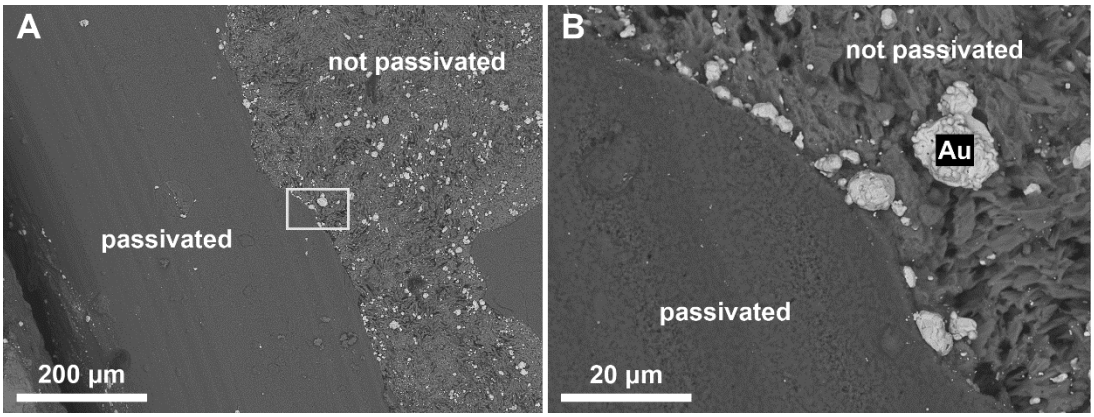

Figure 2-4: Back-scattered electron (BSE) images of passivated and not passivated surfaces of a titanium disk in contact with the brine during the partition experiment; image B shows a higher-magnification view of the area shown in A.

Gold particles accumulated on the 10 µm-pore size titanium filter frits, which filtered or absorbed even much smaller gold particles in the nm range (Figure 2-5). Loss of gold to the frits may have led to issues with erroneously low measured gold concentrations and contributed to low calculated gold recovery. Secondary electron microscopy images of the bottom titanium filter frit showed bright particles <1 µm in size, which were confirmed to be gold by EDX spectroscopy. Particles in the low nm range are not supposed to be filtered by the 10 µm pore sized titanium frit filter, yet the surface of the frit that was oriented toward the liquids was covered by the gold particles, very likely due to the same process as the gold precipitation on to the Ti-cell walls. The relative gold concentration reproducibility did not increase or decrease in a setup with or without titanium filter frits. We therefore recommend the omission of the titanium filter frits to reduce the possibility of filtering gold nanoparticles.

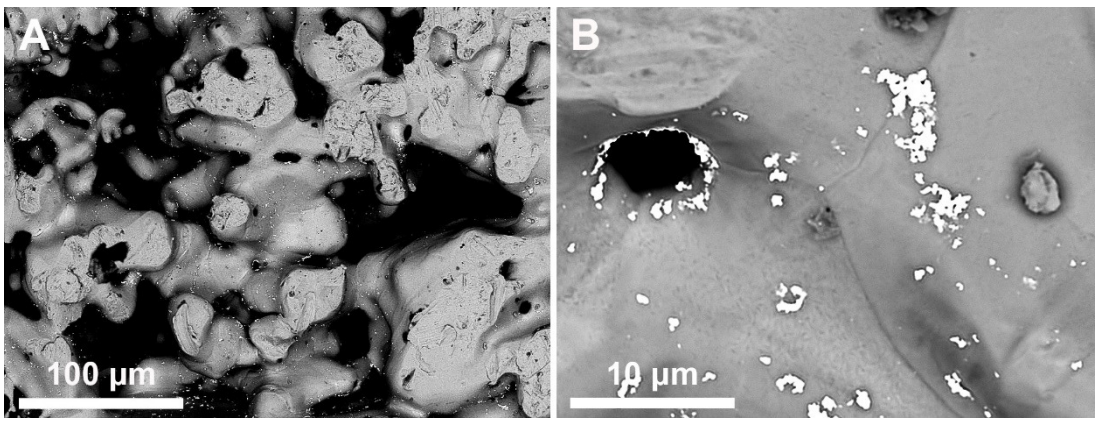

Figure 2-5: BSE images (15 keV, uncoated) of the titanium frit filters, with bright gold (nano-) particles.

2.3.2 GC-MS

The initial *n*-dodecane (170.34 g/mol) and the *n*-dodecane that has undergone contact with the 10 wt% NaCl aqueous solution at 105 °C and 150 °C show identical peaks at the same retention time at 9.45 s and the same mass spectra with the identifying peaks at the. *m/z* ratio of 170 (Figure 2-6). No other mass peaks at other retention times were observed. Thus, the GC-MS data indicates that elevated temperatures and contact with the aqueous brine have no influence on the majority of the *n*-dodecane for this temperature and pressure range. However, the large volume of *n*-hexane used to dilute the sample prior to GC-MS analysis prevents the detection of compounds with a smaller carbon number than n-hexane, compounds with concentrations significantly lower than wt% in the undiluted sample, and polar compounds that are not soluble in *n*-hexane (detection limit: ~1 wt%).

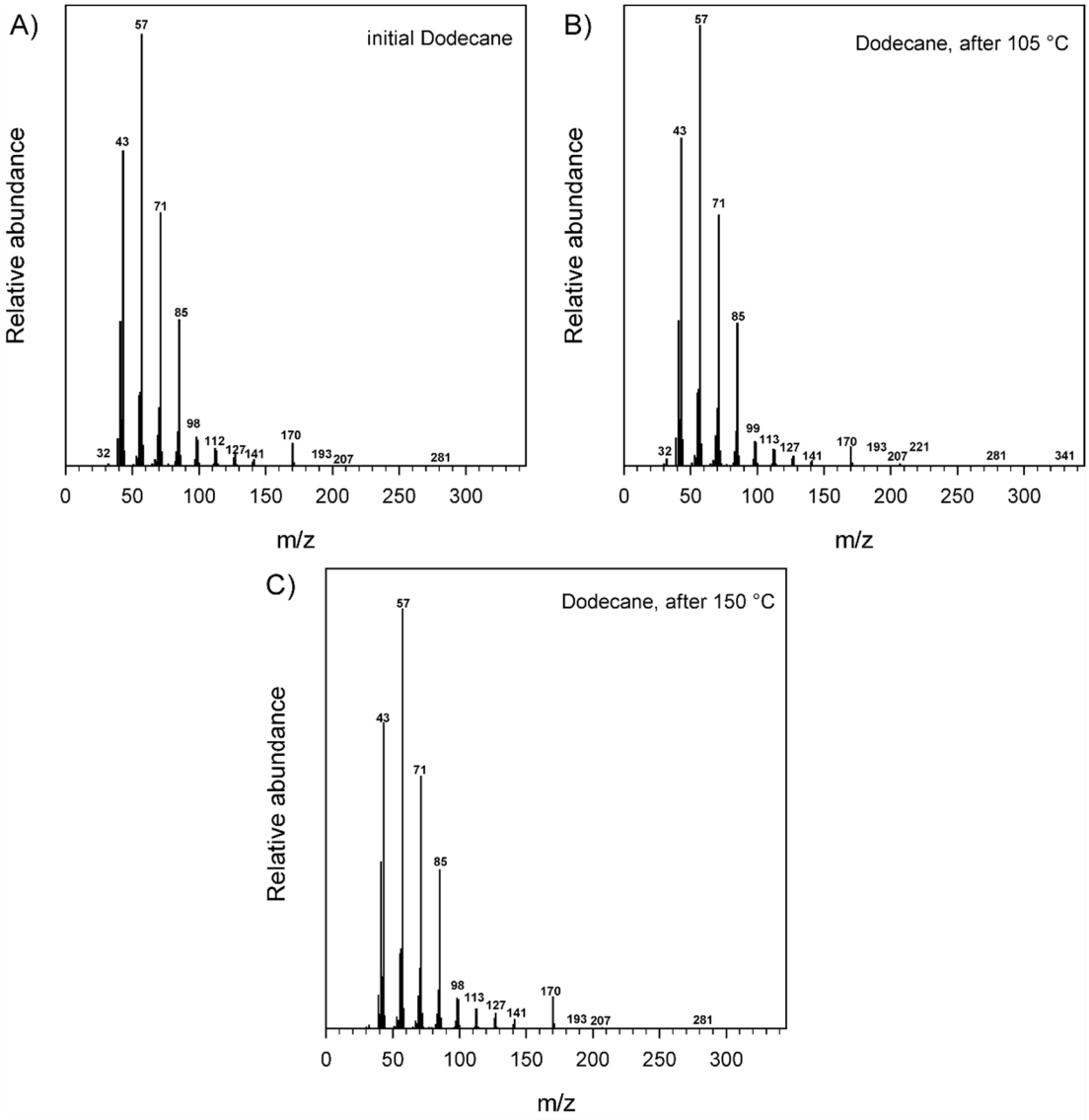

Figure 2-6: Relative abundance versus the m/z ratio of n-dodecane, and n-dodecane after a 105 °C and 150 °C experiment.

2.3.3 Gold stability over time in processed samples and Na and Cl in *n*-dodecane in preliminary experiments

To test if gold concentrations remain stable in the processed sample solutions during the time between sample processing and ICP-MS analyses, the processed sample solutions of PE X42, originally analyzed two weeks after the experiment, were re-analyzed 9 months after the experiment (Table 2-2, Figure 2-7). The results show that, after 9 months, gold concentrations in *n*-dodecane and brine are within error of the original values. The average c_{Au}^{org} of the 4 samples of PE X42 was 427 ± 172 ppb after two weeks, and 396 ± 161 ppb after

nine months -- within error the same concentration. In the brine, c_{Au}^{aq} concentrations were 42 ppb ± 3 ppb and 46 ± 1 ppb at two weeks and nine months respectively. The resulting partition coefficients are therefore within error of each other after 2 weeks and after 9 months. The average Na concentration of the 4 *n*-dodecane samples is 1460 ppm, and the average Cl concentration is 36150 ppm resulting in a Na:Cl ratio of 0.04 (Table 2-2). The expected Na:Cl ratio by mass for NaCl is 0.66.

Table 2-2: Gold concentrations of PE X42 in the 4 processed samples 2 weeks and 9 months after the experiment

	C_{Au}^{Org}	Δx^{b}	C_{Au}^{Aq}	Δx	$D^{org/aq}$	$D^{org/aq}_{mean}$	$\Delta D^{org/aq}_{mean}$	C_{Na}^{Org}	C_{Cl}^{Org}
time[a]	[ppb]	[ppb]	[ppb]	[ppb]	n = 1	n = 3	1 σ[c]	[ppm]	[ppm]
2 weeks	450	20	40	<5	11			-	-
	580	30	40	<5	15	9.7	3.5	-	-
	240	10	45	<5	5.3			-	-
	390	20	50	<5	7.8			-	-
9 months	440	20	45	<5	9.8			50	63140
	530	30	50	<5	11	8.3	3.1	2630	23770
	220	10	50	<5	4.4			690	29900
	370	20	50	<5	7.4			2450	27780

[a] time between experiment and ICP-MS analyzes

[b] analytical error (including balance, volume, and mass spectrometer uncertainties)

[c] total error by error propagation (2σ)

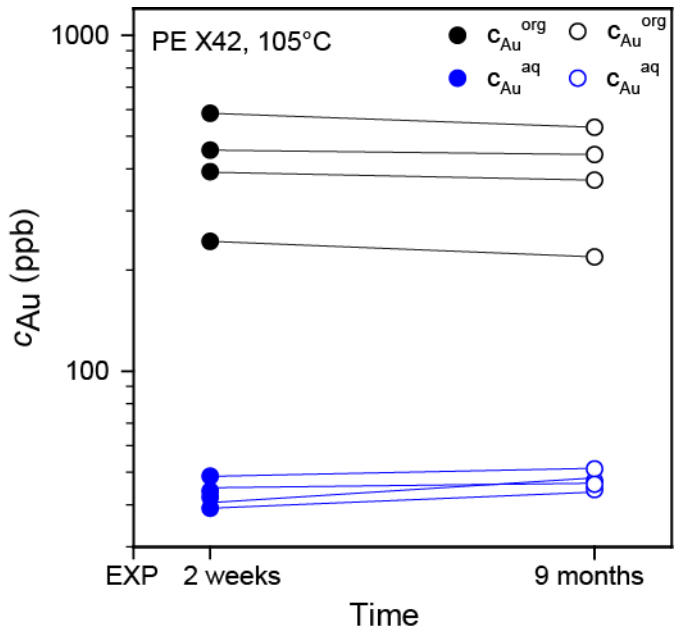

Figure 2-7: Gold concentration in processed samples, n-dodecane and brine, 2 weeks (filled symbols) and 9 months (open symbols) after the experiment (PE X42). Errors are omitted for clarity (see Table 2-2).

Cl concentrations of organic samples (X4 to X6, X42, and X20 to X22; Table 2-2 and Table 2-3) were also determined for six partition experiments during an earlier stage of the method development (Figure 2-8), and yielded up to 2700 ppm Cl in the average of three *n*-dodecane samples, and 36150 ppm in the average of the four *n*-dodecane samples of PE X42. There is no systematic correlation between Cl concentration and c_{Au}^{org} or $D_{Au}^{org/aq}$ in these preliminary experiments (Figure 2-8).

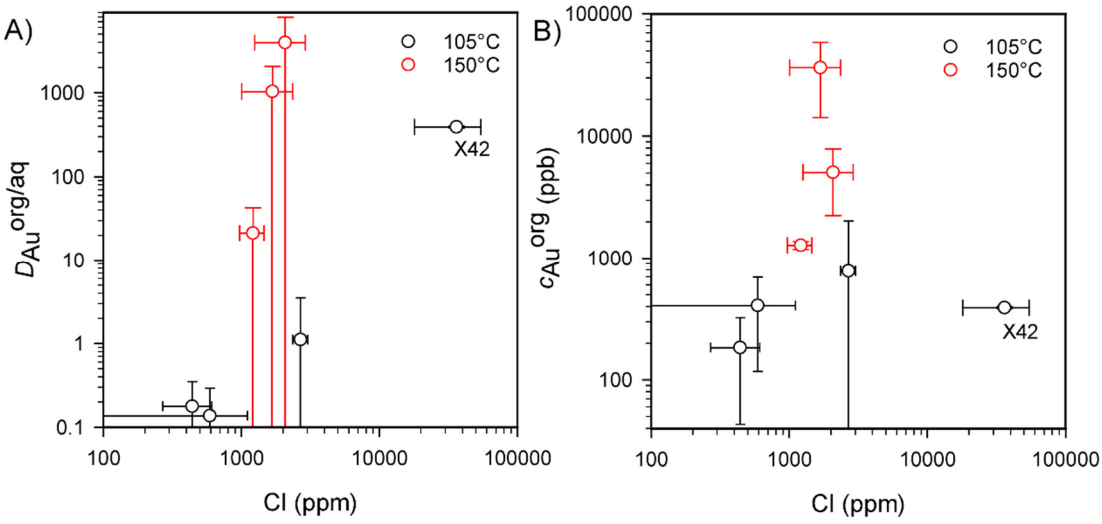

Figure 2-8: (A) Partion coefficient and Cl concentrations in n-dodecane and (B) c_{Au}^{org} and Cl concentrations in n-dodecane of X4 to X6 and X42 (105 °C) and X20 to X22 (150 °C).

2.3.4 Results of the preliminary method development stage

Partition coefficients of all partition experiments (PE) were plotted against gold recovery (Figure 2-9). Preliminary experiments discussed in the text are marked with an X (Table 2-3), where different gold sources (Au(I)Cl or Au(III)Cl_3 powder), sampling techniques, and the influence of titanium filter frits were tested. With a few exceptions, the majority of preliminary experimental results are useful only as a cautionary tale and are presented to help future researchers avoid the discussed issues. The experiments PE 1 to 10 (Table 2-3; Figure 2-9) were doped with the Au plasma standard and were conducted using the final method described in section 2 in all respects except for the regular passivation of the Ti-cell (passivated experiments are identified in the figures and in Table 2-3).

The $D_{Au}^{org/aq}$ in the brine – *n*-dodecane system is highly variable when gold recovery is low (<50%), and ranges from <1 to ~10^3 at 105°C and 150°C, while $D_{Au}^{org/aq}$ for experiments with higher gold recoveries (>50%) are reproducible and <1 (Figure 2-9). Values of $D_{Au}^{org/aq}$ on

the order of 10^3 are obtained when gold is at ppm levels in the organic liquid (e.g., X20 with 60 ppm Au in *n*-dodecane, Table 2-3) and less than 50 ppb in the brine, and coincide with several experiments in a row without passivation of the Ti-cell. Passivation of the Ti-cell before each experiment coincides with gold recoveries over 75%. The correlation between passivation, assumed to be proportional to Au recovery and $D_{Au}^{org/aq}$, is a useful diagnostic that can be monitored to recognize faulty experiments. Variation in $D_{Au}^{org/aq}$ at low Au_{recov} also suggests contamination by remains of Au bearing *n*-dodecane, brine, or aqua regia of previous experiments, when the Ti-cell was not passivated and thus cleaned again (section 5.3).

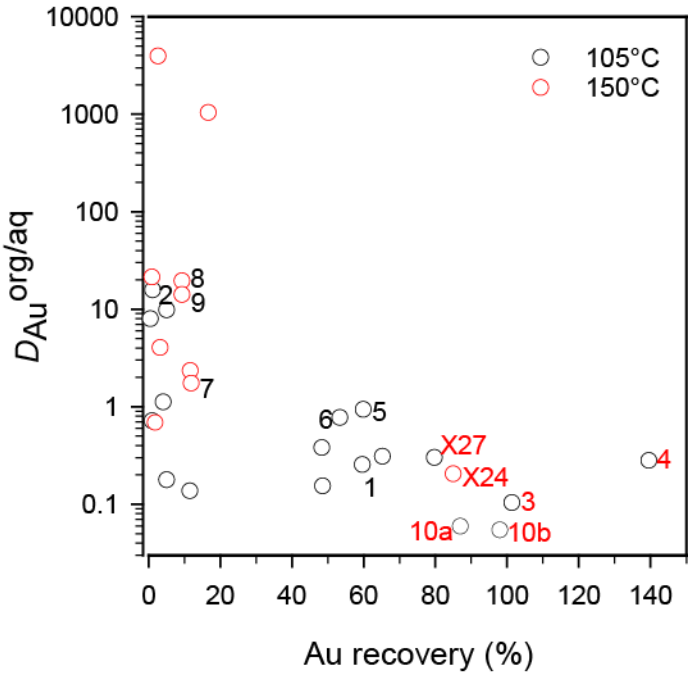

Figure 2-9: Partition coefficients versus gold recovery for all experiments conducted during the method development, independent of sampling technique, the use of titanium filter frits in the setup, or gold species used to dope the brine. Error bars are not shown to aid clarity. The numbers identify the partition experiments using the final methodology (PE, see Figure 2-10 and section 4); red numbers indicate passivation of the Ti-cell prior to the experiment. X24 and X27 were passivated, but were conducted during early stages of the method development, not using the final methodology. The other preliminary experiments are not numbered for clarity. PE 10a was sampled after 21 h and PE 10b after 48 h.

2.4 Results

2.4.1 Effects of passivation of the Ti-Cell

The partition experiments selected and numbered in Figure 2-10 and Figure 2-11 were performed using the final method, with the exception that passivation of the Ti-cell was not performed before every experiment. In these experiments, gold was added *via* the gold

plasma standard solution, titanium frits were omitted, and samples were taken by directly transferring the liquids into the vials (brine) or the titanium autoclaves (*n*-dodecane). The experiments for which the Ti-cell was passivated prior to the experiment are indicated in Table 2-3. The $D_{Au}^{org/aq}$ of the *n*-dodecane brine within the selected experiments at 105 °C and 150 °C (Table 2-3, Figure 2-10) ranges from 0.1 ± 0.02 when Au_{recov} = 100% and 16 ± 7.6 when Au_{recov} = 1%, for both temperatures. Experiments with Au_{recov} below 50% result in $D_{Au}^{org/aq}$ >1, and those with Au_{recov} above 50% result in $D_{Au}^{org/aq}$ < 1. Taking into account the variation of $D_{Au}^{org/aq}$ at low Au_{recov} in the preliminary experiments may indicate that experiments with low Au_{recov} are affected by contamination (section 5.3).

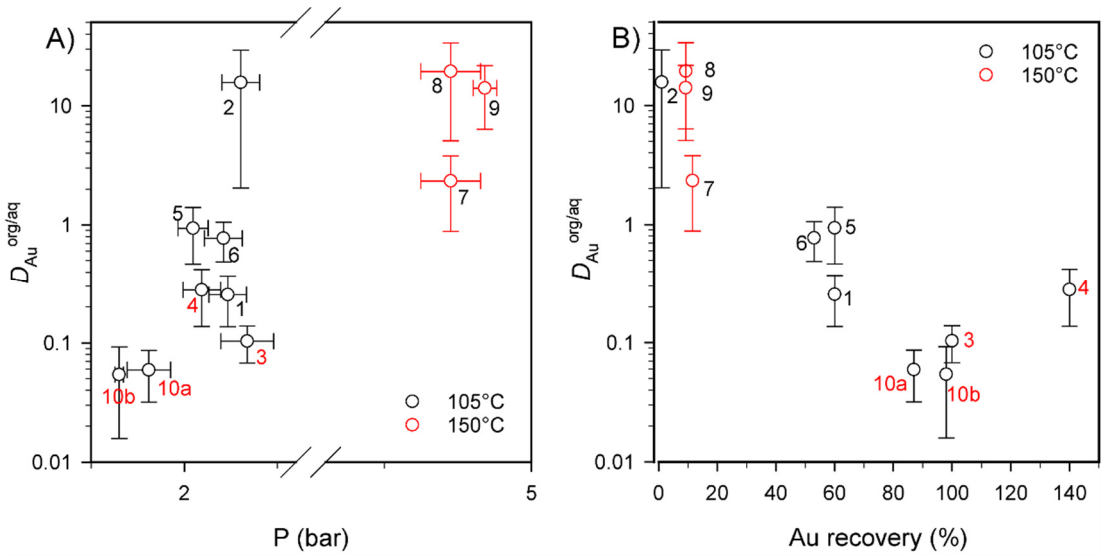

Figure 2-10: Partition coefficients versus pressure at 105 °C and 150 °C (A) and versus gold recovery (B). The numbers identify the partition experiment (PE); red numbers indicate passivation of the Ti-cell prior to the experiment. PE 10a was sampled after 18 h and 10b was sampled after 42 h (Table 2-3).

Initial Au in the brine varied from 90 µg to 3500 µg per 125 ml brine (except for PE 10 with 90 ml brine and 60 ml *n*-dodecane). The initial gold concentration does not show a statistically significant relationship with the partition coefficients (Figure 2-11). Higher initial amounts of Au result in higher concentrations in the liquids, than lower initial amounts of Au, but with no effect on the partition coefficients.

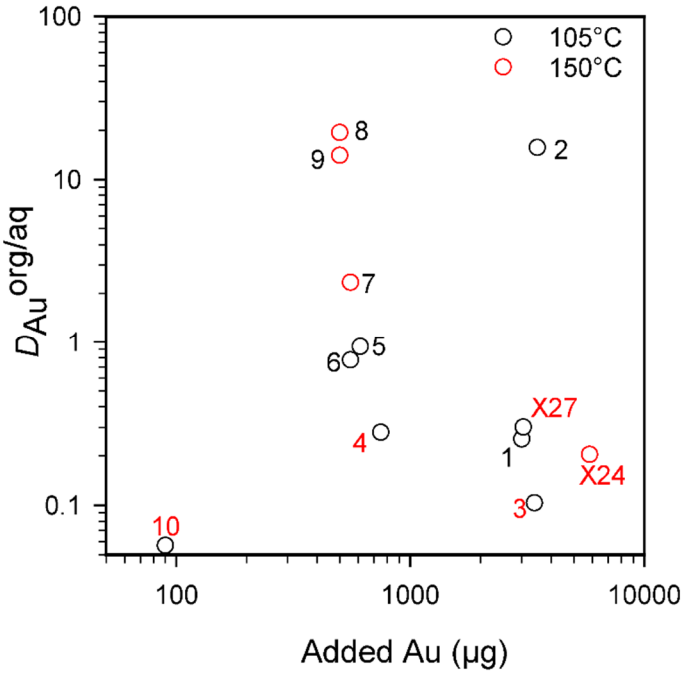

Figure 2-11: Partition coefficients versus the overall added gold of PE 1 to 10 and X24 and X27. PE 10 displays the average partition coefficient of the samples after 18 h and after 42 h. Red numbers identify successful passivation of the Ti-cell.

2.4.2 Effects of temperature, pressure and pH

All PE with $D_{Au}^{org/aq}$ < 1 were conducted at 105 °C, and three of the four experiments with $D_{Au}^{org/aq}$ > 1 were conducted at 150°C (PE 2, 7-9, Au_{recov} max. 12%), which at first sight suggests an increase $D_{Au}^{org/aq}$ of with temperature. However, $D_{Au}^{org/aq}$ increases with decreasing Au_{recov} at 105 °C and at 150 °C, and the majority of low Au_{recov} experiments took place at 150 °C (Figure 2-10 b). It is therefore possible that the apparent temperature dependence is related to Au_{recov} or contamination of *n*-dodecane rather than temperature.

There is no detectable correlation between pressure, and $D_{Au}^{org/aq}$ at these low *P-T* conditions (105 °C to 150 °C, ≤ 5 bar), though the scatter in the data caused by variable gold recovery could obscure a correlation. We tested different pH_{Start} for the brine, ranging from 1.5 to 10.0, and found that regardless of pH_{Start} the pH_{End} ranges from 2.4 to 3.7 with the majority of experiments between a *pH* of 2.4 and 2.9. It was, therefore, not possible to determine the influence of the *pH* on $D_{Au}^{org/aq}$ because experiments with the same pH_{Start} have variable $D_{Au}^{org/aq}$ due to the different gold recoveries, and because all experiments ended in a similar *pH* range of 2.4 to 2.9 with one outlier of 3.7, and the very low *pH* of PE 10. Reasons for the low *pH* in PE 10 are discussed in section 5.2.

2.4.3 Time series: Results after 18 h and after 42 h in PE 10 at 105 °C

Sample 4, the first sample taken from run PE 10 after 42 h was not included in the calculations, as it has a c_{Au}^{org} of 1170 ppb, which is up to three magnitudes higher than in the other *n*-dodecane samples taken from PE 10 (Table 2-3). The high value was probably attributed to Au contamination. Lower Au values than 1170 ppb could also result from Au contamination but the consistency between the other five samples from PE10 is such that contamination is not suspected in these cases. The *n*-dodecane and brine were sampled after 18 h and 42 h and resulted in a $D_{Au}^{org/aq}$ of 0.06 ± 0.03 and of 0.05 ± 0.04 (Figure 2-12). The pH_{End} in the brine was 1.4 after 18 h, and decreased to a pH_{End} of 1.0 after 42 h. The Au_{recov} was 87% after 18 h and 98% in the samples after 42 h. $[Au^{III}Cl_4]^-$ was added in this experiment directly into the Ti-cell after loading the brine, followed by *n*-dodecane. The average Na concentration in the triplicate samples of *n*-dodecane after 21 h is 350 ppm, and the average Cl concentration is 14670 ppm (Na:Cl ratio of 0.02).

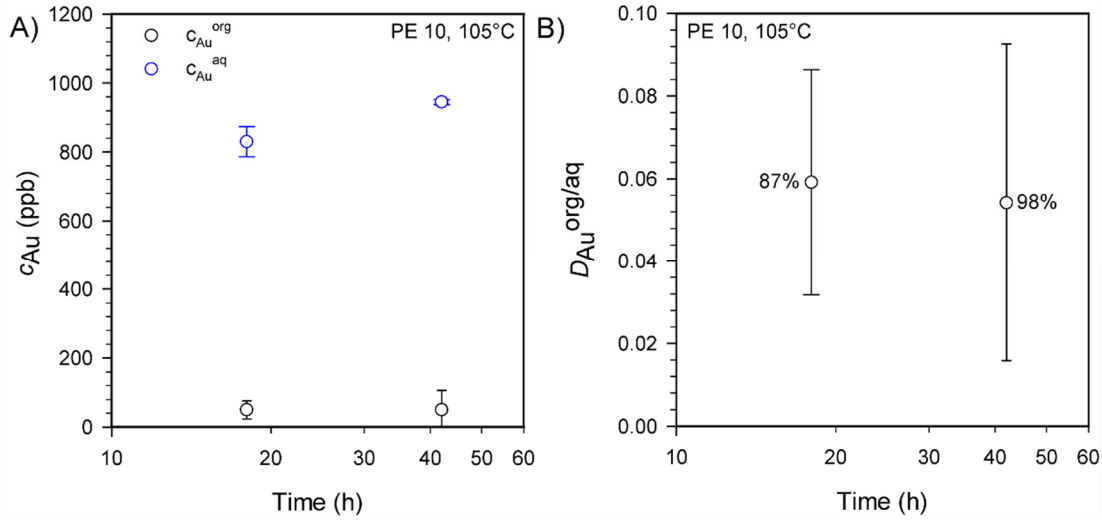

Figure 2-12: (A) Gold concentrations after 18 h and after 42 h (errors are standard deviations of c_{Au}) and (B) the corresponding partition coefficients (errors are total errors as in Table 2-3). The percentages are the Au_{recov}

Table 2-3: Partition coefficients and gold concentrations for experiments at 105 °C and 150 °C

PE[a]	T [°C]	pH_{Start}	pH_{End}	Smpl#[b]	P ± 0.1 [bar]	Au_{start}[g] [µg]	C_{Au}^{Org} [ppb]	Δx[c] [ppb]	C_{Au}^{Aq} [ppb]	Δx [ppb]	Na^{Org} [ppm]	Cl^{Org} [ppm]	$D^{org/aq}$ n=1	$D^{org/aq}_{mean}$ n=3	$\Delta D^{org/aq}_{mean}$ 2 σ[d]	Au recovery [%]	time[f] [h]
				1	2.4		4070	210	13300	690	-	-	0.3				
1	105	1.5	-	2	2.3	3000	2500	130	12590	650	-	-	0.2	0.3	0.1	60	18
				3	2.0		3030	160	11780	610	-	-	0.3				
				1	2.5		640	30	70	4	-	-	9.3				
2	105	10.0	-	2	2.3	3500	970	50	40	2	-	-	22	16	14	1	18
				3	2.1		540	30	40	2	-	-	15				
				1	2.6		2760	140	22920	1190	-	-	0.1				
3[pass]	105	7.5	-	2	2.4	3400	2670	140	24530	1280	-	-	0.1	0.1	0.04	101	18
				3	2.1		2220	120	27580	1430	-	-	0.1				
				1	2.3		2650	140	7150	370	-	-	0.4				
4[pass]	105	4.4	-	2	2.1	750	1340	70	7510	390	-	-	0.2	0.3	0.1	140	18
				3	1.9		2110	110	7390	380	-	-	0.3				
				1	2.2		1490	80	1880	100	-	-	0.8				
5	105	4.7	2.4	2	2.0	612	2130	110	2170	110	-	-	1.0	0.9	0.5	60	18
				3	1.9		2410	130	2350	120	-	-	1.0				
				1	2.4		1590	80	1830	100	-	-	0.9				
6	105	5.7	2.8	2	2.2	556	1460	80	1850	100	-	-	0.8	0.8	0.3	53	18
				3	2.0		1110	60	1690	90	-	-	0.7				
				1	4.9		820	40	300	20	-	-	2.8				
7	150	5.1	2.7	2	4.7	556	830	40	280	10	-	-	3.0	2.3	1.5	12	21
				3	4.6		350	20	280	10	-	-	1.3				

PE[a]	T [°C]	pH_{Start}	pH_{End}	Smpl#[b]	P ± 0.1 [bar]	Au_{start}[g] [µg]	C_{Au}^{Org} [ppb]	Δx[c] [ppb]	C_{Au}^{Aq} [ppb]	Δx [ppb]	Na^{Org} [ppm]	Cl^{Org} [ppm]	$D^{org/aq}$ n=1	$D^{org/aq}_{mean}$ n=3	Δ$D^{org/aq}_{mean}$ 2 σ[d]	Au recovery [%]	time[f] [h]
				1	4.9		1220	60	70	0	-	-	16				
8	150	5.1	2.9	2	4.7	500	890	50	60	0	-	-	15	19	14	9	21
				3	4.6		910	50	30	0	-	-	27				
				1	4.9		950	50	60	0	-	-	16				
9	150	5.0	3.7	2	4.8	500	1110	60	70	0	-	-	17	14	7.7	9	21
				3	4.8		790	40	90	0	-	-	9.0				
				1	2.0		20	<5	850	40	170	16300	0.02				
10[pass]	105	-	1.4	2	1.7	90.0	70	<5	860	40	350	14320	0.08	0.06	0.03	87	18
				3	1.7		60	<5	780	40	520	13380	0.08				
				4[h]	1.7		*1170*	*<5*	*930*	*50*	-	-	*1.25*				
10	105	1.4	1.0	5	1.6	90.0	90	<5	950	50	-	-	0.09	0.05	0.04	98	42
				6	1.6		10	<5	940	50	-	-	0.01				
X3[e]	105	-	-	1	-	2627	110	-	160	-	-	-	0.7	-	-	1	24
				1	2.0		260	10	2830	150	-	960	0.1				
X4	105	-	-	2	1.7	3729	220	10	3020	160	-	810	0.1	0.1	0.2	12	21
				3	1.5		740	40	3030	160	-	0	0.2				
				1	2.4		340	20	939	50	-	630	0.4				
X5	105	-	-	2	2.2	3136	70	5	1122	60	-	300	0.1	0.2	0.2	5	24
				3	1.8		140	10	1219	60	-	390	0.1				
				1	2.5		50	5	1090	60	-	2890	0.05				
X6	105	-	-	2	2.0	3730	2230	120	690	40	-	2300	3.2	1.1	2.4	4	18
				3	1.8		60	5	820	40	-	2850	0.1				

PE[a]	T [°C]	pH_{Start}	pH_{End}	Smpl#[b]	P ± 0.1 [bar]	Au_{start}[g] [µg]	C_{Au}^{Org} [ppb]	Δx[c] [ppb]	C_{Au}^{Aq} [ppb]	Δx [ppb]	Na^{Org} [ppm]	Cl^{Org} [ppm]	$D^{org/aq}$ n=1	$D^{org/aq}_{mean}$ n=3	$\Delta D^{org/aq}_{mean}$ 2 σ[d]	Au recovery [%]	time[f] [h]
				1	2.0		2710	140	15300	800	-	-	0.2				
X23	105	-	-	2	1.7	5000	2120	110	17050	890	-	-	0.1	0.2	0.1	49	19
				3	1.5		2790	150	17690	920	-	-	0.2				
				1	-		680	40	100	5	-	-	6.9				
X25	105	-	-	2	-	8475	1000	50	70	5	-	-	14	8	6.7	0.4	18
				3	-		230	10	70	5	-	-	3.0				
X27[pass]				1	2.3		5260	170	11190	580	-	-	0.5				
		-	-	2	2.0		5030	260	9270	480	-	-	0.5				
X27[pass]				3	1.8	3051	5080	260	11210	580	-	-	0.5	0.3	0.1	80	15
				Aq4	1.7		5130	270	16850	880	-	-	0.3				
				Aq5	1.7		5130	270	17040	890	-	-	0.3				
				1	2.2		6100	320	12550	650	-	-	0.5				
X28	105	-	-	2	2.1		5560	290	10500	550	-	-	0.5				
				3	1.7	4153	5650	290	12320	640	-	-	0.5	0.3	0.1	65	18
				Aq4	1.6		5770	300	17990	940	-	-	0.3				
				Aq5	1.6		5770	300	18590	970	-	-	0.3				
				1	2.5		2240	120	4300	220	-	-	0.5				
X31	105	-	-	2	2.3	1356	1360	70	4410	230	-	-	0.3	0.4	0.2	48	19.0
				3	2.0		1420	70	4680	240	-	-	0.3				
				1	2.7		450	20	40	2	-	-	11.6				18
X42	105	7.5	2.2	2	2.5	500	580	30	40	2	-	-	13.9	9.8	3.4	5	18
				3	2.3		240	10	45	2	-	-	5.5				42
				4	2.3		390	20	50	3	-	-	8.1				42

PE[a]	T [°C]	pH_{Start}	pH_{End}	Smpl#[b]	P ± 0.1 [bar]	Au_{start}[g] [µg]	C_{Au}^{Org} [ppb]	Δx[c] [ppb]	C_{Au}^{Aq} [ppb]	Δx [ppb]	Na^{Org} [ppm]	Cl^{Org} [ppm]	$D^{org/aq}$ n=1	$D^{org/aq}_{mean}$ n=3	$\Delta D^{org/aq}_{mean}$ 2 σ[d]	Au recovery [%]	time[f] [h]
				1	5.2		60820	3160	30	5	-	940	2186				
X20	150	-	-	2	4.8	8983	30910	1600	50	5	-	1840	641	1033	834	17	22
				3	4.7		17470	910	70	5	-	2250	271				
				1	3.4		8300	430	2	0	-	2920	3667				
X21	150	-	-	2	3.2	7288	3150	160	1	0	-	1270	4019	3940	5759	3	22
				3	3.0		3750	200	1	0	-	2040	4133				
				1	5.0		1390	70	70	5	-	950	19				
X22	150	-	-	2	4.7	7119	1210	60	50	5	-	1430	23	21	4.3	1	22
				3	4.4		1250	70	60	5	-	1260	21				
				1	-		12350	640	34030	1770	-	-	0.4				
$X24^{pass}$	150	-	-	2	-	5847	3390	180	33210	1730	-	-	0.1	0.2	0.2	85	21
				3	-		4830	250	32850	1710	-	-	0.1				
				1	-		470	20	344	20	-	-	1.4				
X26	150	-	-	2	-	4746	190	10	530	30	-	-	0.4	0.7	0.6	2	21
				3	-		210	10	630	30	-	-	0.3				
				1	4.6		980	50	250	10	-	-	3.9				
X29	150	-	-	2	4.5	2966	1370	70	280	20	-	-	5.0	4.0	2.8	3	21
				3	4.2		1150	60	360	20	-	-	3.2				
				1	5.5		1590	80	610	30	-	-	2.6				
X30	150	-	-	2	5.3	1525	1200	60	970	50	-	-	1.2	1.7	1.0	12	22
				3	4.8		1470	80	1090	50	-	-	1.3				

PE[a]	T [°C]	pH_{Start}	pH_{End}	Smpl#[b]	P ± 0.1 [bar]	Au_{start}[g] [µg]	C_{Au}^{Org} [ppb]	Δx[c] [ppb]	C_{Au}^{Aq} [ppb]	Δx [ppb]	Na^{Org} [ppm]	Cl^{Org} [ppm]	$D^{org/aq}$ n=1	$D^{org/aq}_{mean}$ n=3	$\Delta D^{org/aq}_{mean}$ 2 σ[d]	Au recovery [%]	time[f] [h]
[a] partition experiment																	
[b] sample number																	
[c] analytical error (including balance, volume, and mass spectrometer uncertainties)																	
[d] total error by error propagation (2σ)																	
[e] X indicates experiments of the early method development stage																	
[f] time between loading the Ti-cell and sampling. Heating to 105°C was 12 h, and 15 h to 150°C																	
[g] PE 1 to 10: Au added as $HAuHCl_4$. Variable in preliminary experiments (X): Au(I)Cl powder or $Au(III)Cl_3$ powder																	
[h] sample 4 was not included in calculations of $D^{org/aq}$, Au_{recov} and P																	
[pass] Ti-cell was passivated before the experiment for 24 h at 100 °C																	

2.5 Discussion

The final method, exemplified by experiment PE10, produces repeatable results and can therefore be used to measure the partitioning of gold, and other metals with similar characteristics, between oil and aqueous fluids, so long as a rigorous routine for passivation of the Ti-cell is applied. Partition coefficients can be used to identify the ability of fluids to transport gold or other metals. A number of processes that may have caused artefacts in the experiments were recognized during the experiment development phase. These processes shed light on the transport of gold in aqueous and organic fluids and are discussed further here.

2.5.1 Evaluation of the relationship between $D_{Au}^{org/aq}$, c_{Au}^{org} and c_{Au}^{aq} for speciation

The relationship between $D_{Au}^{org/aq}$, c_{Au}^{org} and c_{Au}^{aq} is a useful first order indication of the quality of the results. If the experiments are at equilibrium, and if speciation in the experiments is consistent, then a plot of c_{Au}^{org} *versus* c_{Au}^{aq} on a log plot, should produce a straight line with a slope of 1 (Pokrovski et al., 2002). A linear regression through the results of PE 1 to 9 (final method other than regular passivation) in a c_{Au}^{org} *versus* c_{Au}^{aq} log plot (Figure 2-13 A) has a slope of 0.21 (r^2=0.17). Given the variation in gold recovery, this indicates that the data cannot be used to extract equilibrium constants or speciation information. However, if the regression is restricted to experiments, including the preliminary experiments, with $D_{Au}^{org/aq}$ <1, then the data plot parallel to the reference line with a slope of 1 (Figure 2-13 B). This first assessment enables some confidence in the results, although, clearly, a full set of experiments performed using the final method and with regular passivation are needed. However, the high Au_{recov} and consistent Au concentrations in PE 10 lead us to believe that PE 10 produced a partition coefficient between brine and *n*-dodecane that can be treated with a high degree of confidence. Thus, it is assumed that experiments with $D_{Au}^{org/aq}$ > 0.2 were affected by contamination or processes that led to low Au_{recov}. This will be discussed further in the section 5.3.

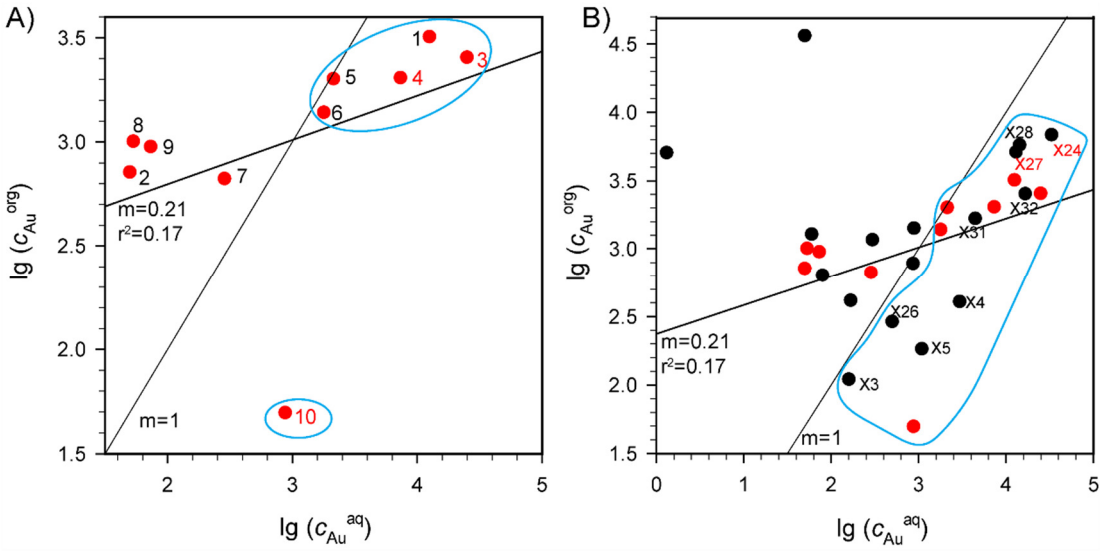

Figure 2-13: Gold concentrations (ppb) in the n-dodecane versus gold concentrations in the brine (lg=log$_{10}$) of (A) PE 1 to 10 (red) and of all (B) partition experiments. The blue areas contain the experiments with $D_{Au}^{org/aq} < 1$, while the $D_{Au}^{org/aq}$ of the experiments outside the blue areas are >1. The line with a slope of 0.21 is a linear regression line through the data of PE 1 to 10 (red). The line with a slope of 1 is given for reference. Red numbers indicate the passivated Ti-cell. Errors are not shown for clarity.

2.5.2 Equilibration

Thermodynamically valid results require that equilibrium between the organic and aqueous phases is reached prior to sampling and analysis. The heating rate of ~10 °C/h is very slow, and the apparatus was left at operating temperature for 6 h before sampling. This method step was included to facilitate equilibration of the system prior to sampling. This time should be sufficient for equilibration between the aqueous and organic fluids based on known equilibration kinetics of fluids and gases (Bischoff et al., 1986; Hovey et al., 1990; Bischoff, 1991; Pokrovski et al., 2002; Pokrovski et al., 2005). In PE 10, where samples were taken 24 h apart (Table 2-3; Figure 2-12), the average c_{Au}^{org} is effectively constant at ~50 ppb, when the outlying sample 4 is not included (section 4.3; Table 2-3). The average c_{Au}^{aq} increases by 110 ppb from 830 ± 40 to 940 ± 10 ppb. This increase coincides with an increase in Au_{recov} from 87% to 98% and is attributed to acidification of the brine from a *pH* of 1.35 to 1.00 due to the extended time available for *n*-dodecane decomposition (see section 5.2 for discussion). However, the *pH* change does not affect the $D_{Au}^{org/aq}$, which is the same average for both measurements, within error (Table 2-3).

Full equilibration of the system requires not only equilibration between gold concentrations in the brine and organic phase, but also equilibrium between *n*-dodecane, dissolved Au, the air present in the system, and the walls of the vessel. Consistent values for

$D_{Au}^{org/aq}$ obtained for PE10 after 18 h and 42 h, as discussed above, suggest that the former is achieved, but changes in *pH* observed in the same experiment, plus the Au precipitation discussed below (section 5.2.2 and 5.2.3) suggest that the latter is not. The extent to which these non-equilibrium processes could have affected the results is discussed below.

2.5.2.1 Acidification by n-dodecane decomposition

Time dependent, and therefore non-equilibrium, behavior is recorded by the decrease in *pH* in the brine that occurred in all experiments (Table 2-2) and it is necessary to consider the possibility that *n*-dodecane broke down to form molecules with polar functional groups, such as carboxylic acids that partitioned into the aqueous phase and caused a *pH* decrease. The *pH*-decrease in the brine is independent of the initial *pH (*Table 2-3*)*. The GC-MS data indicates that the major component in the organic sample is *n*-dodecane after the experiments, but compounds generated by decomposition could have been obscured due to the high dilution of the *n*-dodecane with *n*-hexane to allow GC-MS (detection limit is ~1 wt%). Additionally, polar compounds that transferred to the aqueous phase would not have been detected by GC-MS analysis of the organic phase, while decomposition products such as CO_2, CH_4, and CO could also be released into the gas phase without being sampled.

2.5.2.2 Gold loss

Low Au recoveries for unpassivated experiments suggest that gold loss somewhere in the system needs to be accounted for. Blank measurements and gold recoveries suggest that gold loss to the sampling lines and during the digestion process is minor when the final method is used (Table 2-1 and Table 2-3). The autoclaves used for the digestions are passivated during each digestion resulting in an inert TiO_2 surface and analyses of blank digestions in all autoclaves were below ≤ 6 ppb after 30 digestions. In the second step of the digestion process, the remaining Au is dissolved in aqua regia, and subsequently cleaned in an aqua regia bath. However, as a precautionary measure the Ti-autoclaves should be monitored with regular blank measurements and passivated with HNO_3 at 150 °C (24 h) every few experiments, or replaced after being used for a significant number of digestions.

The variable gold loss/gold recovery indicates different degrees of passivation of the Ti-cell between the experiments. This may only be an issue for Au rather than all metals, as gold is known to be sensitive to reduction during experiments at elevated temperatures

(Pokrovski et al., 2009; Liu et al., 2014). The observation of metallic gold particles in the removable parts of the Ti-cell (Figure 2-4 and Figure 2-5) indicate that dissolved gold is reduced to metallic gold at the experimental conditions in one or both phases. It was not possible to take BSE images of the vertical parts of the Ti-cell in contact with the *n*-dodecane or brine without destroying the Ti-cell. Thus, this did not allow to determine if metallic gold precipitated from the *n*-dodecane only, the brine only, or both. However, the linear correlation between the Au concentrations and the Au_{recov} plotted in Figure 2-14 indicates that Au loss is proportional to c_{Au}^{aq} and c_{Au}^{org}, and thus Au is lost from both liquids (section 5.2).

2.5.2.3 Systematics of Au precipitation

Au^0 precipitation from aqueous solutions in single phase aqueous experiments is known to be temperature dependent – for example, Murphy et al. (2000) demonstrated that the Au(III) complex $[AuCl_4]^-$ breaks down and precipitates Au^0 at temperatures above 250 °C and at low *pH*. Further, in synchrotron XAS experiments on Au in aqueous solution, metallic gold precipitation was noted at ≥ 150 °C (Pokrovski et al., 2009; Liu et al., 2014). These workers proposed that processes related to their experimental conditions, such as Au reduction by the X-ray beam and the use of a glassy carbon tube to contain samples, facilitated precipitation. Precipitation of Au(0) from Au(III) chloride in our system occurs at lower temperatures than that noted in previous investigations of aqueous solutions, somewhere between 25 ° and 150 °C.

Reduction of the Au(III) complex $[AuCl_4]^-$ to Au^0 in the partition experiments indicates that conditions were more reducing than those required for Au(III) stability, either in the solution, or at the Ti surface. Due to the reducing conditions, gold accumulates on unpassivated titanium surfaces. The gold accumulates may act further as a catalyst for Au precipitation by acting as nucleii. In contrast, after successful passivation most of the gold stays in solution either dissolved or as nanoparticles. Precipitation may be enhanced in each subsequent unpassivated experiment due to the previously-precipitated gold acting as nucleii for the gold still in solution, as indicated by decreasing gold recoveries as the time since passivation increases (PE 3 to 9, Table 2-3).

Precipitation of Au when an unpassivated Ti-surface is available suggests either (1) that Au(III) is metastable in solution relative to Au^0, and/or (2) that the Ti surface provides a local environment where Au(III) is not stable. In either case, partition coefficients should be robust

at high Au recovery, because the high Au recovery means that Au precipitation is slow compared to partitioning between the organic and aqueous phases.

Organic matter is commonly thought to act as a reducing agent in ore deposits (Gatellier and Disnar, 1989; Giże, 1999; Giże, 2000). For example, Gatellier and Disnar (1988) found that Au was reduced and precipitated in the presence of lignite in an Au chloride solution, which is in agreement with gold reduction at the relatively low temperatures of our experiments. It may be, therefore, that the organic liquid provides the reducing conditions that drives reduction of Au(III) in the brine. This is discussed further in section 5.5 below.

2.5.3 Contamination

The experimental results indicate two sources of contamination: Contamination of *n*-dodecane by the brine and contamination by remains (Au and Cl bearing *n*-dodecane, brine, or aqua regia of previous experiments) in the Ti-cell, when the Ti-cell was not passivated before the experiments, which is an additional cleaning step.

2.5.3.1 Contamination by boiling-induced mixing of the brine and *n*-dodecane

Brine and *n*-dodecane are theoretically chemically immiscible, but it is possible that traces of the brine can be found in the organic liquid and vice versa due to physical mixing. A vapor phase is generated in experiments at 105 °C and 150 °C (internal pressures of 1.9 bar to 4.9 bar; halite + water + vapor liquid). The water vapor has a lower density than *n*-dodecane, and would migrate to the top of the Ti-cell, filling the headspace (well above the position of the *n*-dodecane sampling line), so vapor-sampling is not considered to be a major source of contamination. *N*-Dodecane boils at 215 °C and was therefore not boiling during the experiments. The brine however, could be boiling in the 150 °C experiments. The brine boiling point ranges from 149.8 °C to 152.8 °C for the respective pressures ranging from 4.6 to 4.9 bar (Meranda and Furter, 1977; Driesner and Heinrich, 2007; and references therein), while the brine is always below the boiling point in the 105 °C experiments. If the brine was boiling at 150 °C mixing could have been induced between the two liquids at the phase interface by generating a turbulent boundary between the two liquids. The sampled liquids can be checked visually to avoid mixed samples, which is especially important for the oil phase, due to the top sampling inlet being closer to the phase boundary than the bottom

sampling inlet. However, the possibility of trace amounts of one component mixed into the other cannot be eliminated, and adds to the experimental uncertainty. Contamination by mixing of the phases would be expected to occur to different extents between samples, and lead to highly variable Au concentrations. In experiments where Au concentrations were consistent between samples, contamination by mixing was assumed not to have occurred.

2.5.3.2 *N*-dodecane contamination by brine

The ~2000 ppm Cl in the *n*-dodecane samples from experiments X4 to X6 and X20 to X22, and the 36150 ppm Cl in X42 may indicate that Cl may have entered the *n*-dodecane as contamination, by droplets of brine mixed into the *n*-dodecane samples. However, the low Na concentration (Na:Cl ratio = 0.04 by weight in PE 42 and 0.02 in PE 10) suggests that simple NaCl contamination is not the only cause of the high values, because contamination with either solid salt or brine droplets would be expected to produce a Na:Cl ratio of 0.66 by weight, and a molar Na:Cl ratio of 1. A possible process to explain the low Na:Cl ratios is discussed in section 5.3.4.

The c_{Au}^{org} in the triplicate samples of PE X6, X20, and X21 varies by factors from 2 to 44, which may indicate contamination of some of the *n*-dodecane samples with Au bearing brine (second sample of X6 and the first sample of X20 and X21). The Cl concentrations vary by factors of up to 2.3 in these experiments, which also indicates a Cl^- contamination. However, Cl^- contamination does not correlate with Au contamination. Taking PE X42 as an example to calculate the possible Au contamination due to brine droplets into the *n*-dodecane samples, we assume that the brine droplet has 10 wt% NaCl. The measured average of 1460 ppm Na in PE X42 would relate to a brine droplet of ~36.7 mg in 1 ml *n*-dodecane, which is ~4.9 wt% or 3.4 vol%. It seems unlikely that such brine droplet of this size got past the visual examination unnoticed, but if it did, the 50 ppb Au in the brine of PE X42 results in an increase in c_{Au}^{org} of *n*-dodecane by 2.5 ppb. Given the experimental uncertainties and high c_{Au}^{org}, the effect of the contamination should be negligible, even for the lowest measured c_{Au}^{org}. However, $D_{Au}^{org/aq} > 1$ in the unpassivated PE 2, 7, 8, 9 indicate Au contamination of *n*-dodecane possibly by another process (Figure 2-9 and Figure 2-14). This will be discussed in the next section 5.3.3.

2.5.3.3 Contamination by remains in the Ti-cell

Another contamination source that would explain the elevated NaCl and/or Cl, and Au concentrations in *n*-dodecane are remains (Au and Cl bearing *n*-dodecane, brine, or aqua regia) from previous experiments in the Ti-cell due to insufficient cleaning. For example, the unpassivated final PE 2, 7, 8, and 9 resulted in $D_{Au}^{org/aq} > 1$ (Figure 2-9 and Figure 2-14) and Au_{recov} below 20%. On the other hand $D_{Au}^{org/aq}$ of all experiments (preliminary and final) ranges from ~0.15 to 10^3 (Figure 2-9) at Au_{recov} below 20%. This suggests that Au (and NaCl) may have accumulated in the lines leading to the high $D_{Au}^{org/aq}$ in PE 2, 7, 8, and 9, and that the reason for the high $D_{Au}^{org/aq}$ at low Au_{recov} is not the Au loss, but the lack of passivation and thus the additional cleaning of the Ti-cell. This would further indicate that $D_{Au}^{org/aq}$ would not be effected by the unpassivated surfaces of the Ti-cell, if the Ti-cell is absolutely clean. This is supported by $D_{Au}^{org/aq}$ of unpassivated preliminary experiments with low Au_{recov}, which are comparable to the $D_{Au}^{org/aq}$ of PE 10.

Cl added by brine contamination or by remains from previous experiments of these mechanisms would be expected to produce (1) inconsistent Cl contents in the triplicate samples, because the extent of contamination would vary; and (2) molar Na:Cl ratios close to 1. A possible process to explain the low Na:Cl ratios is discussed in section 5.3.4.

2.5.4 Chlorination on *n*-dodecane

Alternatively, *n*-dodecane or its decomposition products became chlorinated resulting in the measured Cl concentrations. It is unlikely that the polar Cl^- ion, which is not soluble in non-polar and saturated n-alkanes, partitioned to any extent into an organic phase consisting of pure *n*-dodecane. However, any decomposition of *n*-dodecane, and the associated decrease in *pH* in the aqueous phase would contribute to production of free radicals that could enable hydrogen atom abstraction of *n*-dodecane and consequent chlorination or di-chlorination (Shilov and Shul'pin, 1997). It has been demonstrated that chlorination reaction rates are very fast, within minutes, in photo induced reaction experiments (Ramage and Eckert, 1975) at temperatures <35 °C. Furthermore, $AuCl_4^-$ is used for photochlorination of alkanes (e.g., Shilov and Shul'pin, 1997). The photo-induced effect is necessary to produce radicals, such as ketones, to enable the hydrogen atom release which then allows alkane chlorination. In our experiments, instead of the photo-induced effect, the elevated

temperatures and longer experimental run time, and also acidic conditions may have facilitated the production of radicals (e.g., decomposition of *n*-dodecane). Thus, it must be considered if formation of alkyl halides is partially responsible for the observed Cl concentrations in the *n*-dodecane samples, especially as the Na:Cl ratio in PE X42 and PE 10 is lower than expected for the salt NaCl (Table 2-2 and Table 2-3). The molar Cl concentration in *n*-dodecane in experiment PE X42 is ~ 0.22 mole Cl per mole *n*-dodecane and ~0.012 mole Cl per mole *n*-dodecane in PE 10, while in the other preliminary experiments with ~2000 ppm Cl the mole fraction is around 0.013 mol Cl per mole *n*-dodecane. These concentrations imply a maximum chlorination of 22 %, 1.2 %, and 1.3 % of *n*-dodecane, respectively. The inconsistency in these proportions may be linked to different degrees of passivation and cleanliness of the Ti-cell, which may affect the Cl concentrations as well.

The increase in the amount of oil and decrease in the amount of brine in PE 10 compared to earlier experiments moved the brine further away from the oil-sampling line, and indeed PE 10 samples exhibit lower Na and Cl concentrations compared to PE X42. Still, the presence of Na and Cl and the low Na:Cl ratio indicates a combined effect of chlorination, small brine droplets mixed into n-dodecane, remains of previous experiments, and possibly Cl contamination in the digestion process of n-dodecane (aqua regia cleaning of titanium autoclaves). The 1 cm long PVC tube attached to the valves could account for the low Na:Cl ratios, by contamination of Cl from the tube. To avoid the issues discussed here, regular passivation and monitoring of Na^+ and Cl^- concentrations in both liquids is recommended to reduce possible contamination.

2.5.5 Statistical correlation between *c*Au and Au_{recov}

A plot of the c_{Au}^{aq} and c_{Au}^{org} normalized by the initially added Au against the Au_{recov} shows a temperature independent linear correlation of the Au concentration with the Au_{recov}, when results possibly biased by contamination are not included (Figure 2-14). The simplified criteria for contamination discussed in section 5.3 are $c_{Au}^{org} > c_{Au}^{aq}$ or $D_{Au}^{org/aq} > 1$ and would apply to the *n*-dodecane samples of PE 2, 5, 6, 7, and 9 (Figure 2-14). The correlation has to be interpreted carefully, due to variations in the experimental methods used to acquire the data and the large uncertainties. However, this correlation can be used to extrapolate c_{Au}^{aq} and c_{Au}^{org} to $Au_{recov} = 100$, as long as sufficient data are available and Au_{recov} cover enough range that the extrapolation is robust. The extrapolated c_{Au}^{aq} and c_{Au}^{org} could then be used to calculate $D_{Au}^{org/aq}$

for Au_{recov} = 100 %. Based on PE 1 to 10 and excluding results thought to be biased by contamination, the equation for c_{Au}^{aq} is (Figure 2-14)

$$c_{\mathrm{Au},100\%}^{\mathrm{aq}} = -0.4315 + 0.07349 * 100\% \quad \text{Eq. 2-3}$$

and the equation for the brine is (Figure 2-14),

$$c_{\mathrm{Au},100\%}^{\mathrm{org}} = -0.5076 + 0.02013 * 100\% \quad \text{Eq. 2-4}$$

where $c_{\mathrm{Au},\,100\%}^{\mathrm{aq}}$ and $c_{\mathrm{Au},\,100\%}^{\mathrm{org}}$ are the c_{Au}^{aq} and c_{Au}^{org} for Au_{recov} = 100 %. The $D_{Au}^{org/aq}$ derived from the $c_{\mathrm{Au},\,100\%}^{\mathrm{aq}}$ and $c_{\mathrm{Au},\,100\%}^{\mathrm{org}}$ is 0.22 ± 0.09 and is larger than the $D_{Au}^{org/aq}$ from PE 10 due to the influence of the less good experiments. Plotting c_{Au}^{aq} and c_{Au}^{org} against the Au_{recov} also highlights, if samples are possibly contaminated, for example for PE 2, 5, 6, 7, and 9, where the c_{Au}^{org} plots close to or above the regression line of c_{Au}^{aq}. Furthermore, this plot highlights that Au loss is proportional to c_{Au}^{aq} and c_{Au}^{org} and that the $D_{Au}^{org/aq}$ can be meaningful at low Au_{recov}, when no contamination occurred.

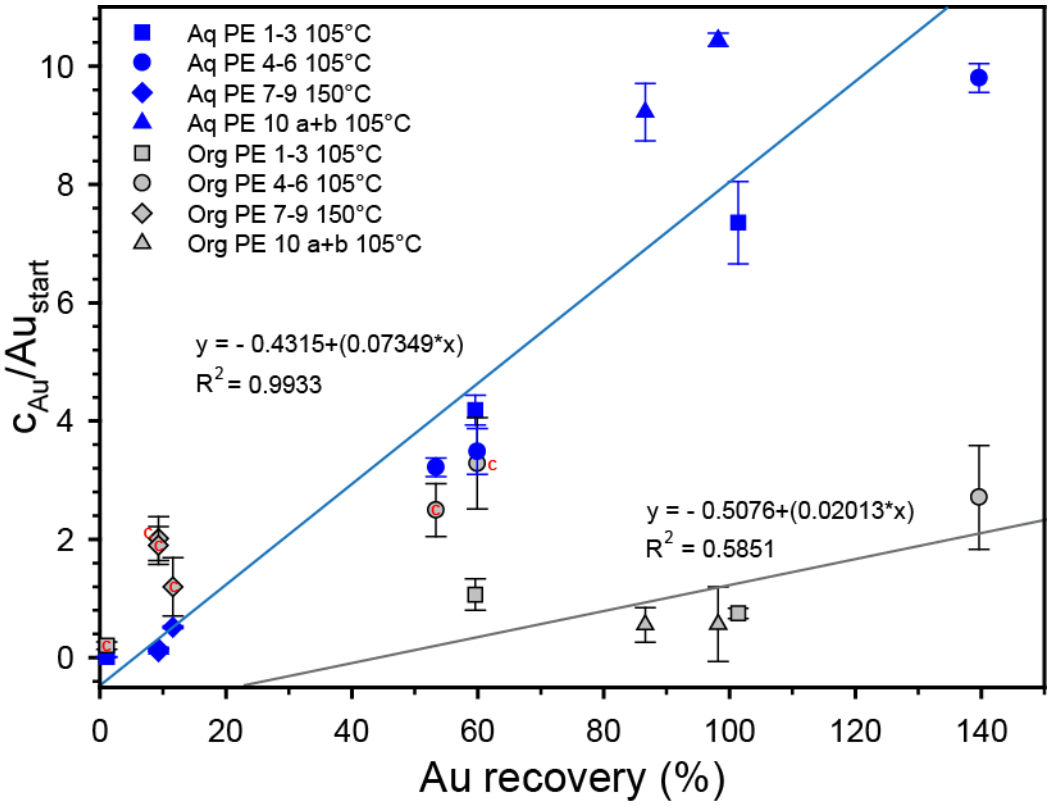

Figure 2-14: The c_{Au}^{aq} and c_{Au}^{org} normalized by the initially added Au content plotted against the Au_{recov}. The data labelled with a red "c" for contamination (PE 2, 5, 6, 7, and 9) are not included in the calculation of the regression lines.

A bigger dataset of final method experiments would enable to derive $D_{Au}^{org/aq}$ with confidence, and thus this technique should be applied at least to investigate the quality of the experiments.

2.5.6 Gold species in *n*-dodecane

The discovery of significant concentrations of gold in *n*-dodecane is surprising (not regarding the possibly contaminated samples), because *n*-dodecane, as an alkane, does not belong to the typical group of hydrocarbon NSO-compounds and porphyrins with functional groups that are expected to complex with metals and thus dissolve significant concentrations of metals (Giordano, 2000 and references therein). Two possible explanations are explored here; (1) *n*-dodecane partially decomposed to produce hydrocarbons more capable of complexing with Au(I), and (2) that a Au(III) complex such as $[AuCl_4]^-$ was present in the organic phase in the 105°C experiments (in addition to possible decomposition products acting as ligands), which is reduced to Au(0) in the 150 °C experiments (Crede et al., 2017; Crede et al., 2019).

(1) Partial decomposition of *n*-dodecane in the presence of water and air could produce strong ligands for Au, such as carbonyls that can form weakly polar Au(I)-Cl-carbonyl complexes (Antes et al., 1996; Kokh et al., 2016). Such complexes would have an affinity for the organic phase and could account for the ppb levels of Au in *n*-dodecane. In most cases, the reaction would involve reduction of Au(III) to Au(I), a transformation that is expected given the relatively reducing combination of hydrocarbons and Ti-metal, and the eventual precipitation of Au(0).

(2) However, X-ray absorption spectroscopy (XAS) results provide evidence for a $[AuCl_4]^-$ species in the organic phase (Crede et al., 2017; Crede et al., 2019). In these experiments, XAS spectra were measured at the Au L_{III}-edge in an *n*-dodecane plus acidified water system doped with $Au(III)Cl_3$ in a glassy carbon tube and equilibrated for 7 h. Below 125 °C the Au(III) complex $[AuCl_4]^-$ is dominant in *n*-dodecane and the aqueous liquid. Metallic gold precipitation was observed at T ≥125 °C from both liquids. This raises the question of whether there could be an Au(III) or Au(III)-Cl-R complex in the organic phase in the < 125 °C partition experiments, and metallic Au in the ≥ 150 °C partition experiments. The presence of a Au(III)-complex is difficult to explain, given that experiments were performed in the glassy carbon tube in the XAS study, or the Ti-cell in this study, and these materials plus *n*-dodecane are expected to have been sufficiently reducing to destabilize an Au(III) complex (e.g., Pokrovski et al., 2009a; Pokrovski et al., 2009b; Brugger et al., 2016). Further work is necessary to resolve this question.

2.6 Conclusion

The method presented here generates reproducible results for metal partitioning between immiscible liquids at hydrothermal P-T conditions, when a rigorous passivation of the Ti-cell is applied and the oil brine interface is far away from the top-sampling line. The data obtained can be used to determine partitioning behavior of elements of interest and can also be used to generate fundamental data of scientific and economic interest for other chemical systems of interest. However, further work is needed to characterize and interpret the transformation of Au to its metallic state, and the possibility of an Au(III) species in the organic phase. *N*-dodecane, or more likely its decomposition or possibly chlorinated products coexisting with brine, can transport an appreciable concentration of gold, indicating that the common presence of hydrocarbons in gold deposits may be the record of a hydrocarbon ore fluid.

Acknowledgments

This work was supported by a Discovery Project (DP140103995) and Future Fellowship (FT120100579) from the Australian Research Council and funding from The Institute for Geoscience Research. We want to thank the reviewer G. Pokrovski, whose suggestions helped to improve the paper, and we also want to thank the editor Mr. Krishnaveni.

References

Antes, I., Dapprich, S., Frenking, G. and Schwerdtfeger, P. (1996) Stability of Group 11 Carbonyl Complexes Cl− M− CO (M= Cu, Ag, Au). *Inorg. Chem.* **35**, 2089-2096.

Bischoff, J.L. (1991) Densities of liquids and vapors in boiling NaCl-H2O solutions: A PVTX summary from 300 to 500 C. *Am. J. Sci.* **291**, 309-338.

Bischoff, J.L., Rosenbauer, R.J. and Pitzer, K.S. (1986) The system NaCl-H2O: Relations of vapor-liquid near the critical temperature of water and of vapor-liquid-halite from 300 to 500 C. *Geochim. Cosmochim. Acta* **50**, 1437-1444.

Bowell, R.J., Baumann, M., Gingrich, M., Tretbar, D., Perkins, W.F. and Fisher, P.C. (1999) The occurrence of gold at the Getchell mine, Nevada. *J. Geochem. Explor.* **67**, 127-143.

Crede, L. S., Liu, W., Evans, K. A., Rempel, K. U., Testemale, D., & Brugger, J. (2019). Crude oils as ore fluids: An experimental in-situ XAS study of gold partitioning between brine and organic fluid from 25 to 250° C. *Geochim. Cosmochim. Acta*, *244*, 352-365.

Crede, L.-S., Remple, K., Brugger, J. and Liu, W. (2017) The role of organics in gold transport: An investigation of gold speciation in organic liquids: European Synchrotron Facility, Experiment number: ES-552.

Driesner, T. and Heinrich, C.A. (2007) The system H2O–NaCl. Part I: Correlation formulae for phase relations in temperature–pressure–composition space from 0 to 1000°C, 0 to 5000bar, and 0 to 1 XNaCl. *Geochim. Cosmochim. Acta* **71**, 4880-4901.

Emsbo, P. and Koenig, A.E. (2007) Transport of Au in petroleum: Evidence from the northern Carlin trend, Nevada, in: al., C.J.A.e. (Ed.), *Mineral Eploration and Research: Digging Deeper*. Proc. 9th Biennial SGA Meeting, Millpress, Dublin, pp. 695-698.

Emsbo, P., Williams-Jones, A.E., Koenig, A.E. and Wilson, S.A. (2009) Petroleum as an Agent of Metal Transport: Metallogenic and Exploration Implications, in: Williams, P.J. (Ed.), In, P.J. Williams (ed.) *Smart Science for Exploration and Mining*. Proc. 10th Biennial SGA Meeting, James Cook Univ. Earth & Enviro. Studies, pp. 99-101.

Fuchs, S., Migdisov, A. and Williams-Jones, A.E. (2011) The transport of gold in petroleum: An experimental study, Goldschmidt. *Mineral Mag.*, Prague, Czech Republic, p. 871.

Fuchs, S., Schumann, D., Williams-Jones, A.E. and Vali, H. (2015) The growth and concentration of uranium and titanium minerals in hydrocarbons of the Carbon Leader Reef, Witwatersrand Supergroup, South Africa. *Chem. Geol.* **393-394**, 55-66.

Fuchs, S., Williams-Jones, A.E., Jackson, S.E. and Przybylowicz, W.J. (2016) Metal distribution in pyrobitumen of the Carbon Leader Reef, Witwatersrand Supergroup, South Africa: Evidence for liquid hydrocarbon ore fluids. *Chem. Geol.* **426**, 45-59.

Gatellier, J.-P. and Disnar, J.-R. (1988) Mécanismes et aspects cinétiques de la réduction de l'or (III) par la matière organique sédimentaire. Importance métallogénique. *Comptes Rendus Acad. Sci. Série 2, Mécanique, Physique, Chimie, Sciences de l'univers, Sciences de la Terre* **306**, 979-984.

Gatellier, J.-P. and Disnar, J.-R. (1989) Organic matter and gold-ore association in a hydrothermal deposit, France. *Applied Geochem.* **4**, 143-149.

Giordano, T. (2000) Organic matter as a transport agent in ore-forming systems. *Rev. Econ. Geol.* **9**, 133-155.

Giże, A. (2000) The organic geochemistry of gold, platinum, uranium and mercury deposits. *Rev. Econ. Geol.: Ore Genesisis and Exploration: The Roles of Organic Matter*, 217-250.

Gize, A.P. (1999) A special issue on organic matter and ore deposits: Interactions, applications, and case studies - Introduction. *Econ. Geol. and the Bull. Soc. of Economic Geologists* **94**, 963-965.

Hofstra, A.H., Leventhal, J.S., Northrop, H.R., Landis, G.P., Rye, R.O., Birak, D.J. and Dahl, A.R. (1991) Genesis of Sediment-Hosted Disseminated-Gold Deposits by Fluid Mixing and Sulfidization - Chemical-Reaction-Path Modeling of Ore-Depositional Processes Documented in the Jerritt Canyon District, Nevada. *Geology* **19**, 36-40.

Hovey, J.K., Pitzer, K.S., Tanger, J.C., Bischoff, J.L. and Rosenbauer, R.J. (1990) Vapor-liquid phase equilibria of potassium chloride-water mixtures: equation-of-state representation for potassium chloride-water and sodium chloride-water. *J. Phys. Chem.* **94**, 1175-1179.

Jana, N.R., Gearheart, L. and Murphy, C.J. (2001) Evidence for seed-mediated nucleation in the chemical reduction of gold salts to gold nanoparticles. *Chem. Mater.* **13**, 2313-2322.

Kokh, M.A., Lopez, M., Gisquet, P., Lanzanova, A., Candaudap, F., Besson, P. and Pokrovski, G.S. (2016) Combined effect of carbon dioxide and sulfur on vapor–liquid partitioning of metals in hydrothermal systems. *Geochim. Cosmochim. Acta* **187**, 311-333.

Landais, P. (1996) Organic geochemistry of sedimentary uranium ore deposits. *Ore Geol. Rev.* **11**, 33-51.

Liu, J., Fu, J. and Lu, J. (1993) Experimental study on interaction between organic matter and gold. *'Sci. Geol. Sin.' In Chinese.* **28**, 246-253.

Liu, W., Etschmann, B., Testemale, D., Hazemann, J.-L., Rempel, K., Müller, H. and Brugger, J. (2014) Gold transport in hydrothermal fluids: Competition among the Cl^-, Br^-, HS^- and NH_3(aq) ligands. *Chem. Geol.* **376**, 11-19.

Lu, J. and Zhuang, H. (1996) Experimental studies on role of organic matter during mineralization of gold and silver at low temperatures. *'Gechim.' In Chinese.* **25**, 173-180.

Meranda, D. and Furter, W.F. (1977) Elevation of the boiling point of water by salts at saturation: Data and correlation. *J. Chem. Eng. Data* **22**, 315-317.

Miedaner, M.M., Migdisov, A.A. and Williams-Jones, A.E. (2005) Solubility of metallic mercury in octane, dodecane and toluene at temperatures between 100 degrees C and 200 degrees C. *Geochim. Cosmochim. Acta* **69**, 5511-5516.

Parnell, J. (1988) Metal Enrichments in Solid Bitumens - a Review. *Miner. Deposita* **23**, 191-199.

Pokrovski, G.S., Borisova, A.Y. and Harrichoury, J.C. (2008) The effect of sulfur on vapor-liquid fractionation of metals in hydrothermal systems. *Earth Planet. Sc. Lett.* **266**, 345-362.

Pokrovski, G.S., Roux, J. and Harrichoury, J.-C. (2005) Fluid density control on vapor-liquid partitioning of metals in hydrothermal systems. *Geology* **33**, 657-660.

Pokrovski, G.S., Tagirov, B.R., Schott, J., Bazarkina, E.F., Hazermann, J.L. and Proux, O. (2009) An in situ X-ray absorption spectroscopy study of gold-chloride complexing in hydrothermal fluids. *Chem. Geol.* **259**, 17-29.

Pokrovski, G.S., Zakirov, I.V., Roux, J., Testemale, D., Hazemann, J.-L., Bychkov, A.Y. and Golikova, G.V. (2002) Experimental study of arsenic speciation in vapor phase to 500 C: Implications for As transport and fractionation in low-density crustal fluids and volcanic gases. *Geochim. Cosmochim. Acta* **66**, 3453-3480.

Ramage, M.P. and Eckert, R.E. (1975) Kinetics of the liquid phase chlorination of n-dodecane. *Industrial & Engineering Chemistry Fundamentals* **14**, 214-221.

Rempel, K.U., Liebscher, A., Meixner, A., Romer, R.L. and Heinrich, W. (2012) An experimental study of the elemental and isotopic fractionation of copper between aqueous vapour and liquid to 450° C and 400bar in the CuCl–NaCl–H_2O and CuCl–NaHS–NaCl–H_2O systems. *Geochim. Cosmochim. Acta* **94**, 199-216.

Sherlock, R. (2000) The association of gold—mercury mineralization and hydrocarbons in the coast ranges of northern California, Organic Matter and Mineralisation: Thermal Alteration, Hydrocarbon Generation and Role in Metallogenesis. Springer, pp. 378-399.

Shilov, A.E. and Shul'pin, G.B. (1997) Activation of C− H bonds by metal complexes. *Chem. Rev.* **97**, 2879-2932.

Spirakis, C.S. (1996) The roles of organic matter in the formation of uranium deposits in sedimentary rocks. *Ore Geol. Rev.* **11**, 53-69.

Turkevich, J., Stevenson, P.C. and Hillier, J. (1951) A study of the nucleation and growth processes in the synthesis of colloidal gold. *Faraday Disc.* **11**, 55-75.

Venables, J.A. (1973) Rate Equation Approaches to Thin-Film Nucleation Kinetics. *Philos. Mag.* **27**, 697-738.

Williams-Jones, A. and Migdisov, A. (2007) The solubility of gold in crude oil: implications for ore genesis, Proceedings of the 9th Biennal SGA Meeting, Millpress, Dublin, pp. 765-768.

Wondimu, T., Goessler, W. and Irgolic, K.J. (2000) Microwave digestion of "residual fuel oil" (NIST SRM 1634b) for the determination of trace elements by inductively coupled plasma-mass spectrometry. *Fresen. J. Anal. Chem.* **367**, 35-42.

Yao, T., Sun, Z.H., Li, Y.Y., Pan, Z.Y., Wei, H., Xie, Y., Nomura, M., Niwa, Y., Yan, W.S., Wu, Z.Y., Jiang, Y., Liu, Q.H. and Wei, S.Q. (2010) Insights into Initial Kinetic Nucleation of Gold Nanocrystals. *J. Am. Chem. Soc.* **132**, 7696-7701.

Zhuang, H.P., Lu, J.L., Fu, J.M., Ren, C.G. and Zou, D.G. (1999) Crude oil as carrier of gold: petrological and geochemical evidence from Lannigou gold deposit in southwestern Guizhou, China. *Sci. China Ser. D* **42**, 216-224.

Copyright statement

Chapter 3

Gold partitioning between 1-dodecanethiol and brine at elevated temperatures: Implications of Au transport in hydrocarbons for oil-brine ore systems

Lars-S. Crede, Katy A. Evans, Kirsten U. Rempel, Kliti Grice, Ichiko Sugiyama

A modified version of this chapter was published with Chemical Geology (https://doi.org/10.1016/j.chemgeo.2018.11.011)

Abstract

Gold can be associated with hydrocarbons in hydrothermal gold deposits, but the near-absence of experimental data on gold-hydrocarbon interactions at hydrothermal conditions prevents a quantitative interpretation of this relationship. In this study, we investigate the ability of liquid hydrocarbons to act as gold-transporting ore fluids using experiments on the partitioning of gold between brine (10 wt% NaCl) and 1-dodecanethiol (DDT). Experiments were conducted at 105 °C and 150 °C and < 5 bar in a batch reactor vessel. Partition coefficients ($D_{Au}^{org/aq}$) obtained from the 105 °C and 150 °C experiments range from 10 ± 3.0 to 91 ± 30 at 105 °C and from 4.9 ± 0.9 to 33 ± 6.9 at 150 °C, with averages of 37 ± 33 and 21 ± 12, respectively. Gold concentrations in both the brine (< 1 ppm) and DDT (up to 10 ppm) are dependent on the initial bulk concentration of gold (up to 4 ppm) and on the Au loss to the vessel walls during the experiment, as the Au concentrations correlate linearly with Au loss, while $D_{Au}^{org/aq}$ appears independent of bulk composition and Au loss. This linear dependency results in a stronger Au loss from the oil that bears more Au (DDT), and enables the calculation of $D_{Au}^{org/aq}$ for zero Au loss, which is 19 ± 21. These findings indicate that $D_{Au}^{org/aq}$ is a constant at the P-T-X conditions investigated. While these experiments did not directly assess Au solubility in DDT, no indication of Au saturation was observed, suggesting that higher concentrations are possible. The *pH* of the brine decreases during the experiments, indicating that the DDT underwent deprotonation and possibly decomposition during the partitioning reaction, but the *pH* does not have an observable effect on the gold concentrations in the brine and DDT. Preferential partitioning of gold into DDT is attributed to bonding with the thiol group, and as thiols compose up to 7 wt% of the total organic sulfur content of crude oils, liquid hydrocarbons have the potential to transport significant amounts of gold in ore formation processes. This is of importance for ore systems forming at relatively low temperatures and ore deposits known to be associated with organic matter such as Carlin type Au deposits.

3.1 Introduction

The common association of metals with carbonaceous material (CM) in various types of hydrothermal ore deposits (Glikson and Mastalerz, 2000 and references therein), anomalously high gold concentrations in CM (Bowell et al., 1999; Sherlock, 2000; Emsbo and Koenig, 2007; Hu et al., 2015; Hu et al., 2016; Robert et al., 2016; Hu et al., 2017; Mirasol-Robert et al., 2017) and the high concentrations of ore metals measured in natural crude oil and bitumen (Samedova et al., 2009) raise the possibility of petroleum-phase metal transport in ore-forming processes. Gold may be associated with CM in a wide variety of deposit types, including epithermal Au-Ag (-Hg) deposits (Sherlock, 1992; Pearcy and Burruss, 1993; Mastalerz et al., 2000; Sherlock, 2000), Carlin-type Au deposits (Radtke and Scheiner, 1970; Hausen and Park, 1986; Emsbo and Koenig, 2007; Gu et al., 2012; Groves et al., 2016), orogenic Au deposits (Mirasol-Robert et al., 2017), and Witwatersrand-type Au-U deposits (Fuchs et al., 2016), indicating that CM plays an important genetic role in gold deposition. However, few experimental data exist for hydrocarbon-gold interactions under hydrothermal conditions, precluding accurate assessment or quantitative models of the role of CM in ore genesis.

Elevated concentrations of gold and other metals in immobilized CM is insufficient evidence for metal transport in liquid hydrocarbons, so CM has been historically interpreted to act as a reducing or scavenging agent during metal precipitation rather than as a transport agent (e.g., Parnell, 1988; Manning and Giże, 1993; Gize, 1999; Giże, 2000, and references therein). Hydrocarbon-mediated metal precipitation is envisaged to occur when CM constituents (bitumen, oil and gas) encounter metal-rich aqueous solutions, leading to reduction and precipitation of metals and sulfides (Leventhal and Giordano, 2000). However, a few studies have used the above lines of evidence to suggest that a liquid hydrocarbon phase may contribute to metal transport (Connan, 1979; Giordano and Barnes, 1981; Mauk and Hieshima, 1992). Possible mechanisms include complexation of metals by oil-based fluids, formation of metal-organic complexes in aqueous fluids (e.g., Saxby, 1976; Giże and Barnes, 1989; Sicree and Barnes, 1996), or a combination of these processes, i.e., partitioning of metals between coexisting aqueous and hydrocarbon fluids and complexing of gold nanoparticles (AuNP). For example, petroleum-phase transport was proposed for the Witwatersrand Basin in South Africa in the form of mobile liquid hydrocarbons that

originated from shales and contributed to the mobilization and re-deposition of uranium and gold (Fuchs et al., 2015; Fuchs et al., 2016).

Many studies have focused on the solubility, transport mechanisms, and speciation of gold in aqueous hydrothermal fluids (e.g., Henley, 1973; Seward, 1973; Renders and Seward, 1989; Shenberger and Barnes, 1989; Hayashi and Ohmoto, 1991; Seward, 1993; Gammons and Williams-Jones, 1995; Benning and Seward, 1996; Gammons et al., 1997; Murphy and LaGrange, 1998; Murphy et al., 2000; Stefánsson and Seward, 2004; Tagirov et al., 2005; Pokrovski et al., 2009a; Pokrovski et al., 2009b; Pokrovski et al., 2014; Seward et al., 2014; Mei et al., 2017). It has been shown that hydrosulfide complexes dominate in acidic to neutral, sulfur-bearing aqueous fluids at temperatures up to 350 °C, whereas chloride complexes become more important in acidic, sulfur-poor acidic fluids, particularly above 350 °C (Williams-Jones et al., 2009). Gold solubilities range from low-ppb values in vapors to ~7000 ppm in sulfide solutions, with composition and temperature acting as the first order controls on Au concentrations (e.g., Henley, 1973; Shenberger and Barnes, 1989; Hayashi and Ohmoto, 1991; Zezin et al., 2007; Zezin et al., 2011; Pokrovski et al., 2014).

In contrast, little is known about metals in liquid hydrocarbons at temperatures and pressures applicable to hydrothermal ore deposits, though some data are available for ambient conditions. In liquid hydrocarbons, compounds containing nitrogen, sulfur and oxygen (NSO-compounds) may act as ligands (e.g., Wood, 1996; Giordano, 2000; Greenwood et al., 2013). This premise is supported by an observed positive correlation of gold and heterocompounds enriched in N, S, and O in crude oil samples in the Jiyang Depression in the Shandong province, China (Sun et al., 2009). Gold complexes bond most strongly with S-bearing functional groups, and then, with decreasing effectiveness, with nitrogen and oxygen (Vlassopoulos et al., 1990; Ta et al., 2014). The preference of gold for soft, easily polarizable ligands such as sulfur-based anions is based on the Lewis acid-like behaviour of the Au^{+} ion (Pearson, 1968; Lewis and Shaw III, 1986). This behavior is observed in biological systems, in which gold taken up by cells is mainly bonded to sulfur-bearing molecules, especially thiols, sodium gold thiomalate and thioglucose (Cotton and Wilkinson, 1988; Giże, 2000 and references therein; Etschmann et al., 2016; Zammit et al., 2016). Au(I) cyanide complexes can survive for extended periods of time in environmental surface waters (Ta et al., 2014), rendering CN^{-} a potential ligand for gold transport (La Brooy et al., 1994). In addition, the following species, Carboxyl (-COOH), phenolic hydroxyl (-OH), amino ($-NH_2$), and thiol (-SH) groups (Figure 3-1) are known to form metal-organic complexes in aqueous solution

(Giordano, 2000 and references therein) and may be relevant for ore systems involving coexisting aqueous and hydrocarbon fluids. Thiolate ligands such as 1-dodecanethiol (DDT) are also used in organic chemistry (Häkkinen, 2012; Alex and Tiwari, 2015 and references therein) to form self-assembled monolayers (SAMs) on gold nanoparticles that stabilize the gold nanoparticles, which raises the possibility of Au transport in the form of nanoparticles. Thiol groups form up to 7 wt% of the total sulfur content in crude oils (Krein, 1993), and thus thiolate ligands may contribute to gold complexation and gold transport in oil-based fluids. Sulfur ranges from 0.1 % to 14 % (sweet to sour oils) in crude oils and is held in thiols, thioethers and thiophenes (Krein, 1993; Robbins and Hsu, 2000). The sulfur content of crude oils is controlled by the depositional environment, thermal history, mineral catalytic effects, and the reservoir environment of the oils (Krein, 1993). The majority of sulfur bearing compounds in crude oils have higher molecular weights than thiols e. g., thiophenes (Krein, 1993 and references therein).

A limited number of experimental studies have been conducted on the transport of gold and other precious metals in liquid hydrocarbons, but the results so far demonstrate that liquid hydrocarbons are able to dissolve substantial concentrations of metals and thus act as an ore fluid. Gold solubility experiments document that 2 to 3 ppb gold can be dissolved in crude oil at 100°C, with increasing gold solubility with temperature up to 250 °C, where Au can reach concentrations of 39–48 ppb (Williams-Jones and Migdisov, 2007). Further increases in temperature result in decreasing gold solubility, as does the use of more refined oil fractions with a smaller proportion of large molecules like porphyrins (Fuchs et al., 2011). Migdisov et al. (2017) showed that liquid hydrocarbons have the potential to mobilize and concentrate metals at concentrations of up to 50 ppb Au in solubility experiments at 250 °C. Such concentrations in aqueous ore fluids are considered to be more than sufficient to form ore deposits (Williams-Jones et al., 2009).

For coexisting brine and oil, mixing experiments between brines spiked with 8 to 10 ppm of Au, Pd, Pt, or V have demonstrated that the metals, except for V, were almost entirely sequestered into the oil phase, at concentrations ranging between 50 ppm and 100 ppm (Emsbo et al., 2009). Gold partitioning experiments by Liu et al. (1993) at 25°C, using crude oil and an aqueous solution containing 500 ppm gold, resulted in a transfer of 98% of the gold to the oil. Similarly, 99% of the gold was transferred into the oil phase in experiments at 150 °C in a coexisting system of crude oil, brine and rock (Zhuang et al., 1999). These studies indicate that liquid hydrocarbon may carry more Au than aqueous fluids in brine-oil systems,

but more rigorous experiments are needed to quantify the concentrations of gold that may be transported and the conditions at which this may occur.

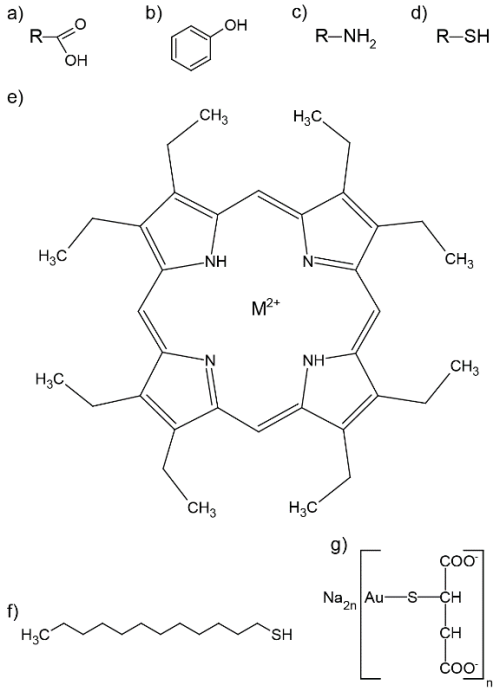

Figure 3-1: Molecular structure of potential organic ligands for metals and metal organic complexes: (a) carboxyls; (b) phenolic hydroxyls; (c) amino groups; (d) thiols (Giordano, 2000), (e) metal porphyrin complex (Robert et al., 2016), (f) 1-dodecanethiol (DDT), and (g) sodium aurothiomalate (Elder and Eidsness, 1987). M^{2+} refers to any divalent metal ion, and R is any free radical species (e.g., unbonded H^+ or hydrocarbon chain).

To investigate the potential of organic compounds such as thiols to transport gold, we have performed gold partitioning experiments (PE) between an aqueous brine (10 wt% NaCl) and a co-existing organic phase, DDT, at 105 °C and 150 °C. The temperatures were chosen to be within the oil window (ca. <160 °C).

An overview of typical concentrations of mercaptans/thiols in sulfur rich and sulfur poor crude oils is given in table 3-1 after Bol'shakov (1986, and references therein). The listed concentrations are average concentrations based on crude oils from different geological ages and do not differentiate the sulfur content of different depth occurrences. Individual sulfur concentrations of certain depths for example can be higher or lower (see Table 4 in Bol'shakov, 1986). Sulfur concentrations depend on the initial organic matter and on the environmental conditions such as lithology and depth (Bol'shakov, 1986). Thiols can host up to 7 wt% to 8 wt% of the total sulfur content in crude oils originating from carbonic lithologies (Tissot and Welte, 1978; Bol'shakov, 1986). Thiol concentrations of oils associated with

terrigenous lithologies are usually below 2 wt% of the total sulfur compound content in crude oils.

Table 3-1: Chemical composition of organic sulfur compounds in crude oils after Bol'shakov (1986)

Lithology	total sulfur	total sulfur range	wt% of total sulfur compound contents			
	≤ 1wt%	> 1wt%	elemental sulfur	mercaptans	sulfide	residual
Terrigeneous	0.87		0.0	0.0	8.0	92.0
Terrigeneous		1.00 - 1.91	0.0	0.0 - 0.9	17.9 - 19.7	80.0 - 82.9
Carbonic		1.23 - 5.75	0.0 - 0.6	0.3 - 4.3	5.5 - 17.8	78.7 - 94.2

Thiols were chosen for the experiments in contrast to the more abundant thiophenes, due to their better experimental suitability and health and safety properties. DDT is a suitable representative for the thiols and thus was used as a proxy for the mercaptans.

3.2 Experimental

3.2.1 Partitioning experiments

Experiments investigating the partitioning of gold between brine and DDT were conducted at 105 °C and 150 °C. The method was described in detail by Crede et al. (2018-B). In brief, the batch reactor used for the experiments (HFS-340Z, from Coretest Systems, Inc.) comprises a flexible titanium sampling cell loaded with the immiscible liquids, which are contained within a stainless steel pressure vessel partially filled with a low viscosity liquid (H_2O) that applies a confining pressure to the reactor cell (Figure 3-2). The pressure vessel and titanium cell are installed within a tube furnace. The titanium cell was passivated with nitric acid before each experiment to generate high gold recoveries (sampled gold concentration divided by added gold concentration), by reducing the amount of gold lost to the titanium cell walls (Crede et al., 2018-B).

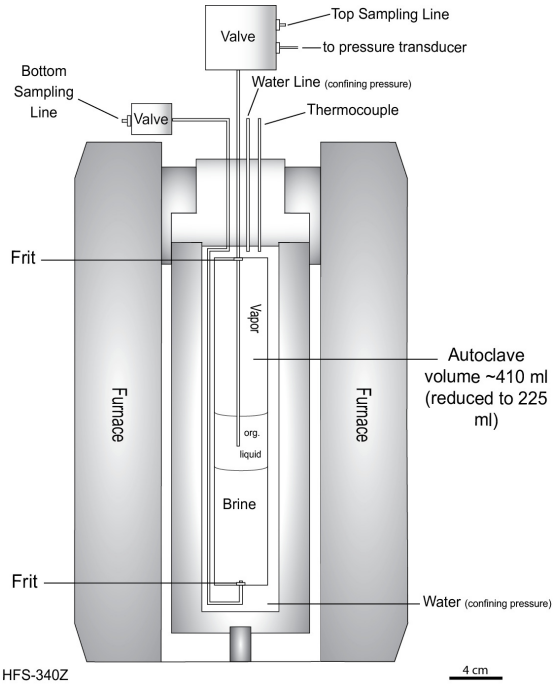

Figure 3-2: Schematic diagram of the HFS-340Z batch reactor system, Coretest Systems, Inc. The volume of the titanium cell was reduced to 225 mL by inserting Teflon rods after Crede et al. (2018-B).

For each experiment, the titanium cell was loaded with ~125 mL brine that was doped with 0.1 mL to 0.5 mL of a 1000 ppm Au plasma standard solution ($Au(III)Cl_4^-$ in 10 wt% $HCl_{(aq)}$); and ~40 mL of DDT, then heated to 105 °C or 150 °C. The added Au is equivalent to 800 to 4000 ppb Au in the brine. Due to liquid immiscibility and the density difference between the brine (1.06 g/mL) and DDT (0.845 g/mL), sampling lines at the top and bottom of the titanium cell allow for simultaneous *in-situ* sampling of both liquids at experimental conditions. The *pH* of the brine was adjusted with HCl and NaOH to test the influence of the acidity of the brine on gold partitioning behavior. For each experiment, three sample pairs of brine and DDT were taken at roughly equal *P-T* conditions, with each brine sample directly followed by one of organic liquid. Samples for the 105 °C and 150 °C experiments were taken 18 h and 21 h after loading the Ti-cell, respectively, which was 6 h after the specified temperature was reached (Crede et al., 2018-B). Proof of concept experiments by Crede et al. (2018-B; Chapter 2) demonstrate that near-equilibrium conditions with respect to the partitioning are reached after that time.

After sampling and visually checking that the brine sample was not contaminated by DDT, Au in the brine samples was stabilized by the addition of 5 mL of concentrated aqua regia (1:3 ratio of HNO_3 to HCl). Visually-checked DDT samples were digested in a mix of HNO_3 and H_2O_2, and the subsequent solutions were analyzed by ICP-MS at LabWest Minerals

Analysis Pty Ltd in Perth. The sample processing is described in more detail in Crede et al. (2018-B; Chapter 2). After each experiment, the Ti-cell, sampling lines and valves were rinsed several times with Milli-Q water, then with a diluted aqua regia solution (35% HCl and 67% HNO_3, 3:1 ratio), followed by Milli-Q water again. After cleaning, the Ti-cell was passivated with HNO_3 at 150 °C for 24 h. The passivation also decomposes any lingering traces of DDT.

The partition coefficients for gold between DDT (org) and the aqueous solution (aq) were calculated using a mass concentration ratio:

$$D_{Au}^{org/aq} = c_{Au}^{org} / c_{Au}^{aq} \qquad \text{Eq. 3-1}$$

In the above equation, $D_{Au}^{org/aq}$ is the partition coefficient, c_{Au}^{org} is the gold concentration in DDT, and c_{Au}^{aq} is the gold concentration in the brine. Uncertainties in the partition coefficients were calculated by standard error propagation, assuming the individual components of the error are uncorrelated. The largest contribution to the uncertainty originates from the standard deviation of the gold concentrations in the three samples taken for each experiment (i.e., each set of sampling conditions). The contact zone of DDT and brine is closer to the top sampling line than it is to the bottom sampling line (Crede et al., 2018-B). Thus, cross contamination could arise from brine droplets in DDT samples, and visual checks were made to check for immiscible brine in the sampled DDT. Mass balance calculations indicate that, even in the event of a 10 wt% brine contamination, the decrease of the $D_{Au}^{org/aq}$ due to contamination would be within the experimental error. Thus, the effect of cross-contamination is considered negligible. Partition coefficients were not systematically related to the initially added amount of Au, as was also the case in the method development work described in Crede et al. (2018-B).

Gold recovery (Au_{recov}) was calculated by dividing the total gold determined from the samples by total gold loaded.

$$Au_{recov} = m_{Au\ total}^{sampled} / m_{Au\ total}^{loaded} \qquad \text{Eq. 3-2}$$

The gold recovery is a useful monitor of gold loss during the partition experiment, and was found to depend mainly on the effectiveness of passivation of the titanium cell with nitric

acid (see Crede et al., 2018-B, for more details). Passivation of the inner titanium cell walls prior to each experiment led to high gold recoveries of >75%.

3.2.2 Gas Chromatography- Mass Spectrometry (GC-MS)

To determine whether DDT was modified during the partitioning experiments, DDT samples from selected experiments at 105 °C and 150 °C were analyzed with gas chromatography-mass spectrometry (GC-MS). The samples were prepared by rinsing through a column of anhydrous magnesium sulfate (pre-washed with *n*-hexane) to desorb water from the samples and then diluted with *n*-hexane. The sample results were compared to the GC-MS spectra of the pure chemical component (>98%). GC-MS analyzes were performed using a Hewlett Packard 6890A gas chromatograph interfaced to a Hewlett Packard 5973 mass spectrometer. The GC was fitted with a 60 m x 0.25 mm in diameter WCOT (wall coated open tubular) fused silica column coated with a 0.25 µm phenyl arylene polymer phase (DB-5MS, J&W Scientific). The GC oven was programmed to begin at 40 °C (hold time of 1 minute), then heated to 320 °C at 20 °C/min with a final hold time of 15 minutes. Ultra-high purity helium was used as carrier gas with a constant flow of 1.1 mL/min. Sample injection was 1 µl, pulsed splitless at 310 °C. The MS was operated at 70 *eV* with a source temperature of 230 °C. Mass spectra were acquired in full scan mode (50-550 Daltons at 2.9 scans/sec).

3.3 Results

3.3.1 GC-MS

GC-MS data of DDT for pre- and post-experiment liquids are indistinguishable (see supplementary data). The initial pre-run DDT (202.18 g/mol) and the post-run DDT sampled at 105 °C and 150 °C show a dominant peak at 11.9 s and an identical mass spectrum with the diagnostic peak at the *m/z* of 202 corresponding to the molecular weight of DDT. The GC-MS data indicate that the elevated temperatures and contact with the aqueous brine have no discernible influence on DDT for this temperature and pressure range, although the strong dilution of DDT with *n*-hexane does not allow detection of decomposition products present at ppm levels.

3.3.2 Gold partitioning

The individual experimental parameters, the gold concentrations in the brine (c_{Au}^{aq}) and in DDT (c_{Au}^{org}), $D_{Au}^{org/aq}$, and the Au_{recov} are given in Table 3-2. Partition coefficients, given as the average of triplicate measurements for each experiment, are plotted *versus* gold recovery in Figure 3-3, along with selected previously-reported data for $D_{Au}^{org/aq}$ between brine and *n*-dodecane (DD) for comparison (Crede et al., 2018-B).

3.3.3 T = 105°C

In all partitioning experiments (PE), Au partitioned preferentially from the brine into the DDT. At 105 °C and 2.1-2.7 bar, $D_{Au}^{org/aq}$ ranges from 10 ± 3.0 to 91 ± 30 with a neutral *pH* in the initial brine and a post-run *pH* ranging from 2.0 to 3.7 and Au_{recov} ranging from 5% to 141%. The gold recoveries in PE 43 and 50 are above 100%. The gold concentrations in the brine and DDT correlate with the initially-added bulk composition of gold, but the partition coefficient itself is not affected. For example, in PE 43, 500 µg gold were added, resulting in c_{Au}^{org} ranging from 6550 to 13260 ppb and a c_{Au}^{aq} ranging from 890 ppb to 950 ppb at an Au_{recov} of 118%. PE 49 and 50, on the other hand, both had 87 µg added gold, resulting in proportionally lower c_{Au}^{org} and c_{Au}^{aq} than in PE 43 (by factors of up to 6 and 30).

3.3.4 T = 150°C

At 150 °C and 3.2-4.7 bar, $D_{Au}^{org/aq}$ ranges from 4.9 ± 0.9 to 33 ± 6.9 with on outlier of 545 ± 357. Without the outlier, the average $D_{Au}^{org/aq}$ is 21 ± 12. The *pH* of PE 46, 47 and 55 decreased from near-neutral at the start of the experiment to 3.2, 2.7 and 1.7, respectively, and the *pH* of PE 51 and 52 decreased from 3.0 to 2.1 and 2.2. The gold recoveries of experiments at 150 °C were all greater than 75%, except for PE 52 with 42%. In the three experiments with gold recoveries >75%, the average c_{Au}^{org} ranges from 880 ppb (PE 51) to 1650 ppb (PE46), and c_{Au}^{aq} ranges from 80 ppb (PE 46 and 55) to 185 ppb (PE 51).

3.3.5 Influence of *pH* and temperature

The range of $D_{Au}^{org/aq}$ at 105 °C coincides with the range of $D_{Au}^{org/aq}$ at 150 °C, with the exception of the outlier. As shown in Figure 3-3, $D_{Au}^{org/aq}$ also appear to be independent of

gold recovery, though Crede et al. (2018-B) show that low recoveries may cause significant scatter in partitioning coefficients. Experiments at 105 °C were all conducted at a starting *pH* with near-neutral values (6.7 to 7.2; Table 3-2), which decreased during the experiments to end *pH* of 2.0-2.5, but *pH* variation had no discernible effect on the partition coefficients (Figure 3-4 A and B). Experiments at 150°C were conducted with starting *pH* values that were either near-neutral (6.8-7.1) or acidic (3.0), and, like the lower-temperature experiments, decreased during the experiments to an end *pH* of 1.7-3.2 with no effect on $D_{Au}^{org/aq}$ (Table 3-1). In PE 46 and PE 55, at 150 °C and neutral starting *pH*, gold concentrations in the brine and DDT were comparable, although the *pH* decreased to 3.2 in PE 46 and 1.7 in PE 55; these experiments had similar gold recoveries of 88 and 89%, respectively. In PE 51 and 52, the *pH* decreased from 3.0 to 2.1 and 2.2, respectively, with similar gold concentrations in DDT, but in the brine, PE 51 and 52 yielded average Au concentrations of 190 and 20 ppb, respectively (gold recoveries of 76% and 42% respectively). A plot of pH_{Start} against pH_{End} (Figure 3-4 C) shows that the pH_{End} is variable and independent of pH_{Start}. To summarize, any trends in Au partitioning as a function of start or end *pH* (Figure 3-4) or temperature fell within the uncertainties of analysis, so partitioning is treated as independent of these parameters in the following discussion.

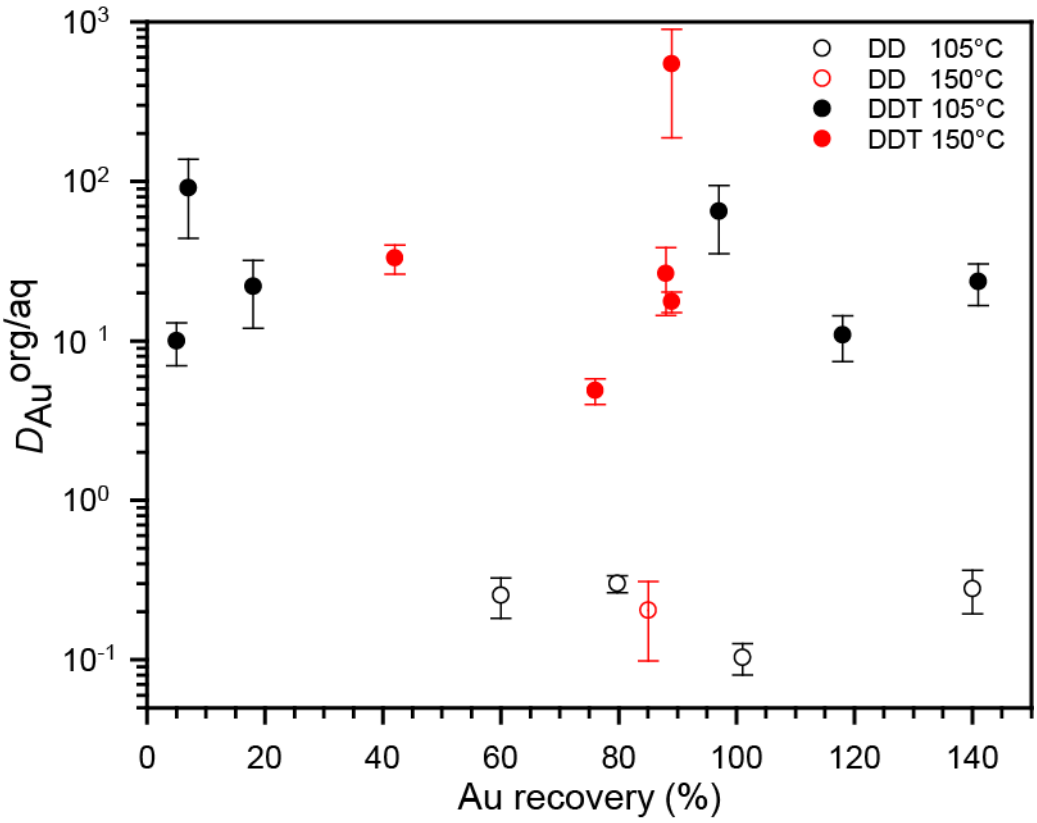

Figure 3-3: Partition coefficients versus Au recovery of the brine-dodecanethiol system (DDT; filled symbols) and a brine n-dodecane system (DD; open symbols, from Crede et al. (2018-B) experiments at 105 and 150°C.

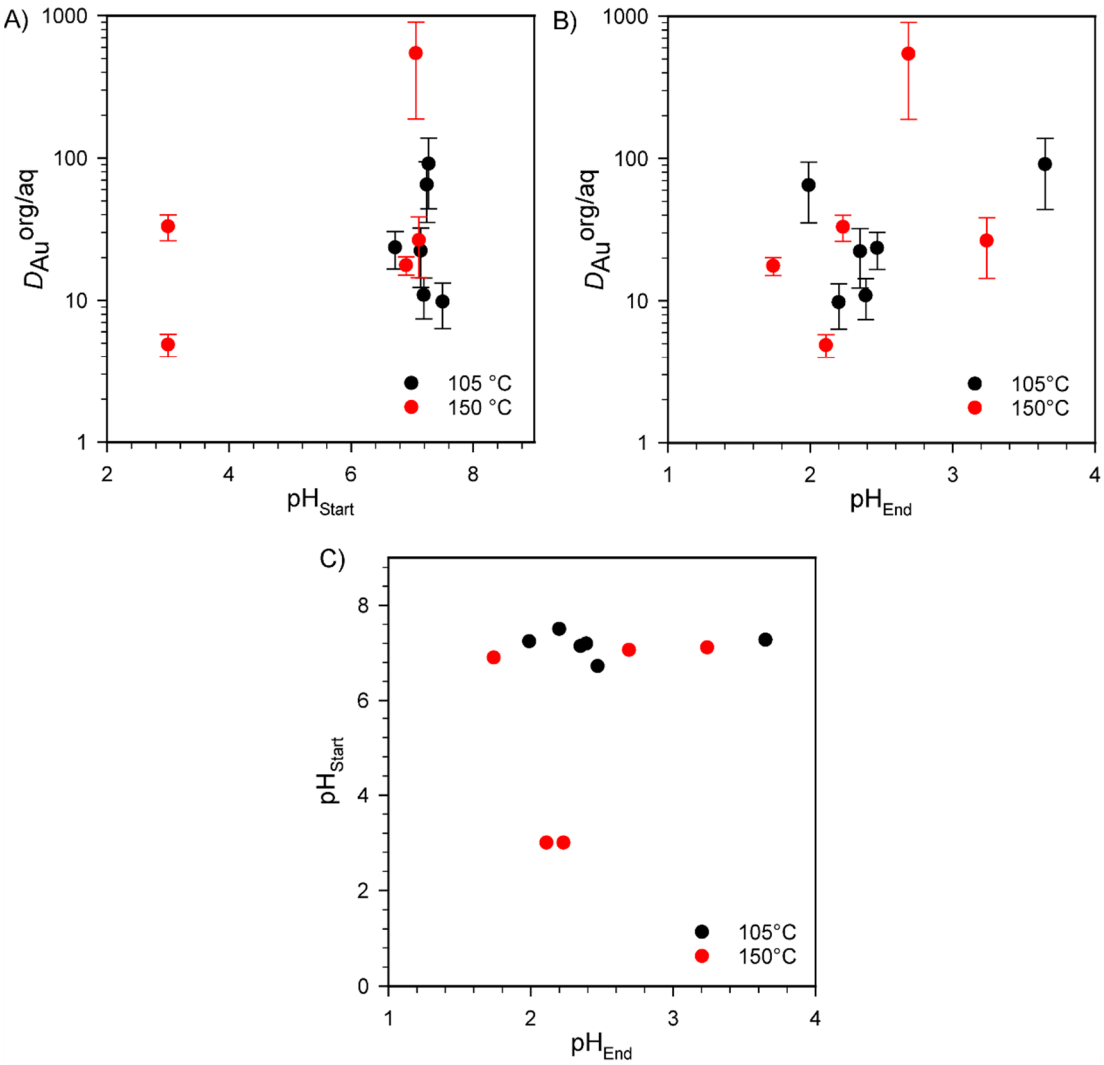

Figure 3-4: Results for the brine-dodecanethiol system. (A) Partition coefficient against pH_{Start}, (B) against pH_{End}, and (C) pH_{Start} against pH_{End}.

Table 3-2: Gold concentrations and $D_{Au}^{org/aq}$ of the partition experiments

PE[a]	T [°C]	pH_{Start}	pH_{End}	Smpl#	P ± 0.1 [bar]	Au_{start} [µg]	C_{Au}^{Org} [ppb]	$\Delta x^{Org, b}$ [ppb]	C_{Au}^{Aq} [ppb]	Δx^{Aq} [ppb]	$D^{org/aq}$ n=1	$D^{org/aq}_{mean}$ n=3	$\Delta D^{org/aq}_{mean}$ 1 σ[c]	time[d] [h]	Au recovery [%]
				1	2.33		820	80	1830	100	54				
41	105	7.3	3.7	2	2.26	500	1160	80	1850	100	89	91	47	18	7
				3	2.12		710	60	1690	90	130				
				1	2.68		450	40	300	20	12				
42	105	7.5	2.2	2	2.54	500	580	40	280	10	14	10	3	18	5
				3	2.26		240	20	280	10	6				
				1	2.6		9850	510	890	50	11				
43	105	7.2	2.4	2	2.4	500	13260	690	900	50	15	11	3.5	18	118
				3	2.0		6550	340	950	50	6.9				
				1	2.3		490	30	20	<5	30				
48	105	7.1	2.4	2	2.0	87	250	10	20	<5	16	22	10	18	18
				3	1.8		250	10	10	<5	21				
				1	2.3		2270	120	20	<5	96				
49	105	7.2	2.0	2	2.2	87	1830	90	30	<5	69	65	30	18	97
				3	2.1		1240	60	40	<5	30				
				1	2.7		3010	160	100	10	30				
50	105	6.7	2.5	2	2.6	87	2280	120	100	10	23	24	7	18	141
				3	2.4		1700	90	90	<5	18				
				1	3.9		1800	90	120	10	15				
46	150	7.1	3.2	2	3.7	96	1570	80	80	<5	20	26	12	21	88
				3	3.2		1590	80	40	<5	44				

PE[a]	T [°C]	pH_{Start}	pH_{End}	Smpl#	P ± 0.1 [bar]	Au_{start} [µg]	C_{Au}^{Org} [ppb]	$\Delta x^{Org, b}$ [ppb]	C_{Au}^{Aq} [ppb]	Δx^{Aq} [ppb]	$D^{org/aq}$ n=1	$D^{org/aq}_{mean}$ n=3	$\Delta D^{org/aq}_{mean}$ 1 σ[c]	time[d] [h]	Au recovery [%]
47	150	7.1	2.7	1	4.1	100	2130	110	2	<5	985	545	357	21	89
				2	4.1		790	40	4	<5	189				
				3	3.9		2630	140	10	<5	460				
51	150	3.0	2.1	1	4.1	87	860	40	170	10	5.0	4.9	0.9	21	76
				2	3.9		930	50	200	10	4.7				
				3	3.4		860	40	-	-	-				
52	150	3.0	2.2	1	4.2	87	730	40	20	<5	32	33	6.9	21	42
				2	4.1		730	40	20	<5	31				
				3	3.7		670	30	20	<5	36				
55	150	6.9	1.7	1	4.7	87	1440	70	80	<5	19	18	2.6	21	89
				2	4.4		1370	70	80	<5	16				
				3	4.1		1410	70	80	<5	18				

[a] partition experiment

[b] analytical error (including balance, volume, and mass spectrometer uncertainties)

[c] total error by error propagation (1σ)

[d] time from loading the Ti-cell to sampling

3.4 Discussion

The experimental results show that gold partitions preferentially into DDT in the presence of brine, and $D_{Au}^{org/aq}$ for DDT is up to 3.5 orders of magnitude higher than $D_{Au}^{org/aq}$ reported for high gold-recovery experiments made in the brine and *n*-dodecane system at 105 °C and 150 °C (Crede et al., 2018-B). A plausible explanation for this observation is that the higher $D_{Au}^{org/aq}$ is a consequence of the presence of the thiol group in the DDT and the strong attraction between gold and sulfur (Vlassopoulos et al., 1990; Ta et al., 2014). This preference for the hydrocarbon phase is in agreement with previous experiments on mixed oils (Liu et al., 1993; Zhuang et al., 1999; Emsbo et al., 2009). While these experiments did not directly assess Au solubility in DDT, no indication of Au saturation was observed, suggesting that higher concentrations are possible. These first results on a pure phase confirm the potential importance of liquid hydrocarbons for gold transport in ore systems that involve coexisting oil and hydrothermal fluid.

3.4.1 Au concentrations, Au loss, and calculation of $D_{Au}^{org/aq}$ for Au_{recov} = 100%

The calculated $D_{Au}^{org/aq}$, enables use of the results from this study as inputs for thermodynamic models, although the uncertainties must also be propagated through any quantitative calculations.

Because of the potential increase in the scatter of the data due to variable Au recovery (Crede et al., 2018-B), we have used the temperature-independent correlation between Au concentrations in the brine and DDT *versus* Au recovery to calculate $D_{Au}^{org/aq}$ at Au_{recov} = 100% (Figure 3-5). The Au concentrations in the brine and DDT, normalized to the initially-added Au to enable comparison (c_{Au}/Au_{Start}), show a linear correlation with the calculated Au_{recov} (Figure 3-5). The Au concentrations plot on the same line in the 105 °C and the 150 °C experiments, but with a different slope for the Au concentrations in the brine and in DDT due to the preference of Au for DDT. Thus, the Au concentration in the brine and in DDT have to be calculated for Au_{recov} = 100% to derive the $D_{Au}^{org/aq}$. The equation for Au in DDT is

$$c^{org}_{Au,\ norm} = 0.1843\ Au_{recov} + 0.1567 \qquad \text{Eq. 3}$$

($R^2 = 0.9567$, $p < 0.001$), where R^2 is the square of the correlation coefficient and p is the probability that the points are unrelated to the regression line, based on a two-tailed significance test of the Pearson's correlation coefficient. The equation for Au in the brine is

$$c^{aq}_{Au,\ norm} = 0.0096\ Au_{recov} + 0.0266 \qquad \text{Eq. 4}$$

($R^2 = 0.3586$, $p < 0.05$). The linear relationship enables removal of the effects of variable gold recovery to calculate c^{org}_{Au} and c^{aq}_{Au}, and subsequently $D^{org/aq}_{Au}$ by projecting c^{org}_{Au} and c^{aq}_{Au} to $Au_{recov} = 100\%$. The standard deviations on the projected values are low for most experiments, except for the six organic samples with the highest Au_{recov}. For these samples, the uncertainties are high because Au concentrations in the triplicate samples were variable. Combining all 12 experiments, and using triplicate samples for each phase per experiment, the best estimate of $D^{org/aq}_{Au}$ (with the corrected c^{org}_{Au} and c^{aq}_{Au} calculated using equations 3 and 4) is 19 ± 21. Calculations done individually for each temperature do not show any significant variation. This value is consistent with the partition coefficients for the experiments with the best recovery rates (PE 46, Au_{recov} of 88%, 150 °C, $D^{org/aq}_{Au} = 26 \pm 12$ and PE 55, Au_{recov} of 89%, $D^{org/aq}_{Au} = 18 \pm 2.6$), although the error is large due to the nature of the calculation of the meaningful $D^{org/aq}_{Au}$ for $Au_{recov} = 100\%$.

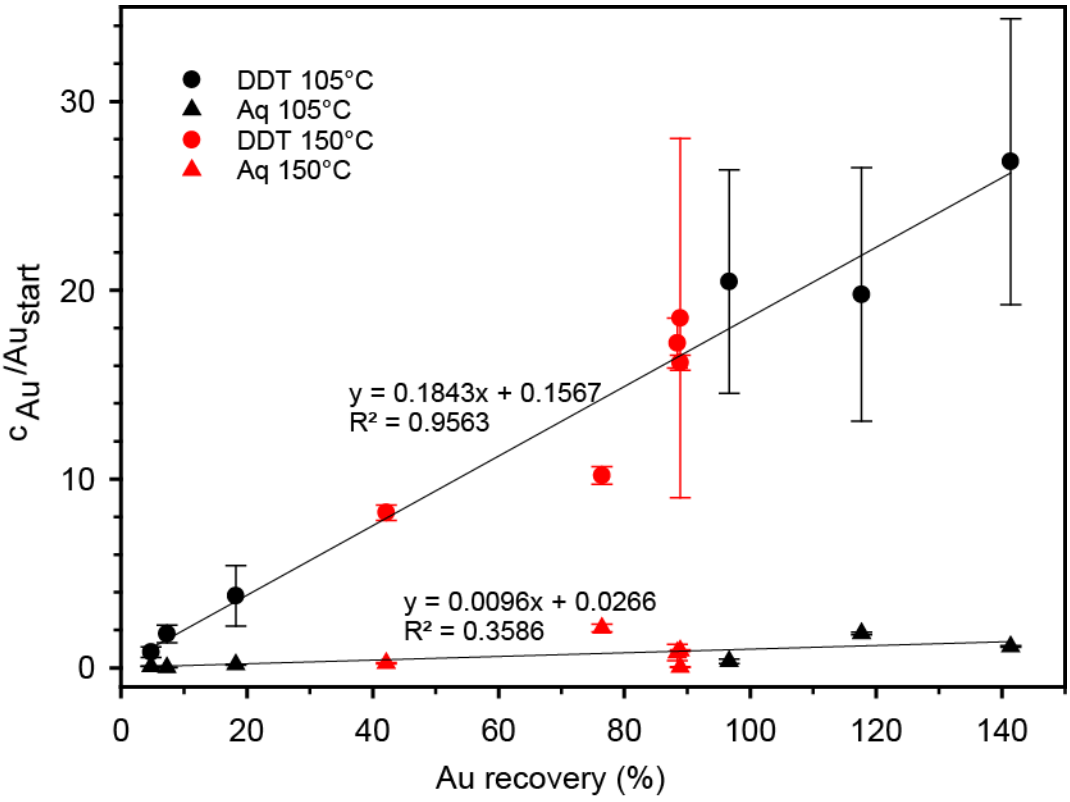

Figure 3-5: (A) Au concentrations in the DDT (circles) and brine (triangles) normalized with Au_{start} and plotted against Au_{recov}. Error bars are the standard deviations of the three Au concentrations measured in the triplicate samples for each experiment. Solid lines are linear regression lines through the Au concentrations in the DDT and brine.

3.4.2 Implications of the statistical correlation between c_{Au} and Au loss for $D_{Au}^{org/aq}$

The linear relationship between Au concentrations and Au_{recov} enables calculation of a meaningful $D_{Au}^{org/aq}$ (Figure 3-5), even if only one or two experiments have Au_{recov} between ~80% and 100%. The strategy is robust when there is a sufficient number of experiments with a wide range of Au_{recov} available, and so long as the Au concentrations are not significantly affected by other factors, such as cross contamination or Au contamination after the experiment, e.g., in the sample processing step. However, significant effects from such factors can be recognized because they would cause a scattered data set without a statistically significant correlation between Au_{recov} and the relevant concentrations. The use of triplicate samples and the resulting calculated average Au concentrations also aid confidence in this method, especially as Au concentrations are variable at high Au_{recov} in DDT samples (Table 3-2, Figure 3-5).

3.4.3 Sources of uncertainty

Variability in calculated $D_{Au}^{org/aq}$ is attributed to a combination of factors. The main factor is the processes that cause low Au_{recov} (Crede et al., 2018-B; section 4.2.1). These effects combine with *pH* effects related to decomposition of DDT. However, the magnitude of such effects are hard to judge because while DDT decomposition was not detected by GC-MS, some DDT breakdown may have been masked by the high degree of dilution required to prevent contamination of the GC column by the DDT (detection limit of the order of ~1wt%). With varying *pH* comes varying deprotonation of the thiol group to bond with Au – these effects are discussed in section 4.3.1. Pressure and temperature are not considered explicitly here because there is no detectable trend in $D_{Au}^{org/aq}$ as a function of pressure or temperature.

3.4.4 Gold recovery

Crede et al. (2018-B) showed that gold recovery was inversely correlated with $D_{Au}^{org/aq}$ in Aubrine – *n*-dodecane partition experiments. Low gold recovery and thus high Au loss were attributed to breakdown of the passivated layer on the Ti-cell and subsequent Au precipitation. Precipitated Au was observed when passivation was not performed after every run.

In contrast to the *n*-dodecane experiments, $D_{Au}^{org/aq}$ values for DDT show no significant correlation with gold recovery and are all within an order of magnitude (Figure 3-3), if the outlier of PE 47 is excluded. This result indicates that $D_{Au}^{org/aq}$ in these experiments are not affected by gold loss to the same extent as the DD experiments (Figure 3-3). This may be due to lower Au concentrations in the brine, or to differing kinetics in the DD and DDT systems. Experiments with gold recoveries >100% may indicate addition of residual gold in the Ti-cell from prior experiments (incomplete cleaning), that more gold was added than intended, or that either the AuHCl solution or sample solutions were not well mixed. Nevertheless, the experiments with $Au_{recov} \geq 100\%$ still plot on the same linear trend (Figure 3-5) and indicate that these factors do not significantly affect the certainty of the calculated partition coefficient.

3.4.5 pH

The use of variable starting *pH* in PE at 150 °C was intended to enable assessment of the effect of *pH* on Au partitioning. However, *pH* effects, if present, were masked by variability in the experimental results related to Au_{recov}. The observed *pH* decrease is thought to be the result of two factors: the decomposition of DDT (section 4.2.3) and the deprotonation of the S in DDT (section 4.3.1).

3.4.6 Influence of decomposition products

Decomposition of DDT in the presence of an initially oxygenated brine at the elevated temperatures of the experiments is likely to produce carboxylic acids, CO_2, CH_4, and CO that could act as ligands for Au and theoretically add to the data scatter. This would have little effect on the Au concentration in DDT, as the thiol group would be expected to have a stronger affinity for Au than any of those products.

In contrast, partitioning of DDT decomposition products, for example, polar carboxylic acids, into the brine could affect calculated Au partition coefficients to a greater extent. Some addition of DDT decomposition products to the brine is suggested by the *pH* decrease that was also observed in the DD experiments by Crede et al. (2018-B), consistent with similar equilibration kinetics in both the DD and DDT experiments. If DDT-derived polar compounds complex with Au, then changes to c_{Au}^{aq} due to DDT decomposition may affect $D_{Au}^{org/aq}$. For example, an increase of c_{Au}^{aq} by 25% in PE 55 would change the $D_{Au}^{org/aq}$ from 18 to 14. Ideally, it would be possible to quantify uncertainties arising from this source of error, but this would require knowledge of the species involved and their concentrations, and acquisition of these data is beyond the scope of this study.

3.4.7 Gold speciation in brine and 1-dodecanethiol

In a related study based on chapter 4, the speciation of gold in coexisting aqueous fluid and DDT were assessed *in-situ* with X-ray absorption spectroscopy (XAS) within a glassy carbon cell up to 250 °C (Crede et al., 2017; Crede et al., 2019). The chemicals and experimental conditions are comparable to this study and may allow to interpret the Au speciation in the experiments of this chapter.

In the XAS experiments gold was added as $HAuCl_4 \bullet 3H_2O$ powder (Au(III) complex). Spectra from XAS experiments at 30 °C for coexisting aqueous solution and DDT showed an Au(I) complex (*pH*=1.85) in both fluids. Au(III) complexes are thermodynamically stable in aqueous fluids at low T and high $f(O_2)$ (Pokrovski et al., 2009a; Pokrovski et al., 2009b; Usher et al., 2009; Williams-Jones et al., 2009; Liu et al., 2014; Brugger et al., 2016). However, sufficiently high $f(O_2)$ to stabilize Au(III) complexes are unlikely to be sustained in the presence of DDT, so the initially present Au(III) complexes would have been metastable and the production of Au(I) complexes is expected in the experiments of this chapter

At temperatures below 125 °C, XANES and EXAFS data were consistent with the structure of a sodium aurothiomalate(I) -like compound (Figure 3-1 g) in the aqueous and organic fluids (same Au speciation and Au-S bond lengths). The laboratory experiments described here were conducted over somewhat longer timescales than the synchrotron experiments, so it is likely that Au(III) was reduced to Au(I) in the brine and DDT within the Ti-cell once the chemicals were loaded. Results of the synchrotron work indicate that one gold atom bonds to two DDTs at 105 °C (Crede et al., 2019), to preferentially produce a formally negatively-charged, quasi-linear [RS-Au-SR] complex (Ning et al., 2012). The geometry of such a species is similar to that of $Au(HS)_2^-$ in aqueous solutions (Liu et al., 2014; Brugger et al., 2016). In the synchrotron experiments at temperatures ≥ 125 °C, however, Au(I) was reduced to Au(0), possibly forming Au(0) nanoparticles, which may be stabilized by or bonded to DDT. Similarities in redox buffering capacity and fluids used for the Ti-cell and synchrotron experiments suggest that the same species are probably present in both studies.

3.4.8 The role of Au(0)

If Au speciation in the Ti-cell experiments is similar to that of the synchrotron experiments, then it is likely that Au in the DDT at 150 °C was present as Au(0), and may have been held in the form of nanoparticles bonded to DDT (Daniel and Astruc, 2004).

Thiols bond *via* S to the gold nanoparticle (Daniel and Astruc, 2004), so that the unreactive end, the hydrocarbon chain, points away from the nanoparticle (Figure 3-6). This configuration shields the surface of the nanoparticle, and protects it from direct interaction with other ligands or reactive molecules. The adsorption of organothiols onto gold nanoparticles is accompanied by an acidification of the solution, because protons are released from the thiol group upon the formation of the covalent Au-S bonds. Thus, the

number of released protons is proportional to the amount of adsorbed organothiols (Ansar et al., 2013). Protons are highly polar and would therefore have an affinity for the aqueous phase relative to the less polar organic phase. The acidification observed in our partition experiments is consistent with deprotonation of the thiol group of DDT, although a quantification of the magnitude of the effect is not possible due to a combination of the fact that the Au to DDT ratio is not known, and that the DDT may have partially decomposed as discussed above and in Crede et al. (2018-B).

If the Au species in this study are the same as in the XAS study (Crede et al., 2017; Crede et al., 2019), the 105 °C and the 150 °C experiments should have involved different Au species. In this case, the well correlated linear regression line and lack of temperature dependence is surprising. There are, broadly speaking, three possibilities here. The first is that the species are, in fact, different in the synchrotron and laboratory experiments, due to the longer runtimes, the different cell material, and the absence of the X-ray beam in the experiments conducted here. Alternatively, it may be that the NP formation simply transforms Au already present in solution, and that the kinetics of any further loss/gain of Au are too slow for changes in solubility to be detected. A third possibility is that the solubility of the two species is different but insufficiently so to be detected through the scatter associated with heterogeneity of Au concentrations in the triplicate sample sets. Further work is necessary to distinguish between these possibilities.

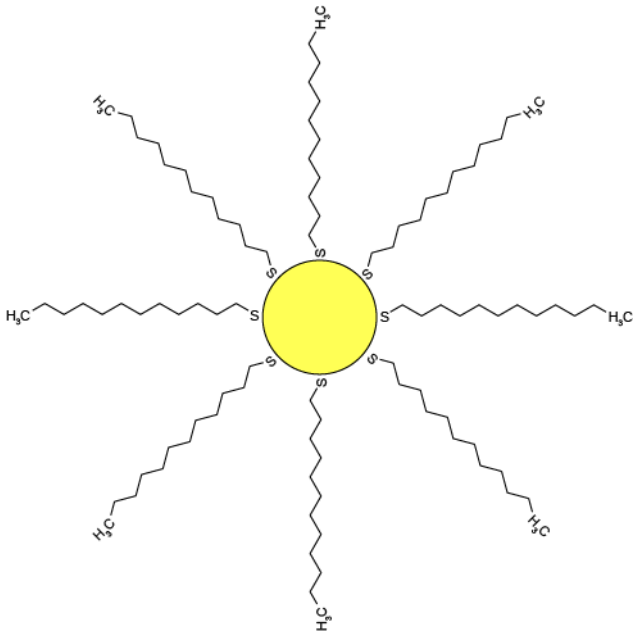

Figure 3-6: AuNP coted with organic shell (DDT) after Daniel and Astruc (2004) and references therein.

3.4.9 Geological implications

In these experiments, DDT is used as an analogue for S-bearing compounds in the organic phase in natural ore systems. The melting point, boiling point, and stability under a broad range of redox and temperature conditions of DDT are representative of other thiol bearing oil molecules, and up to 7 wt% of the total sulfur content of crude oils is held in thiol groups (Krein, 1993). Therefore, DDT provides a practical analogue for thiol-compounds in oils. The strong preference of gold for the liquid hydrocarbon phase suggests that oils may act as ore fluids and contribute to gold transport at low to moderate temperatures in natural systems when liquid oil is present. Oil degradation and significant gas generation start at ca. 160 °C (Khorasani and Murchison, 1988), which is below the boiling point of 275 °C of DDT; thus DDT may be able to mobilize gold at temperatures outside the oil window if the compound does not break down in response to oxidation.

Liquid hydrocarbons may transport precious metals until immobilization occurs due to changing *P-T-X* conditions (pressure, temperature and unknown factors). For example, thermally-induced degradation of liquid oil to immobile organic matter may occur as a consequence of the addition of heat or redox budget from active hot springs or hydrothermal brines. Alternatively, in basinal settings, Au may be deposited when the hydrocarbon liquid is trapped and thermally degraded after subsidence. A natural limit on the temperatures at which Au may be transported by oils is provided by the limited stability of oils to <200 °C. Thus oils may be particularly important for gold transport in lower-temperature environments such as sedimentary basins e.g., Carlin-type Au deposits, for which hydrocarbon ore fluids were proposed (Zhuang et al., 1999; Emsbo and Koenig, 2007; Gu et al., 2012), or sub-volcanic environments (epithermal Ag-Au deposits). On the other hand, maturation modelling shows that organic matter at the Carlin deposit was matured beyond the oil and gas windows before gold mineralization (Gize et al.; 2000). Thus, gold transport in organics is not necessarily a general feature of Carlin-type deposits indicating that the individual deposit settings have to be considered. However, more work is needed to secure direct evidence, for example by analysis of hydrocarbon fluid inclusions in ore deposits.

3.4.10 Metal enriched oils/brine interactions

The elevated brine-DDT partition coefficients found from the experiments also suggest that metal-enriched crude oils may form by leaching metals from metal-bearing brines (Filby,

1994; Samedova et al., 2009). In this scenario, Au may switch between the competing fluids, bringing a new level of complexity to Au transport and distribution. Removal of Au into the organic phase would deplete the hydrothermal ore fluids in Au and other metals with similar properties. Under these circumstances, it is interesting to consider whether it is possible to recognize the chemical signature of this process, in, for example, ratios of metals compatible and incompatible in the organic phase. However, such work is beyond the scope of this project.

3.5 Conclusions

The calculated partition coefficient determined here is the first pure-phase partition coefficient derived for a fluid system involving a brine and single-phase, sulfur-bearing organic liquid. The results indicate that Au demonstrates a strong preference for DDT over brine. The linear relationship between the Au concentrations and Au recovery demonstrate that the calculated partition coefficient is robust, despite variability in $D_{Au}^{org/aq}$ as a function of Au_{recov}. The results indicate that, at the investigated temperature range, hydrocarbon-phase transport for Au may be effective.

Acknowledgements

This work was supported by a Discovery Project to K. R. (DP140103995) and Future Fellowship (FT120100579) from the Australian Research Council (ARC) and funding from The Institute for Geoscience Research

References

Alex, S. and Tiwari, A. (2015) Functionalized gold nanoparticles: synthesis, properties and applications—a review. *J. Nanosci. Nanotechnol.* **15**, 1869-1894.

Ansar, S.M., Perera, G.S., Jiang, D., Holler, R.A. and Zhang, D. (2013) Organothiols self-assembled onto gold: evidence for deprotonation of the sulfur-bound hydrogen and charge transfer from thiolate. *J. Phys. Chem. C* **117**, 8793-8798.

Benning, L.G. and Seward, T.M. (1996) Hydrosulphide complexing of Au (I) in hydrothermal solutions from 150–400 C and 500–1500 bar. *Geochim. Cosmochim. Acta* **60**, 1849-1871.

Bol'shakov, G. F. (1986). Organic sulfur compounds of petroleum. *Sulfur reports*, *5*(2), 103-393.

Bowell, R.J., Baumann, M., Gingrich, M., Tretbar, D., Perkins, W.F. and Fisher, P.C. (1999) The occurrence of gold at the Getchell mine, Nevada. *J. Geochem. Explor.* **67**, 127-143.

Brugger, J., Liu, W., Etschmann, B., Mei, Y., Sherman, D.M. and Testemale, D. (2016) A review of the coordination chemistry of hydrothermal systems, or do coordination changes make ore deposits? *Chem. Geol.* **447**, 219-253.

Connan, J. (1979) Genetic relation between oil and ore in some Pb-Zn-Ba ore deposits. *Special Publication of the Geological Society of South Africa* **5**, 263-274.

Cotton, F.A. and Wilkinson, G. (1988) Advanced inorganic chemistry. Wiley New York.

Crede, L. S., Liu, W., Evans, K. A., Rempel, K. U., Testemale, D., & Brugger, J. (2019). Crude oils as ore fluids: An experimental in-situ XAS study of gold partitioning between brine and organic fluid from 25 to 250° C. *Geochim. Cosmochim. Acta*, *244*, 352-365.

Crede, L. S., Rempel, K. U., Hu, S. Y., & Evans, K. A. (2018-B). An experimental method for gold partitioning between two immiscible fluids: Brine and n-dodecane. *Chem. Geol.*

Crede, L.-S., Remple, K., Brugger, J. and Liu, W. (2017) The role of organics in gold transport: An investigation of gold speciation in organic liquids: European Synchrotron Facility, Experiment number: ES-552.

Daniel, M.-C. and Astruc, D. (2004) Gold nanoparticles: assembly, supramolecular chemistry, quantum-size-related properties, and applications toward biology, catalysis, and nanotechnology. *Chem. Rev.* **104**, 293-346.

Elder, R.C. and Eidsness, M.K. (1987) Synchrotron X-ray studies of metal-based drugs and metabolites. *Chem. Rev.* **87**, 1027-1046.

Emsbo, P. and Koenig, A.E. (2007) Transport of Au in petroleum: Evidence from the northern Carlin trend, Nevada, in: al., C.J.A.e. (Ed.), *Mineral Eploration and Research: Digging Deeper*. Proc. 9th Biennial SGA Meeting, Millpress, Dublin, pp. 695-698.

Emsbo, P., Williams-Jones, A.E., Koenig, A.E. and Wilson, S.A. (2009) Petroleum as an Agent of Metal Transport: Metallogenic and Exploration Implications, in: Williams, P.J. (Ed.), In, P.J. Williams (ed.) *Smart Science for Exploration and Mining*. Proc. 10th Biennial SGA Meeting, James Cook Univ. Earth & Enviro. Studies, pp. 99-101.

Etschmann, B., Brugger, J., Fairbrother, L., Grosse, C., Nies, D., Martinez-Criado, G. and Reith, F. (2016) Applying the Midas touch: Differing toxicity of mobile gold and platinum complexes drives biomineralization in the bacterium Cupriavidus metallidurans. *Chem. Geol.* **438**, 103-111.

Filby, R.H. (1994) Origin and nature of trace element species in crude oils, bitumens and kerogens: implications for correlation and other geochemical studies. *Geol. Soc. Spec. Publ.* **78**, 203-219.

Fuchs, S., Migdisov, A. and Williams-Jones, A.E. (2011) The transport of gold in petroleum: An experimental study, Goldschmidt. *Mineral Mag.*, Prague, Czech Republic, p. 871.

Fuchs, S., Schumann, D., Williams-Jones, A.E. and Vali, H. (2015) The growth and concentration of uranium and titanium minerals in hydrocarbons of the Carbon Leader Reef, Witwatersrand Supergroup, South Africa. *Chem. Geol.* **393-394**, 55-66.

Fuchs, S., Williams-Jones, A.E., Jackson, S.E. and Przybylowicz, W.J. (2016) Metal distribution in pyrobitumen of the Carbon Leader Reef, Witwatersrand Supergroup, South Africa: Evidence for liquid hydrocarbon ore fluids. *Chem. Geol.* **426**, 45-59.

Gammons, C.H. and Williams-Jones, A. (1995) The solubility of Au Ag alloy+ AgCl in HCl/NaCl solutions at 300° C: New data on the stability of Au (1) chloride complexes in hydrothermal fluids. *Geochim. Cosmochim. Acta* **59**, 3453-3468.

Gammons, C.H., Yu, Y. and Williams-Jones, A. (1997) The disproportionation of gold (I) chloride complexes at 25 to 200 C. *Geochim. Cosmochim. Acta* **61**, 1971-1983.

Giordano, T. (2000) Organic matter as a transport agent in ore-forming systems. *Rev. Econ. Geol.* **9**, 133-155.

Giordano, T. and Barnes, H. (1981) Lead transport in Mississippi Valley-type ore solutions. *Econ. Geol.* **76**, 2200-2211.

Giże, A. (2000) The organic geochemistry of gold, platinum, uranium and mercury deposits. *Rev. Econ. Geol.: Ore Genesisis and Exploration: The Roles of Organic Matter*, 217-250.

Giże, A. and Barnes, H. (1989) Organic processes in Mississippi Valley-type ore genesis, 28th International Geological Congress Abstracts, pp. 557-558.

Gize, A.P. (1999) A special issue on organic matter and ore deposits: Interactions, applications, and case studies - Introduction. *Econ. Geol. and the Bull. Soc. of Economic Geologists* **94**, 963-965.

Gize, A. P., Kuehn, C. A., Furlong, K. P., & Gaunt, J. M. (2000). Organic maturation modeling applied to ore genesis and exploration. *Rev. Econ. Geol.*, *9*, 87-104.

Glikson, M. and Mastalerz, M. (2000) Organic matter and mineralisation: thermal alteration, hydrocarbon generation and role in metallogenesis. Springer Science & Business Media.

Greenwood, P.F., Brocks, J.J., Grice, K., Schwark, L., Jaraula, C.M.B., Dick, J.M. and Evans, K.A. (2013) Organic geochemistry and mineralogy. I. Characterisation of organic matter associated with metal deposits. *Ore Geol. Rev.* **50**, 1-27.

Groves, D.I., Goldfarb, R.J. and Santosh, M. (2016) The conjunction of factors that lead to formation of giant gold provinces and deposits in non-arc settings. *Geosc. Frontiers* **7**, 303-314.

Gu, X.X., Zhang, Y.M., Li, B.H., Dong, S.Y., Xue, C.J. and Fu, S.H. (2012) Hydrocarbon- and ore-bearing basinal fluids: a possible link between gold mineralization and hydrocarbon accumulation in the Youjiang basin, South China. *Miner. Deposita* **47**, 663-682.

Häkkinen, H. (2012) The gold-sulfur interface at the nanoscale. *Nature chemistry* **4**, 443-455.

Hausen, D.M. and Park, W.C. (1986) Observations on the association of gold mineralization with organic matter in Carlin-type ores. *Organics and ore deposits, Proceedings: Denver Region Exploration Geologists Society*, 119-136.

Hayashi, K.-i. and Ohmoto, H. (1991) Solubility of gold in NaCl-and H2S-bearing aqueous solutions at 250–350°C. *Geochim. Cosmochim. Acta* **55**, 2111-2126.

Henley, R.W. (1973) Solubility of gold in hydrothermal chloride solutions. *Chem. Geol.* **11**, 73-87.

Hu, S.-Y., Evans, K., Craw, D., Rempel, K. and Grice, K. (2017) Resolving the role of carbonaceous material in gold precipitation in metasediment-hosted orogenic gold deposits. *Geology* **45**, 167-170.

Hu, S.-Y., Evans, K., Fisher, L., Rempel, K., Craw, D., Evans, N.J., Cumberland, S., Robert, A. and Grice, K. (2016) Associations between sulfides, carbonaceous material, gold and other trace elements in polyframboids: implications for the source of orogenic gold deposits, Otago Schist, New Zealand. *Geochim. Cosmochim. Acta* **180**, 197-213.

Hu, S., Evans, K., Craw, D., Rempel, K., Bourdet, J., Dick, J. and Grice, K. (2015) Raman characterization of carbonaceous material in the Macraes orogenic gold deposit and metasedimentary host rocks, New Zealand. *Ore Geol. Rev.* **70**, 80-95.

Khorasani, G.K. and Murchison, D.G. (1988) Order of generation of petroleum hydrocarbons from liptinic macerals with increasing thermal maturity. *Fuel* **67**, 1160-1162.

Krein, E.B. (1993) Organic sulfur in the geosphere: analysis, structures and chemical processes. *Sulphur-Containing Functional Groups (1993)*, 975-1032.

La Brooy, S., Linge, H. and Walker, G. (1994) Review of gold extraction from ores. *Miner. Eng.* **7**, 1213-1241.

Leventhal, J. and Giordano, T. (2000) The nature and roles of organic matter associated with ores and ore-forming systems: An introduction. *Rev. Econ. Geol* **9**, 1-26.

Lewis, G. and Shaw III, C.F. (1986) Competition of thiols and cyanide for gold (I). *Inorg. Chem.* **25**, 58-62.

Liu, J., Fu, J. and Lu, J. (1993) Experimental study on interaction between organic matter and gold. *'Sci. Geol. Sin.' In Chinese.* **28**, 246-253.

Liu, W., Etschmann, B., Testemale, D., Hazemann, J.-L., Rempel, K., Müller, H. and Brugger, J. (2014) Gold transport in hydrothermal fluids: Competition among the Cl^-, Br^-, HS^- and NH_3(aq) ligands. *Chem. Geol.* **376**, 11-19.

Manning, D.A. and Giże, A.P. (1993) The role of organic matter in ore transport processes, Org. Geochem. Springer, pp. 547-563.

Mastalerz, M., Bustin, R., Sinclair, A., Stankiewicz, B. and Thomson, M. (2000) Implications of hydrocarbons in gold-bearing epithermal systems: Selected examples from the Canadian Cordillera, Organic Matter and Mineralisation: Thermal Alteration, Hydrocarbon Generation and Role in Metallogenesis. Springer, pp. 359-377.

Mauk, J.L. and Hieshima, G. (1992) Organic matter and copper mineralization at White Pine, Michigan, USA. *Chem. Geol.* **99**, 189-211.

Mei, Y., Liu, W., Brugger, J., Migdisov, A.A. and Williams-Jones, A.E. (2017) Hydration Is the Key for Gold Transport in CO2–HCl–H2O Vapor. *ACS Earth and Space Chemistry*.

Migdisov, A., Guo, X., Williams-Jones, A., Sun, C., Vasyukova, O., Sugiyama, I., Fuchs, S., Pearce, K. and Roback, R. (2017) Hydrocarbons as ore fluids. *Geochem. Persp. Lett.* **5**, 47-52.

Mirasol-Robert, A., Grotheer, H., Bourdet, J., Suvorova, A., Grice, K., McCuaig, T.C. and Greenwood, P.F. (2017) Evidence and origin of different types of sedimentary organic matter from a Paleoproterozoic orogenic Au deposit. *Precambrian Research* **299**, 319-338.

Murphy, P. and LaGrange, M. (1998) Raman spectroscopy of gold chloro-hydroxy speciation in fluids at ambient temperature and pressure: a re-evaluation of the effects of pH and chloride concentration. *Geochim. Cosmochim. Acta* **62**, 3515-3526.

Murphy, P.J., Stevens, G. and LaGrange, M.S. (2000) The effects of temperature and pressure on gold-chloride speciation in hydrothermal fluids: A Raman spectroscopic study. *Geochim. Cosmochim. Acta* **64**, 479-494.

Ning, C.-G., Xiong, X.-G., Wang, Y.-L., Li, J. and Wang, L.-S. (2012) Probing the electronic structure and chemical bonding of the "staple" motifs of thiolate gold nanoparticles: Au (SCH 3) 2− and Au 2 (SCH 3) 3−. *Phys. Chem. Chem. Phys.* **14**, 9323-9329.

Parnell, J. (1988) Metal Enrichments in Solid Bitumens - a Review. *Miner. Deposita* **23**, 191-199.

Pearcy, E. and Burruss, R. (1993) Hydrocarbons and gold mineralization in the hot-spring deposit at Cherry Hill, California, Bitumens in Ore Deposits. Springer, pp. 117-137.

Pearson, R.G. (1968) Hard and soft acids and bases, HSAB, part 1: Fundamental principles. *J. chem. Educ* **45**, 581.

Pokrovski, G.S., Akinfiev, N.N., Borisova, A.Y., Zotov, A.V. and Kouzmanov, K. (2014) Gold speciation and transport in geological fluids: insights from experiments and physical-chemical modelling. *Geol. Soc. Spec. Publ.* **402(1)**, 9-70.

Pokrovski, G.S., Tagirov, B.R., Schott, J., Bazarkina, E.F., Hazermann, J.L. and Proux, O. (2009a) An in situ X-ray absorption spectroscopy study of gold-chloride complexing in hydrothermal fluids. *Chem. Geol.* **259**, 17-29.

Pokrovski, G.S., Tagirov, B.R., Schott, J., Hazemann, J.L. and Proux, O. (2009b) A new view on gold speciation in sulfur-bearing hydrothermal fluids from in situ X-ray absorption spectroscopy and quantum-chemical modeling. *Geochim. Cosmochim. Acta* **73**, 5406-5427.

Radtke, A.S. and Scheiner, B.J. (1970) Studies of hydrothermal gold deposition - (pt.) 1, carlin gold deposit, nevada, the role of carbonaceous materials in gold deposition. *Econ. Geol.* **65**, 87-102.

Renders, P. and Seward, T. (1989) The stability of hydrosulphido-and sulphido-complexes of Au (I) and Ag (I) at 25 C. *Geochim. Cosmochim. Acta* **53**, 245-253.

Robbins, W. K., & Hsu, C. S. (2000). Petroleum, Composition. *Kirk-Othmer Encyclopedia of Chem. Technology*.

Robert, A.M., Grotheer, H., Greenwood, P.F., McCuaig, T.C., Bourdet, J. and Grice, K. (2016) The hydropyrolysis (HyPy) release of hydrocarbon products from a high maturity kerogen associated with an orogenic Au deposit and their relationship to the mineral matrix. *Chem. Geol.* **425**, 127-144.

Samedova, F., Guseinova, B., Kuliev, A. and Alieva, F. (2009) Trace elements in crude oil from some new South Caspian oil fields. *Petroleum Chemistry* **49**, 288-291.

Saxby, J. (1976) The significance of organic matter in ore genesis. *Handbook of strata-bound and stratiform ore deposits* **2**, 111-133.

Seward, T. (1993) The hydrothermal geochemistry of gold, Gold metallogeny and exploration. Springer, pp. 37-62.

Seward, T., Williams-Jones, A. and Migdisov, A. (2014) 13.2 The Chemistry of Metal Transport and Deposition by Ore-Forming Hydrothermal Fluids. *Treatise on Geochemistry (Second Edition), Elsevier, Oxford*, 29-57.

Seward, T.M. (1973) Thio complexes of gold and the transport of gold in hydrothermal ore solutions. *Geochim. Cosmochim. Acta* **37**, 379-399.

Shenberger, D.M. and Barnes, H.L. (1989) Solubility of gold in aqueous sulfide solutions from 150 to 350°C. *Geochim. Cosmochim. Acta* **53**, 269-278.

Sherlock, R. (1992) The empirical relationship between gold-mercury mineralization and hydrocarbons, in the northern Coast Ranges, California, GAC-MAC Joint Annual Meeting, Program with Abstracts.

Sherlock, R. (2000) The association of gold—mercury mineralization and hydrocarbons in the coast ranges of northern California, Organic Matter and Mineralisation: Thermal Alteration, Hydrocarbon Generation and Role in Metallogenesis. Springer, pp. 378-399.

Sicree, A.A. and Barnes, H.L. (1996) Upper Mississippi Valley district ore fluid model: the role of organic complexes. *Ore Geol. Rev.* **11**, 105-131.

Stefánsson, A. and Seward, T. (2004) Gold (I) complexing in aqueous sulphide solutions to 500 C at 500 bar. *Geochim. Cosmochim. Acta* **68**, 4121-4143.

Sun, Y., Jiao, W., Zhang, S. and Qin, S. (2009) Gold enrichment mechanism in crude oils and source rocks in Jiyang Depression. *Energ. Explor. Exploit.* **27**, 133-142.

Ta, C., Reith, F., Brugger, J.l., Pring, A. and Lenehan, C.E. (2014) Analysis of gold (I/III)-complexes by HPLC-ICP-MS demonstrates gold (III) stability in surface waters. *Environ. Sci. Technol.* **48**, 5737-5744.

Tissot, B. and Welte, D. (1978) The fate of organic matter in sedimentary basins: generation of oil and gas. *Petroleum Formation and Occurrence*, 69-253.

Tagirov, B.R., Salvi, S., Schott, J. and Baranova, N.N. (2005) Experimental study of gold-hydrosulphide complexing in aqueous solutions at 350–500°C, 500 and 1000 bars using mineral buffers. *Geochim. Cosmochim. Acta* **69**, 2119-2132.

Usher, A., McPhail, D.C. and Brugger, J. (2009) A spectrophotometric study of aqueous Au(III) halide–hydroxide complexes at 25–80 °C. *Geochim. Cosmochim. Acta* **73**, 3359-3380.

Vlassopoulos, D., Wood, S.A. and Mucci, A. (1990) Gold speciation in natural waters: II. The importance of organic complexing—Experiments with some simple model ligands. *Geochim. Cosmochim. Acta* **54**, 1575-1586.

Williams-Jones, A. and Migdisov, A. (2007) The solubility of gold in crude oil: implications for ore genesis, Proceedings of the 9th Biennal SGA Meeting, Millpress, Dublin, pp. 765-768.

Williams-Jones, A.E., Bowell, R.J. and Migdisov, A.A. (2009) Gold in solution. *Elements* **5**, 281-287.

Wood, S. (1996) The role of humic substances in the transport and fixation of metals of economic interest (Au, Pt, Pd, U, V). *Ore Geol. Rev.* **11**, 1-31.

Zammit, C.M., Weiland, F., Brugger, J., Wade, B., Winderbaum, L.J., Nies, D.H., Southam, G., Hoffmann, P. and Reith, F. (2016) Proteomic responses to gold (III)-toxicity in the bacterium Cupriavidus metallidurans CH34. *Metallomics* **8**, 1204-1216.

Zezin, D.Y., Migdisov, A.A. and Williams-Jones, A.E. (2007) The solubility of gold in hydrogen sulfide gas: An experimental study. *Geochim. Cosmochim. Acta* **71**, 3070-3081.

Zezin, D.Y., Migdisov, A.A. and Williams-Jones, A.E. (2011) The solubility of gold in H2O–H2S vapour at elevated temperature and pressure. *Geochim. Cosmochim. Acta* **75**, 5140-5153.

Zhuang, H.P., Lu, J.L., Fu, J.M., Ren, C.G. and Zou, D.G. (1999) Crude oil as carrier of gold: petrological and geochemical evidence from Lannigou gold deposit in southwestern Guizhou, China. *Sci. China Ser. D* **42**, 216-224.

Copyright statement

Every reasonable effort has been made to acknowledge the owners of copyright material. I would be pleased to hear from any copyright owner who has been omitted or incorrectly acknowledged.

Chapter 4

Crude oil as ore fluids: an experimental *in-situ* XAS study of gold partitioning between brine and organic fluid from 25 to 250 °C

Lars-S. Crede, Weihua Liu, Katy A. Evans, Kirsten U. Rempel, Denis Testemale, Joël Brugger

A modified version of this chapter was published with Geochimica et Cosmochimica et Acta (https://doi.org/10.1016/j.gca.2018.10.007)

Abstract

Organic matter is often associated with mineralization in hydrothermal ore deposits. One hypothesis is that this organic matter represents remnants of organic fluids (crude oils) that were competing with aqueous fluids for metal transport and contributed to metal endowment. We investigated the transport of gold (Au) in model oil compounds (S-free *n*-dodecane, $CH_3(CH_2)_{10}CH_3$, DD; and S-bearing 1-dodecanethiol, $CH_3(CH_2)_{10}CH_2SH$; DDT) from 25 °C to 250 °C using *in-situ* synchrotron X-ray absorption spectroscopy (XAS) experiments to determine the speciation and the structural properties of gold complexes in the aqueous- and oil-based fluids. For most experiments, DD or DDT were in contact with Au-bearing acidified water, or acidified water plus 10 wt% NaCl ($pH_{25°C}$=1.85 in both cases). Gold rapidly partitioned from the aqueous phase into DD and DDT. Below 125 °C, Au(III)Cl is dominant in the DD and the adjacent water with a refined coordination number (CN) of chloride of 4.0(3) and an Au-Cl bond length of 2.28 Å, consistent with the tetrachloroaurate complex ($AuCl_4^-$) being stable in both the aqueous and organic phases. In contrast, Au(III) is rapidly reduced in the presence of DDT and an Au(I) complex dominates in both water and adjacent DDT with a CN of sulfur ~2.0, suggesting a $[RS\text{-}Au\text{-}SR]^-$ (RS = DDT with deprotonated thiol group) complex with Au-S bond lengths ranging from 2.29(1) Å to 2.31(3) Å. In an open system of DDT in contact with water, of which the water and DDT were analyzed separately, $AuCl_4^-$ was dominant in the water phase, and $Au(RS)_2^-$ dominant in DDT, possibly due to different equilibration kinetics in the beaker and glassy carbon tube.

Since sulfur and organothiol compounds are ubiquitous and abundant components in natural oils, this study demonstrates the potential of natural oils to scavenge and enrich gold from co-existing gold-bearing brines. In particular, Au(I) organothiol complexes may contribute to transport in low-temperature (<125 °C) ore fluids such as those in basinal environments – in both hydrothermal fluids and oils. At temperatures ≥ 125 °C, gold was reduced to metallic gold in all experiments, suggesting that organo-stabilized nanoparticles may be the major form of gold to be scavenged, concentrated or transported in crude oils at these conditions. The results imply that brine-oil interactions may enrich Au in oils, and that oils may be an effective ore fluid in sedimentary environments.

4.1 Introduction

Organic matter is a common constituent in many types of ore deposits, including epithermal Au-Ag(-Hg) deposits (Sherlock, 1992; Pearcy and Burruss, 1993; Mastalerz et al., 2000; Sherlock, 2000); Carlin-type Au deposits (Radtke and Scheiner, 1970; Hausen and Park, 1986; Emsbo and Koenig, 2007; Gu et al., 2012; Groves et al., 2016); orogenic Au deposits (Mirasol-Robert et al., 2017); Mississippi Valley-type Pb-Zn deposits (e.g., Parnell, 1988; Giże and Barnes, 1989; Kesler et al., 1994), 'Kupferschiefer' copper deposits (e.g., Kucha, 1981; Kucha and Przylowicz, 1999; Sawlowicz et al., 2000), sediment-hosted U deposits (Landais, 1996; Spirakis, 1996), and Witwatersrand-type Au-U deposits (Fuchs et al., 2016), but the significance of this occurrence for ore-forming processes remains poorly understood and controversial (e.g., Manning and Giże, 1993; Parnell et al., 1993; Gize, 1999; Giże et al., 2000; Greenwood et al., 2013; Groves et al., 2016). Organic matter is often interpreted to act as a redox barrier for metal deposition (e.g., Radtke and Scheiner, 1970; Giże, 2000; Glikson and Mastalerz, 2000; Sherlock, 2000). However, a few studies challenge the consensus that aqueous fluids are the only medium responsible for metal transport and deposition in sedimentary basins, and suggest that hydrocarbon/petroleum may contribute to Au transport in some sediment-hosted gold deposits, including World-class Carlin-type gold deposits in Nevada, USA (Emsbo and Koenig, 2007) and in South China (Zhuang et al., 1999; Sun et al., 2009; Gu et al., 2012). Just recently, Migdisov et al. (2017) demonstrated experimentally that natural crude oils have the ability to mobilize metals (Zn, Au) from source rocks, and transport them in concentrations sufficient to contribute to ore-forming processes. Further understanding the capacity of organic-based fluids to mobilize metals is not only important for mineral exploration, it is key information for assessing the cycling of metals in the Earth's crust.

Since aqueous hydrothermal fluids are expected to form most economic gold deposits within the Earth's crust (Pokrovski et al. 2014), and chloride and hydrosulfide are the most abundant ligands in these fluids (Brugger et al., 2016), a large number of experimental studies have focused on the geochemical behavior of gold in aqueous hydrothermal chloride- and sulfide-bearing hydrothermal fluids (e.g., Henley, 1973; Seward, 1973; Renders and Seward, 1989; Shenberger and Barnes, 1989; Hayashi and Ohmoto, 1991; Seward, 1993; Gammons and Williams-Jones, 1995; Benning and Seward, 1996; Gammons et al., 1997; Murphy and LaGrange, 1998; Murphy et al., 2000; Stefánsson and Seward, 2004; Tagirov et al., 2005;

Pokrovski et al., 2009a; Pokrovski et al., 2009b; Pokrovski et al., 2014). These experiments give a broad consensus that gold hydrosulfide complexes predominate in acidic to neutral sulfur-bearing aqueous fluids up to 350 °C, and that chloride gold complexes can become important above 350 °C in sulfur-poor acidic fluids (Williams-Jones et al., 2009; Zhong et al., 2015).

Despite the common association of gold and organic matter, only a few experimental studies have investigated the solubility of gold in oils and/or the partitioning of gold between aqueous and oil-based liquids (Liu et al., 1993; Lu and Zhuang, 1996; Zhuang et al., 1999; Williams-Jones and Migdisov, 2007; Emsbo et al., 2009; Fuchs et al., 2011). Aside from Migdisov et al. (2017), all of these studies are preliminary, and none investigated the speciation or possible ligands of gold in oils. Apart from metal porphyrin complexes (Figure 4-1), that are especially relevant for Ni and V, there is little data available for metal-organic species in nature (Maryutina and Timerbaev, 2017). However, a number of species that are stable in aqueous fluids may be relevant for gold: carboxyl (-COOH), phenolic hydroxyl (-OH), amino ($-NH_2$), and thiol (-SH) groups (Figure 4-1) are known to form metal-organic complexes in aqueous solution (Giordano, 2000 and references therein), and as they are present in crude oil, they may contribute to metal and in particular gold transport in the organic phase. The capacity of organic-rich fluids to carry gold is also supported by a positive correlation of gold and hetero-compounds enriched in N, S, O in crude oil samples from the Jiyang Depression in the Shandong province, China (Sun et al., 2009).

The Au^+ ion is classified as a soft Lewis acid that forms complexes with soft, easily polarizable ligands (Pearson, 1968). Consequently, Au(I) bonds strongly with CN^-, which is produced by some plants and microorganisms (Fairbrother et al., 2009), and with S-bearing functional groups, and then, with decreasing effectiveness, with nitrogen (e.g., amine) and oxygen (Vlassopoulos et al., 1990; Wood, 1996; Liu et al., 2014; Ta et al., 2014). Bonds with thiols (Figure 4-1), thiomalate, and thioglucose are the main gold-active species in biological systems (Cotton and Wilkinson, 1988; Giże, 2000; Etschmann et al., 2016; Zammit et al., 2016), and Au(I) cyanide complexes have been shown to survive for extended periods of time in environmental surface waters (Ta et al., 2014), rendering CN^- a potential ligand for gold transport.

Another possibility for gold transport in organic ore fluids is *via* gold nanoparticles (AuNP). Organothiols have long been used to stabilize and passivate AuNPs (e.g., Weisbecker

et al., 1996; Edinger et al., 1997; Fink et al., 1998; Lavrich et al., 1998; Brust and Kiely, 2002; Daniel and Astruc, 2004; Häkkinen, 2012; Lohman et al., 2012; Ansar et al., 2013; Alex and Tiwari, 2015), and the role of AuNPs as a potentially critical factor for metal migration in the environment and the formation of ore deposits is attracting increasing attention (Reith et al., 2010; Hough et al., 2011, and references therein; Reith and Cornelis, 2017; Shuster et al., 2017).

The aim of this study is to investigate gold speciation and complexation in crude oils in contact with aqueous solutions by *in-situ* XAS spectroscopy to identify potential gold ligands in oils and the effect of two competing liquids at low temperatures (25 °C to 200 °C). To represent the many types of organic groups that exist in the oil, we chose the model compounds *n*-dodecane ($CH_3(CH_2)_{10}CH_3$) and 1-dodecanethiol ($CH_3(CH_2)_{10}CH_2SH$; Figure 4-1) as they are common components of crude oils. XAS spectroscopy has been successfully applied in previous work to identify and characterize the molecular-level structure of aqueous gold species with inorganic ligands such as Cl^-, Br^-, HS^- and NH_3 in aqueous hydrothermal fluids (Pokrovski et al., 2009a; Pokrovski et al., 2009b; Liu et al., 2014). As in chapter 3, thiols were chosen for the experiments in contrast to the more abundant thiophenes, due to their better experimental suitability and health and safety properties. Di-benzothiophene was tried but solidified during the experiment and destroyed the glassy carbon capsule.

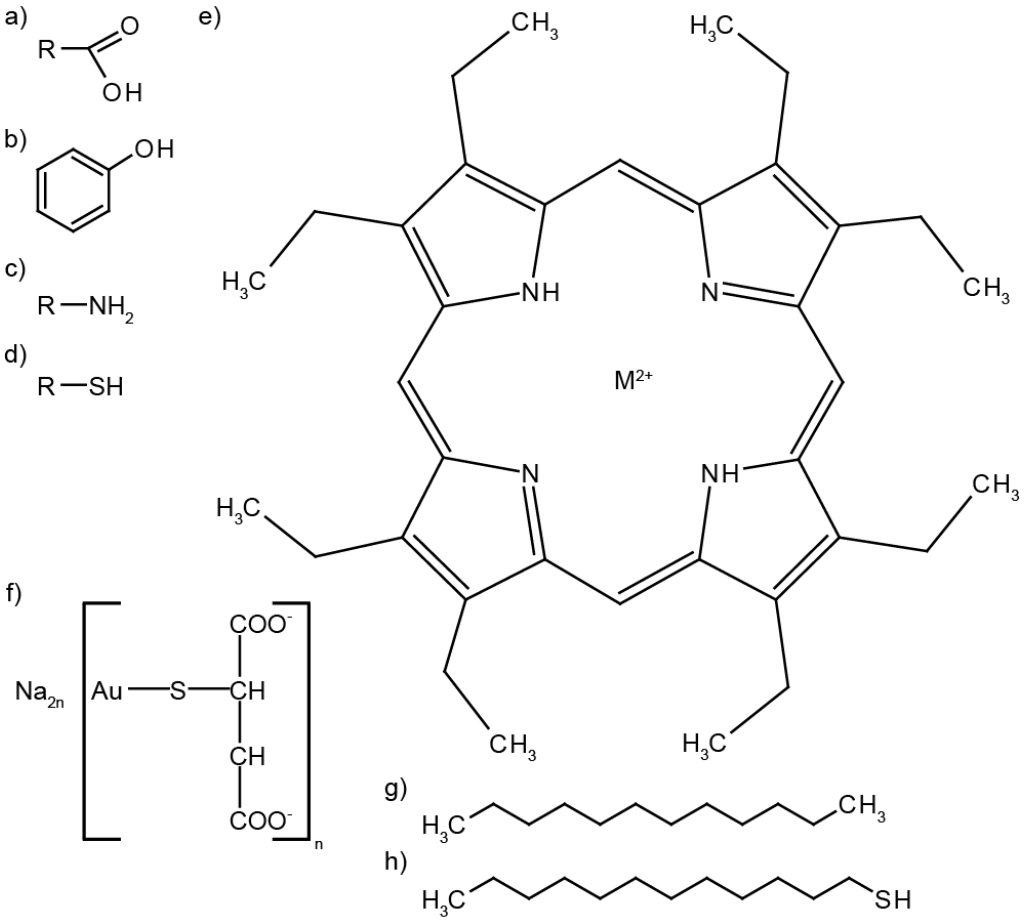

Figure 4-1: Some of the ligands that can form metal organic complexes. (a) carboxyls; (b) phenolic hydroxyls; (c) amino groups; (d) thiol; (e) metal porphyrin complex, and the compounds of this study: sodium aurothiomalate (f), n-dodecane (g) and 1-dodecanethiol (h).

4.2 Experimental

4.2.1 Sample preparation

The aqueous solutions were prepared by adding Au(III) chloride powder ($HAuCl_4 \bullet 3H_2O$) to three aqueous solutions: either pure water (Milli-Pore grade), water acidified to $pH_{25^\circ C}$ = 1.85 using HCl, or an acidified brine plus 10 wt% NaCl ($pH_{25^\circ C}$ = 1.85). Each aqueous solution was simultaneously loaded with *n*-dodecane (99%) or 1-dodecanethiol (98%) directly into either a glassy carbon cell for XAS measurement, or into a beaker, from which the aqueous solution and the oil were sampled separately and individually measured by XAS. The aqueous solutions and the oils do not mix and were density-stratified within one hour, allowing collection of XANES (X-ray absorption near edge structure) and EXAFS (extended X-ray absorption fine structure) spectra from both liquids in the same experiment. The oils and adjacent aqueous phase were distinguishable under the X-ray beam by the difference in absorbance, except for the DDT and brine solutions, which have similar

absorption coefficients (Table 4-1). DD plus brine experiments were only conducted in the beaker, and thus DD and the brine were sampled and measured separately in glassy carbon tubes, that were open at the top.

Table 4-1: Absorption lengths ($L_{\mu=1}$) at 11.85 keV

Composition	Density [g/cm^3]	$L_{\mu=1}$ [cm]
H_2O	1.00	0.308
H_2O + 10wt% NaCl	1.069	0.172
n-dodecane	0.749	0.765
1-dodecanethiol	0.845	0.168

XAS standards were a sodium aurothiomalate(I) ($C_4H_3AuNa_2O_4S$, Figure 4-1) solution chosen to represent the Au-S bond; a 2% solution of gold nanoparticles stabilized by *n*-dodecanethiol in toluene; and a metallic gold foil to represent Au(0). Sodium aurothiomalate(I) dissociates into a gold(I) thiomalate complex (Bau, 1998) and free sodium ions in aqueous solution. Dissolved aurothiomalate retains to some degree the structure of crystalline aurothiomalate(I) (Grootveld and Sadler, 1983; Graham et al., 1985; Bau, 1998), and Elder and Eidsness (1987) suggest that the solid-state chain structure is maintained in solution.

4.2.2 XAS measurements and data treatment

Gold L_{III}-edge XANES and EXAFS spectra were measured at the FAME (BM-30B) beamline, at the European Synchrotron Research Facility (ESRF) in Grenoble, France. The ESRF has a 6.03 GeV ring, and when operating in 7/8 multi-bunch mode, it has a maximum current of 200 mA. FAME is a bending magnet beamline with a double crystal Si(220) monochromator, and an energy resolution of 0.61 eV at the Au L3-edge (Proux et al., 2005). A focused beam size of FWHM 300 × 150 µm^2 was used.

Silicon diodes were used to measure the incident and transmitted beam intensities, and a 30-element solid-state fluorescence detector (Canberra) was used for detecting fluorescence data. The maximum of the first derivative was set to 11.919 keV by calibrating the energy with a metallic gold foil. The high T–P cell developed by the CNRS (Testemale et al., 2005) was used for data collection. As described in Etschmann et al. (2010) and Liu et al. (2011), the temperature at the beam position was calibrated using measurements of the

density of water. Measurements were conducted 1–5 hours after sample solutions had been prepared to allow full unmixing of organic and aqueous fluids. Spectra for each sample solution were collected from at least four vertical positions, from the top to the bottom of the solutions, to investigate gold in the aqueous liquid and in the oil (when both were loaded). Experiments all started at 30 °C and progressively heated to 250 °C; pressures ranged from 1 to 600 bar, but the pressure was found to have no effect other than reducing measurement noise in some solutions.

The XANES and EXAFS data were processed and refined using the HORAE package (Ravel and Newville, 2005) with the theoretical standards calculated by FEFF6 (Zabinsky et al., 1995). The k^3-weighted data were refined in R space. For the DDT solutions, optimum fits were obtained for a fitting range of 1 to 3.5 Å in R-space. For DD, the best fits were obtained for a fitting range of 1 to 5 Å. The range chosen for the Fourier transformation from k to R space was selected depending on data quality (Table 4-3). The amplitude-reduction factor (S_0^2) of 0.82 was obtained by fitting the known structure of gold(I) thiomalate (Bau, 1998) to the spectrum of a gold(I) thiomalate solution, and was used to fit all sample spectra. The fits included the first 5 scattering paths, and the fitting results are listed in Table 4-3.

4.3 Results

The first spectrum for each experiment was collected at 30 °C in all solutions. Gold partitioned rapidly (within less than one hour) from the aqueous phase into DD and DDT (Figure 4-2; more details in sections 3.2 and 3.3). At this point the Au-L_{III}-edge spectra was measured in both the organic and the aqueous phase. Figure 4-2 shows the yellow coloration of aqueous solution containing $AuCl_4^-$ (Au^{III}, t=0 h; Usher et al. 2009) and the disappearance of this yellow color after adding DDT and waiting for t=24 h, while the added, former colorless, DDT turns slightly yellow. The Au L_{III}-edge XANES and EXAFS spectra were collected at various temperatures and pressures (30-250 ˚C and 1-600 bar) for *n*-dodecane (99%, DD) or 1-dodecanethiol (98%, DDT) coexisting with H_2O, or with H_2O and NaCl. Sample compositions are listed in Table 4-2.

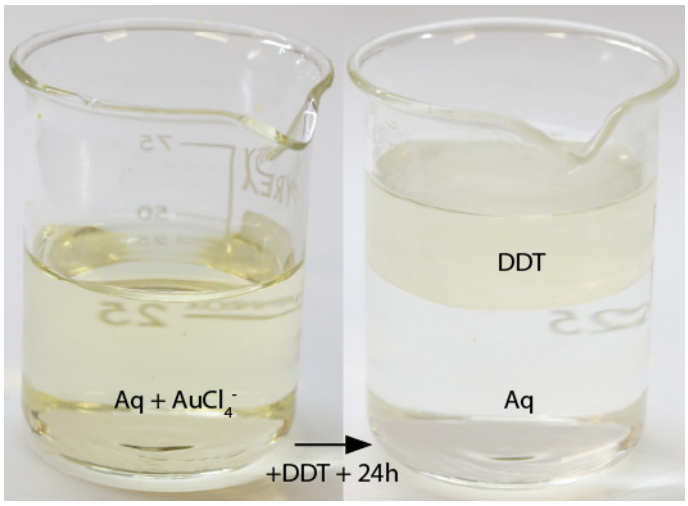

Figure 4-2: Water with $AuCl_{4\,(aq)}^-$ (left; t = 0) and its change in color after adding DDT, right image taken at t = 24 h.

Table 4-2: Starting compositions and measurement conditions of experimental solutions

Sample	Starting Compositions	Conditions
Au-thiomalate std	49.2 m*m*[a] $C_4H_3AuNa_2O_4S$ in H_2O	30-150 °C, 600 bar
S7 $_{AuNP\ standard}$	2.5 ml DDT+ 0.25 ml *n*-Dodecanethiol gold nanoparticles[d]	30-250 °C, 15-400 bar
S11	10.2 m*m* $AuCl_3$ in H_2O + DDT	30-70 °C, 1-200 bar
S13	10.2 m*m* $AuCl_3$ in H_2O, $pH_{25°C}$=1.85[b] + DDT	30-125 °C, 1-400 bar
S14	10.2 m*m*$AuCl_3$ in H_2O, $pH_{25°C}$=1.85[b] + DD	30-130 °C, 15-200 bar
S16	39.8 m*m* $AuCl_3$ + 1.74 *m* NaCl[c] in H_2O, $pH_{25°C}$=1.85[b] + DDT	30-130 °C, 1-400 bar
S17	39.8 m*m* $AuCl_3$ + 1.74 *m* NaCl[c] in H_2O, $pH_{25°C}$=1.85[b] + DDT	30-130 °C, 1-200 bar
S18	DDT sampled from beaker, composition = S16	30-150 °C, 1bar
S19	Brine sampled from beaker, composition = S16	30 °C, 2 bar

[a] milli molal; [b] adjusted with HCl; [c] equals 10wt% NaCl in the aqueous phase;[d] 2% solution in toluene.

4.3.1 XANES spectra for Au references

The Au L_{III}-edge XANES spectra for representative solutions and standards are plotted in Figure 4-3. Two examples of the changes in XANES spectra changes with increasing temperature are shown in Figure 4-4. The XANES spectrum of the solid gold(I) thiomalate standard was identical to that of the gold(I) thiomalate (Au-thiomalate std) in solution and is thus not shown. The gold(I) thiomalate standard is representative of Au(I) complexes and Au-S bonds with an alkyl chain attached to the S and a Au : S ratio of 1 : 2, and thus a CN for S of 2. The XANES spectrum of gold(I) thiomalate shows a small peak at ~11922 eV (band I) and a small peak at ~11929 eV (band II). The XANES spectrum of the AuNP standard solution ($S7_{AuNP}$) is similar to that collected for the metallic gold foil, though it exhibits a less pronounced peak at 11945 eV, which reflects the state of Au on the surface of the foil, and in particular, capping by thio-groups from DDT molecules (Zhang and Sham, 2002).

4.3.2 1-Dodecanethiol (DDT) – water system < 125 °C

The absorbance of the DDT and the aqueous liquid (with and without NaCl) and the gold fluorescence signal intensity across the two solutions were determined to identify spectra derived from the DDT and the aqueous liquid, and to qualitatively determine the gold distribution between the two liquids. Absorbance measurements were made before collection of the first XANES spectrum and a maximum of ~2h after the solutions were prepared and loaded into the carbon cell. Gold was found to be present in DDT and the aqueous phase, with a 5 to 6 times higher step height at the AuL_{III}-edge in the DDT than in the aqueous liquid.

All XANES spectra collected for the samples with DDT in contact with the aqueous solution with and without NaCl (10 wt%) display similar sequences of spectra at temperatures between 30 °C to 125 °C in DDT and in the adjacent aqueous phase (Figure 4-3, Figure 4-4 a; S11, S13, S16, S18). At temperatures below 125 °C all the spectra resemble the spectrum of the gold(I) thiomalate standard, with a small peak at ~11922 eV (band I) and a small peak at ~11929 eV (band II). It is also notable that the second peak (edge energy position) in all the solution XANES spectra and Au(I) thiomalate is located at 11929 eV, which is a 2 eV shift relative to the position of the second peak (11927 eV) in the $Au(HS)_2^-$ complex, so these spectra are distinct from that of $Au(HS)_2^-$. The edge energy position is shifted to slightly lower eV compared to that of the Au foil and the AuNPs. The gold(I) thiomalate resemblance suggests a Au complex in the DDT experiments that is similar to that of an $Au(RS)_2^-$ complex, where RS symbolizes DDT with a deprotonated thiol group. The same spectral observations in DDT and in the adjacent aqueous phase indicate the same gold complex in both liquids.

Since DDT and the brine have similar absorption coefficients (Table 4-1), it was not possible to identify the analyzed liquid in experiments S16 and S17. However, all XANES spectra across the sample profile resemble the gold(I) thiomalate, and are very different from the XANES spectrum of $Au(HS)_2^-$(Figure 4-3 and 4a).

4.3.3 Open system DDT – brine solution

A XANES spectrum identical to that of $AuCl_4^-$ was collected in the brine (S19) that was sampled and analyzed individually from a brineDDT solution in an open beaker. This is in

contrast with an Au(I) thiomalate-like spectrum measured in the aqueous liquid (S11) that was in direct contact with the DDT in the glassy carbon cell. The XANES spectrum of S19 (Figure 4-3) shows a sharp pre-edge feature at ~11920 eV that rises above the post-edge feature region and is in agreement with the spectra reported for $AuCl_4^-$ in Pokrovski et al. (2009a) and Liu et al. (2014). The spectrum of the $AuCl_4^-$ complex has an intense peak at this energy due to the 2p-5d transition (Berrodier et al., 2004).

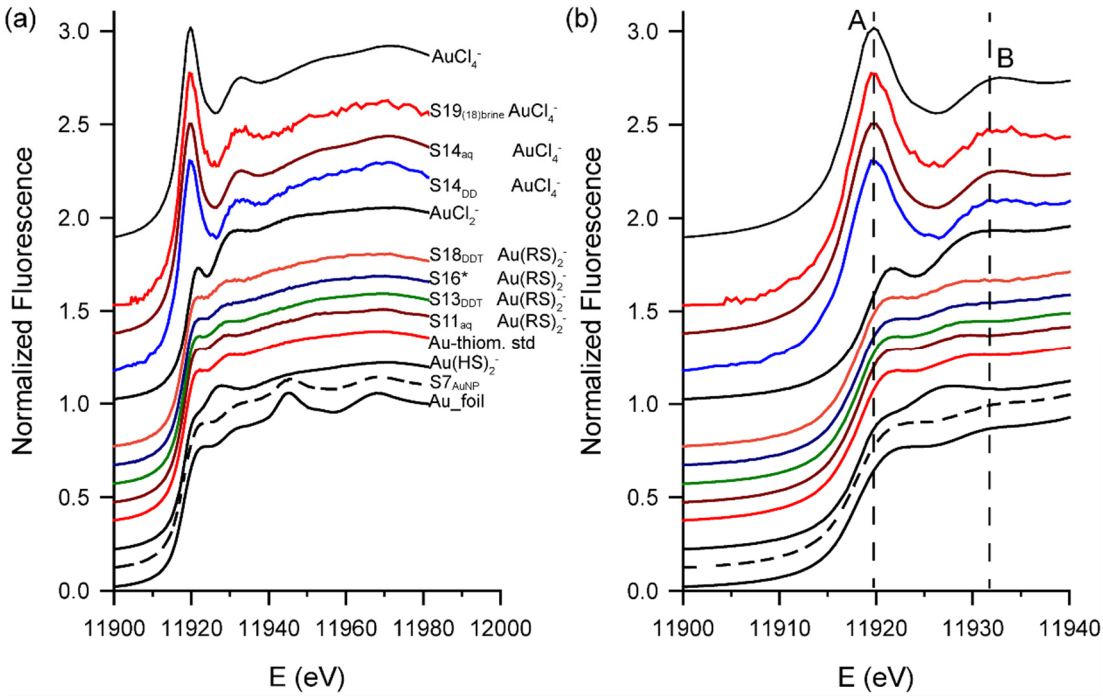

Figure 4-3: Normalized Au L_3-edge XANES spectra of the solutions and the complexes they resemble, shown labelled in (a) and the same (b) on a different scale to emphasize the pre-edge (A) and edge (B) energy position (right dashed line to aid the eye, as it is not always at the edge). The $AuCl_2^-$ spectrum is from Pokrovski et al. (2009a). The $Au(HS)_2^-$ and the $AuCl_4^-$ spectra are from Liu et al. (2014). S7 at 100 °C; S11, S13, and S19 at 30 °C; S14 at 75 °C; S16 at 70 °C; S18 at 100 °C. The subscript abbreviations indicate whether the spectrum was collected in water (aq), brine, n-dodecane (DD), 1-dodecanethiol (DDT), or if the phase was unclear (*).

Table 4-3: EXAFS model parameters

Fit EXAFS parameters for selected sample spectra. N: ligand number; R: bond length (Å); σ^2: magnitude scale factor; χ^2_{red}: reduced chi-squared parameter.

Solution	T (°C)	Ligand	N	R (Å)	σ^2 x 10^3	χ^2_{red}	k weight	Data range ($Å^{-1}$)
Au-thiomalate std	30	S	2 (fix)	2.31(3)	2.8(5)	5.1	3	2-12.3
$S11_{aq}$	30	S	2.59 ± 0.41	2.30(4)	5.2(1)	2.05	3	2-11
$S13_{DDT}$	30	S	1.83 ± 0.30	2.29(1)	0.9(1)	19.9	3	2-11.2
S16*	70	S	1.60 ± 0.50	2.30(2)	0.2(5)	20.3	3	2-11
S17*	30	S	2.31 ± 0.45	2.29(3)	2.0(2)	17	3	2-11
$S14_{DD}$	75	Cl	4.36 ± 0.77	2.27(6)	2.0(0)	5.62	3	2-10
$S14_{aq}$	75	Cl	3.94 ± 0.34	2.280(3)	2.0(1)	55.81	3	2-11.5

*not clear if DDT or brine was analyzed.

4.3.4 *n*-Dodecane (DD) – water system < 125 °C

The step height at the L_{III}-edge was found to be ~50 times smaller in DD than in the adjacent aqueous phase. All XANES spectra collected in DD and in the adjacent water and/or brine below ~125 °C resemble that of the $AuCl_4^-$ complex (S14, Figure 4-3) with a peak at ~11920 eV rising above the post-edge region and a small peak at 11932 eV.

4.3.5 Metallic gold

At 125 ˚C and 130 °C, the X-ray-absorption at the Au-edge of all sample solutions (DD, DDT, water, and water plus NaCl, from all experiments) decreased and exhibit an increase in signal noise (Figure 4-4a). This was accompanied by the disappearance of features representative of Au(I) and Au(III) complexes ($Au(RS)_2^-$ and $AuCl_4^-$), and the concurrent appearance of features characteristic for metallic gold in the Au XANES spectra in DD, DDT, water, and water plus NaCl (Figure 4-3 and Figure 4-4).

The time periods between spectrum collection at 30 °C and 125 °C/130 °C for solutions 11, 13, 14, 16, 17, and 18 were 5 h, 7 h, 7 h, 8 h, 6 h, and 3.5 h respectively. Features representative of metallic gold appeared in the first spectrum collected at 125 °C/130 °C, with the only time delay between inserting the loaded glassy carbon tube and the first measurement being the beam position adjustment in the above named solutions 11 to 17. Features typical of metallic gold did not appear in S18 until the second spectrum was collected– there was a delay of 30 min at 130 °C under the X-ray beam between the last

$AuCl_4^-$ like spectrum and the first Au(0)-spectrum. After heating to 130 °C in the DD-water experiment (S14), which had produced only Au(III) spectra below 130 °C, no intermediate Au(I) complexes (e.g., $AuCl_2^-$) were detected at any point in time between collection of the last Au(III) spectrum and the first Au(0) spectrum. This result is consistent with the results of a Raman study by Murphy et al. (2000), where metallic gold precipitated at 250 °C from an $AuCl_4^-$ solution, without a detectable intermediate stage of reduction to $Au(I)Cl_2^-$.

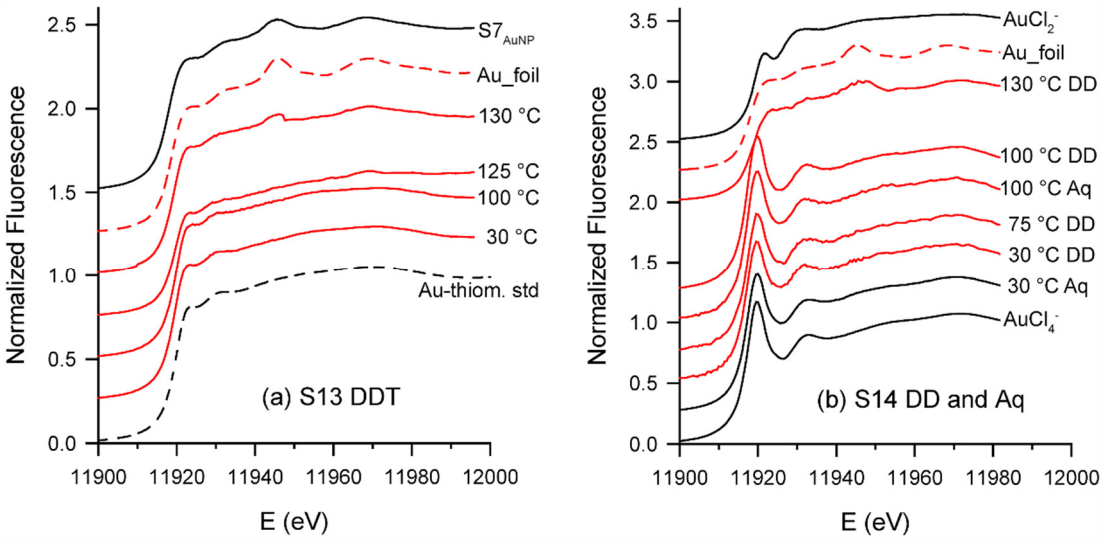

Figure 4-4: The change in Au L_{III}-edge XANES spectra for S13 in DDT (a) and for S14 in DD and the aqueous phase (b) with increasing temperatures and the appearance of Au(0) at 130 °C. The $AuCl_2^-$ spectrum is from Pokrovski et al. (2009a), and the $AuCl_4^-$ spectrum is from Liu et al. (2014).

4.3.6 EXAFS

The results of the EXAFS refinement of selected spectra are given in Table 4-3, and the fitted spectra of the k^3 weighted EXAFS data and the Au L_3-edge Fourier-transformed EXAFS data are plotted in Figure 4-5 and Figure 4-6. The refined Au-S bond lengths for the gold(I) thiomalate and for the solutions with XANES spectra that resemble the gold(I) thiomalate range from 2.29(1) Å to 2.31(2) Å. These distances are equivalent to, within error of, the Au-S bond distances found in sodium aurothiomalate crystals (Au_1-S at 2.289(8) Å; Au_2-S at 2.285(7) Å; Bau (1998)), and are in agreement with the bond lengths of 2.29 Å reported in earlier studies for aurothiomalate in solution (Elder et al., 1985). The refined coordination number of sulfur of 2 (within uncertainties; Table 4-3) is in agreement with the gold(I) thiomalate resemblance of the XANES spectra and its CN of 2.

In the DD experiments, a refined coordination number of chloride of 4.0(3) and Au-Cl bond length of 2.280(3) Å (Table 4-3) are in agreement with tetrachloroaurate ($AuCl_4^-$) and

the reported Au-Cl bond lengths of ~2.29 Å (Welter et al., 2001) and 2.28(1) Å (Liu et al., 2014), and thus the EXAFS data is in agreement with the $AuCl_4^-$ resembling XANES spectra.

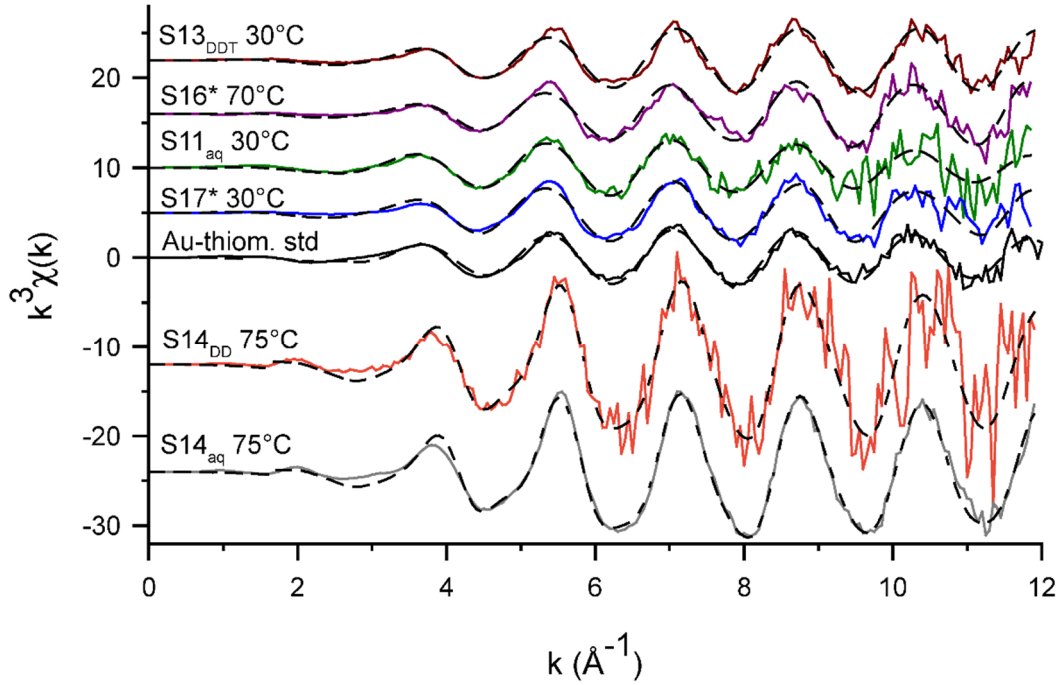

Figure 4-5: Normalized k^3 weighted EXAFS data. The solid lines are the raw data, and the dashed lines are fitted spectra from the parameters listed in Table 4-3. In S15 to S17 it is not clear whether the DDT or brine phase was analyzed due to similar absorption length of the two fluids.

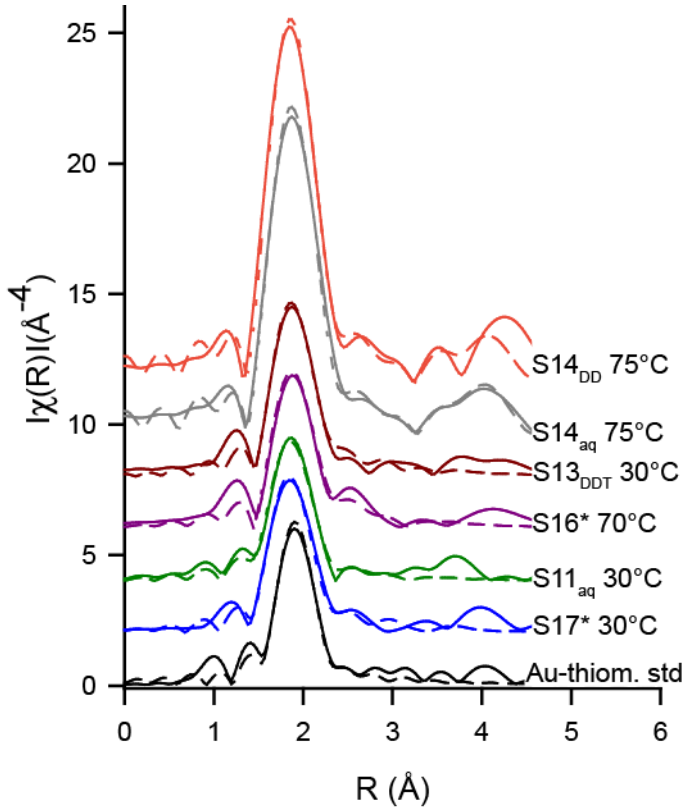

Figure 4-6: Au L_3-edge Fourier-transformed EXAFS data and fits. The solid lines are the raw data, and the dashed lines are fitted spectra from the parameters listed in Table 4-3. All solutions shown resembled the Au(I) thiomalate in XANES except for S14, which resembled $AuCl_4^-$. In S15 to S17 it is not clear whether the DDT or brine phase was analyzed.

4.4 Nature of Au transport in model hydrocarbons

4.4.1 Interpretation of the DDT experiments below 125 °C

The yellow coloration of the water doped with $AuCl_4^-{}_{(aq)}$ (Figure 4-2) and the change to colorless after addition of DDT indicate that Au partitions preferentially into DDT. This is confirmed by the up to 5 times higher step height at the L_{III}-edge in DDT, which translates to a higher Au concentration in DDT, in comparison to adjacent aqueous liquid. No differences were observed in the spectra between the experiments with acidified, neutral, NaCl-containing and NaCl-free aqueous liquids, suggesting that the *pH* and the NaCl content of the aqueous liquid have no influence on the Au speciation at these conditions.

The XANES spectra collected in the DDT and in the adjacent aqueous solution are identical, and closely match the XANES spectrum of the Au(I) thiomalate standard. Together with the CN for S of 2 and the Au-S bond lengths refined from the EXAFS data, this shows that Au exists as a Au(I) complex bonded to two sulfur atoms, which are each bonded to an alkyl

chain, resulting in a complex similar to Au(I) thiomalate (Bau, 1998) in both the aqueous and organic phases. An important difference between the XANES data of the inorganic $Au(HS)_2^-$ complex and thiol-ligand is the position of the second peak, which is located at 11929 eV in Au thiomalate, 2 eV higher than its position (11927 eV) in $Au(HS)_2^-$. In all spectra for the DDT and coexisting waters, this second peak is located at 11929 eV. Since Au(I) is coordinated in distorted linear fashion to two sulfur ligands in both complexes, the shift of this second peak is a strong indication that the sulfur ligands are not free bisulfide ions but are S-radicals attached to an organic group in these DDT experiments. To create a covalent Au-S bond with a Au:S ratio of 2, the sulfhydryl group of two DDT molecules needs to be deprotonated, creating thiyl radicals (e.g., Häkkinen, 2012; Ansar et al., 2013). The hydrogen ions released by deprotonation would go into solution and cause acidification of the solution (Ansar et al., 2013). Density functional theory (DFT) calculations for $RS(AuSR)_n$, with R being a methyl group, suggest that the lowest unoccupied molecular orbital (LUMO) of the neutral $RS(AuSR)_n$ (n = 1) has an antibonding Au-S character, and that the neutral complex is an odd-valence-electron system (radical). The neutral complex is therefore less stable than the anionic complex (Häkkinen, 2012 and references therein). Thus, the anionic complex may be dominant over the neutral complex. Hence, the overall reaction involving reduction of Au(III), complexing of the Au(I) product, and partitioning among aqueous (aq) and organic (o) phases can be written as

$$Au^{(III)}Cl_4^-{}_{(aq)} + 2RH_{(o)} + 2e^- = Au^{(I)}R_2^-{}_{(o/aq)} + 4Cl^-_{(o/aq)} + 2H^+_{(o/aq)} \qquad \text{Eq. 4-1}$$

with $R = [CH_3(CH_2)_{10}CH_2S]^-$. Thiol groups are the most likely electron donor, since DD, which does not contain thiol groups, did not reduce Au(III) to Au(I) at room temperature under similar conditions as the DDT-induced reduction. XANES and EXAFS spectra suggest that the same gold complex is present in DDT (indicated by "o" for organic liquid) and in the adjacent aqueous phase. Thus, the $Au(RS)_2^-$ complex is to some degree soluble in water, although the step height at the Au L_{III}-edge remained consistently higher in the DDT throughout the period of data collection.

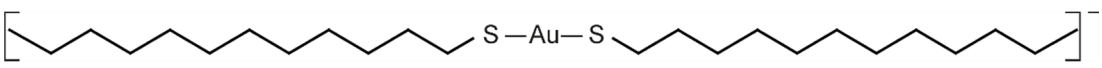

Figure 4-7: $Au(RS)_2^-$ 2D-structure.

4.4.2 Interpretation of the open system DDT – brine solution

In contrast to the Au(I) complexes in the aqueous liquids in contact with DDT in the glassy carbon tubes, gold remained as $AuCl_4^-$ in the acidic brine (S19) in contact with DDT (S18) at room temperature that was sampled and analyzed separately from the DDT. The DDT (S18) was analyzed over a time period of 4 h. It may be that the $AuCl_4^-$-like spectra record a metastable Au(III) complex and that an extended period of equilibration could have resulted in reduction to Au(0). However, a time series of analyzes was not made so it is not possible to assess this possibility.

Reduction from Au(III) to Au(0) could be enhanced by the X-ray beam, which could accelerate the equilibration process by creating turbulence in the solution within the glassy carbon tube and/or redox-active radiolysis products. Neither of these factors would operate in the beaker experiment, where DDT and the brine were analyzed separately. Alternatively, the open system of the brine/DDT system could have stabilized the $AuCl_4^-$ complex, although the brine is shielded from the oxidizing atmosphere by the overlying low density DDT phase.

4.4.3 Interpretation of the DD experiments below 125 °C

The XANES and EXAFS results indicate that $AuCl_4^-$ is the dominant species in DD and in the adjacent acidified water below ~125 °C. Based on the ~10 times lower step height at the L_{III}-edge in DD compared to the brine, $AuCl_4^-$ is weakly soluble in DD. This is consistent with the known chemical properties of DD, including the low solubility of polar groups in DD and an absence of functional groups available for bonding with Au. Furthermore, DD did not reduce the Au(III) complex over the time frame of the experiments at these conditions, even in the presence of the X-ray beam, which catalyzes reactions by induction of the formation of redox-active radiolysis radicals (review in Brugger et al., 2016). In the presence of thiol-held sulfur or other bonded S, significant Au transport in the form of $AuCl_4^-$ dissolved in or bonded to an alkane, such as DD, seems improbable, because the always present S in natural oils would induce reduction of the Au(III) complex within a few hours or less.

4.4.4 Formation of gold nanoparticles at 125 °C/130 °C

In aqueous solutions, Au(III) complexes are only thermodynamically stable at low *pH* and low temperature in the presence of free oxygen, but can remain metastable for days at

room temperature (Usher et al., 2009; Ta et al., 2014). Heating at constant fO_2(g) will cause reduction of Au(III) and possibly of Au(I) as a thermodynamic reduction process. Au(III) complexes are stabilized relative to Au(I) complexes by high chloride and low HS^- activities.

Reduction to metallic gold was observed in all solutions at 125 and 130 °C, though from different low temperature species. In the DDT experiments the organic-Au(I) complex was reduced to Au(0), while in the DD experiment, the Au(III) complex ($AuCl_4^-$) was reduced to Au(0) without a detectable intermediate Au(I) complex (e.g., $AuCl_2^-$; S14). The spectroscopic Raman study by Murphy et al. (2000) observed similar Au(0) formation at 250 °C in the $HAuCl_4$ – HCl aqueous system. Pokrovski et al. (2009a) reported metallic gold precipitation from $HAuCl_4$-NaCl-HCl solutions but with an accompanied increase of $AuCl_2^-$ at the expanse of $AuCl_4^-$, at the same beamline as in this study with the same set-up at 150 °C in the carbon cell and in addition at 250 °C in a sapphire cell. It is not clear whether $AuCl_2^-$ was present in the Murphy et al. (2000) experiment but not detected due to instrumental constraints (Pokrovski et al., 2009a), or whether different redox conditions may have caused the discrepancy. The possible reduction path from Au(III) to Au(I) and then Au(0) in the DD experiments, may have been concealed in our experiments in the time needed to heat from 100 °C to 125 °C/130 °C and to adjust the beam spot position.

The carbon cell appears to generate more reducing conditions than the sapphire cell consisting of Al_2O_3 that was used in the Pokrovski et al. (2009a) experiments at 250 °C, so that metallic gold appears at a lower temperature in the carbon cell. This proposal is consistent with the metallic gold precipitation at 150 °C in the Pokrovski et al. (2009a) experiments in the glassy carbon cell and with the conclusions of Murphy et al. (2000), who proposed that the exact temperature of metallic gold formation depends on the oxygen fugacity; note that equilibration times in the Murphy study were 10 to 15 min, in contrast to several hours in this study.

Interestingly, the temperature at which Au(0) forms in our experiments is the same in sulfur-free (DD) and sulfur-rich (DDT) experiments. Thus, the formation temperature of metallic gold is independent of solution composition in our experiments, and is in agreement with the study of Au in aqueous liquids by Pokrovski et al. (2009a), where Au(0) appeared at 150 °C using the carbon cell, whereas spectra collected at 100 °C in the same experiments did not show Au(0). The similar temperature of metallic gold appearance in the carbon cell with a different chemical system, and the higher temperature of metallic gold appearance in

the sapphire cell in the HC- and S-free experiments by Pokrovski et al. (2009a) further emphasize that, rather than fluid composition, factors related to the experimental set-up such as X-ray beam, temperature and carbon cell induced reduction control the reduction of Au(I) or Au(III) to Au(0).

The extent of X-ray beam-induced photoreduction depends strongly on the ratio of the volume affected by the beam to the sample volume (Brugger et al., 2016). In that study, redox-active radicals generated by the X-ray beam occur at relatively low concentrations because the sample volume is large compared to the beam-affected volume. Nevertheless, these species may have accelerated the Au reduction process by catalyzing the conversion to the thermodynamically-stable species *via* a decrease in the activation energy required for the reduction and speciation changes. Consequently, the observed temperature at which speciation changes occur needs to be interpreted with caution in XAS studies. In other studies, X-rays have been used to synthesize and precipitate AuNPs from Au(III) chloride complex solutions onto a substrate (Karadas et al., 2005), or in solution (Wang et al., 2007; Plech et al., 2008); the latter work used citrate as a reductant, and demonstrated an increase in reduction kinetics when X-rays were used. The situation of our experiment is similar to that of Wang et al. (2007), i.e., reduction to metallic gold occurs at 125 °C/130 °C even in the absence of the beam, but the beam may have affected the reduction kinetics.

In summary, temperature is the first order control on Au(0) formation at our experimental conditions. However, different redox conditions and catalysts may increase or decrease the temperature at which Au(0) forms.

4.5 Alkanes and organothiols as ore fluids

4.5.1 Crude oil and gold transport

The temperatures employed in this study are typical of low temperature hydrothermal systems near the surface and in non-hydrothermal systems (e.g., sedimentary basins) generally not deeper than ~3 km, and are well within the liquid oil window (< 160 °C). Obvious examples include the Carlin-type gold deposits where evidence of gold transport by hydrocarbon/petroleum has already been proposed (e.g., Carlin-type Au deposits in Nevada, US, (Emsbo and Koenig, 2007); and Southwest China, (Gu et al., 2012).

The organic S content (S bound to an organic compound) in low and high S petroleum ranges from < 0.1 wt% to 1 wt% organic S, and can be up to 10 wt% in carbonate-hosted biodegraded oils (Tissot and Welte, 1978; see also section 3.1). Up to 7 wt % of the total sulfur content of crude oils is held in thiol groups (Krein, 1993). Assuming the Au : S atomic ratio of 1 : 2 based on $AuRS_2^-$, 1 g of oil with 1 wt% S, of which 7 wt% is held by thiolate ligands, would account for 55 ppb Au if only the thiols bond with Au. If all the S bonds with Au (Au : S ratio of 1 : 2), the S would account for 792 ppb Au in an oil with 1 wt% S, or 7920 ppb Au in a carbonate-hosted oil with 10 wt% S. These concentrations are in agreement with the 50 ppb Au in crude oils at 250 °C in solubility experiments by Migdisov et al. (2017) and Williams-Jones and Migdisov (2007), but are still below the hundreds of ppm Au in crude oils in partition experiments between crude oils and aqueous solutions (Liu et al., 1993; Zhuang et al., 1999; Emsbo et al., 2009).

This concentration discrepancy suggests that there is an additional factor at play in the chemical transport of gold in crude oil. For instance, Au may be in the form of AuNPs, which would allow a decrease in the number of S-bearing ligands required for bonding of individual gold atoms, yet increase the amount of Au carried by the solution (Hough et al., 2011). Although other functional groups (-COOH, -OH, $-NH_2$) are present in oil and may complex with Au and increase the Au solubility, the formation of AuNPs would be the most efficient to increase Au solubility. We also note that our experiment deals with partitioning between a brine and the oil, whereas Migdisov et al. (2017) studied the dissolution of metallic Au in (natural) oils.

The marked partitioning of Au into DDT suggests that organothiols such as DDT act as effective ligands for Au transport at temperatures below 160 °C (within the liqiuid oil window), either in dissolved form (monomeric Au(I) complex) or potentially in the form of metallic Au, possibly AuNPs capped with organic (thiolate) ligands (Zhang and Sham, 2002).

4.5.2 Au transport in nanoparticulate form

The importance of AuNPs as an alternative form to dissolved complexes for contributing to the migration and concentration of Au and the formation of ore deposits from aqueous fluids or organic ore fluids, is still a hotly debated topic (Hough et al., 2011, and references therein).

Gold nanoparticles (AuNPs) have different physical properties from molecular macro-scale metallic compounds, due to their special electronic structures arising from quantum mechanical rules (Daniel and Astruc, 2004, and references therein). The physical properties strongly depend on size, shape, crystallinity, interparticle distance, and the nature of the protecting organic shell. AuNPs can act as delocalized redox molecules, and thus exhibit different oxidation states within a single AuNP (Daniel and Astruc, 2004, and references therein). Alkanethiolate ligands such as DDT are used to synthesize self-assembled monolayers (SAMs) onto the surface of the AuNP to stabilize and passivate AuNP. The alkanethiol-stabilized AuNPs are thermally stable, air-stable, size-controllable (e.g., Brust–Schiffrin method), re-dissolvable in organic solvents without aggregation or decomposition, can be handled and functionalized like organic and molecular compounds and have a reduced dispersity, (Daniel and Astruc, 2004, and references therein).

Zhang and Sham (2002) measured XANES spectra of AuNPs capped with thiols, and interpreted a less-pronounced peak at 11945 eV, compared to the peak of Au(0) as an indicator that Au(0) is capped by DDT. The spectra in this study at temperatures above 125 °C were too noisy to identify a possibly reduced peak at 11945 eV, so further information on the speciation of AuNP could not be obtained.

However, as noted above, DDT and other organothiols are used to stabilize Au(0) NPs (Daniel and Astruc, 2004), *via* self-assembling of the deprotonated thiol-groups onto the gold surface (Ansar et al. 2013). DDT reduces the surface energy of the AuNP as long as the size of the AuNP provides an energetic advantage for the thiol (Leff et al., 1995), and the unreactive ends of the thiol group create a passivation shell around the exterior of the AuNP-thiol structure (e.g., Daniel and Astruc, 2004). This suggests that AuNPs may be a stable form of gold in DDT, and given enough time, Au(0) would form at the expanse of Au(I) at some point.

It has also been proposed that AuNPs are an important factor in the formation of economic deposits because the unique properties of AuNPs, such as the variety of possible shapes and the high surface areas may contribute towards Au transport and deposition mechanisms in hydrothermal and supergene environments (e.g., Hough et al., 2011). AuNPs capped with alkane thiolate ligands would be very soluble in oils (e.g., Daniel and Astruc, 2004), which raises the question whether they do exist in oil-based ore fluids in nature. We note that AuNP were first observed in a sediment-hosted Carlin-type Au deposit (Palenik et

al., 2004). Experiments in water (ambient conditions) by Stankus et al. (2010) showed that the adsorption of natural organic matter onto AuNPs is more effective for the AuNPs colloidal stability of the particles, in contrast to the one-compound capping agents, which were either anionic, neutral, or cationic. This suggests that in the presence of complex oils and natural organic matter, a stabilization of AuNPs by only one compound like DDT is not realistic, but a capping by natural organic matter is within the realms of possibility (Stankus et al., 2010).

4.6 Conclusions

The abundance of sulfur in thiols and the ability of thiols to stabilize AuNPs suggest that organothiols or natural organic matter in general (Stankus et al., 2010) may contribute to Au migration in low temperature hydrothermal fluids. For example, this is of importance in basinal environments, where organothiols could contribute to the Au endowment of some Carlin-type gold deposits. One scenario for immobilization of the gold transported in oil is an increase in temperature, e.g. *via* mixing with hotter hydrothermal fluids leading to an increase in temperature and the degradation of oil resulting in its immobilization along with the AuNPs.

In our experiments, both the Au(III) complex in DD and the Au(I) complex in DDT were stable up to a temperature between 100 °C and 125 °C, even after exposure to the X-ray beam for 7 h (DD) and 8 h (DDT). At elevated temperatures, metallic Au is formed. The experiments reveal that the presence of oil can contribute to the formation of Au deposits in a number of manners. (i) Crude oil may act as an ore-fluid, transporting gold either *via* the formation of Au organothiol complexes, or, at higher temperatures, through the formation of AuNPs, possibly capped and stabilized by organic molecules. In natural systems metallic Au would either precipitate and drop out of solution in the presence of organic oils, or form nanoparticles that could be transported until the oil is degraded and immobilized. (ii) An important lesson from our experiments is that DDT is able to scavenge and enrich Au from adjacent aqueous gold-bearing brines; this provides a new process for concentrating Au from hydrothermal fluids to levels that are high enough to contribute to ore formation. (iii) Conversely, the strong organic complexes that form in oils can also be transferred to a coexisting aqueous fluid, increasing Au solubility in the aqueous phase.

The new results show that the commonly observed gold-enriched organic matter in gold deposits may reflect an active role of OM in gold transport and concentration, either *via*

scavenging, transport and/or concentration of Au(I) from aqueous fluids at low T (<125 °C) or in the form of AuNPs at higher T (~125-250 °C). Thus, organic matter has the potential to transport Au and does not simply act as a reducing agent only, and this possibility needs to be considered in the study of genetic models of Au deposits that are closely associated with organic matter, in particular some Carlin-type gold deposits where evidence of gold transport by hydrocarbon/petroleum has already been proposed (e.g., Carlin-type Au deposits in Nevada, US, Emsbo and Koenig, 2007; and Southwest China, Gu et al., 2012). In the case of aqueous fluids, studies of modern ore-forming environments were critical in providing a definitive proof of their capacity to form large Au deposits (e.g., Simmons and Brown, 2006 and references therein). Hence, further experimental work associated with studies of oil geochemistry in Au-bearing sedimentary basins is needed in order to further constrain and quantitatively model the role of gold-organic complexes in the formation of hydrothermal gold deposits.

Acknowledgements

Research funding was provided by the Australian Research Council (ARC) to K. R. (DP140103995) and W. L. (FT130100510). We are grateful to the European Synchrotron Research Facility and SOLEIL (Grenoble, France) for providing beam time. We acknowledge travel funding provided by the International Synchrotron Access Program (ISAP) managed by the Australian Synchrotron and funded by the Australian Government.

References

Alex, S. and Tiwari, A. (2015) Functionalized gold nanoparticles: synthesis, properties and applications—a review. *J. Nanosci. Nanotechnol.* **15**, 1869-1894.

Ansar, S.M., Perera, G.S., Jiang, D., Holler, R.A. and Zhang, D. (2013) Organothiols self-assembled onto gold: evidence for deprotonation of the sulfur-bound hydrogen and charge transfer from thiolate. *J. Phys. Chem. C* **117**, 8793-8798.

Bau, R. (1998) Crystal structure of the antiarthritic drug gold thiomalate (myochrysine): a double-helical geometry in the solid state. *J. Am. Chem. Soc.* **120**, 9380-9381.

Benning, L.G. and Seward, T.M. (1996) Hydrosulphide complexing of Au (I) in hydrothermal solutions from 150–400 C and 500–1500 bar. *Geochim. Cosmochim. Acta* **60**, 1849-1871.

Berrodier, I., Farges, F., Benedetti, M., Winterer, M., Brown, G.E. and Deveughèle, M. (2004) Adsorption mechanisms of trivalent gold on iron-and aluminum-(oxy) hydroxides. Part 1: X-ray absorption and Raman scattering spectroscopic studies of Au (III) adsorbed on ferrihydrite, goethite, and boehmite. *Geochim. Cosmochim. Acta* **68**, 3019-3042.

Brugger, J., Liu, W., Etschmann, B., Mei, Y., Sherman, D.M. and Testemale, D. (2016) A review of the coordination chemistry of hydrothermal systems, or do coordination changes make ore deposits? *Chem. Geol.* **447**, 219-253.

Brust, M. and Kiely, C.J. (2002) Some recent advances in nanostructure preparation from gold and silver particles: a short topical review. *Colloids and Surf. A: Physicochemical and Engineering Aspects* **202**, 175-186.

Cotton, F.A. and Wilkinson, G. (1988) Advanced inorganic chemistry. Wiley New York.

Daniel, M.-C. and Astruc, D. (2004) Gold nanoparticles: assembly, supramolecular chemistry, quantum-size-related properties, and applications toward biology, catalysis, and nanotechnology. *Chem. Rev.* **104**, 293-346.

Edinger, K., Grunze, M. and Wöll, C. (1997) Corrosion of gold by alkane thiols. *Phys. Chem. Chem. Phys.* **101**, 1811-1815.

Elder, R., Ludwig, K., Cooper, J. and Eidsness, M. (1985) EXAFS and WAXS structure determination for an antiarthritic drug, sodium gold (I) thiomalate. *J. Am. Chem. Soc.* **107**, 5024-5025.

Elder, R.C. and Eidsness, M.K. (1987) Synchrotron X-ray studies of metal-based drugs and metabolites. *Chem. Rev.* **87**, 1027-1046.

Emsbo, P. and Koenig, A.E. (2007) Transport of Au in petroleum: Evidence from the northern Carlin trend, Nevada, in: al., C.J.A.e. (Ed.), *Mineral Eploration and Research: Digging Deeper*. Proc. 9th Biennial SGA Meeting, Millpress, Dublin, pp. 695-698.

Emsbo, P., Williams-Jones, A.E., Koenig, A.E. and Wilson, S.A. (2009) Petroleum as an Agent of Metal Transport: Metallogenic and Exploration Implications, in: Williams, P.J. (Ed.), In, P.J. Williams (ed.) *Smart Science for Exploration and Mining*. Proc. 10th Biennial SGA Meeting, James Cook Univ. Earth & Enviro. Studies, pp. 99-101.

Etschmann, B., Brugger, J., Fairbrother, L., Grosse, C., Nies, D., Martinez-Criado, G. and Reith, F. (2016) Applying the Midas touch: Differing toxicity of mobile gold and platinum complexes drives biomineralization in the bacterium Cupriavidus metallidurans. *Chem. Geol.* **438**, 103-111.

Etschmann, B., Liu, W., Testemale, D., Mueller, H., Rae, N., Proux, O., Hazemann, J.-L. and Brugger, J. (2010) An in situ XAS study of copper (I) transport as hydrosulfide complexes in hydrothermal solutions (25–592 C, 180–600bar): speciation and solubility in vapor and liquid phases. *Geochim. Cosmochim. Acta* **74**, 4723-4739.

Fairbrother, L., Shapter, J., Brugger, J., Southam, G., Pring, A. and Reith, F. (2009) Effect of the cyanide-producing bacterium Chromobacterium violaceum on ultraflat Au surfaces. *Chem. Geol.* **265**, 313-320.

Fink, J., Kiely, C.J., Bethell, D. and Schiffrin, D.J. (1998) Self-organization of nanosized gold particles. *Chem. Mater.* **10**, 922-926.

Fuchs, S., Migdisov, A. and Williams-Jones, A.E. (2011) The transport of gold in petroleum: An experimental study, Goldschmidt. *Mineral Mag.*, Prague, Czech Republic, p. 871.

Fuchs, S., Williams-Jones, A.E., Jackson, S.E. and Przybylowicz, W.J. (2016) Metal distribution in pyrobitumen of the Carbon Leader Reef, Witwatersrand Supergroup, South Africa: Evidence for liquid hydrocarbon ore fluids. *Chem. Geol.* **426**, 45-59.

Gammons, C.H. and Williams-Jones, A. (1995) The solubility of Au Ag alloy+ AgCl in HCl/NaCl solutions at 300° C: New data on the stability of Au (1) chloride complexes in hydrothermal fluids. *Geochim. Cosmochim. Acta* **59**, 3453-3468.

Gammons, C.H., Yu, Y. and Williams-Jones, A. (1997) The disproportionation of gold (I) chloride complexes at 25 to 200 C. *Geochim. Cosmochim. Acta* **61**, 1971-1983.

Giordano, T. (2000) Organic matter as a transport agent in ore-forming systems. *Rev. Econ. Geol.* **9**, 133-155.

Giże, A. (2000) The organic geochemistry of gold, platinum, uranium and mercury deposits. *Rev. Econ. Geol.: Ore Genesisis and Exploration: The Roles of Organic Matter*, 217-250.

Giże, A. and Barnes, H. (1989) Organic processes in Mississippi Valley-type ore genesis, 28th International Geological Congress Abstracts, pp. 557-558.

Gize, A.P. (1999) A special issue on organic matter and ore deposits: Interactions, applications, and case studies - Introduction. *Econ. Geol. and the Bull. Soc. of Economic Geologists* **94**, 963-965.

Giże, A.P., Kuehn, C., Furlong, K. and Gaunt, J. (2000) Organic maturation modeling applied to ore genesis and exploration. *Rev. Econ. Geol.* **9**, 87-104.

Graham, G.G., Bales, J.R., Grootveld, M.C. and Sadler, P.J. (1985) 1H, 13C NMR, and electronic absorption spectroscopic studies of the interaction of cyanide with aurothiomalate. *J. Inorg. Biochem.* **25**, 163-173.

Greenwood, P.F., Brocks, J.J., Grice, K., Schwark, L., Jaraula, C.M.B., Dick, J.M. and Evans, K.A. (2013) Organic geochemistry and mineralogy. I. Characterisation of organic matter associated with metal deposits. *Ore Geol. Rev.* **50**, 1-27.

Grootveld, M.C. and Sadler, P.J. (1983) Differences between the structure of the anti-arthritic gold drug "myocrisin" in the solid state and in solution: a kinetic study of dissolution. *J. Inorg. Biochem.* **19**, 51-64.

Groves, D.I., Goldfarb, R.J. and Santosh, M. (2016) The conjunction of factors that lead to formation of giant gold provinces and deposits in non-arc settings. *Geosc. Frontiers* **7**, 303-314.

Gu, X.X., Zhang, Y.M., Li, B.H., Dong, S.Y., Xue, C.J. and Fu, S.H. (2012) Hydrocarbon- and ore-bearing basinal fluids: a possible link between gold mineralization and hydrocarbon accumulation in the Youjiang basin, South China. *Miner. Deposita* **47**, 663-682.

Häkkinen, H. (2012) The gold-sulfur interface at the nanoscale. *Nature chemistry* **4**, 443-455.

Hausen, D.M. and Park, W.C. (1986) Observations on the association of gold mineralization with organic matter in Carlin-type ores. *Organics and ore deposits, Proceedings: Denver Region Exploration Geologists Society*, 119-136.

Hayashi, K.-i. and Ohmoto, H. (1991) Solubility of gold in NaCl-and H2S-bearing aqueous solutions at 250–350°C. *Geochim. Cosmochim. Acta* **55**, 2111-2126.

Henley, R.W. (1973) Solubility of gold in hydrothermal chloride solutions. *Chem. Geol.* **11**, 73-87.

Hough, R., Noble, R. and Reich, M. (2011) Natural gold nanoparticles. *Ore Geol. Rev.* **42**, 55-61.

Karadas, F., Ertas, G., Ozkaraoglu, E. and Suzer, S. (2005) X-ray-induced production of gold nanoparticles on a SiO2/Si system and in a poly (methyl methacrylate) matrix. *Langmuir* **21**, 437-442.

Kesler, S., Jones, H., Furman, F., Sassen, R., Anderson, W. and Kyle, J. (1994) Role of crude oil in the genesis of Mississippi Valley-type deposits: Evidence from the Cincinnati arch. *Geology* **22**, 609-612.

Krein, E.B. (1993) Organic sulfur in the geosphere: analysis, structures and chemical processes. *Sulphur-Containing Functional Groups (1993)*, 975-1032.

Kucha, H. (1981) Precious metal alloys and organic matter in the Zechstein copper deposits, Poland. *Mineral. Petrol.* **28**, 1-16.

Kucha, H. and Przylowicz, W. (1999) Noble metals in organic matter and clay-organic matrices, Kupferschiefer, Poland. *Econ. Geol.* **94**, 1137-1162.

Landais, P. (1996) Organic geochemistry of sedimentary uranium ore deposits. *Ore Geol. Rev.* **11**, 33-51.

Lavrich, D.J., Wetterer, S.M., Bernasek, S.L. and Scoles, G. (1998) Physisorption and chemisorption of alkanethiols and alkyl sulfides on Au (111). *J. Phys. Chem. B* **102**, 3456-3465.

Leff, D.V., Ohara, P.C., Heath, J.R. and Gelbart, W.M. (1995) Thermodynamic control of gold nanocrystal size: experiment and theory. *J. Phys. Chem.* **99**, 7036-7041.

Liu, J., Fu, J. and Lu, J. (1993) Experimental study on interaction between organic matter and gold. *'Scientia Geologica Sinica' In Chinese* **28**, 246-253.

Liu, W., Borg, S.J., Testemale, D., Etschmann, B., Hazemann, J.-L. and Brugger, J. (2011) Speciation and thermodynamic properties for cobalt chloride complexes in hydrothermal fluids at 35–440 C and 600bar: an *in-situ* XAS study. *Geochim. Cosmochim. Acta* **75**, 1227-1248.

Liu, W., Etschmann, B., Testemale, D., Hazemann, J.-L., Rempel, K., Müller, H. and Brugger, J. (2014) Gold transport in hydrothermal fluids: Competition among the Cl^-, Br^-, HS^- and NH_3(aq) ligands. *Chem. Geol.* **376**, 11-19.

Lohman, B.C., Powell, J.A., Cingarapu, S., Aakeroy, C.B., Chakrabarti, A., Klabunde, K.J., Law, B.M. and Sorensen, C.M. (2012) Solubility of gold nanoparticles as a function of ligand shell and alkane solvent. *Phys. Chem. Chem. Phys.* **14**, 6509-6513.

Lu, J. and Zhuang, H. (1996) Experimental studies on role of organic matter during mineralization of gold and silver at low temperatures. *'Gechim.' In Chinese.* **25**, 173-180.

Manning, D.A. and Giże, A.P. (1993) The role of organic matter in ore transport processes, Org. Geochem. Springer, pp. 547-563.

Maryutina, T.A. and Timerbaev, A.R. (2017) Metal speciation analysis of petroleum: Myth or reality? *Anal. Chim. Acta*.

Mastalerz, M., Bustin, R., Sinclair, A., Stankiewicz, B. and Thomson, M. (2000) Implications of hydrocarbons in gold-bearing epithermal systems: Selected examples from the Canadian Cordillera, Organic Matter and Mineralisation: Thermal Alteration, Hydrocarbon Generation and Role in Metallogenesis. Springer, pp. 359-377.

Migdisov, A., Guo, X., Williams-Jones, A., Sun, C., Vasyukova, O., Sugiyama, I., Fuchs, S., Pearce, K. and Roback, R. (2017) Hydrocarbons as ore fluids. *Geochem. Persp. Lett.* **5**, 47-52.

Mirasol-Robert, A., Grotheer, H., Bourdet, J., Suvorova, A., Grice, K., McCuaig, T.C. and Greenwood, P.F. (2017) Evidence and origin of different types of sedimentary organic matter from a Paleoproterozoic orogenic Au deposit. *Precambrian Research* **299**, 319-338.

Murphy, P. and LaGrange, M. (1998) Raman spectroscopy of gold chloro-hydroxy speciation in fluids at ambient temperature and pressure: a re-evaluation of the effects of pH and chloride concentration. *Geochim. Cosmochim. Acta* **62**, 3515-3526.

Murphy, P.J., Stevens, G. and LaGrange, M.S. (2000) The effects of temperature and pressure on gold-chloride speciation in hydrothermal fluids: A Raman spectroscopic study. *Geochim. Cosmochim. Acta* **64**, 479-494.

Parnell, J. (1988) Metal Enrichments in Solid Bitumens - a Review. *Miner. Deposita* **23**, 191-199.

Parnell, J., Kucha, H. and Landais, P. (1993) Bitumens in ore deposits. Springer Science & Business Media.

Pearcy, E. and Burruss, R. (1993) Hydrocarbons and gold mineralization in the hot-spring deposit at Cherry Hill, California, Bitumens in Ore Deposits. Springer, pp. 117-137.

Pearson, R.G. (1968) Hard and soft acids and bases, HSAB, part 1: Fundamental principles. *J. chem. Educ* **45**, 581.

Plech, A., Kotaidis, V., Siems, A. and Sztucki, M. (2008) Kinetics of the X-ray induced gold nanoparticle synthesis. *Phys. Chem. Chem. Phys.* **10**, 3888-3894.

Pokrovski, G.S., Akinfiev, N.N., Borisova, A.Y., Zotov, A.V. and Kouzmanov, K. (2014) Gold speciation and transport in geological fluids: insights from experiments and physical-chemical modelling. *Geol. Soc. Spec. Publ.* **402(1)**, 9-70.

Pokrovski, G.S., Tagirov, B.R., Schott, J., Bazarkina, E.F., Hazermann, J.L. and Proux, O. (2009a) An in situ X-ray absorption spectroscopy study of gold-chloride complexing in hydrothermal fluids. *Chem. Geol.* **259**, 17-29.

Pokrovski, G.S., Tagirov, B.R., Schott, J., Hazemann, J.L. and Proux, O. (2009b) A new view on gold speciation in sulfur-bearing hydrothermal fluids from in situ X-ray absorption spectroscopy and quantum-chemical modeling. *Geochim. Cosmochim. Acta* **73**, 5406-5427.

Proux, O., Biquard, X., Lahera, E., Menthonnex, J., Prat, A., Ulrich, O., Soldo, Y., Trévisson, P., Kapoujyan, G. and Perroux, G. (2005) FAME: a new beamline for X-ray absorption investigations of very-diluted systems of environmental, material and biological interests. *Phys. Scr.* **2005**, 970.

Radtke, A.S. and Scheiner, B.J. (1970) Studies of hydrothermal gold deposition - (pt.) 1, carlin gold deposit, nevada, the role of carbonaceous materials in gold deposition. *Econ. Geol.* **65**, 87-102.

Ravel, B. and Newville, M. (2005) ATHENA, ARTEMIS, HEPHAESTUS: data analysis for X-ray absorption spectroscopy using IFEFFIT. *J. Synchrotron Radiat.* **12**, 537-541.

Reith, F. and Cornelis, G. (2017) Effect of soil properties on gold-and platinum nanoparticle mobility. *Chem. Geol.* **466**, 446-453.

Reith, F., Fairbrother, L., Nolze, G., Wilhelmi, O., Clode, P.L., Gregg, A., Parsons, J.E., Wakelin, S.A., Pring, A. and Hough, R. (2010) Nanoparticle factories: Biofilms hold the key to gold dispersion and nugget formation. *Geology* **38**, 843-846.

Renders, P. and Seward, T. (1989) The stability of hydrosulphido-and sulphido-complexes of Au (I) and Ag (I) at 25 C. *Geochim. Cosmochim. Acta* **53**, 245-253.

Sawlowicz, Z., Gize, A. and Rospondek, M. (2000) Organic matter from Zechstein copper deposits (Kupferschiefer) in Poland, Organic Matter and Mineralisation: Thermal Alteration, Hydrocarbon Generation and Role in Metallogenesis. Springer, pp. 220-242.

Seward, T. (1993) The hydrothermal geochemistry of gold, Gold metallogeny and exploration. Springer, pp. 37-62.

Seward, T.M. (1973) Thio complexes of gold and the transport of gold in hydrothermal ore solutions. *Geochim. Cosmochim. Acta* **37**, 379-399.

Shenberger, D.M. and Barnes, H.L. (1989) Solubility of gold in aqueous sulfide solutions from 150 to 350°C. *Geochim. Cosmochim. Acta* **53**, 269-278.

Sherlock, R. (1992) The empirical relationship between gold-mercury mineralization and hydrocarbons, in the northern Coast Ranges, California, GAC-MAC Joint Annual Meeting, Program with Abstracts.

Sherlock, R. (2000) The association of gold—mercury mineralization and hydrocarbons in the coast ranges of northern California, Organic Matter and Mineralisation: Thermal Alteration, Hydrocarbon Generation and Role in Metallogenesis. Springer, pp. 378-399.

Shuster, J., Reith, F., Cornelis, G., Parsons, J.E., Parsons, J.M. and Southam, G. (2017) Secondary gold structures: Relics of past biogeochemical transformations and implications for colloidal gold dispersion in subtropical environments. *Chem. Geol.* **450**, 154-164.

Spirakis, C.S. (1996) The roles of organic matter in the formation of uranium deposits in sedimentary rocks. *Ore Geol. Rev.* **11**, 53-69.

Stefánsson, A. and Seward, T. (2004) Gold (I) complexing in aqueous sulphide solutions to 500 C at 500 bar. *Geochim. Cosmochim. Acta* **68**, 4121-4143.

Sun, Y., Jiao, W., Zhang, S. and Qin, S. (2009) Gold enrichment mechanism in crude oils and source rocks in Jiyang Depression. *Energ. Explor. Exploit.* **27**, 133-142.

Ta, C., Reith, F., Brugger, J.l., Pring, A. and Lenehan, C.E. (2014) Analysis of gold (I/III)-complexes by HPLC-ICP-MS demonstrates gold (III) stability in surface waters. *Environ. Sci. Technol.* **48**, 5737-5744.

Tagirov, B.R., Salvi, S., Schott, J. and Baranova, N.N. (2005) Experimental study of gold-hydrosulphide complexing in aqueous solutions at 350–500°C, 500 and 1000 bars using mineral buffers. *Geochim. Cosmochim. Acta* **69**, 2119-2132.

Testemale, D., Argoud, R., Geaymond, O. and Hazemann, J.-L. (2005) High pressure/high temperature cell for X-ray absorption and scattering techniques. *Rev. Sci. Instrum.* **76**, 043905.

Tissot, B. and Welte, D. (1978) The fate of organic matter in sedimentary basins: generation of oil and gas. *Petroleum Formation and Occurrence*, 69-253.

Usher, A., McPhail, D.C. and Brugger, J. (2009) A spectrophotometric study of aqueous Au(III) halide–hydroxide complexes at 25–80 °C. *Geochim. Cosmochim. Acta* **73**, 3359-3380.

Vlassopoulos, D., Wood, S.A. and Mucci, A. (1990) Gold speciation in natural waters: II. The importance of organic complexing—Experiments with some simple model ligands. *Geochim. Cosmochim. Acta* **54**, 1575-1586.

Wang, C.-H., Chien, C.-C., Yu, Y.-L., Liu, C.-J., Lee, C.-F., Chen, C.-H., Hwu, Y., Yang, C.-S., Je, J.-H. and Margaritondo, G. (2007) Structural properties of 'naked' gold nanoparticles formed by synchrotron X-ray irradiation. *J. Synchrotron Radiat.* **14**, 477-482.

Weisbecker, C.S., Merritt, M.V. and Whitesides, G.M. (1996) Molecular self-assembly of aliphatic thiols on gold colloids. *Langmuir* **12**, 3763-3772.

Welter, R., Omrani, H. and Vangelisti, R. (2001) Sodium tetrabromoaurate (III) dihydrate. *Acta Crystallogr. Sect. Sect. E: Struct. Rep. Online* **57**, i8-i9.

Williams-Jones, A. and Migdisov, A. (2007) The solubility of gold in crude oil: implications for ore genesis, Proceedings of the 9th Biennal SGA Meeting, Millpress, Dublin, pp. 765-768.

Williams-Jones, A.E., Bowell, R.J. and Migdisov, A.A. (2009) Gold in solution. *Elements* **5**, 281-287.

Wood, S. (1996) The role of humic substances in the transport and fixation of metals of economic interest (Au, Pt, Pd, U, V). *Ore Geol. Rev.* **11**, 1-31.

Zabinsky, S., Rehr, J., Ankudinov, A., Albers, R. and Eller, M. (1995) Multiple-scattering calculations of X-ray-absorption spectra. *Phys. Rev. B* **52**, 2995.

Zammit, C.M., Weiland, F., Brugger, J., Wade, B., Winderbaum, L.J., Nies, D.H., Southam, G., Hoffmann, P. and Reith, F. (2016) Proteomic responses to gold (III)-toxicity in the bacterium Cupriavidus metallidurans CH34. *Metallomics* **8**, 1204-1216.

Zhang, P. and Sham, T. (2002) Tuning the electronic behavior of Au nanoparticles with capping molecules. *Appl. Phys. Lett.* **81**, 736-738.

Zhong, R., Brugger, J., Chen, Y. and Li, W. (2015) Contrasting regimes of Cu, Zn and Pb transport in ore-forming hydrothermal fluids. *Chem. Geol.* **395**, 154-164.

Zhuang, H.P., Lu, J.L., Fu, J.M., Ren, C.G. and Zou, D.G. (1999) Crude oil as carrier of gold: petrological and geochemical evidence from Lannigou gold deposit in southwestern Guizhou, China. *Sci. China Ser. D* **42**, 216-224.

Copyright statement

Chapter 5

Hydrocarbon phase mobilization of Au in the Au-Hg McLaughlin Mine, Geysers/Clear Lake area, California

Lars-S. Crede, Katy A. Evans, Kirsten U. Rempel, Joël Brugger, Barbara Etschmann, Julien Bourdet, Frank Reith

Abstract

Hydrocarbon (HC) – enriched silica is co-located with gold (Au) mineralization in the Au-Hg McLaughlin deposit, Geysers/Clear Lake area, California. This co-location suggests that HC material may be involved in the mineralization and metal concentration process, but in general little is known about the role of HC material in the formation of ore deposits. Previous studies noted liquid oil inclusions in samples from the McLaughlin deposit, and proposed that the hydrocarbons were liquid at the time of ore deposition. Hydrocarbon materials in the McLaughlin deposit range from solid to liquid forms. Textural evidence suggests that hydrocarbon-rich and aqueous, silica-rich fluids were present simultaneously, as well as separately in alternating pulses. Synchrotron X-ray fluorescence microscopy of microscopically silica free carbonaceous material (CM) reveals that the CM contains abundant ore metals e.g., Au, Ag, Hg, and Pb. The CM could have become metal enriched by scavenging metals from other ore fluids, or it could have transported metals when the CM was still liquid, with subsequent *in-situ* degradation due to hydrothermal heat. Au concentrations of up to 18 mg/kg in HC and CM were measured *via* acid digestion of solid and liquid HC material and subsequent inductively coupled plasma – mass spectrometry (ICP-MS) analyzes. HC material with liquid to medium viscous properties bearing 10.8 mg/kg Au provides evidence that Au in liquid HC in the McLaughlin Au-Hg deposit is still mobile and that remobilization and/or transport of metals to the deposit by HC liquids cannot be ruled out.

5.1 Introduction

Carbonaceous matter (CM) or hydrocarbon matter can be a common constituent of hydrothermal ore deposits (Bowell et al., 1999; Zhuang et al., 1999; Sherlock, 2000; Emsbo and Koenig, 2007). Still the role of CM in ore formation processes is controversial and often uncertain. Solid CM has been commonly proposed to act as a trap for the deposition of metals from hydrothermal ore fluids, either *via* reduction (Giże, 1999; Giże, 2000) or *via* sorption or complexation (Etschmann et al., 2017; Cumberland et al., 2018). In contrast, some researchers of crude oils and petroleum or CM associated with Au deposits, e.g., Carlin-type Au deposits in Guizhou, China and Nevada, USA (e.g., Zhuang et al., 1999; Emsbo and Koenig, 2007), Pb-Zn-Ba ore deposits (Connan, 1979), Pb deposits, e.g., Mississippi Valley-type deposits (Giordano and Barnes, 1981), Cu deposits, Zechstein Cu deposits (e.g., Kucha, 1981; Kucha and Przylowicz, 1999; Sawlowicz et al., 2000), or with U-Ti deposits, Witwatersrand

Supergroup, South Africa (Fuchs et al., 2015; Fuchs et al., 2016) argue that the hydrocarbon phase contributed to metal transport. It is thought that hydrocarbons may have played a major role for example in the formation of the giant Carlin-type deposit province in Nevada (Groves et al., 2016). Out of 41 Carlin-type deposits, 39 are reported to have CM in the original mineralized horizon (Berger and Bagby, 1993). The two deposits without CM indicate that the formation of Carlin deposits is not dependent on CM. The bitumen in the Upper Zone of the Rodeo deposit, northern Carlin trend, Nevada contains up to 100 mg/kg Au, and there is evidence suggesting that Au and associated metals were remobilized in petroleum as organo-metallic compounds during oil generation and migration (Emsbo and Koenig, 2007). However, organic matter at the original Carlin deposit was matured beyond the oil and gas windows before gold mineralization (Gize et al.; 2000). Thus, it is important to consider individual deposit settings in context if Au transport in organic fluids is to be proposed.

A few experimental results indicate that metal transport in a hydrocarbon phase is viable (Liu et al., 1993; Lu and Zhuang, 1996; Miedaner et al., 2005; Fuchs et al., 2011; Crede et al., 2017; Migdisov et al., 2017; Crede et al., 2019; Crede et al., 2018-A; Crede et al., 2018-B).

For example, in mixing experiments between a brine (20 % NaCl, doped with metals) and crude oil (Wyoming, Barbour Crude), 50 to 100 mg/kg of platinum, palladium and gold were present in the oil after a 24 h agitation at room temperature (Emsbo et al., 2009). Crede et al. (2018-A) showed in partition experiments between brine and 1-dodecanethiol that more than 95% of the Au partitions into the oil phase between 105 °C and 150 °C, and the study by Crede et al. (2019) showed that at temperatures ≥ 125 °C gold transport as nanoparticle was possible.

This study focuses on samples from the epithermal McLaughlin Au-Hg deposit, Geysers/Clear Lake area, California to understand the roles of CM in the ore formation, where CM is present in liquid and solid form. Oils in hydrothermal systems are generated instantaneous in geological time compared to the accepted conventional petroleum formation and differ in composition from conventional petroleum by being relatively enriched in unsubstituted aromatic hydrocarbons (Simoneit, 1993; Simoneit, 2000b). Bitumen in the McLaughlin Au-Hg deposit was found to have Au concentrations of up to 15.1 mg/kg, and 46.2 mg/kg Au was measured in bitumen from the Scorpion vein area in the Sulphur Creek District, ~20 km north of the McLaughlin mine (Sherlock, 2000). Furthermore,

Au is strongly associated with hydrocarbon-enriched chalcedony and opal in the McLaughlin deposit (Sherlock, 2000), and rocks in the Geysers/Clear Lake area and the McLaughlin mine have been documented to contain hydrocarbon fluid inclusions (FLINCS; Peters, 1991; Sherlock, 2000) and various types of CM in the form of pyrobitumen in sinter materials, vug fillings of tars and light oils, and hydrocarbon-enriched opal (Sherlock, 1992; Rytuba, 1993; Sherlock and Lehrman, 1995). In the McLaughlin deposit, Au concentrations of up to 240 µg/kg were found in bitumen, up to ~450 µg/kg in low viscosity oils, and Au concentrations elevated above background sinter values of 4.49 mg/kg are associated with hydrocarbon-rich silica (Tosdal et al., 1993; Sherlock and Lehrman, 1995). The McLaughlin deposit is therefore a suitable locality for this study on Au-CM associations. Despite these observations, Sherlock (2000) concluded that hydrocarbons were not instrumental in forming the McLaughlin deposit, although CM is present throughout the entire paragenetic history of the hydrothermal system, and suggested instead that particulate Au was scavenged and immobilized by hydrocarbons from aqueous ore fluids *via* the action of opposing surface charges. However, new experimental measurements of the partitioning coefficients of ore metals between liquid hydrocarbons and aqueous hydrothermal fluids by Crede et al. (2018-A) and experiments of Au solubility in oil (Migdisov et al., 2017) suggest that a metal transport by liquid hydrocarbons is possible, and thus liquid hydrocarbons may have acted as an ore transport medium in this deposit. Consideration of such non-aqueous fluids is a potentially critical factor missing from most current ore deposit models. This is related to the observation, that bitumen enriched in Au is often pre- or postAu mineralization and rarely syn-genetic and that it is difficult to attain information on the genetic role of hydrocarbons in the mineralization process (Parnell and McCready, 2000).

In this work, textural interpretation of the association between CM, Au-Ag alloys, and silica which are combined with the results of acid digestion of CM and Au analyses by inductively coupled mass spectrometry (ICP-MS) and with synchrotron X-ray fluorescence (SXFM) mapping, reveal insights into the possibility of a hydrocarbon phase gold transport in the McLaughlin deposit.

5.1.1 Geological setting

The McLaughlin deposit is associated with the Clear Lake volcanic field and is part of the hydrothermally active Geysers/Clear Lake area in north-western California (Figure 5-1). The major Mesozoic lithologies in the area comprise the Great Valley Sequence, Coast Range

Ophiolite and Franciscan Complex (Blake, 1981; Blake and Jones, 1981; Dickinson, 1981). The Franciscan Complex is thought to be an accretionary wedge formed by the subduction of the Pacific plate under the North American plate (Blake, 1981; Blake and Jones, 1981; Dickinson, 1981). The Great Valley sequence is proposed to have been deposited in a fore-arc environment (Dickinson, 1981) and is thought to have been deposited on top of the tectonically emplaced oceanic crust of the Coast Range ophiolite. The Mesozoic units are overlain by Late Tertiary and Quaternary volcanic rocks of the Clear Lake volcanic field (Hearn et al., 1981). Magma was introduced into the crust of the Clear Lake area in relation to an east-southeast extensional field together with the northward propagation of the San Andreas transform (Hearn et al., 1981). Regional normal, strike-slip and thrust faults, along with tectonic interleaving of the underlying Great Valley Sequence, Coast Range Ophiolite, and Franciscan complex, occurred during multiple episodes of Mesozoic and Cenozoic tectonic activity (McLaughlin, 1981). The basaltic andesite Clear Lake volcanic rocks of the McLaughlin mine have a whole-rock age of 2.2 ± 0.2 Ma and indicate the maximum mineralization age (Lehrman, 1986).

The McLaughlin deposit lies on the Stony Creek Fault, which forms the contact between the Great Valley Sequence and the Coast Range Ophiolite (Figure 5-1). (Tosdal et al., 1993). The deposit is a sheeted vein complex built almost entirely of hydrothermal silica-rich veins, emplaced between the tholeiitic basalts and the polymictic sediment-serpentinite mélange of the Coast Range Ophiolite, and capped by a hot spring-type silica sinter terrace (Sherlock and Lehrman, 1995). At the base of the sinter is an alunite-bearing vein that has K – Ar ages between 0.75 and the 2.2 Ma recorded by the basaltic andesite (Lehrman, 1986; Tosdal et al., 1993). This suggests that hydrothermal activity took place during the late Pliocene to Pleistocene age (Lehrman, 1986; Tosdal et al., 1993). The McLaughlin mine was opened when Au mineralization was discovered at the Manhattan mercury deposit in 1978, which was then renamed to McLaughlin. The total resources of the deposit, now mined out and remediated, has been estimated at 109.1 tons of Au (Tosdal et al., 1993).

Mineralization consists of electrum or native gold, silver sulfosalts, cinnabar and native mercury, along with stibnite, arsenic phases, and base metal sulfides. The metals are vertically zoned; the upper Hg-rich sinter overlies the Au-rich upper levels of the sheeted veins (<50 m depth), located in turn above an Au-Ag transitional zone (50200 m) which grades to more Ag-rich veins at 200-350 m, and finally to base metal sulfides at depth (Sherlock et al., 1995).

The fluid source of the ore fluids in the McLaughlin deposit is meteoric fluids, based on $\delta^{18}O$ and δD data. Isotope characteristics for $\delta^{18}O$ and δD are typical of meteoric water dominated hydrothermal systems that interacted with large volumes of marine sedimentary rocks such as the hanging wall Great Valley sequence (Peters, 1991; Thompson, 1993; Sherlock et al., 1995, and references therein). The interaction with marine sedimentary rocks is consistent with the high abundance of hydrocarbon material in the McLaughlin Deposit (Sherlock et al., 1995; Sherlock, 2005).

Based on fluid inclusion data, Sherlock et al. (1995) interpreted metal precipitation to result from boiling of the hydrothermal fluids and consequent chemical and physical changes. The homogenization temperatures of the aqueous fluid inclusions at McLaughlin average ~235 °C, but range from cooler temperatures (down to 121 °C) at the surface and higher temperatures (up to 263 °C) at depth (Sherlock et al., 1995). The average salinity of aqueous fluid inclusions is ~2.4 eq. wt% NaCl (Sherlock et al., 1995). A small second population of fluid inclusions has salinities of up to 14.5 eq. wt% NaCl; these are interpreted to have resulted from sustained boiling in a low permeability fracture (Sherlock et al., 1995).

Both Au and hydrocarbons are present at relatively shallow depths (<200 m) and Au is often associated with hydrocarbon-rich hydrothermal silica, such as opal and chalcedony (Sherlock, 1992; Sherlock and Lehrman, 1995). Sherlock and Lehrman (1995) show images of dendritic Au aligned parallel and perpendicular to colloform hydrocarbon-silica banding, and of dendritic Au cross-cutting opaline spheres. These textures are suggestive of co-precipitation of silica, hydrocarbons and dendritic Au, especially as the Au dendrites are only observed in association with hydrocarbon-rich opaline silica (Sherlock, 2000). A spatial and temporal association of Au mineralization with hydrocarbon migration is also supported by mg/kg levels of Au found in hydrocarbons throughout the nearby Sulphur Creek District and elevated Au levels, compared to other crude oils, in thick tar and low viscosity oils from the McLaughlin deposit of up to ~0.45 mg/kg and one bitumen sample with 15.1 mg/kg Au (Pearcy and Burruss, 1993; Sherlock, 2000).

The close spatial association of the McLaughlin deposit with the Great Valley Sequence (Figure 5-1) is consistent with an origin of the hydrocarbons in the Great Valley Sequence, which produced small amounts of petroleum at the Terhel 1 well, 2 km east of the Sulfur Creek District (Brabb et al., 2001; Sherlock, 2005).

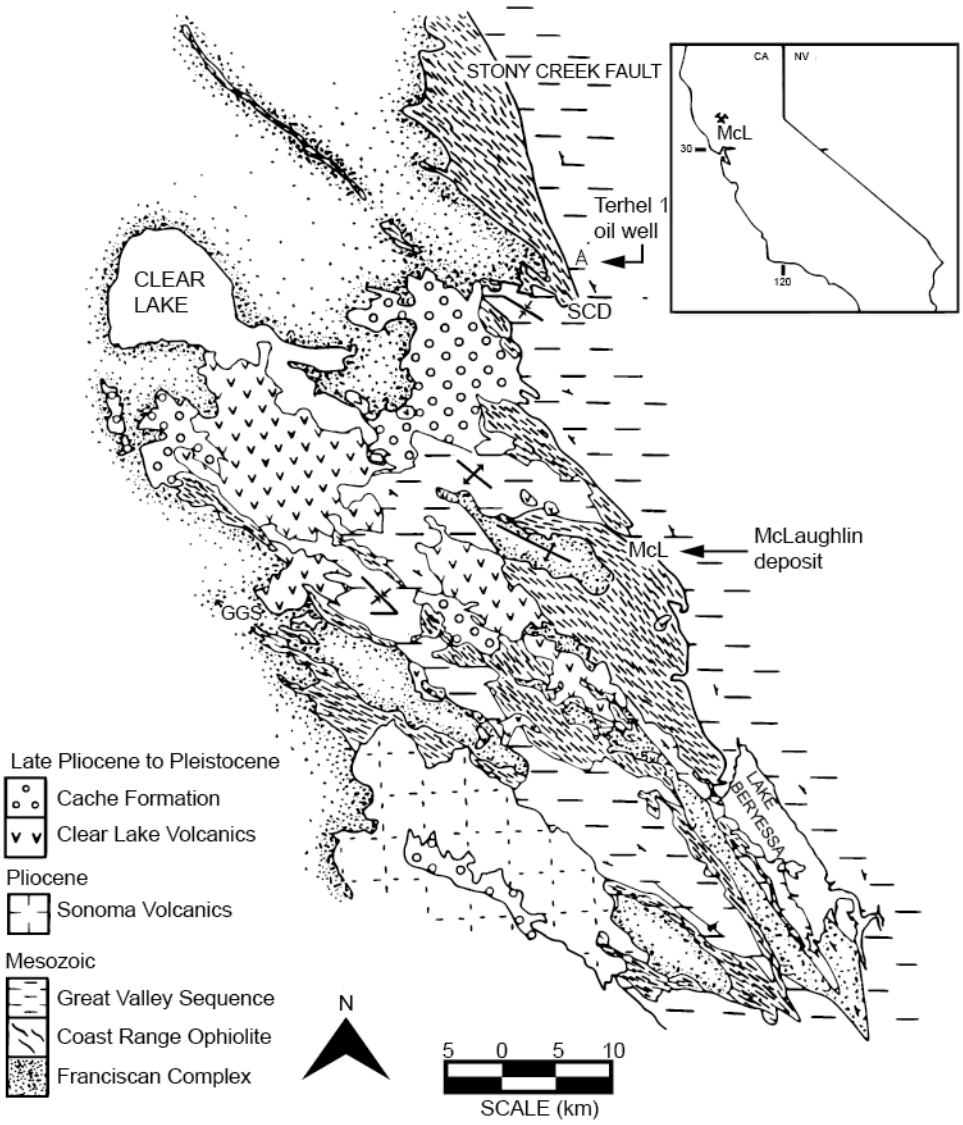

Figure 5-1: Geological map of the Clear Lake area in the northern Coast Ranges of California. McL: McLaughlin Deposit; GGS Geysers geothermal system; SCD: Sulphur Creek district. Modified after Sherlock et al. (1995) and compiled from McLaughlin (1978), McLaughlin et al. (1985), Wagner and Bortugno (1982), and Chapman et al. (1972).

5.2 Materials and methods

We chose three samples with different forms of CM from approximately 100 McLaughlin samples provided by the administrators of the McLaughlin Natural Reserve (University of California, Davis) for this study. The selected samples bear various forms of CM, liquid to solid (section 3), and Au and are thus suitable for the study on the role of the CM in the ore formation.

5.2.1 Synchrotron X-ray fluorescence microscopy (SXFM)

SXFM on a billet of sample 2 (section 3.1.2) was performed at the X-ray fluorescence microscopy (XFM) beamline at the Australian Synchrotron (Kirkham et al., 2010; Paterson et al., 2011; Ryan et al., 2014). The setup enables a 2 μm^2 spot size in the 4-20 keV range and is equipped with a Maia 384 large angle detector array with an integrated real-time processor. The beam is focused by Kirkpatrick-Baez mirrors. SXRF maps and Au-XANES stacks (Etschmann et al., 2010; Etschmann et al., 2014) were collected with the Maia fluorescence detector (Ryan et al., 2010a; Ryan et al., 2010b; Ryan et al., 2014). Images of up to 100M pixels can be acquired using the Maia detector.

Element mapping was performed on the polished billet of sample 2 (section 2.3 and 3) over an area of 40.25 × 18.38 mm^2 with a beam energy of 18.5 keV, a step size of 5 µm and a dwell time of 0.5 ms per 5 µm pixel. A rough XANES stack was constructed by collecting SXRF maps on the thin section of sample 2 at 26 monochromator energy points across the Au L_3-edge starting at ~12 keV with a pixel size of 2 μm^2 over an area of 2.27 × 0.28 mm^2. Standard metal foils were measured to account for self-absorption, absorption in air and the efficiency response of the detector. X-rays can penetrate into the sample resulting in relative average pixel concentrations representing the sampled volume (Ryan et al., 2014); in comparison to electron-based microanalysis, this relatively large penetration of X-rays is advantageous for revealing the distribution of rare (sub)micron size particles below the surface (Li et al., 2016). Data reduction was performed with the GeoPIXE^{TM} software (Ryan et al., 2005), which includes a fundamental parameter model, the Maia detector array efficiency model, and a dynamic analysis (DA) matrix method to deconvolute spectra and create images. By fitting multiple lines per element, it becomes possible to distinguish between elements that have overlapping X-ray lines, that are difficult to separate using the traditional region-of-interest approach: As Kα1 and Pb Lα1, Pb Mα and S Kα (Ryan et al., 2010b). DA matrix analysis was used to generate images of the mapped area (Ryan et al., 2010b).

5.2.2 Petrography to locate fluid inclusions

Thirteen thin sections (30 µm thick) and fifteen doubly polished thin sections (250 µm thick) from the quartz veins visually assessed as enriched in hydrocarbons were prepared for the fluid inclusion study. Quartz veins were investigated using fluid inclusion techniques. This mineral has suitable mechanical properties for preserving primary fluid inclusions and optical

properties allowing their observations (Roedder, 1984; Van den Kerkhof and Hein, 2001). Fluorescing oil inclusions and/or CM were identified by UV illumination using a petrographic Olympus AX 70 microscope with a 100 W high pressure mercury-vapor light source (Olympus BH2-RFL-T3) that was filtered through a broad 330 - 385 nm band pass filter giving a high peak intensity at 365 nm.

5.2.3 Digestion of CM for Au analysis

Au concentration in CM was determined in three samples (Figure 5-3): viscous CM covering and filling the pore spaces of quartz in sample 1; CM in a polymictic mudstone-sandstone-CM breccia with fractured CM-quartz infill in sample 2; and CM vug fillings in colloform layers of chalcedony and quartz in sample 3 (Figure 5-3). Au concentrations were determined by digesting 0.0098 g to 1.042 g of the bitumen in 7.5 ml HNO_3 (67 %) and 2 ml H_2O_2 (30 %) at 125°C in titanium autoclaves (V = 40 ml) for three days. After decanting the solution, *aqua regia* was added to the autoclaves and heated to 150°C (24 h) to dissolve any remaining Au that may have precipitated onto the autoclave walls during the digestion, thus generating two solutions per sample for ICP-MS analyses. ICP-MS analyses were performed by LabWest Minerals Analysis Pty Ltd. A blank digestion produced concentrations of ~300 µg/kg Au, which was attributed to earlier experiments using the same autoclaves. However, an uncertainty of around 300 µg/kg is negligible in comparison to the orders of magnitude higher Au concentrations (~10000 µg/kg) in the CM.

5.2.4 Feasibility of LA-ICP-MS on the OFLINCS

One purpose of this study was to directly analyze the metal contents in fluid inclusions. The small sizes (< 5 µm) and irregular shapes of the hydrocarbon fluid inclusions are poorly suited to laser ablation techniques and the maximum of one to three hydrocarbon fluid inclusions per section in our samples, on average 0.5 oil inclusions per section, is far too few to obtain robust and statistically significant results by LA-ICP-MS. The low OFLINC (organic fluid inclusion) abundance means that 100 to 200 thin sections would be needed to find 50 to 100 hydrocarbon fluid inclusions, which would require the equivalent of 20 kg to 70 kg of pure quartz samples from the McLaughlin deposit, assuming that 200 g to 350 g are needed per thin section (Figure 5-2). Future studies of oil inclusions in hydrothermal deposits should therefore plan for large sample volumes and high numbers of thin sections, and carefully choose the samples.

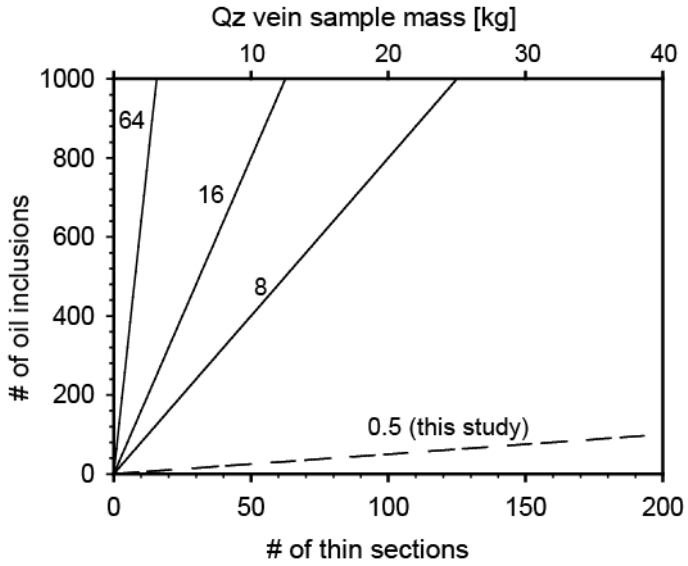

Figure 5-2: Predicted number of oil inclusions vs number of thin sections (300 µm thickness) based on the results of this study. Labels for each line are the average number of inclusions per thin section.

5.3 Results

5.3.1 CM and textures in samples from the McLaughlin mine

The three samples used to determine the Au concentration in CM exhibit different textural relationships between the CM and associated host rock material (Figure 5-3). CM is present as liquid oils and relatively low to high viscous CM (tar), solid bitumen, bituminous vug infills, and as fluid inclusions. The main phases of interest are the CM enriched phases that are either pure or associated with silica (usually quartz and chalcedony), pure quartz, or pure chalcedony.

5.3.1.1 Sample 1

Sample 1 consists purely of coarse, crystalline quartz that is dominated by euhedral grains with c-axis lengths ranging from 0.1 mm up to 3 mm. The outside of the sample is covered with viscous CM, which is also found in late stage macroscopic vugs (Figure 5-3 A), and in the macroscopic and microscopic pore spaces (section 3.3). A few very fine, loose quartz crystals are present within the CM covering the sample. Liquid oil spreads from the viscous bitumen into and through the sample along connected pore spaces and fractures (Figure 5-3 A; section 3.3). When leaving the sample on paper for a while, the paper becomes stained by liquid oil. While hydrocarbons are found in vugs, fractures, pore spaces and along grain boundaries of the quartz crystals, less than one hydrocarbon fluid inclusion per thin

section was found trapped in quartz crystals from this sample. No metal sulfides or other opaque/ore minerals were found within the quartz of sample 1.

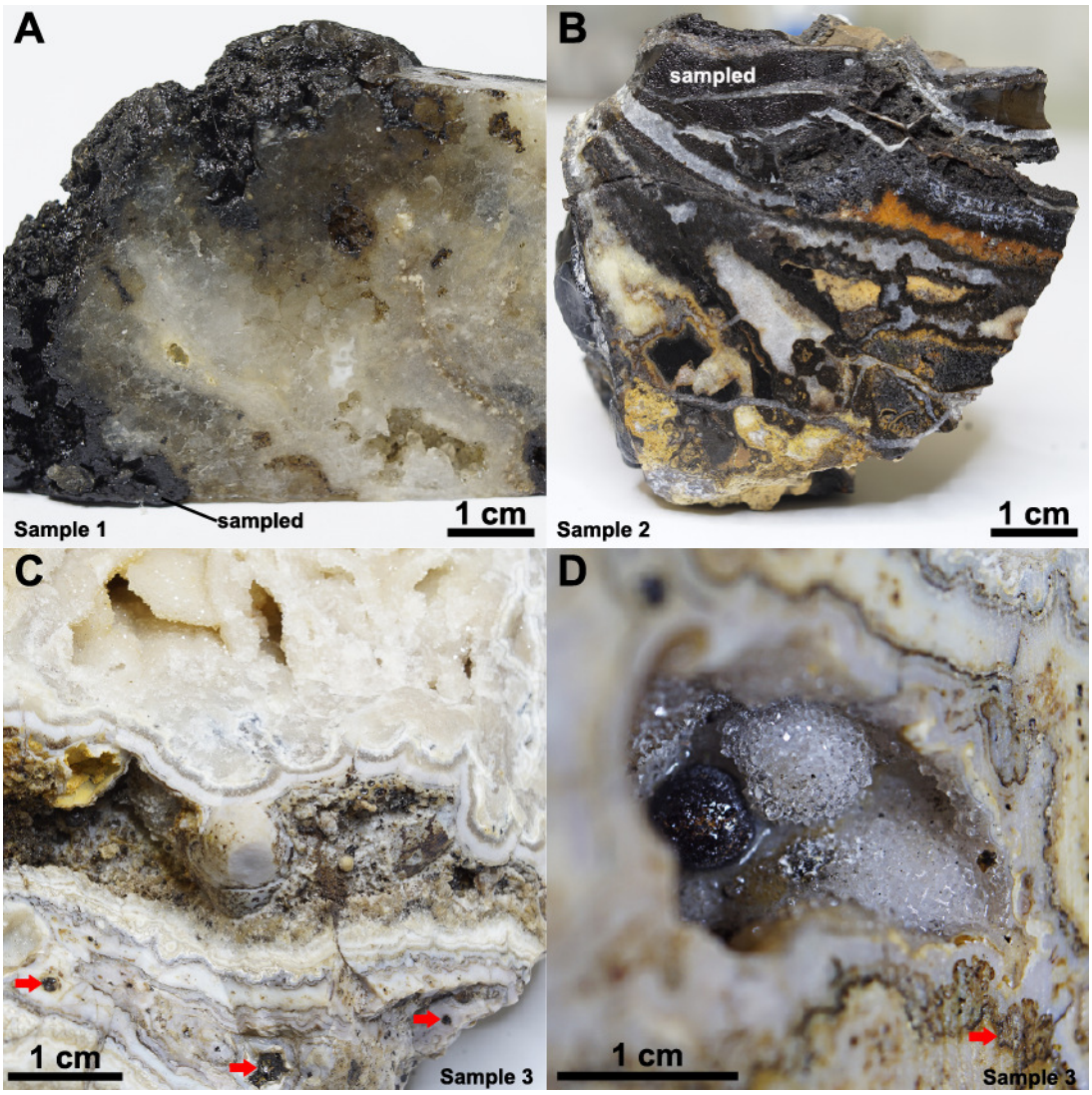

Figure 5-3: Samples 1 to 3 from the McLaughlin mine, Geysers/Clear Lake area, California. Surfaces of samples in images A, B and D were wetted prior to photography. (A) Sample 1: Quartz coated and soaked with viscous CM and liquid light oils. The viscous CM was sampled, digested and analyzed. (B) Sample 2: Brecciated network of solid and brittle brown-black CM, quartz and fine grained weathered material in yellow. The brown-black CM was sampled (labelled sampled in white), digested and analyzed. (C) Sample 3: Colloform layers of chalcedony and quartz showing botryoidal textures, and calcite blades that were replaced by quartz at the top. The CM of the vug infills (red arrows) were sampled, digested, and analyzed. (D) Sample 3: Crystalline CM sphere in quartz cavity from sample 3. The red arrow indicates very fine CM layers in between the silica layers.

5.3.1.2 Sample 2

Sample 2 (Figure 5-3 C) is a brecciated, fractured, and partially layered rock composed of quartz, chalcedony, carbonates and solid but brittle CM. The sample comprises a cockade of carbonate (yellow and orange due to Fe-oxide staining) and CM fragments cemented by layered CM and silica (quartz and chalcedony), as well as a fractured zone of solid, brittle CM.

Dark grey silica veins, which crosscut CM and altered rock, do not crosscut the white silica in the center of the sample. This indicates at least two generations of silica that were introduced into the open space after the CM, as the CM surrounds the silica, indicating inward deposition of CM followed by silica. The brecciated part of the sample is dominated by carbonates with fragments of CM that correspond in texture and coloration to the preserved CM layers at the top of the sample. The top shows well preserved CM around presumable former bladed calcite that was replaced by quartz, as the quartz pseudomorphs now has the typical crystal habit of bladed calcite (Etoh et al., 2002).

In sample 2, hydrocarbon-enriched chalcedony and quartz crystals up to 500 µm in length are crosscut by later hydrocarbon-free quartz veins (Figure 5-4 A; Figure 5-5). The thin section is very complex, so the description here is focused on features that constrain the paragenesis of CM-free and CM-dominant phases. Briefly, the thin section exhibits a primary CM-rich layering (e.g. pure CM band #1 and CM-enriched silica and silica-carbonate layers #4), which is disrupted by crosscutting silica veins #2 (Figure 5-5). The thick pure-CM layer (~5000 µm; #1) lies between two CM-enriched silica layers to the left and right (only a small piece of the right-hand layer is visible). CM also fills pore spaces (#3), from which it seems to spread into the surrounding silica. The silica grains in contact with the CM and the grains within the CM show fringed edges/dissolution textures (Figure 5-4 A).

A few quartz veins crosscut the alternating layered CM and silica veins (Figure 5-5). The full map of the thin section (Fig. 5-5) shows one CM layer (dark brown; #1) to the right of the image that is free of silica (#4 in Figure 5-4 B; Figure 5-5) and several brecciated fragments of almost silica-free CM to the far left within a silica and carbonate matrix. The majority of the remaining CM in the thin section is associated with quartz and chalcedony. Still, in some areas CM is dominant and contains individual grains of quartz (Figure 5-4 A; Figure 5-5 A). These areas appear almost black in cross-polarized light (Figure 5-5 B). Most Au-Ag alloys are associated with CM-enriched silica Figure 5-4; B, C), but can also be found within CM only (Figure 5-4 C), and in association with different sulfides; mostly proustite-pyrargyrite, but also chalcopyrite, pyrite, and sphalerite (Figure 5-4 D) in silica or CM-enriched silica.

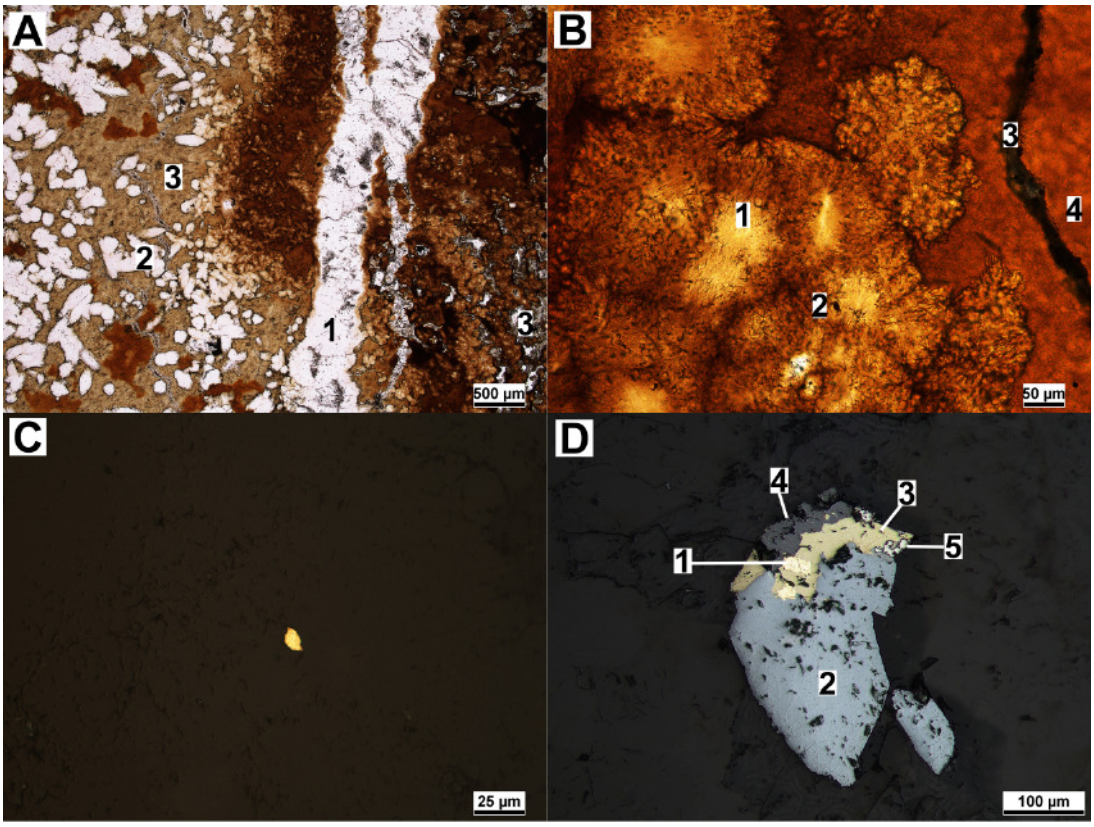

Figure 5-4: Transmitted (A, B) and reflected light (C, D) photomicrographs of sample 2. **A** *Quartz vein (1) crosscutting individual quartz grains (2) with fringed edges and chalcedony enriched in hydrocarbon (brown; 3).* ***B*** *Hydrocarbon-rich chalcedony (1), a single Au-Ag alloy grain (2) in the chalcedony, and a vein filled with sulfides (3), mainly pyrite and some cinnabar, cutting through CM (4).* **C** *Enlarged (50x magnification) reflected light view of Au-Ag alloy within hydrocarbon-rich chalcedony shown in B.* **D** *Au-Ag alloy(1) associated with proustite-pyrargyrite (2), chalcopyrite (3), sphalerite (4), and pyrite (5) surrounded by chalcedony and quartz.*

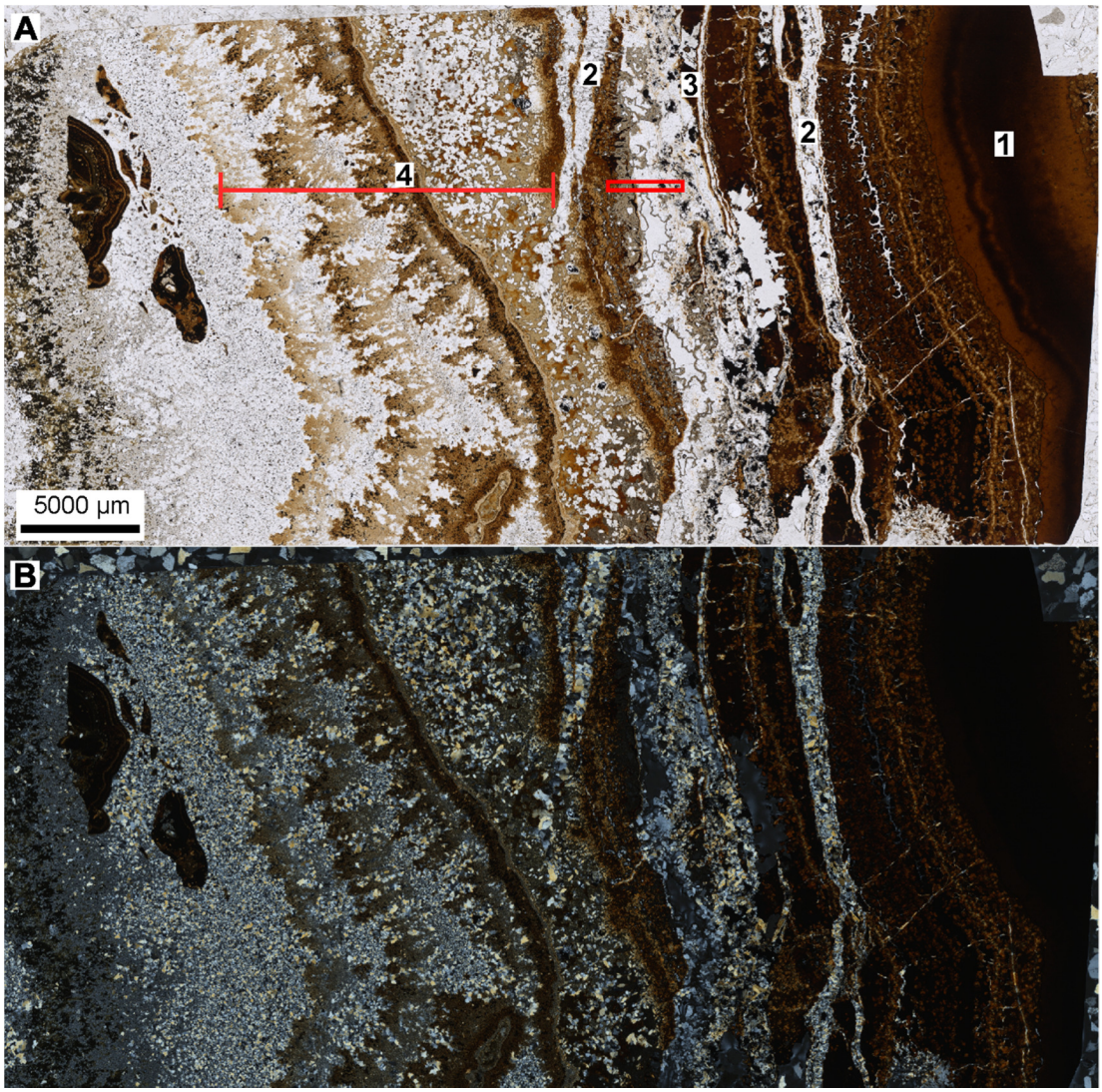

Figure 5-5: Photomicrographs in plane-polarized light (A) and crossed-polarized light (B) of sample 2 (see also Figure 5-4). The red box indicates the region in which Au XANES stack was measured (Figure 5-7). Brown to dark brown colors are CM-enriched silica veins (mainly quartz, chalcedony; #4), and the dark brown region (#1) is pure CM. #2 are silica veins disrupting a silica-CM layer, and #3 is pore space filled with CM.

5.3.1.3 Sample 3

Sample 3 is made up of colloform silica layers, mostly chalcedony and some quartz, with botryoidal texture, and an upper layer of bladed calcite that was completely replaced by quartz. The colloform layers have a maximum thickness of 2 mm and are very fine grained. The bladed calcite was replaced by coarser euhedral quartz crystals with lengths of ~0.2 mm. Vugs within the colloform layers are commonly filled with CM, and some small vugs and fractures are filled with CM and liquid oil (Figure 5-6). In a vug with crystalline quartz (Figure 5-3 D), a large (Ø = 0.5 mm) solid glassy-looking CM sphere and two smaller CM spheres (Ø < 1 mm) are embedded within a quartz cavity. In addition, there are very fine grained layers of disseminated CM between the chalcedony layers, as well as chalcedony layers enriched in

CM, visible in both the hand sample and thin section (Figure 5-3 C and Figure 5-6). In contrast to the chalcedony layers, the quartz layers are usually CM free (Figure 5-6). To summarize, CM is present in sample 3 in the form of hydrocarbon-enriched chalcedony, as liquid oil in small vugs and fractures, and as solid CM in microscopic to macroscopic vugs. The textural relationships indicate that several CM deposition events that occurred both in parallel to, and alternating with, the precipitation of colloform silica. Based on optical microscopy, the only opaque minerals present in sample 3 are small amounts (< 0.5 vol%) of iron sulfides, mostly pyrite; no particulate Au-Ag alloys were observed.

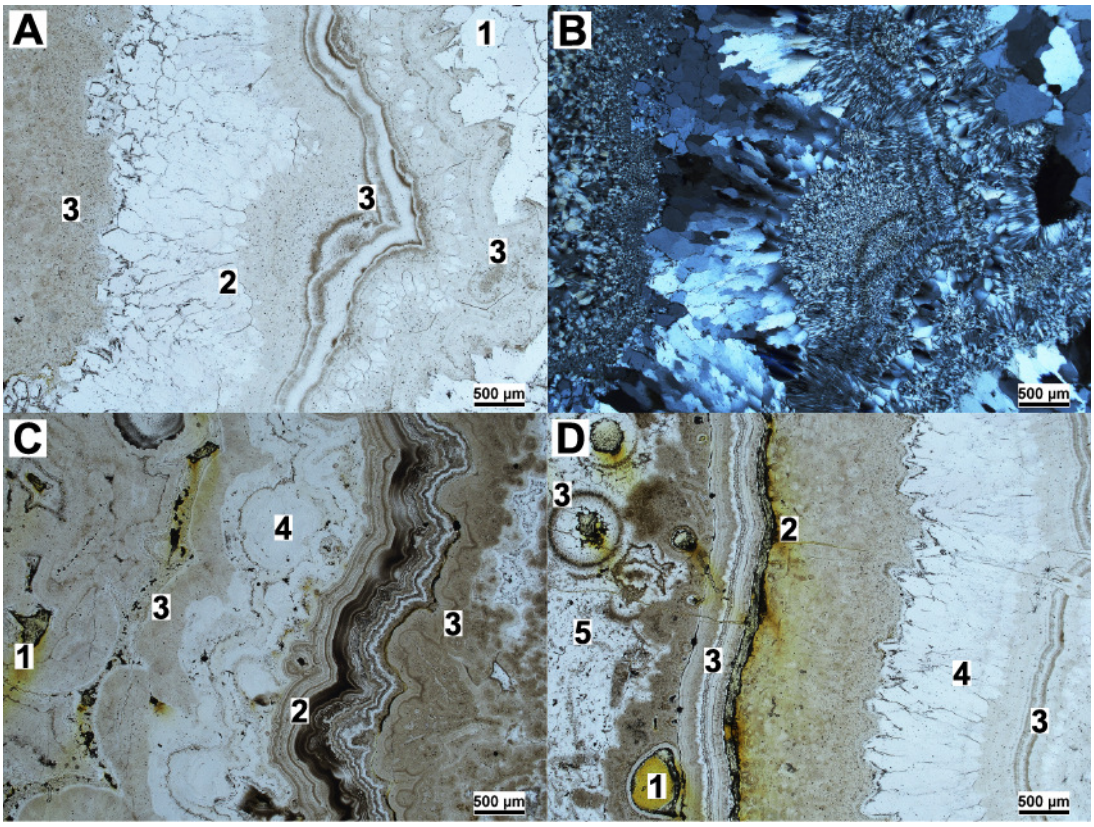

Figure 5-6: Transmitted light photomicrographs of sample 3 in plane-polarized (A, C, D) and cross-polarized light (B). **A** *Quartz (1) and recrystallized quartz (2) in between hydrocarbon-enriched chalcedony (3).* **B** *Image A under crossed polars.* **C** *Vugs filled with liquid oil (1) and solid bitumen (2) and colloform layers of hydrocarbon-rich material (3) and hydrocarbon-free chalcedony (4).* **D** *Liquid oil filing vugs (1), veins, and fractures (2) within different layers of hydrocarbon-enriched chalcedony (3) that is alternating with recrystallized, elongated quartz (4) and fine quartz grains (5).*

5.3.2 Synchrotron X-ray fluorescence microscopy

A gold XANES stack was measured in the area indicated in sample 2 (Figure 5-7); Au XANES were extracted from 6 regions in this area. The spectra of regions 1, 2, 3, 4, and 5 resemble the spectrum of metallic Au. The quality of spectra 6 is low, but may still be in agreement with the spectrum of metallic Au.

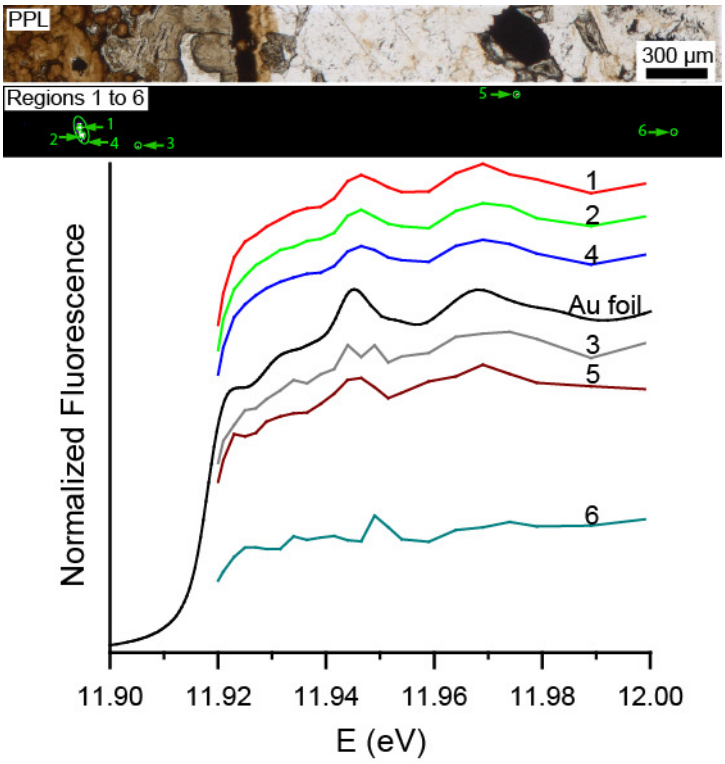

Figure 5-7: At the top is the plane-polarized (PPL) photomicrograph of the greater region selected for the Au XANES stack (see Figure 5-5), and the Au XANES spectra extracted from 6 regions indicated in green are shown below. The metallic Au foil spectrum is from Crede et al. (2017). The spectra indicate that the Au in the selected regions is metallic. Spectra 1, 2, 3, 4, and 5 were measured in CM-enriched silica, while 6 and 7 were measured in a nearly CM-free silica vein.

SXFM element maps collected on the billet of sample 2 and a labeled interpretation of the distribution of different types of dominant vein material in the billet are shown in Figure 5-8. While visual observation of the billet suggests a clear separation of pure CM and silica veins (Figure 5-8 A), the thin section indicates that most of the apparent CM layers are silica layers and veins enriched in CM (Figure 5-5). Thus, both CM and silica are present in most veins and layers, with CM #1 being an exception. The CM #1 layer is silica-free according to optical microscopy (Figure 5-5, section 3.1.2), and a number of these pure, black and apparently CM-only layers are present in the hand sample (Figure 5-3 B). Some CM-free silica veins cross-cut CM-silica veins and layers (e.g., #6 and #9).

The transparent Au SXFM map on top of the photo of the billet illustrates the spatial distribution of Au within the different veins (Figure 5-8 C). Note that due to the depth penetration of the SXFM technique, the element maps may not fit accurately with the vein pattern on the surface of the billet. The SXFM maps may cautiously be compared with the thin section (Figure 5-5) but it has to be kept in mind that the thin section was cut a few millimeters away from the surface of the billet.

5.3.2.1 Au SXFM

The Au SXFM map (Figure 5-8 B) shows distinctive colloform layers and veins that are either low in Au or enriched in Au. Starting from the right side of Figure 5-8 B (Numbered from #1 to #17), the first Au-rich vein is a thin silica vein (#2; <5 µm) dividing a pure CM layer (#1) and a CM-silica layer (#3, Figure 5-8 A). The CM layer and the CM-silica layer appear brown to dark brown in plain-polarized light (Figure 5-5 A), and exhibit a low density distribution of Au, with #3 having a relatively higher Au density than #1. The next distinctive layer (#4) is a mixture of CM and silica (marked as CM-Si in Figure 5-8 D), relatively low in Au (see color coded Figure 5-8) and, like most of the Au in the billet, oriented parallel to the layer pattern. This layer is to the right of a CM-Si layer (#5, Figure 5-8D) that is relatively low in Au and crosscut by a silica (blue chalcedony and quartz)-dominated vein (#6) with a high density of Au and relatively high Au concentrations, and surrounds a fragment of relatively pure CM (#7) (Figure 5-8 A and C). To the left of this Au-rich silica vein is a thicker CM and CM-silica layer (#8) with a relatively higher Au density compared to the previously described CM or CMsilica layers and the vein #6. The silica vein (#9) next to this CMsilica layer is, in comparison, relatively Au free and is in contact with an Au-rich CMsilica wedge (#10), followed by a thick (5000 to 7000 µm) mélange of chalcedony and CM in contact with a quartz layer (#11) showing a high Au density along the contact with CMsilica layer #12. CMsilica layer #12 exhibits a clustered distribution of Au in addition to the high gold intensity along the margin to #11. CM-silica layer #13 has a few Au clusters. The distinctively Au-rich vein to the left is difficult to assign to a particular vein, but is very likely associated with the dark, thin CM rich vein (#15) that can also be seen in the thin section (Figure 5-5) and is in contact with a silica and carbonate rich layer (#14). The area to the left of that vein shows a relatively homogenous Au distribution in a broad CM and silicadominated layer (#16), followed by silica and Fe rich carbonates (#17).

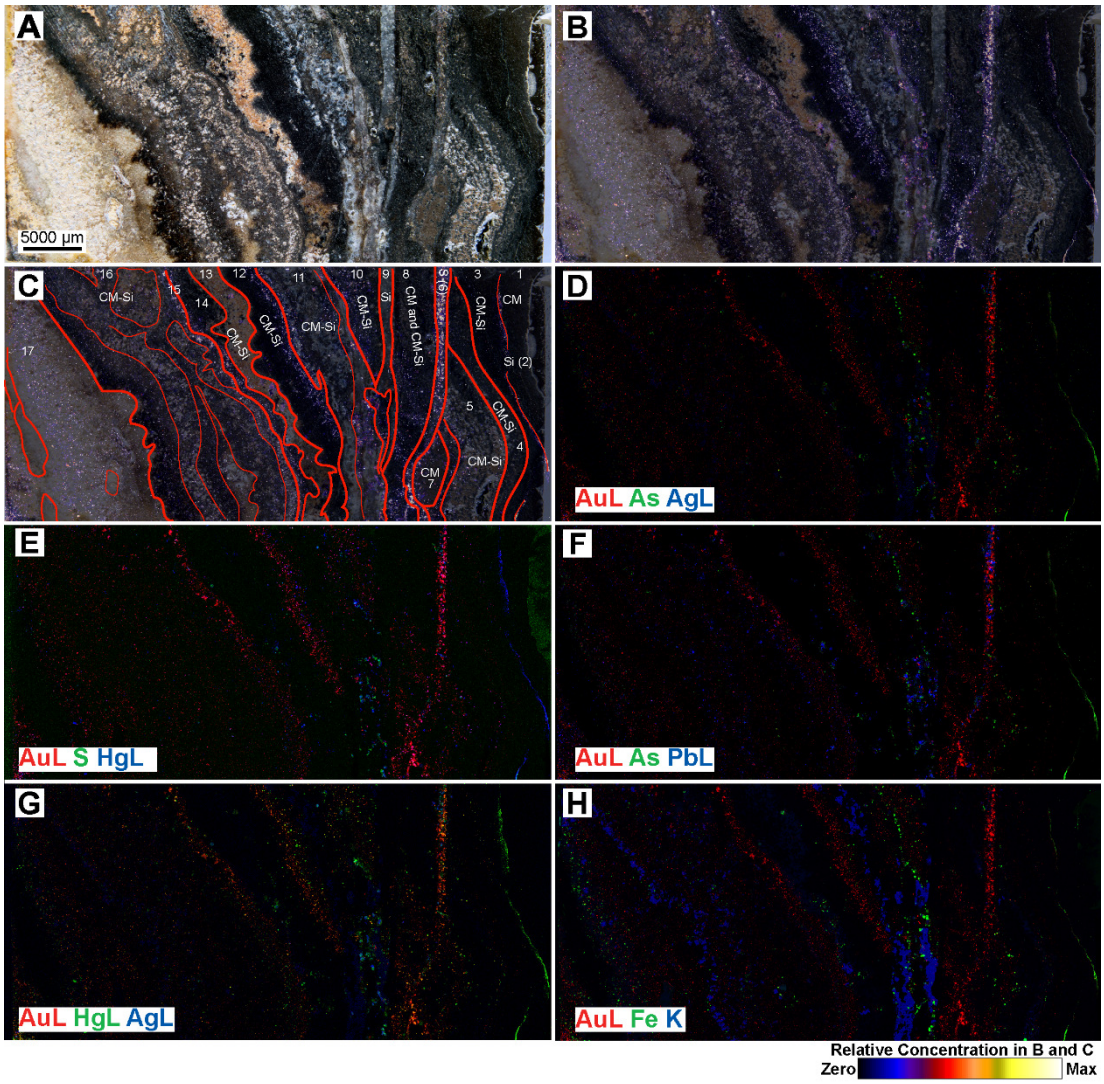

Figure 5-8: (A) Photo of the billet of sample 2; (B) Transparent overlay of the AuSXFM map on top of the billet photo (A); (C) Interpreted layers superimposed on the Au SXFM map and the billet photo (B) with relative concentration of Au in A, B and C (color coded legend in the bottom right). Labels indicate the dominant material (CM=Carbonaceous Matter; S=silica; CM-Si= mix of CM and S); X-rays penetrate into the sample, and thus the overlay in (C) may not be 100% accurate, as veins may dip and change with sample depth. (D to H) Au SXFM Red-Green-Blue maps of the billet with the elements in the color as indicated.

5.3.2.2 SXFM of other elements

The S background is high due to relatively high S concentrations in the epoxy of the billet and the CM (Figure 5-8 E) and therefore the S amount in the sample is close to the detection limit. Most S is associated with the silica- and CM-silica dominated veins (#6, #9, #11), and less so with CM-dominated veins or layers.

Fe is present in the layers/veins #2, 5, 9, 10, 13, and 17, but is spatially not well associated with the distribution of Au. It correlates more strongly with the distribution of As, Pb, Hg and Ag. Iron sulfides identified as pyrite (FeS_2) are present in #2.

The metals Ag, Pb, and Hg correlate strongly with Au in the silica vein #6 and in the two distinctive Au rich layers between #11 and #12 and #14 and #15. Of these metals, Hg shows the strongest spatial correlation with Au distribution. These metals are also present in Au-poor areas of the sample e.g., the area between #11 and #15. Ag, As, and Hg are more abundant within the silica free CM layer #1 than Au and Pb. The presence of As is mostly restricted to the layers/veins #2, 5, 7, 9, and 10. Note that only the Ag hot spots are significant, because Ag X-ray fluorescence lines overlap with those resulting from Ar in the air, which results in high Ag detection limits.

5.3.3 Fluid inclusions and CM

Aqueous fluid inclusions in the McLaughlin samples average 10 to 15 µm in size, with maximum sizes of ~50 µm, and have regular to negative-crystal shapes. The inclusions are two phase, containing a liquid and a vapor bubble (Figure 5-9). Aqueous inclusions dominantly occur along crystal growth boundaries and fractures.

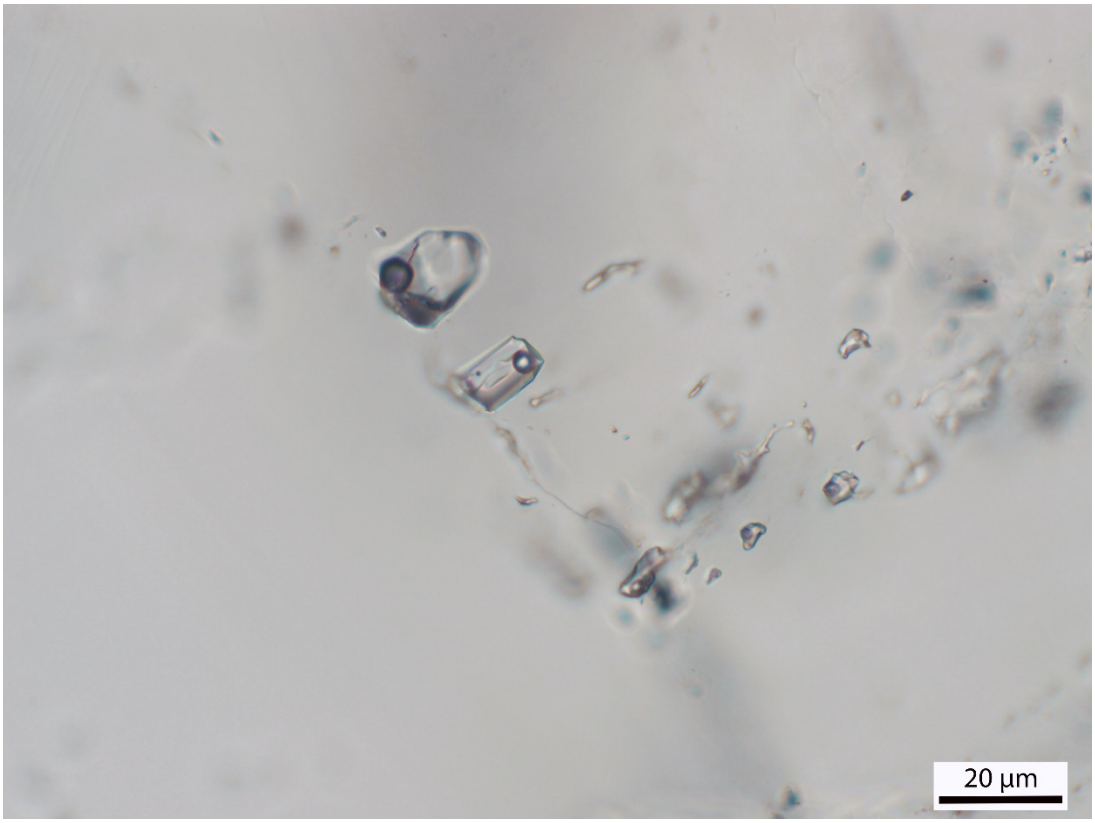

Figure 5-9: Photomicrograph of aqueous fluid inclusions in quartz ranging from 20 µm to < 5 µm in size (sample 1), McLaughlin deposit.

While aqueous fluid inclusions are abundant in the samples, less than one liquid oil inclusion was found on average per double polished thick section, and only one group of several liquid oil inclusions with sizes far smaller than 5 µm. An example of a typical fluorescing hydrocarbon oil or gas inclusion in quartz of sample 1 is shown in Figure 5-10 A-B. The hydrocarbon fluid inclusions have highly irregular shapes, no visible vapor bubble, and show bright white fluorescence. The low number, small sizes and irregular shapes of the oil inclusions were not suitable for LA-ICP-MS, which was originally intended to be used to determine element concentrations in trapped fluids.

The majority of hydrocarbons in the thin sections occur as liquid (especially sample 1) to non-liquid CM filling veins, cracks, or pore spaces along grain boundaries (Figure 5-10; C to F). The CM is grey, dark brown to black under reflected light in the 250 µm thick thin sections and is abundant (Figure 5-10). Fluorescence colors range from white to green and yellow.

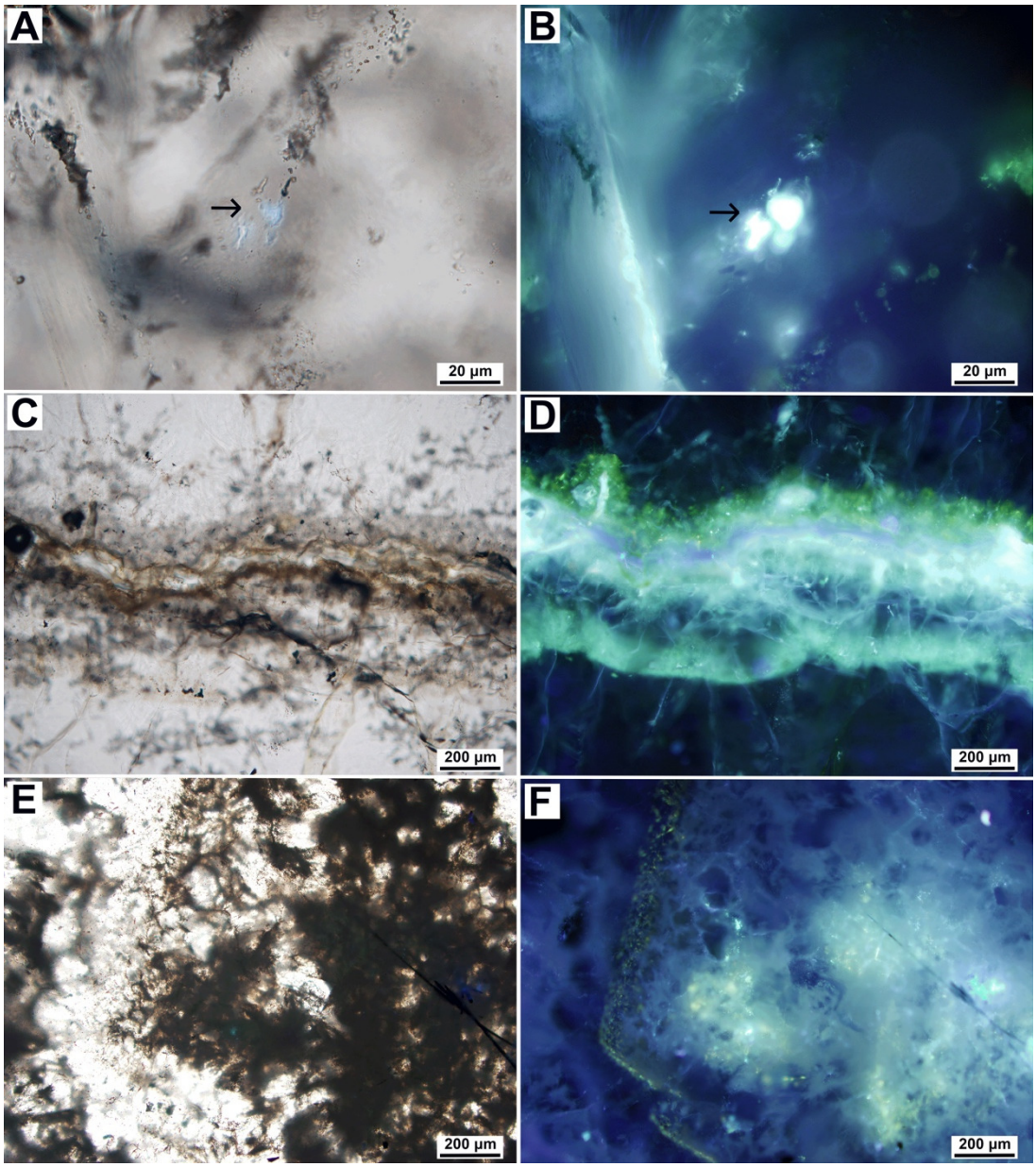

Figure 5-10: Reflected light (left) and UV-light images (right) of sample 1. A and B: Highly irregular hydrocarbon fluid inclusion in quartz. C and D: Vein and cracks filled with hydrocarbons. E and F: Microcrystalline hydrocarbons on grain boundaries and in pore spaces.

5.3.4 Au concentrations in digested CM

The viscous CM covering the quartz and filling the pore spaces of sample 1, although it is soaked in liquid oil, yields an Au concentration of 10800 µg/kg. The solid but brittle silica-free CM of sample 2 has an Au concentration of 5000 µg/kg. The vug fillings in the quartz and chalcedony layers of sample 3 have the highest Au concentration of 18800 µg/kg.

Table 5-1: Au contents in CM digested with acids

Sample	Au (µg/kg)	Mass (g)	Description
Sample 1	10800	0.035	Viscous CM soaked with liquid oil
Sample 2	5000	0.104	Solid, brittle CM (bitumen)
Sample 3	18800	0.010	Vug fillings, solid and brittle CM (bitumen)

5.4 Discussion

Below, the likelihood that metals may have been transported by CM is compared to the likelihood that CM/HC acted only to scavenge metals from aqueous fluid. We discuss the relative timing of deposition of CM, silica and the associated metals, based on textural observations and its implications and the possible importance of the low abundance of hydrocarbon fluid inclusions.

5.4.1 Re-mobilization and mobilization Au by CM

CM is present as liquid oils and viscous CM (tar) soaked with liquid oil, bitumen, bituminous vug infills, as fluid inclusions, and as a solid phase within the McLaughlin deposit. The liquid oil and viscous tar are still mobile, and may have been mobile from the beginning of the formation process of the McLaughlin deposit. This mobile form of CM has ~ 10800 µg/kg Au (Table 5-1) and demonstrates that Au occurs in a mobile hydrocarbon phase within the deposit. Similarly, the high concentrations of Au in the viscous CM soaked in liquid oil in sample 1, in the solid silica free CM of sample 2, in the CM vug infills in sample 3, and in bitumen analyzed by Sherlock (2000) suggest that the Au was at one point in time mobilized by the hydrocarbon phase, and is still mobile in the liquid oils present until today within the deposit. This evidence suggests that the role of hydrocarbons may be underestimated, when they are interpreted to have acted as a scavenging agent only, in ore deposits where mineralization is closely associated with organic matter. Liquid hydrocarbons can act as a transport medium for Au and other metals, and may be a rival ore fluid to aqueous ore fluids and this ability was also demonstrated in a number of experimental studies (Liu et al., 1993; Zhuang et al., 1999; Williams-Jones and Migdisov, 2007; Emsbo et al., 2009; Migdisov et al., 2017; Crede et al., 2019; Crede et al., 2018-A; Crede et al., 2018-B). However, direct evidence of Au-transport by hydrocarbons may not be preserved within the deposit, as the observable CM is usually a decay product, i.e. secondary material that does not necessarily preserve the original Au distribution and concentration in CM, due to

modification by subsequent maturation in response to heat associated with the high temperature fluids that transported the quartz, and due to Au redistribution into the different forms of CM. Whether a hydrocarbon phase migrated from its source and was enriched in Au and transported the Au from the source into the later McLaughlin deposit is beyond the scope of this study to determine given that direct proof is so difficult to attain. Studies to determine the hydrocarbon origin have still to be performed and may help in that matter. Nevertheless, the fact remains that oil can migrate on the km-scale from a source rock into a rock formation that acts as a trap. Under these circumstances we can assume that oil is capable of transporting Au and other metals over long distances and not just within a deposit. This is very important for understanding ore formation processes and the development of ore formation models of deposits associated with CM, like e.g., the McLauhglin deposit, the Witwatersrand Au-U deposits (Fuchs et al., 2016), South Africa, the Erickson Au-Ag deposit (Parnell and McCready, 2000), some Carlin-type deposits (Groves et al., 2016), Nevada and many others.

5.4.2 Au species

Only metallic Au and Au-Ag alloys species where detected by using XANES and optical microscopy. XANES stacks were not collected in a pure CM layer, and thus, although metallic Au was found by optical microscopy in silica-free CM layers (Figure 5-4), we cannot exclude the possibility that Au dissolved in CM may be present within the CM. Due to the high S background, the XFM maps indicate only that S is present, but do not allow to interpret the relationship of Au and S in sample 2. A synchrotron X-ray absorption spectroscopy study by Crede et al. (2019) on Au in 1-dodecanethiol ($CH_3(CH_2)_{10}CH_2SH$) in contact with a 10 wt% Cl bearing brine suggests that Au is transported as metallic Au at temperatures above 125 °C, and in a dissolved form (Au^I) bonded to the thiol group of 1-dodecanethiol below 125 °C. Depending on the timing of CM introduction and current temperature of the hydrothermal deposit, Au could have been transported within CM in both forms.

5.4.3 Do textures preserve information on Au introduction?

The following sections focus on the textural relationships and the information they may have preserved and whether it is possible to determine from the textures only, whether Au and other metals were transported by CM or scavenged by CM from aqueous fluids.

5.4.3.1 Scavenging of Au by CM and interpretation of textural observations

Sherlock (2000) proposed the scavenging theory for the Au-enriched hydrocarbon silica phase and implied that particulate gold precipitated on surfaces with a negative surface charge that may have attracted positively charged protonated areas of hydrocarbons (Frondel, 1938). When exposed to hydrothermal fluids the hydrocarbons would scavenge the Au by absorption. However, the repeated superposition of textural features makes it hard to confirm or refute this hypothesis. If, as suggested by the oxygen and hydrogen isotopes, the source of the ore fluids is meteoric water that interacted with the marine sedimentary rocks of the Great Valley Sequence, and if this process let to a co-migration of hydrocarbons from the marine sedimentary rocks, then metals could have partitioned into the hydrocarbon phase during the migration stage. Partitioning of Au into the HC phase is consistent with the results of Au partition experiments between brine and oil (Crede et al., 2017; Crede et al., 2019; Crede et al., 2018-A; Crede et al., 2018-B).

The metals mapped by SXFM are associated with CM-free silica veins, intermixed CM-silica veins, and CM dominated veins. Some CM and silica are also almost metal-free (#13 and #9). These associations can be used to assess the possibility that metals were transported by the hydrocarbon fluid. The CM in samples 1 and 3 contains Au (Table 5-1), but microscopically visible Au or AuAg alloys were not found in these samples. Since the Au could be in nanoparticulate form within the silica and thus not-visible (for optical microscope imaging), Au could have been scavenged from the silica bearing ore fluids. Thus, these two samples are less informative than sample 2, where the presence of alloy grains and the SXFM data allows more comprehensive interpretation. However, the preserved liquid oil in samples 1 and 3 suggests a late oil fluid migration into the deposits and that temperatures after that event were not much higher than 160 °C. The combined conceptual model discussed in this section is summarized in Figure 5-11.

The silica free CM layer in sample 2 (#1, Figure 5-8 D and Figure 5-5 A) contains Au, As, Ag, Hg, and Fe. Although not much Au is visible *via* SXFM, digestion and ICP-MS analyses of the macroscopically silica free CM of the same sample revealed 5000 µg/kg Au (Table 5-1) and some Au particles were identified *via* optical microscopy (Figure 5-4). The lack of silica in this thick layer is consistent with hydrocarbon phase metal transport. But it is also possible to argue that these metals transferred into the CM in its current location, when the CM or its

precursor hydrocarbon fluid came into contact with metal-bearing hydrothermal silica rich fluids.

The silica-free CM (#1 Figure 5-8 D and Figure 5-5 A) layer in sample 2 shows the same orientation as most layers in the billet and the thin section (e.g., #4 in Figure 5-5; Figure 5-8), suggesting that these layers formed in the same stress-field. Layers with this orientation are crosscut by later silica CM-free veins that can be Au-rich (#6) or Au-free (#9). The metals could have been transported within a hydrocarbon fluid to result in the metal distribution in CM #1 (Figure 5-5; Figure 5-8), but they also could have been scavenged from the later introduced silica.

The layers of sample 2 between #1 and #2 and between #2 and #3 in Figure 5-5A (#1 to #8, Figure 5-8) show chalcedony closely associated and intermixed with CM. This combination is of a light brown to beige color, and is in between layers of a darker brown CM. The Au rich silica dominated vein (#6, Figure 5-8 C) crosscuts both, the Au bearing light brown CM + chalcedony and the dark brown CM, which may be Au bearing. Whether Au spread from the Au rich silica vein into the CM associated layers, was scavenged by the CM associated layers, or whether Au was transported within the CM associated layers is impossible to determine just from these textures. However, the Au free silica vein #9 (Figure 5-8) crosscuts the Au rich CM and CM + quartz grains with the dissolution features (#8 and #10, Figure 5-8). Thus, here Au was possibly introduced in a mix of CM and aqueous fluids that precipitated chalcedony, and did not diffuse from the adjacent Au free silica vein into the CM-rich layers.

The presence of CM is a key factor in explaining the distribution of Au within the deposit e.g., the correlation of Au and CM enriched chalcedony. But, based on the textural observations, it remains mostly inconclusive whether Au and other metals were introduced or transported within any form of CM. Liquid or solid CM enriched in Au is consistent with either Au transport within CM and scavenging of Au from aqueous hydrothermal fluids. CM and aqueous fluids coexisted during the formation of the deposit.

Solid CM may immobilize Au effectively if it contains appropriate ligands, such as S, to bind ionic gold, which would then promote the formation/aggregation of metallic gold (Hough et al., 2008; Hough et al., 2011). This process could promote secondary Au mobility and may contribute to grade increase, but with similar textures as observed here. Thus, in

fossil ore deposit systems like this, it probably is impossible to reconstruct, based on the preserved textures and even the fluid inclusions (due to late metal diffusion), whether CM transported Au and other metals or not. The high Au contents in the liquid hydrocarbons are most likely derived by scavenging from other Au bearing phases and cannot confirm an Au transport in oils into the deposit.

5.4.3.2 Relative timing of fluids

Variation in thermal maturity of the CM phase is thought to record multiple infiltration episodes and with some *in-situ* thermal maturation, synchronous and asynchronous with aqueous fluids. Liquid and viscous properties of the CM are an indicator of the thermal maturity of the CM and the temperature that the CM has seen. Liquid oils for example must have been within the liquid oil temperature window not greater than 160 °C. The coincidence of CM and silica suggests that hydrocarbon and non-hydrocarbon fluids used the same pathways within the McLaughlin deposit both simultaneously, to deposit the CM-enriched chalcedony layers, and alternately. This implies that at some points in time hydrocarbons migrated without aqueous fluids from their source or from some intermediate location between the source and the deposit, into the McLaughlin deposit.

The shared use of the same pathways in spite of the near absence of hydrocarbon fluid inclusions entrapped in the vein quartz, discussed above, is supported by textural analyses of samples 1 to 3 (section 3.1 and 4.3). These textures indicate that oil migration pre-, and post-dated precipitation of vein quartz, and that oil migrated within the deposit. Furthermore, the close association of CM and chalcedony suggests a parallel precipitation of chalcedony and CM. Observations in support of this notion are the viscous nature of the CM and specially the liquid oil in sample 1, and the liquid oil in sample 3. For example, the liquid oil associated with solid CM that is enclosed by colloform chalcedony and quartz (Figure 5-6 C and D) in sample 3 appears to be liquid oil remaining after enclosure and partial degradation of the associated CM. The CM within the liquid oil must have experienced lower temperatures compared to the solid, degraded CM. The remaining liquid oil could then have migrated through micro cracks and along boundaries into the adjacent silica phases.

The glassy CM spheres in sample 3 (Figure 5-3 D) are emplaced on quartz in only partially filled vugs and are thus interpreted to have formed after the quartz. The vugs are residual open spaces left by incomplete filling of a cavity or fracture i.e., the colloform quartz

bands were filling in a fracture. The hydrocarbon fluids then passed through the vugs and deposited the CM that we can observe now (Figure 5-11). The described order of events is consistent with the suggestions of hydrocarbon migration into the deposit with and without aqueous fluid interaction or mixing. This CM material contains 18800 µg/kg Au, but contact with Au-bearing aqueous fluids can't be eliminated as a possibility.

The complex cross-cutting relations between CM, chalcedony and quartz in samples 2 and 3 are interpreted as repeated cycles of CM, chalcedony and quartz deposition. CM is also closely interlayered with chalcedony (but not quartz) indicating that CM introduction was synchronous with silica-bearing fluids (Figure 5-5) and that the source fluids could bear both silica and organic species. However, the thick CM layer (#1 inFigure 5-5 A) free of silica indicates that CM did precipitate, at times, without co-precipitation of chalcedony. The lack of CM + quartz veins suggests that CM did not precipitate together with quartz and that the temperature of the fluids responsible for quartz precipitation was too high for liquid CM to be stable. At these temperatures (>160 °C) bituminous overmature CM is expected. Aqueous fluids at these temperatures would have lost any dissolved CM before the fluids entered the deposit. On the other hand, the co-location of CM and chalcedony is consistent with precipitation of chalcedony at lower temperatures that permit hydrocarbon stability transport of hydrocarbons within the silica bearing fluids into the deposit. The other possibility that must be considered is that CM- bearing fluids did not use the fluid pathways at the same time as aqueous fluids, and that CMfree quartz was simply precipitated from CM-free fluids.

Evidence of hydrocarbon introduction post-dating quartz precipitation is also provided by dissolution features at the margins of the quartz grains in sample 2 and the distribution of these quartz grains within an hydrocarbon matrix (Figure 5-4), if dissolution is assumed to be related to organic acids introduced after the quartz grain precipitation (e.g., Bennett et al., 1988; Bennett, 1991; Drever and Stillings, 1997). An absence of hydrocarbon fluid inclusions in the quartz grains with the dissolution features, and CM filling pore spaces (Figure 5-6) also suggests that the CM was introduced after the quartz was introduced. To summarize, the textural observations imply repeated influxes of fluids that deposited quartz, chalcedony and CM.

5.4.3.3 Fluorescence colors

The variation of fluorescence colors of the liquid and solid CM in this study indicate different compositions and thus can possibly indicate different thermal maturity stages of the hydrocarbons (Khorasani, 1987; Mclimans, 1987; Pradier et al., 1991; Stasiuk and Snowdon, 1997; George et al., 2001). The samples therefore may be either preserved oils from distinct migration or maturation stages in the McLaughlin deposit or alternatively, the oils or CM could be from a single event, with variation due to polar compounds being preferably adsorbed onto charged mineral surfaces leading to a separation of organic compounds and potentially different fluorescence colors (George et al., 2001). However, the range of different forms of CM from liquid to crystalline is more consistent with the expected result of a combination of multiple phases of migration with or without *in-situ* modification by hydrothermal heat, biodegradation or water washing (Pradier et al., 1991; Simoneit, 1993), in addition to the separation of organic compounds. This is an indicator of multiple CM introduction episodes.

5.4.3.4 Fluid Inclusion microthermometry

Fluid inclusion microthermometry suggests that the aqueous fluids were trapped between 121°C and 263°C with an average temperature of 253 °C (Sherlock et al., 1995). This is in agreement with the replacement textures of bladed calcite, which indicates that the aqueous fluid was at P-T-X conditions consistent with boiling (Simmons and Christenson, 1994). CM filling the open spaces between the bladed calcites suggest that hydrocarbons were either introduced or still mobile after boiling took place because at temperatures above 200 °C, hydrocarbons would be thermally mature or over-mature and could not have migrated into the open space (Glikson and Mastalerz, 2000). The viscous CM and liquid oil, which require lower temperatures to preserve the liquidity, support the suggestion that liquid oils migrated into the deposit at temperatures lower than 160 °C with a source rock elsewhere (Jacob, 1993; Simoneit, 1993, 2000a; Simoneit, 2000b). The solid CM is clearly ex-situ and is therefore interpreted as a maturation and degradation product of liquid HC introduced with or without aqueous fluids after the meteoric water interacted with the sedimentary rocks of the Great Valley sequence (Sherlock et al., 1995) and experienced temperatures above 160 °C.

The McLaughlin Au-Hg deposit has a prolonged dual fluid (oil and aqueous fluids) history. The samples bear several indicators supporting a model with multiple phases of CM migration, partially asynchronous with silica-introduction, into the McLaughlin deposit, possibly followed by *in-situ* maturation by hydrothermal heat, biodegradation or water washing and migration of viscous CM and liquid oil within the deposit, and late stage infiltration of liquid oil. The order of events based on samples 1 to 3 is illustrated in Figure 5-11.

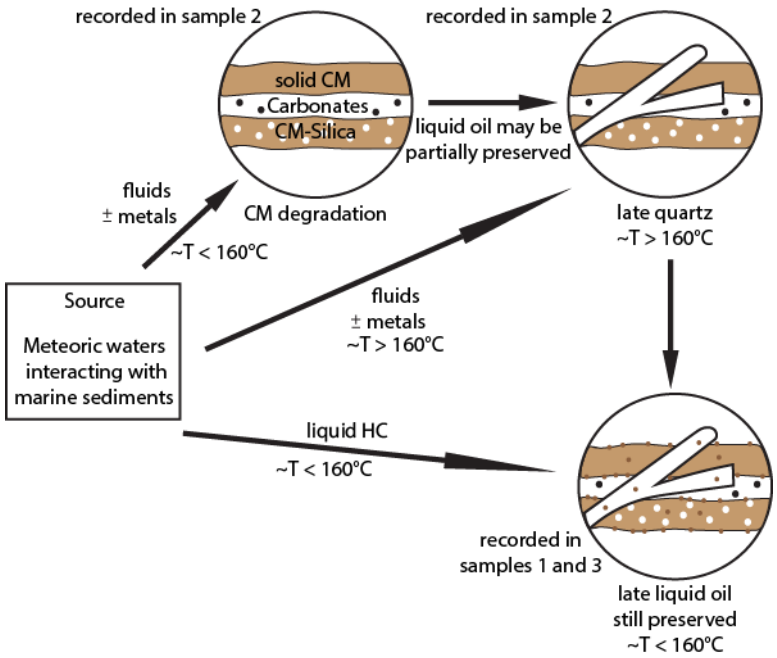

Figure 5-11: Combined conceptual model recorded in samples 1 to 3 as discussed in section 4.3.

5.4.4 Low hydrocarbon FLINCS *versus* abundant aqueous FLINCS

Although some of the McLaughlin vein samples are literally soaked in viscous and liquid hydrocarbons (sample 1), hydrocarbon inclusions that could provide information on the hydrocarbon fluid composition at the time of trapping are present in extremely low abundances, while there are hundreds of aqueous fluid inclusions in quartz. Aqueous and hydrocarbon fluids could have been present in similar amounts at some points in time during the deposit formation, but the different fluid properties and different trapping processes of the two fluids could have led to differential preservation of the two types of fluid inclusions. The absence of a bubble in the oil inclusions indicates entrapment at low pressure or moderate temperature and high pressure (Bourdet et al., 2008).

The samples chosen for our fluid inclusion study lack the oil inclusions reported in the other studies of McLaughlin veins (Peters, 1991; Sherlock et al., 1995; Sherlock, 2000). One explanation of this difference is that liquid oil migration pathways, on which abundant liquid oil inclusions were produced, were missed by our sampling. The probability that this possibility is correct is increased if the fluid pathways are discrete and cover only a small proportion of the deposit. In the samples described here, cross-cutting relationships suggest that some of the quartz veins could have been precipitated without any presence of a hydrocarbon fluid if the rare fluorescing fluid inclusions in these veins are interpreted as inclusions of pre-existing CM similar to that in contact with the veins. Other silica veins have an unambiguously syn-genetic relationship with CM, but still lack abundant oil inclusions. It is therefore not possible to eliminate this possibility.

However, we note that the previous works that reported hydrocarbon fluid inclusions did not publish images or specific information on the amount of hydrocarbon fluid inclusions found in their samples. Peters (1991) stated that half of her sections contained inclusions which fluoresced yellow-green under blue light (405-490 nm), a few of which were also excited by UV light (334-365 nm). According to the author, these wavelengths are indicative of liquid hydrocarbons in the fluid inclusions. Other studies have shown that all oil inclusions, even very light condensates (methane and short-chained hydrocarbons), fluoresce under blue light and fluoresce more strongly at shorter wavelengths (Downare and Mullins, 1995; Liu and Eadington, 2005). Thus, all hydrocarbons, from light to heavy and liquid to solid, would fluoresce under UV light. This inconsistency leads us to suspect that Peters (1991) may have defined all hydrocarbons, including solids, present in the samples as oil inclusions, thus over-representing the number of “true” liquid oil inclusions at McLaughlin.

A likely explanation for the small number of oil inclusions as compared to hundreds of aqueous inclusions in single grains is a difference in wettability of the two fluids, leading to preferential trapping of the aqueous phase. This enables the lack of fluid oil inclusions to be reconciled with the proposal that hydrocarbons are present throughout the whole paragenetic sequence of the McLaughlin deposit (Sherlock, 1992; Sherlock, 2000). While the wettability of aqueous *versus* hydrocarbon fluids are dependent on factors such as fluid composition and temperature, studies of oil reservoirs have shown that silicates may be dominantly wetted by either oil or water (Xie et al., 1997; Morrow et al., 1998). If the oil is not able to wet the growing minerals because it is forced away by the aqueous phase (surfaces are water-wetted), aqueous fluid inclusions will be in the majority compared to oil

inclusions. A low oil wettability would lead to a low number of oil inclusions compared to aqueous inclusions and could explain the near absence of oil inclusions.

5.4.5 Implications

Common genetic models of Au deposits involving hydrocarbons indicate that hydrocarbons are usually not syn-genetic with Au mineralization and are thus not involved in metal transport, but acted as a reductant or when Au was available for uptake were enriched in Au aided in this way in metallogenesis (e.g., Parnell and McCready, 2000). This study in combination with the earlier presented experimental studies suggest that hydrocarbon liquids have to be considered as potential ore fluids. If indicators of a syn-genetic hydrocarbon introduction are observed, it is possible that hydrocarbons were involved in metal transport and further investigations can be applied to investigate the involvement of hydrocarbons. Re-mobilization of metals by liquid hydrocarbons can result in further concentration of metals within the deposit. And lastly, the role of hydrocarbons could be given more prominence in ore deposit exploration, by taking into account the possible migration pathways of hydrocarbon fluids when exploring for deposits that are known to be associated with hydrocarbons (Taylor, 2000).

5.5 Conclusions

Hydrocarbon/CM fluids and aqueous fluids were present synchronously during formation of the McLaughlin deposit, and the CM forms an important reservoir for Au with higher Au concentrations than in the average background sinter of 4490 µg/kg (Tosdal et al., 1993). While textural evidence alone is not enough to constrain the exact role of CM, the high Au concentrations in liquid HC/CM in the McLaughlin deposit, the ability of oil to migrate long distances in addition to experimental studies showing that CM can transport metals better than aqueous fluids in specific environments (low to medium temperatures), and that hydrocarbon and aqueous fluids have used the same pathways could be strong indicators of a HC/CM metal phase transport. It is not clear whether metals such as Au have been transported into the McLaughlin deposit, but they were (re-) mobilized within the deposit.

Acknowledgements

This work was supported by a Discovery Project (DP140103995) and Future Fellowships (FT120100579 and FT100150200) from the Australian Research Council, the Australian Research Centre in Perth, the Commonwealth Scientific and Industrial Research Organisation (CSIRO), and by funding from The Institute for Geoscience Research (TIGeR). Part of this research was undertaken on the X-ray fluorescence microscopy beamline at the Australian Synchrotron, part of ANSTO.

References

Bennett, P., Melcer, M., Siegel, D. and Hassett, J. (1988) The dissolution of quartz in dilute aqueous solutions of organic acids at 25 C. *Geochim. Cosmochim. Acta* **52**, 1521-1530.

Bennett, P.C. (1991) Quartz dissolution in organic-rich aqueous systems. *Geochim. Cosmochim. Acta* **55**, 1781-1797.

Berger, B.R. and Bagby, W.C. (1993) The geology and origin of Carlin-type gold deposits, in: Foster, R.P. (Ed.), Gold Metallogeny and Exploration. Springer Netherlands, pp. 210-248.

Blake, M., Jr (1981) Geologic transect of the northern Diablo Range, California.

Blake, M., Jr and Jones, D. (1981) The Franciscan assemblage and related rocks in northern California: a reinterpretation. *The Geotectonic Development of California*, 306-328.

Bourdet, J., Pironon, J., Levresse, G. and Tritlla, J. (2008) Petroleum type determination through homogenization temperature and vapour volume fraction measurements in fluid inclusions. *Geofluids* **8**, 46-59.

Bowell, R.J., Baumann, M., Gingrich, M., Tretbar, D., Perkins, W.F. and Fisher, P.C. (1999) The occurrence of gold at the Getchell mine, Nevada. *J. Geochem. Explor.* **67**, 127-143.

Brabb, E.E., Powell, C.L. and Brocher, T.M. (2001) Preliminary compilation of data for selected oil test wells in Northern California. US Department of the Interior, US Geological Survey.

Chapman, R.N., O'Neil, J.R. and Mayeda, T.K. (1972) Bouguer gravity map of California, Ukiah sheet: California Division of Mines and Geology.

Connan, J. (1979) Genetic relation between oil and ore in some Pb-Zn-Ba ore deposits. *Special Publication of the Geological Society of South Africa* **5**, 263-274.

Crede, L. S., Liu, W., Evans, K. A., Rempel, K. U., Testemale, D., & Brugger, J. (2019). Crude oils as ore fluids: An experimental in-situ XAS study of gold partitioning between brine and organic fluid from 25 to 250° C. *Geochim. Cosmochim. Acta*, *244*, 352-365.

Crede, L. S., Evans, K. A., Rempel, K. U., Grice, K., & Sugiyama, I. (2018-A). Gold partitioning between 1-dodecanethiol and brine at elevated temperatures: Implications of Au transport in hydrocarbons for oil-brine ore systems. *Chem. Geol.*.

Crede, L. S., Rempel, K. U., Hu, S. Y., & Evans, K. A. (2018-B). An experimental method for gold partitioning between two immiscible fluids: Brine and n-dodecane. *Chem. Geol.*.

Crede, L.-S., Remple, K., Brugger, J. and Liu, W. (2017) The role of organics in gold transport: An investigation of gold speciation in organic liquids: European Synchrotron Facility, Experiment number: ES-552.

Cumberland, S.A., Etschmann, B., Brugger, J., Douglas, G., Evans, K., Fisher, L., Kappen, P. and Moreau, J.W. (2018) Characterization of uranium redox state in organic-rich Eocene sediments. *Chemosphere* **194**, 602-613.

Dickinson, W.R. (1981) Plate tectonics and the continental margin of California. *The geotectonic development of California: Englewood Cliffs, New Jersey, Prentice-Hall*, 1-28.

Downare, T.D. and Mullins, O.C. (1995) Visible and near-infrared fluorescence of crude oils. *Appl. Spectrosc.* **49**, 754-764.

Drever, J. and Stillings, L. (1997) The role of organic acids in mineral weathering. *Colloids and Surfaces A: Physicochemical and Engineering Aspects* **120**, 167-181.

Emsbo, P. and Koenig, A.E. (2007) Transport of Au in petroleum: Evidence from the northern Carlin trend, Nevada, in: al., C.J.A.e. (Ed.), *Mineral Eploration and Research: Digging Deeper*. Proc. 9th Biennial SGA Meeting, Millpress, Dublin, pp. 695-698.

Emsbo, P., Williams-Jones, A.E., Koenig, A.E. and Wilson, S.A. (2009) Petroleum as an Agent of Metal Transport: Metallogenic and Exploration Implications, in: Williams, P.J. (Ed.), In, P.J. Williams (ed.) *Smart Science for Exploration and Mining*. Proc. 10th Biennial SGA Meeting, James Cook Univ. Earth & Enviro. Studies, pp. 99-101.

Etoh, J., Izawa, E., Watanabe, K., Taguchi, S. and Sekine, R. (2002) Bladed quartz and its relationship to gold mineralization in the Hishikari low-sulfidation epithermal gold deposit, Japan. *Econ. Geol.* **97**, 1841-1851.

Etschmann, B., Liu, W., Li, K., Dai, S., Reith, F., Falconer, D., Kerr, G., Paterson, D., Howard, D. and Kappen, P. (2017) Enrichment of germanium and associated arsenic and tungsten in coal and roll-front uranium deposits. *Chem. Geol.* **463**, 29-49.

Etschmann, B., Ryan, C., Brugger, J., Kirkham, R., Hough, R., Moorhead, G., Siddons, D., De Geronimo, G., Kuczewski, A. and Dunn, P. (2010) Reduced As components in highly oxidized environments: Evidence from full spectral XANES imaging using the Maia massively parallel detector. *Am. Mineral.* **95**, 884-887.

Etschmann, B.E., Donner, E., Brugger, J., Howard, D.L., de Jonge, M.D., Paterson, D., Naidu, R., Scheckel, K.G., Ryan, C.G. and Lombi, E. (2014) Speciation mapping of environmental samples using XANES imaging. *Environmental Chemistry* **11**, 341-350.

Fuchs, S., Migdisov, A. and Williams-Jones, A.E. (2011) The transport of gold in petroleum: An experimental study, Goldschmidt. *Mineral Mag.*, Prague, Czech Republic, p. 871.

Fuchs, S., Schumann, D., Williams-Jones, A.E. and Vali, H. (2015) The growth and concentration of uranium and titanium minerals in hydrocarbons of the Carbon Leader Reef, Witwatersrand Supergroup, South Africa. *Chem. Geol.* **393-394**, 55-66.

Fuchs, S., Williams-Jones, A.E., Jackson, S.E. and Przybylowicz, W.J. (2016) Metal distribution in pyrobitumen of the Carbon Leader Reef, Witwatersrand Supergroup, South Africa: Evidence for liquid hydrocarbon ore fluids. *Chem. Geol.* **426**, 45-59.

George, S.C., Ruble, T.E., Dutkiewicz, A. and Eadington, P.J. (2001) Assessing the maturity of oil trapped in fluid inclusions using molecular geochemistry data and visually-determined fluorescence colours. *Appl. Geochem.* **16**, 451-473.

Giordano, T. and Barnes, H. (1981) Lead transport in Mississippi Valley-type ore solutions. *Econ. Geol.* **76**, 2200-2211.

Giże, A. (2000) The organic geochemistry of gold, platinum, uranium and mercury deposits. *Rev. Econ. Geol.: Ore Genesisis and Exploration: The Roles of Organic Matter*, 217-250.

Gize, A. P., Kuehn, C. A., Furlong, K. P., & Gaunt, J. M. (2000). Organic maturation modeling applied to ore genesis and exploration. *Rev. Econ. Geol.*, *9*, 87-104.

Giże, A.P. (1999) A special issue on organic matter and ore deposits: Interactions, applications, and case studies - Introduction. *Econ. Geol. and the Bull. Soc. of Economic Geologists* **94**, 963-965.

Glikson, M. and Mastalerz, M. (2000) Organic matter and mineralisation: thermal alteration, hydrocarbon generation and role in metallogenesis. Springer Science & Business Media.

Groves, D.I., Goldfarb, R.J. and Santosh, M. (2016) The conjunction of factors that lead to formation of giant gold provinces and deposits in non-arc settings. *Geosc. Frontiers* **7**, 303-314.

Hearn, B.C., Jr, Donnelly-Nolan, J. and Goff, F.E. (1981) The Clear Lake volcanics: Tectonic setting and magma sources. *US Geol. Surv. Prof. Pap* **1141**, 25-45.

Hough, R., Noble, R., Hitchen, G., Hart, R., Reddy, S., Saunders, M., Clode, P., Vaughan, D., Lowe, J. and Gray, D. (2008) Naturally occurring gold nanoparticles and nanoplates. *Geology* **36**, 571-574.

Hough, R., Noble, R. and Reich, M. (2011) Natural gold nanoparticles. *Ore Geol. Rev.* **42**, 55-61.

Jacob, H. (1993) Nomenclature, classification, characterization, and genesis of natural solid bitumen (migrabitumen), Bitumens in ore deposits. Springer, pp. 11-27.

Khorasani, G.K. (1987) Novel development in fluorescence microscopy of complex organic mixtures: application in petroleum geochemistry. *Org. Geochem.* **11**, 157-168.

Kirkham, R., Dunn, P., Kuczewski, A., Siddons, D., Dodanwela, R., Moorhead, G., Ryan, C., De Geronimo, G., Beuttenmuller, R. and Pinelli, D. (2010) The Maia Spectroscopy Detector System: Engineering for Integrated Pulse Capture, Low-Latency Scanning and Real-Time Processing, AIP Conference Proceedings. AIP, pp. 240-243.

Kucha, H. (1981) Precious metal alloys and organic matter in the Zechstein copper deposits, Poland. *Mineral. Petrol.* **28**, 1-16.

Kucha, H. and Przylowicz, W. (1999) Noble metals in organic matter and clay-organic matrices, Kupferschiefer, Poland. *Econ. Geol.* **94**, 1137-1162.

Lehrman, N.J. (1986) The McLaughlin mine, Napa and Yolo Counties, California. *Nevada Bureau of Mines and Geology*, 85-89.

Li, K., Etschmann, B., Rae, N., Reith, F., Ryan, C.G., Kirkham, R., Howard, D., Rosa, D.R., Zammit, C. and Pring, A. (2016) Ore petrography using megapixel X-ray imaging: rapid insights into element distribution and mobilization in complex Pt and U-Ge-Cu ores. *Econ. Geol.* **111**, 487-501.

Liu, J., Fu, J. and Lu, J. (1993) Experimental study on interaction between organic matter and gold. *'Sci. Geol. Sin.' In Chinese.* **28**, 246-253.

Liu, K. and Eadington, P. (2005) Quantitative fluorescence techniques for detecting residual oils and reconstructing hydrocarbon charge history. *Org. Geochem.* **36**, 1023-1036.

Lu, J. and Zhuang, H. (1996) Experimental studies on role of organic matter during mineralization of gold and silver at low temperatures. *'Gechim.' In Chinese.* **25**, 173-180.

McLaughlin, R., Ohlin, H., Thormahlen, D., Jones, D., Miller, J. and Blome, C. (1985) Geologic map and structure sections of the Little Indian Valley-Wilbur Springs geothermal area northern Coast Ranges, California. US Geological Survey.

McLaughlin, R.J. (1978) Preliminary Geologic Map and Structural Sections of the Central Mayacamas Mountains and the Geysers Steam Field, Sonoma, Lake and Mendocino Counties, California. United States Geological Survey.

McLaughlin, R.J. (1981) Tectonic setting of pre-Tertiary rocks and its relation to geothermal resources in The Geysers-Clear Lake area. *US Geol. Surv. Prof. Pap* **1141**, 3-23.

Mclimans, R.K. (1987) The application of fluid inclusions to migration of oil and diagenesis in petroleum reservoirs. *Appl. Geochem.* **2**, 585-603.

Miedaner, M.M., Migdisov, A.A. and Williams-Jones, A.E. (2005) Solubility of metallic mercury in octane, dodecane and toluene at temperatures between 100 degrees C and 200 degrees C. *Geochim. Cosmochim. Acta* **69**, 5511-5516.

Migdisov, A., Guo, X., Williams-Jones, A., Sun, C., Vasyukova, O., Sugiyama, I., Fuchs, S., Pearce, K. and Roback, R. (2017) Hydrocarbons as ore fluids. *Geochem. Persp. Lett.* **5**, 47-52.

Morrow, N.R., Tang, G.-q., Valat, M. and Xie, X. (1998) Prospects of improved oil recovery related to wettability and brine composition. *Journal of Petroleum science and Engineering* **20**, 267-276.

Parnell, J. and McCready, A. (2000) Paragenesis of gold-and hydrocarbon-bearing fluids in gold deposits, Organic Matter and Mineralisation: Thermal Alteration, Hydrocarbon Generation and Role in Metallogenesis. Springer, pp. 38-52.

Paterson, D., De Jonge, M., Howard, D., Lewis, W., McKinlay, J., Starritt, A., Kusel, M., Ryan, C., Kirkham, R. and Moorhead, G. (2011) The X-ray Fluorescence Microscopy Beamline at the Australian Synchrotron, AIP Conference Proceedings. AIP, pp. 219-222.

Pearcy, E. and Burruss, R. (1993) Hydrocarbons and gold mineralization in the hot-spring deposit at Cherry Hill, California, Bitumens in Ore Deposits. Springer, pp. 117-137.

Peters, E.K. (1991) Gold-bearing hot spring systems of the northern Coast Ranges, California. *Econ. Geol.* **86**, 1519-1528.

Pradier, B., Bertrand, P., Martinez, L. and Laggoun-Defarge, F. (1991) Fluorescence of organic matter and thermal maturity assessment. *Org. Geochem.* **17**, 511-524.

Roedder, E. (1984) Fluid inclusions: Reviews in mineralogy: Mineralogical Society of American, v. 12.

Ryan, C., Etschmann, B., Vogt, S., Maser, J., Harland, C., Van Achterbergh, E. and Legnini, D. (2005) Nuclear microprobe–synchrotron synergy: towards integrated quantitative real-time elemental imaging using PIXE and SXRF. *Nuclear Instruments and Methods in Physics Research Section B: Beam Interactions with Materials and Atoms* **231**, 183-188.

Ryan, C., Kirkham, R., Hough, R., Moorhead, G., Siddons, D., De Jonge, M., Paterson, D., De Geronimo, G., Howard, D. and Cleverley, J. (2010a) Elemental X-ray imaging using the Maia detector array: The benefits and challenges of large solid-angle. *Nuclear Instruments and Methods in Physics Research Section A: Accelerators, Spectrometers, Detectors and Associated Equipment* **619**, 37-43.

Ryan, C., Siddons, D., Kirkham, R., Dunn, P., Kuczewski, A., Moorhead, G., De Geronimo, G., Paterson, D., De Jonge, M. and Hough, R. (2010b) The new Maia detector system: methods for high definition trace element imaging of natural material, AIP Conference Proceedings. AIP, pp. 9-17.

Ryan, C., Siddons, D., Kirkham, R., Li, Z., de Jonge, M., Paterson, D., Kuczewski, A., Howard, D., Dunn, P. and Falkenberg, G. (2014) Maia X-ray fluorescence imaging: Capturing detail in complex natural samples, Journal of Physics: Conference Series. IOP Publishing, p. 012002.

Rytuba, J.J. (1993) Epithermal precious-metal and mercury deposits in the Sonoma and Clear Lake volcanic fields, California. *Active geothermal systems and gold-mercury deposits in the Sonoma-Clear Lake volcanic fields, California: Society of Economic Geologists, Guidebook Series* **16**, 38-51.

Sawlowicz, Z., Gize, A. and Rospondek, M. (2000) Organic matter from Zechstein copper deposits (Kupferschiefer) in Poland, Organic Matter and Mineralisation: Thermal Alteration, Hydrocarbon Generation and Role in Metallogenesis. Springer, pp. 220-242.

Sherlock, R. (1992) The empirical relationship between gold-mercury mineralization and hydrocarbons, in the northern Coast Ranges, California, GAC-MAC Joint Annual Meeting, Program with Abstracts.

Sherlock, R. (2000) The association of gold—mercury mineralization and hydrocarbons in the coast ranges of northern California, Organic Matter and Mineralisation: Thermal

Alteration, Hydrocarbon Generation and Role in Metallogenesis. Springer, pp. 378-399.

Sherlock, R.L. (2005) The relationship between the McLaughlin gold-mercury deposit and active hydrothermal systems in the Geysers-Clear Lake area, northern Coast Ranges, California. *Ore Geol. Rev.* **26**, 349-382.

Sherlock, R.L. and Lehrman, N.J. (1995) Occurrences of Dendritic Gold at the Mclaughlin Mine Hot-Spring Gold Deposit. *Miner. Deposita* **30**, 323-327.

Sherlock, R.L., Tosdal, R.M., Lehrman, N.J., Graney, J.R., Losh, S., Jowett, E.C. and Kesler, S.E. (1995) Origin of the McLaughlin mine sheeted vein complex: Metal zoning, fluid inclusion, and isotopic evidence. *Econ. Geol.* **90**, 2156-2181.

Simmons, S.F. and Christenson, B.W. (1994) Origins of calcite in a boiling geothermal system. *Am. J. Sci.* **294**, 361-400.

Simoneit, B. (1993) Hydrothermal activity and its effects on sedimentary organic matter, Bitumens in Ore Deposits. Springer, pp. 81-95.

Simoneit, B. (2000a) Submarine and continental hydrothermal systems—a review of organic matter alteration and migration processes, and comparison with conventional sedimentary basins. *Ore genesis and exploration: the roles of organic matter. Rev Econ Geol* **9**, 193-214.

Simoneit, B.R. (2000b) Alteration and migration process of organic matter in hydrothermal systems and implications for metallogenesis, Organic Matter and Mineralisation: Thermal Alteration, Hydrocarbon Generation and Role in Metallogenesis. Springer, pp. 13-37.

Stasiuk, L.D. and Snowdon, L.R. (1997) Fluorescence micro-spectrometry of synthetic and natural hydrocarbon fluid inclusions: crude oil chemistry, density and application to petroleum migration. *Appl. Geochem.* **12**, 229-241.

Taylor, D. (2000) Introduction: A 'soft-rock'petroleum-type approach to exploration for 'hard-rock'minerals in sedimentary basins, Organic Matter and Mineralisation: Thermal Alteration, Hydrocarbon Generation and Role in Metallogenesis. Springer, pp. 1-12.

Thompson, J.M. (1993) Chemical and isotopic constituents in the hot springs along Sulphur Creek, Colusa County, California. *Active Geothermal Systems and Gold–Mercury Deposits in the Sonoma-Clear Lake Volcanic Fields* **16**, 190-206.

Tosdal, R., Enderlin, D., Nelson, G. and Lehrman, N. (1993) Overview of the McLaughlin precious metal deposit, Napa and Yolo counties, northern California. *Active geothermal systems and gold/mercury deposits in the Sonoma/Clear Lake Volcanic Fields, California. Soc. Econ. Geol. Guidebook Series* **16**, 312-329.

Van den Kerkhof, A.M. and Hein, U.F. (2001) Fluid inclusion petrography. *Lithos* **55**, 27-47.

Wagner, D.L. and Bortugno, E.J. (1982) Santa Rosa quadrangle: U. S. Geological Survey, Regional Map Series, Map No. 2A.

Williams-Jones, A. and Migdisov, A. (2007) The solubility of gold in crude oil: implications for ore genesis, Proceedings of the 9th Biennal SGA Meeting, Millpress, Dublin, pp. 765-768.

Xie, X., Morrow, N. and Buckley, J. (1997) Crude oil/brine contact angles on quartz glass, paper SCA-9712 presented at the 1997 SCA International Symposium, Calgary, pp. 8-10.

Zhuang, H.P., Lu, J.L., Fu, J.M., Ren, C.G. and Zou, D.G. (1999) Crude oil as carrier of gold: petrological and geochemical evidence from Lannigou gold deposit in southwestern Guizhou, China. *Sci. China Ser. D* **42**, 216-224.

Copyright statement

Chapter 6

Conclusion and synthesis

6.1 Discussion and conclusions

In this chapter progress towards the objectives of this thesis is summarized, and the implications of the results are discussed

6.1.1 Progress on the objectives

6.1.1.1 Experimental method development and oil as an ore fluid

The experimental method for Au partitioning experiments between oils and aqueous fluids, or any other immiscible and density stratified fluids, was successfully developed. Solutions for the major issues that can arise, such as the Au loss, were devised and described and allow derivation of statistically robust Au partition coefficients, even when the Au recoveries were not 100%.

The objective to determine the capacity and ability of oil in comparison to an aqueous fluid was successfully achieved using the partitioning method at the tested temperature and pressure conditions, The Au--brine--DDT experiments enable calculation of a $D_{Au}^{org/aq}$ of 19, without variation as a function of the range of pressures and temperatures investigated (105 °C to 150 °C, <10 bar). With this partition coefficient, 95% of the Au partitions from the brine to DDT. DDT, were it to be present as a pure fluid in natural systems would be an effective ore fluid with the potential to transport Au at high ppm concentrations with a currently unknown upper limit. Natural oils are not composed of 100% DDT or thiols in general – nevertheless other S bearing ligands in oils may act as ligands for Au as well and small percentages can transport significant amounts of Au for oils to act as ore fluids as demonstrated in Chapter 4, section 5.

6.1.1.2 Au speciation

New information on the speciation of Au in organic liquids as obtained. The speciation and coordination number of Au were determined *in-situ* in *n*-dodecane and *1*-dodecanethiol by EXAFS measurements. At low temperatures (< 125 °C) Au can be expected to form covalent bonds with S in the form of $Au(I)RS_2^-$, where R is a radical attached to the S. However, at T >125 °C Au(I) is reduced to Au(0) suggesting metallic Au transport, possibly in the form of Au nanoparticles (NPs).

6.1.1.3 Natural observations

Analyses and textural observations of samples from the Au-Hg McLaughlin mine allow constraints to be placed on the possible roles of CM in a natural ore deposit environment. While textural observations remain, to some degree, inconclusive, as it is unknown whether the original textures were preserved, Au analysis of liquid oils containing ppm level of Au are consistent with experimental results. Au concentrations at ppm levels in preserved liquid oil indicate the potential importance of oils in ore deposits associated with CM and its capacity to transport Au.

6.1.2 Implications of results

One of the outcomes of this research, the successful method development, enables scientists to produce metal partition data in two-fluid systems with aqueous and oil based fluids in the future. Such data is much needed to understand the mechanisms responsible for ore formation processes in ore deposits associated with organic matter such as e.g., the Carlin Au deposit and province, Nevada, USA; or the McLaughlin Au-Hg deposit and the Sulfur Creek District, California, USA; the Lannigou Au deposit, SW Guizhou, China, and many more.

A key result of this thesis is demonstrated by the partition experiments and the XAS experiments. Liquid hydrocarbons can transport significant amounts of Au and presumably other metals. Thiols such as DDT make up to 7 wt% of the total S content of crude oils, and are thus a strong possible ligand for Au. In addition, crude oils contain many other N, S, and O compounds that can act as ligands increasing the ability to transport Au and other metals even more. Oils have the ability to scavenge Au from aqueous fluids, rendering oils as a competing ore fluid to aqueous ore fluids. If the fluids follow the same pathway, the presence of an oil and an aqueous ore fluid may enhance the effectivity of the ore formation process by transporting more Au from the source to the final destination. Alternatively, hydrocarbon fluids may have a competing role and re-distribute Au and other metals. In other cases, hydrocarbon fluids can simply scavenge the Au from aqueous hydrothermal fluids and concentrate the Au. This highly depends on the chemical composition of the two ore fluids, as aqueous ore fluids can contain sulfur in the lower weight-% range and are able to concentrate >500 ppm Au. Proof that the two fluids use the same pathways was observed in the Au-Hg McLaughlin deposit ore samples.

While Au transport in the form of AuNPs is potentially more effective compared to Au bonded to ligands in the form of $Au(I)RS_2^-$, due to higher Au concentrations being able to be transported in the same amount of fluid (Hough et al., 2011), it remains unclear whether, in natural environments AuNPs are capped and stabilized by single organic compounds, such as DDTs that form SAMs around the individual AuNPs. Based on Stankus et al. (2010) observations, AuNPs are capped and stabilized by more complex natural organic matter in preference over single organic compounds. Thus, in low temperature environments, such as sedimentary basins, where natural organic matter can be abundant in many forms from bitumen to liquid oils, natural organic matter may effectively transport metallic AuNPs.

6.1.2.1 Implications for genetic models for ore deposits

The ability of liquid hydrocarbons to scavenge and transport Au, and thus to support or compete with aqueous ore fluids, add another level of complexity to the formation processes of ore deposits. This affects epithermal Au-Ag(-Hg) deposits (Sherlock, 1992; Pearcy and Burruss, 1993; Mastalerz et al., 2000; Sherlock, 2000); Carlin-type Au deposits (Radtke and Scheiner, 1970; Hausen and Park, 1986; Emsbo and Koenig, 2007; Gu et al., 2012; Groves et al., 2016); orogenic Au deposits (Mirasol-Robert et al., 2017); Mississippi Valley-type Pb-Zn deposits (e.g., Parnell, 1988; Giże and Barnes, 1989; Kesler et al., 1994), 'Kupferschiefer' copper deposits (e.g., Kucha, 1981; Kucha and Przylowicz, 1999; Sawlowicz et al., 2000), sediment-hosted U deposits (Landais, 1996; Spirakis, 1996), and Witwatersrand-type Au-U deposits (Fuchs et al., 2016). Thus, CM is, in addition to aqueous ore fluids, a key factor to the metal influx. CM has the capacity to augment the metal influx and to concentrate and remobilize metals within a deposit. For example, after metals migrate *via* either organic or aqueous fluids and get concentrated at a location, these metals can be scavenged by later liquid hydrocarbons that can redistribute and further concentrate the metals within the deposit. A process like this is a possible explanation for the elevated metal concentrations in the CM associated sequences in the Au-Hg McLaughlin deposit. Such sequences are restricted to shallower depths of the McLaughlin deposit (Sherlock, 2000). The low density of liquid hydrocarbons compared to rocks would ultimately lead to hydrocarbon fluid migration to shallower depths of the deposit, resulting in the metal and CM-enriched sequences. Whatever the specific role of CM in the formation of an ore deposit, the influence of CM should never be disregarded when studying ore deposits associated with CM and derivation of genetic models

In addition to the role as a metal transport agent, oils may become a metal deposit of the future itself, due to its ability to scavenge Au and other metals from aqueous fluids, as demonstrated in this PhD project and based on observed metal rich crude oils (e.g., Samedova et al., 2009). Au and other metals may be recovered from the ashes and remains of burnt fossil fuels (Gilliam et al, 1982).

6.1.3 Recommendations for future work

Regarding the experimental work (partition and XAS experiments), future works would benefit from a focus on more complex fluid compositions to better represent natural conditions. It would be interesting to extend the temperature range to higher temperatures to observe the behavior of Au and/or other metals in fluids as hydrocarbons degrade. Such experiments would enable us to better understand CMassociated textures in ore deposits. A comparison of single organic compounds such as DDT with complex natural organic matter interacting with Au and Au nanoparticles would clarify how the AuCM interaction behaves in a natural environment. Specifically regarding partition experiments, research would benefit from experiments with aqueous fluids with more natural chemical compositions, for example sulfur-bearing brines.

Regarding ore deposits, the next logical step would be to determine the source of CM, the possible pathways, and when and how they were enriched in Au and other metals. This may be achieved *via* fluid inclusion studies, and especially metal fractionation studies depending on mass, atomic radii or isotopes. As Au has no isotopes, indirect fractionation data may be acquired by investigating the fractionation of elements associated or bonded to Au such as sulfur. This could be first investigated experimentally and then compared to isotopic data of CM and fluids in ore deposits.

6.1.4 Conclusions

The objectives of this PhD project were to demonstrate experimentally whether hydrocarbons can act as ore fluids or not, in what form Au may be transported, and to support or rebut the experimental results with observations from an actual Au deposit associated with CM. The overall results of these three main objectives suggest that hydrocarbons can be as effective in transporting Au as aqueous ore fluids and thus have to be considered in genetic models of Au and other metal deposits associated with CM. Apart

from forming Au or metal reservoirs, or act as a reductant, hydrocarbons can mobilize and re-mobilize Au and other metals and compete with hydrothermal aqueous fluids resulting in a metal depletion of aqueous hydrothermal fluids. While hydrocarbon fluids may be able to dissolve higher concentrations of Au and presumably other metals than aqueous fluids, they are less abundant than aqueous ore fluids and are usually restricted to a thin zone of the upper crust. The extent of this zone depends on the temperature stability of hydrocarbons, especially liquid hydrocarbons. Thus, the role of liquid hydrocarbons in metal transport and deposition is restricted to the upper ~3 km of the earth crust, where liquid oil can exist. Therefore, a liquid hydrocarbon fluid metal transport is applicable for deposits forming in low temperature environments, such as Carlin-type deposits, hydrothermal deposits and sedimentary deposits. Summarizing, this PhD thesis demonstrated that at specific conditions liquid hydrocarbons are excellent ore fluids for Au and that hydrocarbons can be a key factor, which is often underestimated, in the formation of ore deposits

References

Emsbo, P. and Koenig, A.E. (2007) Transport of Au in petroleum: Evidence from the northern Carlin trend, Nevada, in: al., C.J.A.e. (Ed.), *Mineral Eploration and Research: Digging Deeper*. Proc. 9th Biennial SGA Meeting, Millpress, Dublin, pp. 695-698.

Fuchs, S., Williams-Jones, A.E., Jackson, S.E. and Przybylowicz, W.J. (2016) Metal distribution in pyrobitumen of the Carbon Leader Reef, Witwatersrand Supergroup, South Africa: Evidence for liquid hydrocarbon ore fluids. *Chem. Geol.* **426**, 45-59.

Gilliam, T. M., Canon, R. M., Egan, B. Z., Kelmers, A. D., Seeley, F. G., & Watson, J. S. (1982). Economic metal recovery from fly ash. *Resources and Conservation*, *9*, 155-168.

Giże, A. and Barnes, H. (1989) Organic processes in Mississippi Valley-type ore genesis, 28th International Geological Congress Abstracts, pp. 557-558.

Groves, D.I., Goldfarb, R.J. and Santosh, M. (2016) The conjunction of factors that lead to formation of giant gold provinces and deposits in non-arc settings. *Geosc. Frontiers* **7**, 303-314.

Gu, X.X., Zhang, Y.M., Li, B.H., Dong, S.Y., Xue, C.J. and Fu, S.H. (2012) Hydrocarbon- and ore-bearing basinal fluids: a possible link between gold mineralization and hydrocarbon accumulation in the Youjiang basin, South China. *Miner. Deposita* **47**, 663-682.

Hausen, D.M. and Park, W.C. (1986) Observations on the association of gold mineralization with organic matter in Carlin-type ores. *Organics and ore deposits, Proceedings: Denver Region Exploration Geologists Society*, 119-136.

Hough, R., Noble, R. and Reich, M. (2011) Natural gold nanoparticles. *Ore Geol. Rev.* **42**, 55-61.

Kesler, S., Jones, H., Furman, F., Sassen, R., Anderson, W. and Kyle, J. (1994) Role of crude oil in the genesis of Mississippi Valley-type deposits: Evidence from the Cincinnati arch. *Geology* **22**, 609-612.

Kucha, H. (1981) Precious metal alloys and organic matter in the Zechstein copper deposits, Poland. *Mineral. Petrol.* **28**, 1-16.

Kucha, H. and Przylowicz, W. (1999) Noble metals in organic matter and clay-organic matrices, Kupferschiefer, Poland. *Econ. Geol.* **94**, 1137-1162.

Landais, P. (1996) Organic geochemistry of sedimentary uranium ore deposits. *Ore Geol. Rev.* **11**, 33-51.

Mastalerz, M., Bustin, R., Sinclair, A., Stankiewicz, B. and Thomson, M. (2000) Implications of hydrocarbons in gold-bearing epithermal systems: Selected examples from the Canadian Cordillera, Organic Matter and Mineralisation: Thermal Alteration, Hydrocarbon Generation and Role in Metallogenesis. Springer, pp. 359-377.

Mirasol-Robert, A., Grotheer, H., Bourdet, J., Suvorova, A., Grice, K., McCuaig, T.C. and Greenwood, P.F. (2017) Evidence and origin of different types of sedimentary organic matter from a Paleoproterozoic orogenic Au deposit. *Precambrian Research* **299**, 319-338.

Parnell, J. (1988) Metal Enrichments in Solid Bitumens - a Review. *Miner. Deposita* **23**, 191-199.

Pearcy, E. and Burruss, R. (1993) Hydrocarbons and gold mineralization in the hot-spring deposit at Cherry Hill, California, Bitumens in Ore Deposits. Springer, pp. 117-137.

Radtke, A.S. and Scheiner, B.J. (1970) Studies of hydrothermal gold deposition - (pt.) 1, carlin gold deposit, nevada, the role of carbonaceous materials in gold deposition. *Econ. Geol.* **65**, 87-102.

Samedova, F., Guseinova, B., Kuliev, A. and Alieva, F. (2009) Trace elements in crude oil from some new South Caspian oil fields. *Petroleum Chemistry* **49**, 288-291.

Sawlowicz, Z., Gize, A. and Rospondek, M. (2000) Organic matter from Zechstein copper deposits (Kupferschiefer) in Poland, Organic Matter and Mineralisation: Thermal Alteration, Hydrocarbon Generation and Role in Metallogenesis. Springer, pp. 220-242.

Sherlock, R. (1992) The empirical relationship between gold-mercury mineralization and hydrocarbons, in the northern Coast Ranges, California, GAC-MAC Joint Annual Meeting, Program with Abstracts.

Sherlock, R. (2000) The association of gold—mercury mineralization and hydrocarbons in the coast ranges of northern California, Organic Matter and Mineralisation: Thermal Alteration, Hydrocarbon Generation and Role in Metallogenesis. Springer, pp. 378-399.

Spirakis, C.S. (1996) The roles of organic matter in the formation of uranium deposits in sedimentary rocks. *Ore Geol. Rev.* **11**, 53-69.

Stankus, D.P., Lohse, S.E., Hutchison, J.E. and Nason, J.A. (2010) Interactions between natural organic matter and gold nanoparticles stabilized with different organic capping agents. *Environ. Sci. Technol.* **45**, 3238-3244.

Copyright statement

Complete reference bibliography

Alex, S. and Tiwari, A. (2015) Functionalized gold nanoparticles: synthesis, properties and applications—a review. *J. Nanosci. Nanotechnol.* **15**, 1869-1894.

Ansar, S.M., Perera, G.S., Jiang, D., Holler, R.A. and Zhang, D. (2013) Organothiols self-assembled onto gold: evidence for deprotonation of the sulfur-bound hydrogen and charge transfer from thiolate. *J. Phys. Chem. C* **117**, 8793-8798.

Antes, I., Dapprich, S., Frenking, G. and Schwerdtfeger, P. (1996) Stability of Group 11 Carbonyl Complexes Cl− M− CO (M= Cu, Ag, Au). *Inorg. Chem.* **35**, 2089-2096.

Bau, R. (1998) Crystal structure of the antiarthritic drug gold thiomalate (myochrysine): a double-helical geometry in the solid state. *J. Am. Chem. Soc.* **120**, 9380-9381.

Bennett, P., Melcer, M., Siegel, D. and Hassett, J. (1988) The dissolution of quartz in dilute aqueous solutions of organic acids at 25 C. *Geochim. Cosmochim. Acta* **52**, 1521-1530.

Bennett, P.C. (1991) Quartz dissolution in organic-rich aqueous systems. *Geochim. Cosmochim. Acta* **55**, 1781-1797.

Benning, L.G. and Seward, T.M. (1996) Hydrosulphide complexing of Au (I) in hydrothermal solutions from 150–400 C and 500–1500 bar. *Geochim. Cosmochim. Acta* **60**, 1849-1871.

Berger, B.R. and Bagby, W.C. (1993) The geology and origin of Carlin-type gold deposits, in: Foster, R.P. (Ed.), Gold Metallogeny and Exploration. Springer Netherlands, pp. 210-248.

Berrodier, I., Farges, F., Benedetti, M., Winterer, M., Brown, G.E. and Deveughèle, M. (2004) Adsorption mechanisms of trivalent gold on iron-and aluminum-(oxy) hydroxides. Part 1: X-ray absorption and Raman scattering spectroscopic studies of Au (III) adsorbed on ferrihydrite, goethite, and boehmite. *Geochim. Cosmochim. Acta* **68**, 3019-3042.

Bischoff, J.L. (1991) Densities of liquids and vapors in boiling NaCl-H2O solutions: A PVTX summary from 300 to 500 C. *Am. J. Sci.* **291**, 309-338.

Bischoff, J.L., Rosenbauer, R.J. and Pitzer, K.S. (1986) The system NaCl-H2O: Relations of vapor-liquid near the critical temperature of water and of vapor-liquid-halite from 300 to 500 C. *Geochim. Cosmochim. Acta* **50**, 1437-1444.

Blake, M., Jr (1981) Geologic transect of the northern Diablo Range, California.

Blake, M., Jr and Jones, D. (1981) The Franciscan assemblage and related rocks in northern California: a reinterpretation. *The Geotectonic Development of California*, 306-328.

Bol'shakov, G. F. (1986). Organic sulfur compounds of petroleum. *Sulfur reports*, *5*(2), 103-393.

Bourdet, J., Pironon, J., Levresse, G. and Tritlla, J. (2008) Petroleum type determination through homogenization temperature and vapour volume fraction measurements in fluid inclusions. *Geofluids* **8**, 46-59.

Bowell, R.J., Baumann, M., Gingrich, M., Tretbar, D., Perkins, W.F. and Fisher, P.C. (1999) The occurrence of gold at the Getchell mine, Nevada. *J. Geochem. Explor.* **67**, 127-143.

Brabb, E.E., Powell, C.L. and Brocher, T.M. (2001) Preliminary compilation of data for selected oil test wells in Northern California. US Department of the Interior, US Geological Survey.

Brugger, J., Liu, W., Etschmann, B., Mei, Y., Sherman, D.M. and Testemale, D. (2016) A review of the coordination chemistry of hydrothermal systems, or do coordination changes make ore deposits? *Chem. Geol.* **447**, 219-253.

Brust, M. and Kiely, C.J. (2002) Some recent advances in nanostructure preparation from gold and silver particles: a short topical review. *Colloids and Surfaces A: Physicochemical and Engineering Aspects* **202**, 175-186.

Chapman, R.N., O'Neil, J.R. and Mayeda, T.K. (1972) Bouguer gravity map of California, Ukiah sheet: California Division of Mines and Geology.

Connan, J. (1979) Genetic relation between oil and ore in some Pb-Zn-Ba ore deposits. *Special Publication of the Geological Society of South Africa* **5**, 263-274.

Cotton, F.A. and Wilkinson, G. (1988) Advanced inorganic chemistry. Wiley New York.

Crede, L. S., Liu, W., Evans, K. A., Rempel, K. U., Testemale, D., & Brugger, J. (2019). Crude oils as ore fluids: An experimental in-situ XAS study of gold partitioning between brine and organic fluid from 25 to 250° C. *Geochim. Cosmochim. Acta*, *244*, 352-365.

Crede, L. S., Evans, K. A., Rempel, K. U., Grice, K., & Sugiyama, I. (2018-A). Gold partitioning between 1-dodecanethiol and brine at elevated temperatures: Implications of Au transport in hydrocarbons for oil-brine ore systems. *Chem. Geol.*.

Crede, L. S., Rempel, K. U., Hu, S. Y., & Evans, K. A. (2018-B). An experimental method for gold partitioning between two immiscible fluids: Brine and n-dodecane. *Chem. Geol.*.

Crede, L.-S., Remple, K., Brugger, J. and Liu, W. (2017) The role of organics in gold transport: An investigation of gold speciation in organic liquids: European Synchrotron Facility, Experiment number: ES-552.

Cumberland, S.A., Etschmann, B., Brugger, J., Douglas, G., Evans, K., Fisher, L., Kappen, P. and Moreau, J.W. (2018) Characterization of uranium redox state in organic-rich Eocene sediments. *Chemosphere* **194**, 602-613.

Daniel, M.-C. and Astruc, D. (2004) Gold nanoparticles: assembly, supramolecular chemistry, quantum-size-related properties, and applications toward biology, catalysis, and nanotechnology. *Chem. Rev.* **104**, 293-346.

Delamarche, E.a.a., Michel, B., Kang, H. and Gerber, C. (1994) Thermal stability of self-assembled monolayers. *Langmuir* **10**, 4103-4108.

Dickinson, W.R. (1981) Plate tectonics and the continental margin of California. *The geotectonic development of California: Englewood Cliffs, New Jersey, Prentice-Hall*, 1-28.

Downare, T.D. and Mullins, O.C. (1995) Visible and near-infrared fluorescence of crude oils. *Appl. Spectrosc.* **49**, 754-764.

Drever, J. and Stillings, L. (1997) The role of organic acids in mineral weathering. *Colloids and Surfaces A: Physicochemical and Engineering Aspects* **120**, 167-181.

Driesner, T. and Heinrich, C.A. (2007) The system H2O–NaCl. Part I: Correlation formulae for phase relations in temperature–pressure–composition space from 0 to 1000°C, 0 to 5000bar, and 0 to 1 XNaCl. *Geochim. Cosmochim. Acta* **71**, 4880-4901.

Edinger, K., Grunze, M. and Wöll, C. (1997) Corrosion of gold by alkane thiols. *Phys. Chem. Chem. Phys.* **101**, 1811-1815.

Elder, R., Ludwig, K., Cooper, J. and Eidsness, M. (1985) EXAFS and WAXS structure determination for an antiarthritic drug, sodium gold (I) thiomalate. *J. Am. Chem. Soc.* **107**, 5024-5025.

Elder, R.C. and Eidsness, M.K. (1987) Synchrotron X-ray studies of metal-based drugs and metabolites. *Chem. Rev.* **87**, 1027-1046.

Ellsworth, H. V. (1928). (I) Thuchohte, a remarkable primary carbon mineral from the vicinity of Parry Sound, Ontario.(II) Cyrtolite intergrowth associated with the Parry Sound thucholite. *American Mineralogist: Journal of Earth and Planetary Materials*, *13*(8), 419-441.

Emsbo, P. and Koenig, A.E. (2007) Transport of Au in petroleum: Evidence from the northern Carlin trend, Nevada, in: al., C.J.A.e. (Ed.), *Mineral Eploration and Research: Digging Deeper*. Proc. 9th Biennial SGA Meeting, Millpress, Dublin, pp. 695-698.

Emsbo, P., Williams-Jones, A.E., Koenig, A.E. and Wilson, S.A. (2009) Petroleum as an Agent of Metal Transport: Metallogenic and Exploration Implications, in: Williams, P.J. (Ed.), In, P.J. Williams (ed.) *Smart Science for Exploration and Mining*. Proc. 10th Biennial SGA Meeting, James Cook Univ. Earth & Enviro. Studies, pp. 99-101.

Etoh, J., Izawa, E., Watanabe, K., Taguchi, S. and Sekine, R. (2002) Bladed quartz and its relationship to gold mineralization in the Hishikari low-sulfidation epithermal gold deposit, Japan. *Econ. Geol.* **97**, 1841-1851.

Etschmann, B., Brugger, J., Fairbrother, L., Grosse, C., Nies, D., Martinez-Criado, G. and Reith, F. (2016) Applying the Midas touch: Differing toxicity of mobile gold and platinum complexes drives biomineralization in the bacterium Cupriavidus metallidurans. *Chem. Geol.* **438**, 103-111.

Etschmann, B., Liu, W., Li, K., Dai, S., Reith, F., Falconer, D., Kerr, G., Paterson, D., Howard, D. and Kappen, P. (2017) Enrichment of germanium and associated arsenic and tungsten in coal and roll-front uranium deposits. *Chem. Geol.* **463**, 29-49.

Etschmann, B., Liu, W., Testemale, D., Mueller, H., Rae, N., Proux, O., Hazemann, J.-L. and Brugger, J. (2010a) An in situ XAS study of copper (I) transport as hydrosulfide complexes in hydrothermal solutions (25–592 C, 180–600bar): speciation and solubility in vapor and liquid phases. *Geochim. Cosmochim. Acta* **74**, 4723-4739.

Etschmann, B., Ryan, C., Brugger, J., Kirkham, R., Hough, R., Moorhead, G., Siddons, D., De Geronimo, G., Kuczewski, A. and Dunn, P. (2010b) Reduced As components in highly oxidized environments: Evidence from full spectral XANES imaging using the Maia massively parallel detector. *Am. Mineral.* **95**, 884-887.

Etschmann, B.E., Donner, E., Brugger, J., Howard, D.L., de Jonge, M.D., Paterson, D., Naidu, R., Scheckel, K.G., Ryan, C.G. and Lombi, E. (2014) Speciation mapping of environmental samples using XANES imaging. *Environmental Chemistry* **11**, 341-350.

Fairbrother, L., Shapter, J., Brugger, J., Southam, G., Pring, A. and Reith, F. (2009) Effect of the cyanide-producing bacterium Chromobacterium violaceum on ultraflat Au surfaces. *Chem. Geol.* **265**, 313-320.

Filby, R.H. (1994) Origin and nature of trace element species in crude oils, bitumens and kerogens: implications for correlation and other geochemical studies. *Geol. Soc. Spec. Publ.* **78**, 203-219.

Fink, J., Kiely, C.J., Bethell, D. and Schiffrin, D.J. (1998) Self-organization of nanosized gold particles. *Chem. Mater.* **10**, 922-926.

Frondel, C. (1938) Stability of colloidal gold under hydrothermal conditions. *Econ. Geol.* **33**, 1-20.

Fuchs, S., Migdisov, A. and Williams-Jones, A.E. (2011) The transport of gold in petroleum: An experimental study, Goldschmidt. *Mineral Mag.*, Prague, Czech Republic, p. 871.

Fuchs, S., Schumann, D., Williams-Jones, A.E. and Vali, H. (2015) The growth and concentration of uranium and titanium minerals in hydrocarbons of the Carbon Leader Reef, Witwatersrand Supergroup, South Africa. *Chem. Geol.* **393-394**, 55-66.

Fuchs, S., Williams-Jones, A.E., Jackson, S.E. and Przybylowicz, W.J. (2016) Metal distribution in pyrobitumen of the Carbon Leader Reef, Witwatersrand Supergroup, South Africa: Evidence for liquid hydrocarbon ore fluids. *Chem. Geol.* **426**, 45-59.

Gammons, C.H. and Williams-Jones, A. (1995) The solubility of Au Ag alloy+ AgCl in HCl/NaCl solutions at 300° C: New data on the stability of Au (1) chloride complexes in hydrothermal fluids. *Geochim. Cosmochim. Acta* **59**, 3453-3468.

Gammons, C.H., Yu, Y. and Williams-Jones, A. (1997) The disproportionation of gold (I) chloride complexes at 25 to 200 C. *Geochim. Cosmochim. Acta* **61**, 1971-1983.

Gatellier, J.-P. and Disnar, J.-R. (1988) Mécanismes et aspects cinétiques de la réduction de l'or (III) par la matière organique sédimentaire. Importance métallogénique. *Comptes Rendus Acad. Sci. Série 2, Mécanique, Physique, Chimie, Sciences de l'univers, Sciences de la Terre* **306**, 979-984.

Gatellier, J.-P. and Disnar, J.-R. (1989) Organic matter and gold-ore association in a hydrothermal deposit, France. *Applied Geochem.* **4**, 143-149.

George, S.C., Ruble, T.E., Dutkiewicz, A. and Eadington, P.J. (2001) Assessing the maturity of oil trapped in fluid inclusions using molecular geochemistry data and visually-determined fluorescence colours. *Appl. Geochem.* **16**, 451-473.

Giordano, T. (2000) Organic matter as a transport agent in ore-forming systems. *Rev. Econ. Geol.* **9**, 133-155.

Giordano, T. and Barnes, H. (1981) Lead transport in Mississippi Valley-type ore solutions. *Econ. Geol.* **76**, 2200-2211.

Giordano, T.H., Kettler, R.M. and Wood, S.A. (2000) Ore genesis and exploration: the roles of organic matter. Society of Economic Geologists.

Gize, A. P., Kuehn, C. A., Furlong, K. P., & Gaunt, J. M. (2000). Organic maturation modeling applied to ore genesis and exploration. *Rev. Econ. Geol.*, *9*, 87-104.

Giże, A. (2000) The organic geochemistry of gold, platinum, uranium and mercury deposits. *Rev. Econ. Geol.: Ore Genesisis and Exploration: The Roles of Organic Matter*, 217-250.

Giże, A. and Barnes, H. (1989) Organic processes in Mississippi Valley-type ore genesis, 28th International Geological Congress Abstracts, pp. 557-558.

Giże, A.P. (1999) A special issue on organic matter and ore deposits: Interactions, applications, and case studies - Introduction. *Econ. Geol. and the Bull. Soc. of Economic Geologists* **94**, 963-965.

Giże, A.P., Kuehn, C., Furlong, K. and Gaunt, J. (2000) Organic maturation modeling applied to ore genesis and exploration. *Rev. Econ. Geol.* **9**, 87-104.

Glikson, M. and Mastalerz, M. (2000) Organic matter and mineralisation: thermal alteration, hydrocarbon generation and role in metallogenesis. Springer Science & Business Media.

Graham, G.G., Bales, J.R., Grootveld, M.C. and Sadler, P.J. (1985) 1H, 13C NMR, and electronic absorption spectroscopic studies of the interaction of cyanide with aurothiomalate. *J. Inorg. Biochem.* **25**, 163-173.

Granger, H.C. (1966) Analytical data on samples collected at Ambrosia Lake, New Mexico, 1958 through 1962. US Geological Survey], 1966.

Greenwood, P.F., Brocks, J.J., Grice, K., Schwark, L., Jaraula, C.M.B., Dick, J.M. and Evans, K.A. (2013) Organic geochemistry and mineralogy. I. Characterisation of organic matter associated with metal deposits. *Ore Geol. Rev.* **50**, 1-27.

Grootveld, M.C. and Sadler, P.J. (1983) Differences between the structure of the anti-arthritic gold drug "myocrisin" in the solid state and in solution: a kinetic study of dissolution. *J. Inorg. Biochem.* **19**, 51-64.

Groves, D.I., Goldfarb, R.J. and Santosh, M. (2016) The conjunction of factors that lead to formation of giant gold provinces and deposits in non-arc settings. *Geosc. Frontiers* **7**, 303-314.

Gu, X.X., Zhang, Y.M., Li, B.H., Dong, S.Y., Xue, C.J. and Fu, S.H. (2012) Hydrocarbon- and ore-bearing basinal fluids: a possible link between gold mineralization and hydrocarbon accumulation in the Youjiang basin, South China. *Miner. Deposita* **47**, 663-682.

Häkkinen, H. (2012) The gold-sulfur interface at the nanoscale. *Nature chemistry* **4**, 443-455.

Hausen, D.M. and Park, W.C. (1986) Observations on the association of gold mineralization with organic matter in Carlin-type ores. *Organics and ore deposits, Proceedings: Denver Region Exploration Geologists Society*, 119-136.

Hayashi, K.-i. and Ohmoto, H. (1991) Solubility of gold in NaCl-and H2S-bearing aqueous solutions at 250–350°C. *Geochim. Cosmochim. Acta* **55**, 2111-2126.

Hearn, B.C., Jr, Donnelly-Nolan, J. and Goff, F.E. (1981) The Clear Lake volcanics: Tectonic setting and magma sources. *US Geol. Surv. Prof. Pap* **1141**, 25-45.

Heath, J.R., Knobler, C.M. and Leff, D.V. (1997) Pressure/temperature phase diagrams and superlattices of organically functionalized metal nanocrystal monolayers: the influence of particle size, size distribution, and surface passivant. *J. Phys. Chem. B* **101**, 189-197.

Henley, R.W. (1973) Solubility of gold in hydrothermal chloride solutions. *Chem. Geol.* **11**, 73-87.

Hennet, R.J.C., Crerar, D.A. and Schwartz, J. (1988) Organic complexes in hydrothermal systems. *Econ. Geol.* **83**, 742-764.

Hofstra, A.H., Leventhal, J.S., Northrop, H.R., Landis, G.P., Rye, R.O., Birak, D.J. and Dahl, A.R. (1991) Genesis of Sediment-Hosted Disseminated-Gold Deposits by Fluid Mixing and Sulfidization - Chemical-Reaction-Path Modeling of Ore-Depositional Processes Documented in the Jerritt Canyon District, Nevada. *Geology* **19**, 36-40.

Hough, R., Butt, C. and Buhner, J. (2009) The mineralogy, crystallography and metallography of gold. *Elements* **5**, 297-302.

Hough, R., Noble, R., Hitchen, G., Hart, R., Reddy, S., Saunders, M., Clode, P., Vaughan, D., Lowe, J. and Gray, D. (2008) Naturally occurring gold nanoparticles and nanoplates. *Geology* **36**, 571-574.

Hough, R., Noble, R. and Reich, M. (2011) Natural gold nanoparticles. *Ore Geol. Rev.* **42**, 55-61.

Hovey, J.K., Pitzer, K.S., Tanger, J.C., Bischoff, J.L. and Rosenbauer, R.J. (1990) Vapor-liquid phase equilibria of potassium chloride-water mixtures: equation-of-state representation for potassium chloride-water and sodium chloride-water. *J. Phys. Chem.* **94**, 1175-1179.

Hu, S.-Y., Evans, K., Craw, D., Rempel, K. and Grice, K. (2017) Resolving the role of carbonaceous material in gold precipitation in metasediment-hosted orogenic gold deposits. *Geology* **45**, 167-170.

Hu, S.-Y., Evans, K., Fisher, L., Rempel, K., Craw, D., Evans, N.J., Cumberland, S., Robert, A. and Grice, K. (2016) Associations between sulfides, carbonaceous material, gold and other trace elements in polyframboids: implications for the source of orogenic gold deposits, Otago Schist, New Zealand. *Geochim. Cosmochim. Acta* **180**, 197-213.

Hu, S., Evans, K., Craw, D., Rempel, K., Bourdet, J., Dick, J. and Grice, K. (2015) Raman characterization of carbonaceous material in the Macraes orogenic gold deposit and metasedimentary host rocks, New Zealand. *Ore Geol. Rev.* **70**, 80-95.

Hulen, J.B. and Collister, J.W. (1999) The oil-bearing, carlin-type gold deposits of Yankee Basin, Alligator Ridge District, Nevada. *Econ. Geol.* **94**, 1029-1049.

Jacob, H. (1993) Nomenclature, classification, characterization, and genesis of natural solid bitumen (migrabitumen), Bitumens in ore deposits. Springer, pp. 11-27.

Jain, P.K., Huang, X., El-Sayed, I.H. and El-Sayed, M.A. (2007) Review of some interesting surface plasmon resonance-enhanced properties of noble metal nanoparticles and their applications to biosystems. *Plasmonics* **2**, 107-118.

Jana, N.R., Gearheart, L. and Murphy, C.J. (2001) Evidence for seed-mediated nucleation in the chemical reduction of gold salts to gold nanoparticles. *Chem. Mater.* **13**, 2313-2322.

Karadas, F., Ertas, G., Ozkaraoglu, E. and Suzer, S. (2005) X-ray-induced production of gold nanoparticles on a SiO2/Si system and in a poly (methyl methacrylate) matrix. *Langmuir* **21**, 437-442.

Kesler, S., Jones, H., Furman, F., Sassen, R., Anderson, W. and Kyle, J. (1994) Role of crude oil in the genesis of Mississippi Valley-type deposits: Evidence from the Cincinnati arch. *Geology* **22**, 609-612.

Khorasani, G.K. (1987) Novel development in fluorescence microscopy of complex organic mixtures: application in petroleum geochemistry. *Org. Geochem.* **11**, 157-168.

Khorasani, G.K. and Murchison, D.G. (1988) Order of generation of petroleum hydrocarbons from liptinic macerals with increasing thermal maturity. *Fuel* **67**, 1160-1162.

Kirkham, R., Dunn, P., Kuczewski, A., Siddons, D., Dodanwela, R., Moorhead, G., Ryan, C., De Geronimo, G., Beuttenmuller, R. and Pinelli, D. (2010) The Maia Spectroscopy Detector System: Engineering for Integrated Pulse Capture, Low-Latency Scanning and Real-Time Processing, AIP Conference Proceedings. AIP, pp. 240-243.

Kokh, M.A., Lopez, M., Gisquet, P., Lanzanova, A., Candaudap, F., Besson, P. and Pokrovski, G.S. (2016) Combined effect of carbon dioxide and sulfur on vapor–liquid partitioning of metals in hydrothermal systems. *Geochim. Cosmochim. Acta* **187**, 311-333.

Krein, E.B. (1993) Organic sulfur in the geosphere: analysis, structures and chemical processes. *Sulphur-Containing Functional Groups (1993)*, 975-1032.

Kucha, H. (1981) Precious metal alloys and organic matter in the Zechstein copper deposits, Poland. *Mineral. Petrol.* **28**, 1-16.

Kucha, H. and Przylowicz, W. (1999) Noble metals in organic matter and clay-organic matrices, Kupferschiefer, Poland. *Econ. Geol.* **94**, 1137-1162.

Kuehn, C.A. (1989) Studies of disseminated gold deposits near Carlin, Nevada: Evidence for a deep geologic setting of ore formation.

La Brooy, S., Linge, H. and Walker, G. (1994) Review of gold extraction from ores. *Miner. Eng.* **7**, 1213-1241.

Landais, P. (1996) Organic geochemistry of sedimentary uranium ore deposits. *Ore Geol. Rev.* **11**, 33-51.

Langmuir, D. (1979) Techniques of estimating thermodynamic properties for some aqueous complexes of geochemical interest.

Large, R.R., Bull, S.W. and Maslennikov, V.V. (2011) A Carbonaceous Sedimentary Source-Rock Model for Carlin-Type and Orogenic Gold Deposits. *Econ. Geol.* **106**, 331-358.

Larocque, A.C., Stimac, J.A., Siebe, C., Greengrass, K., Chapman, R. and Mejia, S.R. (2008) Deposition of a high-sulfidation Au assemblage from a magmatic volatile phase, Volcán Popocatépetl, Mexico. *Journal of Volcanology and Geothermal Research* **170**, 51-60.

Lavrich, D.J., Wetterer, S.M., Bernasek, S.L. and Scoles, G. (1998) Physisorption and chemisorption of alkanethiols and alkyl sulfides on Au (111). *J. Phys. Chem. B* **102**, 3456-3465.

Leff, D.V., Ohara, P.C., Heath, J.R. and Gelbart, W.M. (1995) Thermodynamic control of gold nanocrystal size: experiment and theory. *J. Phys. Chem.* **99**, 7036-7041.

Lehrman, N.J. (1986) The McLaughlin mine, Napa and Yolo Counties, California. *Nevada Bureau of Mines and Geology*, 85-89.

Leventhal, J. (1980) Organic geochemistry and uranium in Grants mineral belt. *Mem.-NM Bur. Mines Miner. Resour.;(United States)* **38**.

Leventhal, J. and Giordano, T. (2000) The nature and roles of organic matter associated with ores and ore-forming systems: An introduction. *Rev. Econ. Geol* **9**, 1-26.

Leventhal, J.S., Daws, T.A. and Frye, J.S. (1986) Organic geochemical analysis of sedimentary organic matter associated with uranium. *Appl. Geochem.* **1**, 241-247.

Leventhal, J.S. and Threlkeld, C.N. (1978) Carbon-13/carbon-12 isotope fractionation of organic matter associated with uranium ores induced by alpha irradiation. *Science* **202**, 430-432.

Lewis, G. and Shaw III, C.F. (1986) Competition of thiols and cyanide for gold (I). *Inorg. Chem.* **25**, 58-62.

Li, K., Etschmann, B., Rae, N., Reith, F., Ryan, C.G., Kirkham, R., Howard, D., Rosa, D.R., Zammit, C. and Pring, A. (2016) Ore petrography using megapixel X-ray imaging: rapid insights into element distribution and mobilization in complex Pt and U-Ge-Cu ores. *Econ. Geol.* **111**, 487-501.

Liu, D., Fu, J. and Jia, R. (1993a) Bitumen and dispersed organic matter related to mineralization in stratabound deposits, South China, Bitumens in Ore Deposits. Springer, pp. 171-177.

Liu, J., Fu, J. and Lu, J. (1993b) Experimental study on interaction between organic matter and gold. *'Sci. Geol. Sin.' In Chinese.* **28**, 246-253.

Liu, K. and Eadington, P. (2005) Quantitative fluorescence techniques for detecting residual oils and reconstructing hydrocarbon charge history. *Org. Geochem.* **36**, 1023-1036.

Liu, W., Borg, S.J., Testemale, D., Etschmann, B., Hazemann, J.-L. and Brugger, J. (2011) Speciation and thermodynamic properties for cobalt chloride complexes in hydrothermal fluids at 35–440 C and 600bar: an *in-situ* XAS study. *Geochim. Cosmochim. Acta* **75**, 1227-1248.

Liu, W., Etschmann, B., Testemale, D., Hazemann, J.-L., Rempel, K., Müller, H. and Brugger, J. (2014) Gold transport in hydrothermal fluids: Competition among the Cl^-, Br^-, HS^- and NH_3(aq) ligands. *Chem. Geol.* **376**, 11-19.

Lohman, B.C., Powell, J.A., Cingarapu, S., Aakeroy, C.B., Chakrabarti, A., Klabunde, K.J., Law, B.M. and Sorensen, C.M. (2012) Solubility of gold nanoparticles as a function of ligand shell and alkane solvent. *Phys. Chem. Chem. Phys.* **14**, 6509-6513.

Lu, J. and Zhuang, H. (1996) Experimental studies on role of organic matter during mineralization of gold and silver at low temperatures. *'Gechim.' In Chinese.* **25**, 173-180.

Manning, D.A. and Giże, A.P. (1993) The role of organic matter in ore transport processes, Org. Geochem. Springer, pp. 547-563.

Maryutina, T.A. and Timerbaev, A.R. (2017) Metal speciation analysis of petroleum: Myth or reality? *Anal. Chim. Acta*.

Mastalerz, M., Bustin, R., Sinclair, A., Stankiewicz, B. and Thomson, M. (2000) Implications of hydrocarbons in gold-bearing epithermal systems: Selected examples from the Canadian Cordillera, Organic Matter and Mineralisation: Thermal Alteration, Hydrocarbon Generation and Role in Metallogenesis. Springer, pp. 359-377.

Mauk, J.L. and Hieshima, G. (1992) Organic matter and copper mineralization at White Pine, Michigan, USA. *Chem. Geol.* **99**, 189-211.

McLaughlin, R., Ohlin, H., Thormahlen, D., Jones, D., Miller, J. and Blome, C. (1985) Geologic map and structure sections of the Little Indian Valley-Wilbur Springs geothermal area northern Coast Ranges, California. US Geological Survey.

McLaughlin, R.J. (1978) Preliminary Geologic Map and Structural Sections of the Central Mayacamas Mountains and the Geysers Steam Field, Sonoma, Lake and Mendocino Counties, California. United States Geological Survey.

McLaughlin, R.J. (1981) Tectonic setting of pre-Tertiary rocks and its relation to geothermal resources in The Geysers-Clear Lake area. *US Geol. Surv. Prof. Pap* **1141**, 3-23.

Mclimans, R.K. (1987) The application of fluid inclusions to migration of oil and diagenesis in petroleum reservoirs. *Appl. Geochem.* **2**, 585-603.

Meeker, K.A., Chuan, R.L., Kyle, P.R. and Palais, J.M. (1991) Emission of elemental gold particles from Mount Erebus, Ross Island, Antarctica. *Geophysical Research Letters* **18**, 1405-1408.

Mei, Y., Liu, W., Brugger, J., Migdisov, A.A. and Williams-Jones, A.E. (2017) Hydration Is the Key for Gold Transport in CO2–HCl–H2O Vapor. *ACS Earth and Space Chemistry*.

Meranda, D. and Furter, W.F. (1977) Elevation of the boiling point of water by salts at saturation: Data and correlation. *J. Chem. Eng. Data* **22**, 315-317.

Miedaner, M.M., Migdisov, A.A. and Williams-Jones, A.E. (2005) Solubility of metallic mercury in octane, dodecane and toluene at temperatures between 100 degrees C and 200 degrees C. *Geochim. Cosmochim. Acta* **69**, 5511-5516.

Migdisov, A., Guo, X., Williams-Jones, A., Sun, C., Vasyukova, O., Sugiyama, I., Fuchs, S., Pearce, K. and Roback, R. (2017) Hydrocarbons as ore fluids. *Geochem. Persp. Lett.* **5**, 47-52.

Mirasol-Robert, A., Grotheer, H., Bourdet, J., Suvorova, A., Grice, K., McCuaig, T.C. and Greenwood, P.F. (2017) Evidence and origin of different types of sedimentary organic matter from a Paleoproterozoic orogenic Au deposit. *Precambrian Research* **299**, 319-338.

Molnár, F., Oduro, H., Cook, N.D., Pohjolainen, E., Takács, Á., O'Brien, H., Pakkanen, L., Johanson, B. and Wirth, R. (2016) Association of gold with uraninite and pyrobitumen in the metavolcanic rock hosted hydrothermal Au-U mineralisation at Rompas, Peräpohja Schist Belt, northern Finland. *Miner. Deposita*, 1-22.

Morrow, N.R., Tang, G.-q., Valat, M. and Xie, X. (1998) Prospects of improved oil recovery related to wettability and brine composition. *Journal of Petroleum science and Engineering* **20**, 267-276.

Murphy, P. and LaGrange, M. (1998) Raman spectroscopy of gold chloro-hydroxy speciation in fluids at ambient temperature and pressure: a re-evaluation of the effects of pH and chloride concentration. *Geochim. Cosmochim. Acta* **62**, 3515-3526.

Murphy, P.J., Stevens, G. and LaGrange, M.S. (2000) The effects of temperature and pressure on gold-chloride speciation in hydrothermal fluids: A Raman spectroscopic study. *Geochim. Cosmochim. Acta* **64**, 479-494.

Ning, C.-G., Xiong, X.-G., Wang, Y.-L., Li, J. and Wang, L.-S. (2012) Probing the electronic structure and chemical bonding of the “staple” motifs of thiolate gold nanoparticles: Au (SCH 3) 2− and Au 2 (SCH 3) 3−. *Phys. Chem. Chem. Phys.* **14**, 9323-9329.

Osterloh, F., Hiramatsu, H., Porter, R. and Guo, T. (2004) Alkanethiol-induced structural rearrangements in silica-gold core-shell-type nanoparticle clusters: An opportunity for chemical sensor engineering. *Langmuir* **20**, 5553-5558.

Palenik, C.S., Utsunomiya, S., Reich, M., Kesler, S.E., Wang, L. and Ewing, R.C. (2004) “Invisible „gold revealed: Direct imaging of gold nanoparticles in a Carlin-type deposit. *Am. Mineral.* **89**, 1359-1366.

Parnell, J. (1988) Metal Enrichments in Solid Bitumens - a Review. *Miner. Deposita* **23**, 191-199.

Parnell, J., Kucha, H. and Landais, P. (1993) Bitumens in ore deposits. Springer Science & Business Media.

Parnell, J. and McCready, A. (2000) Paragenesis of gold-and hydrocarbon-bearing fluids in gold deposits, Organic Matter and Mineralisation: Thermal Alteration, Hydrocarbon Generation and Role in Metallogenesis. Springer, pp. 38-52.

Paterson, D., De Jonge, M., Howard, D., Lewis, W., McKinlay, J., Starritt, A., Kusel, M., Ryan, C., Kirkham, R. and Moorhead, G. (2011) The X-ray Fluorescence Microscopy Beamline at the Australian Synchrotron, AIP Conference Proceedings. AIP, pp. 219-222.

Pearce, M.A., Gazley, M.F., Fisher, L.A., Hough, R., Saunders, M. and Kong, C. (2016) Nanoparticles and Gold Deposit Formation, Goldschmidt, Yokohama, Japan, p. 2455.

Pearcy, E. and Burruss, R. (1993) Hydrocarbons and gold mineralization in the hot-spring deposit at Cherry Hill, California, Bitumens in Ore Deposits. Springer, pp. 117-137.

Pearson, R.G. (1968) Hard and soft acids and bases, HSAB, part 1: Fundamental principles. *J. chem. Educ* **45**, 581.

Peters, E.K. (1991) Gold-bearing hot spring systems of the northern Coast Ranges, California. *Econ. Geol.* **86**, 1519-1528.

Plech, A., Kotaidis, V., Siems, A. and Sztucki, M. (2008) Kinetics of the X-ray induced gold nanoparticle synthesis. *Phys. Chem. Chem. Phys.* **10**, 3888-3894.

Pokrovski, G.S., Akinfiev, N.N., Borisova, A.Y., Zotov, A.V. and Kouzmanov, K. (2014) Gold speciation and transport in geological fluids: insights from experiments and physical-chemical modelling. *Geol. Soc. Spec. Publ.* **402(1)**, 9-70.

Pokrovski, G.S., Borisova, A.Y. and Harrichoury, J.C. (2008) The effect of sulfur on vapor-liquid fractionation of metals in hydrothermal systems. *Earth Planet. Sc. Lett.* **266**, 345-362.

Pokrovski, G.S., Roux, J. and Harrichoury, J.-C. (2005) Fluid density control on vapor-liquid partitioning of metals in hydrothermal systems. *Geology* **33**, 657-660.

Pokrovski, G.S., Tagirov, B.R., Schott, J., Bazarkina, E.F., Hazermann, J.L. and Proux, O. (2009a) An in situ X-ray absorption spectroscopy study of gold-chloride complexing in hydrothermal fluids. *Chem. Geol.* **259**, 17-29.

Pokrovski, G.S., Tagirov, B.R., Schott, J., Hazemann, J.L. and Proux, O. (2009b) A new view on gold speciation in sulfur-bearing hydrothermal fluids from in situ X-ray absorption spectroscopy and quantum-chemical modeling. *Geochim. Cosmochim. Acta* **73**, 5406-5427.

Pokrovski, G.S., Zakirov, I.V., Roux, J., Testemale, D., Hazemann, J.-L., Bychkov, A.Y. and Golikova, G.V. (2002) Experimental study of arsenic speciation in vapor phase to 500 C: Implications for As transport and fractionation in low-density crustal fluids and volcanic gases. *Geochim. Cosmochim. Acta* **66**, 3453-3480.

Pradier, B., Bertrand, P., Martinez, L. and Laggoun-Defarge, F. (1991) Fluorescence of organic matter and thermal maturity assessment. *Org. Geochem.* **17**, 511-524.

Proux, O., Biquard, X., Lahera, E., Menthonnex, J., Prat, A., Ulrich, O., Soldo, Y., Trévisson, P., Kapoujyan, G. and Perroux, G. (2005) FAME: a new beamline for X-ray absorption investigations of very-diluted systems of environmental, material and biological interests. *Phys. Scr.* **2005**, 970.

Radtke, A.S. (1981) Geology of the Carlin gold deposit, Nevada, Open-File Report, - ed.

Radtke, A.S. and Scheiner, B.J. (1970) Studies of hydrothermal gold deposition - (pt.) 1, carlin gold deposit, nevada, the role of carbonaceous materials in gold deposition. *Econ. Geol.* **65**, 87-102.

Ramage, M.P. and Eckert, R.E. (1975) Kinetics of the liquid phase chlorination of n-dodecane. *Industrial & Engineering Chemistry Fundamentals* **14**, 214-221.

Ravel, B. and Newville, M. (2005) ATHENA, ARTEMIS, HEPHAESTUS: data analysis for X-ray absorption spectroscopy using IFEFFIT. *J. Synchrotron Radiat.* **12**, 537-541.

Reich, M., Kesler, S.E., Utsunomiya, S., Palenik, C.S., Chryssoulis, S.L. and Ewing, R.C. (2005) Solubility of gold in arsenian pyrite. *Geochim. Cosmochim. Acta* **69**, 2781-2796.

Reith, F. and Cornelis, G. (2017) Effect of soil properties on gold-and platinum nanoparticle mobility. *Chem. Geol.* **466**, 446-453.

Reith, F., Fairbrother, L., Nolze, G., Wilhelmi, O., Clode, P.L., Gregg, A., Parsons, J.E., Wakelin, S.A., Pring, A. and Hough, R. (2010) Nanoparticle factories: Biofilms hold the key to gold dispersion and nugget formation. *Geology* **38**, 843-846.

Rempel, K.U., Liebscher, A., Meixner, A., Romer, R.L. and Heinrich, W. (2012) An experimental study of the elemental and isotopic fractionation of copper between aqueous vapour and liquid to 450° C and 400bar in the CuCl–NaCl–H_2O and CuCl–NaHS–NaCl–H_2O systems. *Geochim. Cosmochim. Acta* **94**, 199-216.

Renders, P. and Seward, T. (1989) The stability of hydrosulphido-and sulphido-complexes of Au (I) and Ag (I) at 25 C. *Geochim. Cosmochim. Acta* **53**, 245-253.

Robbins, W. K., & Hsu, C. S. (2000). Petroleum, Composition. *Kirk-Othmer Encyclopedia of Chem. Technology*.

Robert, A.M., Grotheer, H., Greenwood, P.F., McCuaig, T.C., Bourdet, J. and Grice, K. (2016) The hydropyrolysis (HyPy) release of hydrocarbon products from a high maturity kerogen associated with an orogenic Au deposit and their relationship to the mineral matrix. *Chem. Geol.* **425**, 127-144.

Roedder, E. (1984) Fluid inclusions: Reviews in mineralogy: Mineralogical Society of American, v. 12.

Ryan, C., Etschmann, B., Vogt, S., Maser, J., Harland, C., Van Achterbergh, E. and Legnini, D. (2005) Nuclear microprobe–synchrotron synergy: towards integrated quantitative real-time elemental imaging using PIXE and SXRF. *Nuclear Instruments and Methods in Physics Research Section B: Beam Interactions with Materials and Atoms* **231**, 183-188.

Ryan, C., Kirkham, R., Hough, R., Moorhead, G., Siddons, D., De Jonge, M., Paterson, D., De Geronimo, G., Howard, D. and Cleverley, J. (2010a) Elemental X-ray imaging using the Maia detector array: The benefits and challenges of large solid-angle. *Nuclear Instruments and Methods in Physics Research Section A: Accelerators, Spectrometers, Detectors and Associated Equipment* **619**, 37-43.

Ryan, C., Siddons, D., Kirkham, R., Dunn, P., Kuczewski, A., Moorhead, G., De Geronimo, G., Paterson, D., De Jonge, M. and Hough, R. (2010b) The new Maia detector system:

methods for high definition trace element imaging of natural material, AIP Conference Proceedings. AIP, pp. 9-17.

Ryan, C., Siddons, D., Kirkham, R., Li, Z., de Jonge, M., Paterson, D., Kuczewski, A., Howard, D., Dunn, P. and Falkenberg, G. (2014) Maia X-ray fluorescence imaging: Capturing detail in complex natural samples, Journal of Physics: Conference Series. IOP Publishing, p. 012002.

Rytuba, J.J. (1993) Epithermal precious-metal and mercury deposits in the Sonoma and Clear Lake volcanic fields, California. *Active geothermal systems and gold-mercury deposits in the Sonoma-Clear Lake volcanic fields, California: Society of Economic Geologists, Guidebook Series* **16**, 38-51.

Samedova, F., Guseinova, B., Kuliev, A. and Alieva, F. (2009) Trace elements in crude oil from some new South Caspian oil fields. *Petroleum Chemistry* **49**, 288-291.

Sardar, R., Funston, A.M., Mulvaney, P. and Murray, R.W. (2009) Gold nanoparticles: past, present, and future. *Langmuir* **25**, 13840-13851.

Saunders, J.A. (1990) Colloidal transport of gold and silica in epithermal precious-metal systems: Evidence from the Sleeper deposit, Nevada. *Geology* **18**, 757-760.

Sawlowicz, Z., Gize, A. and Rospondek, M. (2000) Organic matter from Zechstein copper deposits (Kupferschiefer) in Poland, Organic Matter and Mineralisation: Thermal Alteration, Hydrocarbon Generation and Role in Metallogenesis. Springer, pp. 220-242.

Saxby, J. D. (1973). Diagenesis of metal-organic complexes in sediments: formation of metal sulphides from cystine complexes. Chemical Geology, 12(4), 241-248.

Saxby, J. (1976) The significance of organic matter in ore genesis. *Handbook of strata-bound and stratiform ore deposits* **2**, 111-133.

Seward, T. (1993) The hydrothermal geochemistry of gold, Gold metallogeny and exploration. Springer, pp. 37-62.

Seward, T., Williams-Jones, A. and Migdisov, A. (2014) 13.2 The Chemistry of Metal Transport and Deposition by Ore-Forming Hydrothermal Fluids. *Treatise on Geochemistry (Second Edition), Elsevier, Oxford*, 29-57.

Seward, T.M. (1973) Thio complexes of gold and the transport of gold in hydrothermal ore solutions. *Geochim. Cosmochim. Acta* **37**, 379-399.

Shenberger, D.M. and Barnes, H.L. (1989) Solubility of gold in aqueous sulfide solutions from 150 to 350°C. *Geochim. Cosmochim. Acta* **53**, 269-278.

Sherlock, R. (1992) The empirical relationship between gold-mercury mineralization and hydrocarbons, in the northern Coast Ranges, California, GAC-MAC Joint Annual Meeting, Program with Abstracts.

Sherlock, R. (2000) The association of gold—mercury mineralization and hydrocarbons in the coast ranges of northern California, Organic Matter and Mineralisation: Thermal Alteration, Hydrocarbon Generation and Role in Metallogenesis. Springer, pp. 378-399.

Sherlock, R.L. (2005) The relationship between the McLaughlin gold-mercury deposit and active hydrothermal systems in the Geysers-Clear Lake area, northern Coast Ranges, California. *Ore Geol. Rev.* **26**, 349-382.

Sherlock, R.L. and Lehrman, N.J. (1995) Occurrences of Dendritic Gold at the Mclaughlin Mine Hot-Spring Gold Deposit. *Miner. Deposita* **30**, 323-327.

Sherlock, R.L., Tosdal, R.M., Lehrman, N.J., Graney, J.R., Losh, S., Jowett, E.C. and Kesler, S.E. (1995) Origin of the McLaughlin mine sheeted vein complex: Metal zoning, fluid inclusion, and isotopic evidence. *Econ. Geol.* **90**, 2156-2181.

Shilov, A.E. and Shul'pin, G.B. (1997) Activation of C− H bonds by metal complexes. *Chem. Rev.* **97**, 2879-2932.

Shuster, J., Reith, F., Cornelis, G., Parsons, J.E., Parsons, J.M. and Southam, G. (2017) Secondary gold structures: Relics of past biogeochemical transformations and implications for colloidal gold dispersion in subtropical environments. *Chem. Geol.* **450**, 154-164.

Sicree, A.A. and Barnes, H.L. (1996) Upper Mississippi Valley district ore fluid model: the role of organic complexes. *Ore Geol. Rev.* **11**, 105-131.

Simmons, S.F. and Brown, K.L. (2006) Gold in magmatic hydrothermal solutions and the rapid formation of a giant ore deposit. *Science* **314**, 288-291.

Simmons, S.F. and Brown, K.L. (2007) The flux of gold and related metals through a volcanic arc, Taupo Volcanic Zone, New Zealand. *Geology* **35**, 1099-1102.

Simmons, S.F. and Christenson, B.W. (1994) Origins of calcite in a boiling geothermal system. *Am. J. Sci.* **294**, 361-400.

Simon, G., Huang, H., Penner-Hahn, J.E., Kesler, S.E. and Kao, L.-S. (1999) Oxidation state of gold and arsenic in gold-bearing arsenian pyrite. *Am. Mineral.* **84**, 1071-1079.

Simoneit, B. (1993) Hydrothermal activity and its effects on sedimentary organic matter, Bitumens in Ore Deposits. Springer, pp. 81-95.

Simoneit, B. (2000a) Submarine and continental hydrothermal systems—a review of organic matter alteration and migration processes, and comparison with conventional sedimentary basins. *Ore genesis and exploration: the roles of organic matter. Rev Econ Geol* **9**, 193-214.

Simoneit, B.R. (2000b) Alteration and migration process of organic matter in hydrothermal systems and implications for metallogenesis, Organic Matter and Mineralisation: Thermal Alteration, Hydrocarbon Generation and Role in Metallogenesis. Springer, pp. 13-37.

Spirakis, C.S. (1996) The roles of organic matter in the formation of uranium deposits in sedimentary rocks. *Ore Geol. Rev.* **11**, 53-69.

Stankus, D.P., Lohse, S.E., Hutchison, J.E. and Nason, J.A. (2010) Interactions between natural organic matter and gold nanoparticles stabilized with different organic capping agents. *Environ. Sci. Technol.* **45**, 3238-3244.

Stasiuk, L.D. and Snowdon, L.R. (1997) Fluorescence micro-spectrometry of synthetic and natural hydrocarbon fluid inclusions: crude oil chemistry, density and application to petroleum migration. *Appl. Geochem.* **12**, 229-241.

Stefánsson, A. and Seward, T. (2004) Gold (I) complexing in aqueous sulphide solutions to 500 C at 500 bar. *Geochim. Cosmochim. Acta* **68**, 4121-4143.

Sun, Y., Jiao, W., Zhang, S. and Qin, S. (2009) Gold enrichment mechanism in crude oils and source rocks in Jiyang Depression. *Energ. Explor. Exploit.* **27**, 133-142.

Ta, C., Reith, F., Brugger, J.l., Pring, A. and Lenehan, C.E. (2014) Analysis of gold (I/III)-complexes by HPLC-ICP-MS demonstrates gold (III) stability in surface waters. *Environ. Sci. Technol.* **48**, 5737-5744.

Tagirov, B.R., Salvi, S., Schott, J. and Baranova, N.N. (2005) Experimental study of gold-hydrosulphide complexing in aqueous solutions at 350–500°C, 500 and 1000 bars using mineral buffers. *Geochim. Cosmochim. Acta* **69**, 2119-2132.

Taran, Y.A., Bernard, A., Gavilanes, J.-C. and Africano, F. (2000) Native gold in mineral precipitates from high-temperature volcanic gases of Colima volcano, Mexico. *Appl. Geochem.* **15**, 337-346.

Taylor, D. (2000) Introduction: A 'soft-rock'petroleum-type approach to exploration for 'hard-rock'minerals in sedimentary basins, Organic Matter and Mineralisation: Thermal Alteration, Hydrocarbon Generation and Role in Metallogenesis. Springer, pp. 1-12.

Testemale, D., Argoud, R., Geaymond, O. and Hazemann, J.-L. (2005) High pressure/high temperature cell for X-ray absorption and scattering techniques. *Rev. Sci. Instrum.* **76**, 043905.

Thompson, J.M. (1993) Chemical and isotopic constituents in the hot springs along Sulphur Creek, Colusa County, California. *Active Geothermal Systems and Gold–Mercury Deposits in the Sonoma-Clear Lake Volcanic Fields* **16**, 190-206.

Tissot, B. and Welte, D. (1978) The fate of organic matter in sedimentary basins: generation of oil and gas. *Petroleum Formation and Occurrence*, 69-253.

Tosdal, R., Enderlin, D., Nelson, G. and Lehrman, N. (1993) Overview of the McLaughlin precious metal deposit, Napa and Yolo counties, northern California. *Active geothermal systems and gold/mercury deposits in the Sonoma/Clear Lake Volcanic Fields, California. Soc. Econ. Geol. Guidebook Series* **16**, 312-329.

Turkevich, J., Stevenson, P.C. and Hillier, J. (1951) A study of the nucleation and growth processes in the synthesis of colloidal gold. *Faraday Disc.* **11**, 55-75.

Usher, A., McPhail, D.C. and Brugger, J. (2009) A spectrophotometric study of aqueous Au(III) halide–hydroxide complexes at 25–80 °C. *Geochim. Cosmochim. Acta* **73**, 3359-3380.

Van den Kerkhof, A.M. and Hein, U.F. (2001) Fluid inclusion petrography. *Lithos* **55**, 27-47.

Venables, J.A. (1973) Rate Equation Approaches to Thin-Film Nucleation Kinetics. *Philos. Mag.* **27**, 697-738.

Vlassopoulos, D., Wood, S.A. and Mucci, A. (1990) Gold speciation in natural waters: II. The importance of organic complexing—Experiments with some simple model ligands. *Geochim. Cosmochim. Acta* **54**, 1575-1586.

Vorapalawut, N., Pohl, P., Bouyssiere, B., Shiowatana, J. and Lobinski, R. (2011) Multielement analysis of petroleum samples by laser ablation double focusing sector field inductively coupled plasma mass spectrometry (LA-ICP MS). *J. Anal. At. Spectrom.* **26**, 618-622.

Wagner, D.L. and Bortugno, E.J. (1982) Santa Rosa quadrangle: U. S. Geological Survey, Regional Map Series, Map No. 2A.

Wang, C.-H., Chien, C.-C., Yu, Y.-L., Liu, C.-J., Lee, C.-F., Chen, C.-H., Hwu, Y., Yang, C.-S., Je, J.-H. and Margaritondo, G. (2007) Structural properties of 'naked' gold nanoparticles formed by synchrotron X-ray irradiation. *J. Synchrotron Radiat.* **14**, 477-482.

Warren, H.V. and Delavault, R.E. (1950) Gold and silver content of some trees and horsetails in British Columbia. *Geological Society of America Bulletin* **61**, 123-128.

Weisbecker, C.S., Merritt, M.V. and Whitesides, G.M. (1996) Molecular self-assembly of aliphatic thiols on gold colloids. *Langmuir* **12**, 3763-3772.

Welter, R., Omrani, H. and Vangelisti, R. (2001) Sodium tetrabromoaurate (III) dihydrate. *Acta Crystallogr. Sect. Sect. E: Struct. Rep. Online* **57**, i8-i9.

Williams-Jones, A. and Migdisov, A. (2007) The solubility of gold in crude oil: implications for ore genesis, Proceedings of the 9th Biennal SGA Meeting, Millpress, Dublin, pp. 765-768.

Williams-Jones, A.E., Bowell, R.J. and Migdisov, A.A. (2009) Gold in solution. *Elements* **5**, 281-287.

Wondimu, T., Goessler, W. and Irgolic, K.J. (2000) Microwave digestion of "residual fuel oil" (NIST SRM 1634b) for the determination of trace elements by inductively coupled plasma-mass spectrometry. *Fresen. J. Anal. Chem.* **367**, 35-42.

Wood, S. (1996) The role of humic substances in the transport and fixation of metals of economic interest (Au, Pt, Pd, U, V). *Ore Geol. Rev.* **11**, 1-31.

Wood, S. (2000) Organic matter: supergene enrichment and dispersion. *Ore Genesis and Exploration: The Roles of organic matter. Reviews in Economic Geology* **9**, 157-192.

Xie, X., Morrow, N. and Buckley, J. (1997) Crude oil/brine contact angles on quartz glass, paper SCA-9712 presented at the 1997 SCA International Symposium, Calgary, pp. 8-10.

Yao, T., Sun, Z.H., Li, Y.Y., Pan, Z.Y., Wei, H., Xie, Y., Nomura, M., Niwa, Y., Yan, W.S., Wu, Z.Y., Jiang, Y., Liu, Q.H. and Wei, S.Q. (2010) Insights into Initial Kinetic Nucleation of Gold Nanocrystals. *J. Am. Chem. Soc.* **132**, 7696-7701.

Zabinsky, S., Rehr, J., Ankudinov, A., Albers, R. and Eller, M. (1995) Multiple-scattering calculations of X-ray-absorption spectra. *Phys. Rev. B* **52**, 2995.

Zamborini, F.P. and Crooks, R.M. (1998) Corrosion passivation of gold by n-alkanethiol self-assembled monolayers: effect of chain length and end group. *Langmuir* **14**, 3279-3286.

Zammit, C.M., Weiland, F., Brugger, J., Wade, B., Winderbaum, L.J., Nies, D.H., Southam, G., Hoffmann, P. and Reith, F. (2016) Proteomic responses to gold (III)-toxicity in the bacterium Cupriavidus metallidurans CH34. *Metallomics* **8**, 1204-1216.

Zezin, D.Y., Migdisov, A.A. and Williams-Jones, A.E. (2007) The solubility of gold in hydrogen sulfide gas: An experimental study. *Geochim. Cosmochim. Acta* **71**, 3070-3081.

Zezin, D.Y., Migdisov, A.A. and Williams-Jones, A.E. (2011) The solubility of gold in H2O–H2S vapour at elevated temperature and pressure. *Geochim. Cosmochim. Acta* **75**, 5140-5153.

Zhang, P. and Sham, T. (2002) Tuning the electronic behavior of Au nanoparticles with capping molecules. *Appl. Phys. Lett.* **81**, 736-738.

Zhong, R., Brugger, J., Chen, Y. and Li, W. (2015) Contrasting regimes of Cu, Zn and Pb transport in ore-forming hydrothermal fluids. *Chem. Geol.* **395**, 154-164.

Zhuang, H.P., Lu, J.L., Fu, J.M., Ren, C.G. and Zou, D.G. (1999) Crude oil as carrier of gold: petrological and geochemical evidence from Lannigou gold deposit in southwestern Guizhou, China. *Sci. China Ser. D* **42**, 216-224.

Copyright statement

Appendix

1 Figure (Chapter 3)

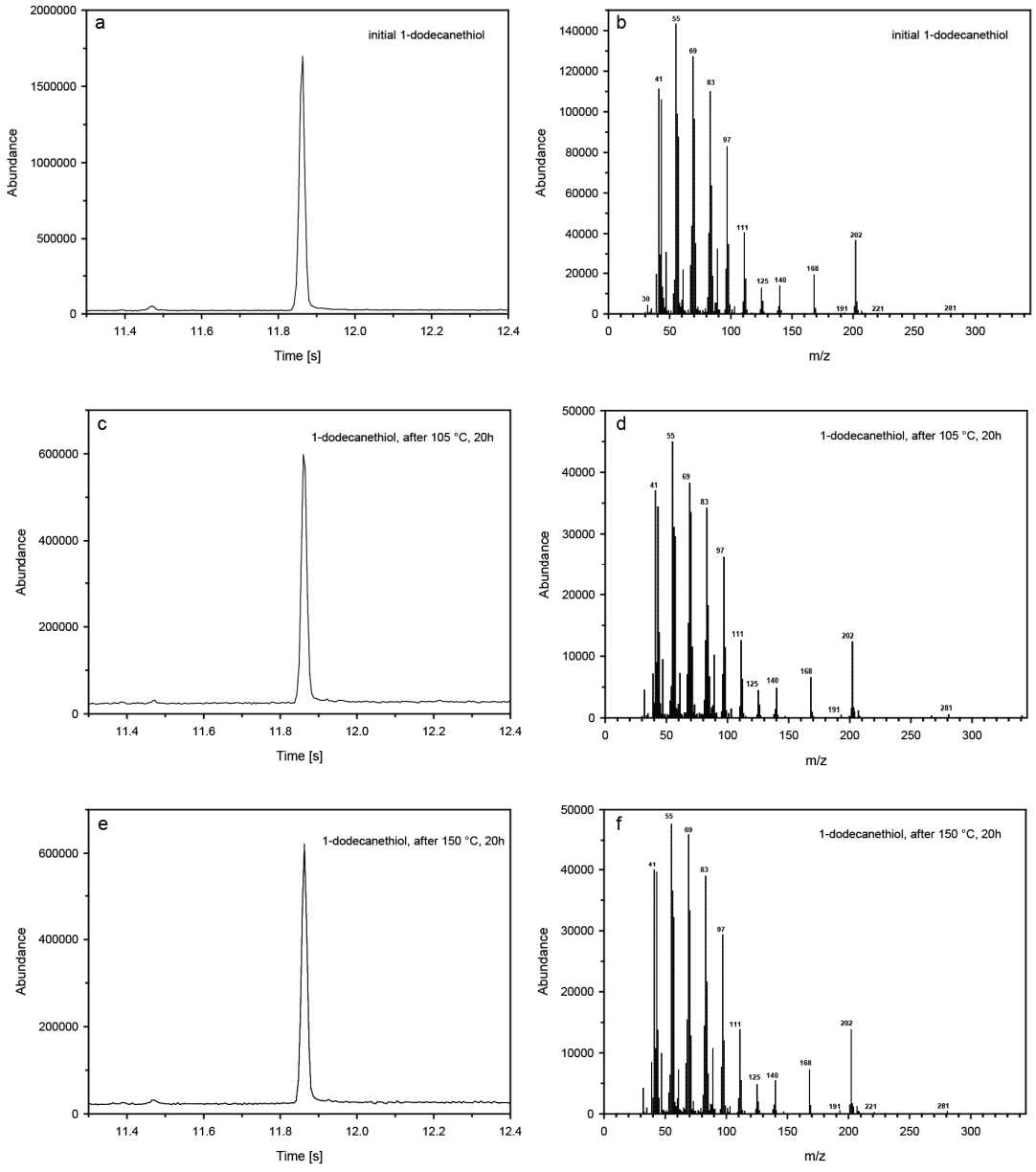

Appendix Figure 1 (Chapter 3): GC-MS spectra of the unaltered 1-dodecanethiol (a, b), and after 20 h at 105 °C while in contact with the Au doped brine (c, d), and after 20 h at 150 °C while in contact with the Au doped brine (e, f).

2 Author contributions of submitted chapters

Chapter 2

To whom it may concern,

The individual (co-) authors confirm the contribution as follows:

Manuscript title: An experimental method for gold partitioning between two immiscible fluids: brine and n-dodecane

Author	L.-S. Crede	K. Rempel	K. Evans	S.-Y. Hu
Percentage (%)	70	14	14	2

Signature: 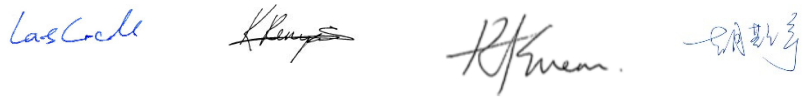

Chapter 3

To whom it may concern,

The individual (co-) authors confirm the contribution as follows (K. Grice was not available):

Manuscript title: *Gold partitioning between 1-dodecanethiol and brine at elevated temperatures: Implications of Au transport in hydrocarbons for oil-brine ore systems*

Author	L.-S. Crede	K. Evans	K. Rempel	K Grice	I. Sugiyama
Percentage (%)	63	20	15	1	1

Signature: 

Chapter 4

To whom it may concern,

The individual (co-) authors confirm the contribution as follows:

Manuscript title: *Gold partitioning between brine and organic fluid: an XAS study of gold in n-dodecane and 1-dodecanethiol and the adjacent brine from 25 to 250 °C*

Author	L.-S. Crede	W. Liu	K. Evans	K. Rempel	D. Testemale	J. Brugger
Percentage (%)	55	17.5	5	2.5	2.5	17.5

Sig-nature: 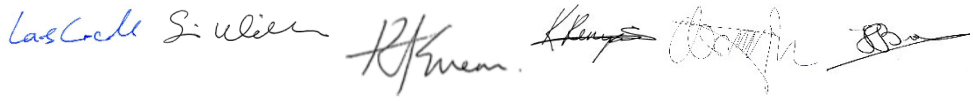

Chapter 5

To whom it may concern,

The individual (co-) authors confirm the contribution as follows:

Manuscript title: *Hydrocarbon phase mobilization of Au in the Au-Hg McLaughlin Mine, Geysers/Clear Lake area, California*

Author	L.-S. Crede	K. Evans	K. Rempel	J. Brugger	B. Etschmann	J. Bourdet	Frank Reith
Percentage (%)	59	15	10	5	5	5	1

Signature: